

University of Alberta
Department of Civil Engineering



Structural Engineering Report 139

BEHAVIOR AND STRENGTH OF MASONRY WALL/SLAB JOINTS

by
TUNDE M. OLATUNJI
J. WARWARUK
J. LONGWORTH

JULY 1986

Structural Engineering Report No. 139

BEHAVIOR AND STRENGTH OF MASONRY WALL/SLAB JOINTS

by

Tunde M. Olatunji¹

J. Warwaruk²

J. Longworth³

July 1986

Department of Civil Engineering

University of Alberta

Edmonton, Alberta

Canada T6G 2G7

-
1. Former Graduate Student, Department of Civil Engineering, Edmonton, Alberta
 2. Professor of Civil Engineering, Edmonton, Alberta
 3. Professor Emeritus of Civil Engineering, Edmonton, Alberta

ABSTRACT

Various methods have been proposed for evaluating maximum moments in the walls at the joint between a vertical masonry wall and a horizontal slab under vertical loadings. The present study examines the various proposed theories in relation to the available experimental data, provides data where there is a gap, and then develops a rational method for design. The behavior of the walls with regards to joint cracking is also investigated.

The experimental program consisted of testing four full-scale simple wall/slab joints and two H-type wall/slab frame specimens. Prism tests were also conducted to obtain stress-strain relations for the walls. The major variables investigated in the joint tests were the type of specimen, the level of axial load on the wall and the application of slab load. The behavior of the full-scale specimens was monitored by measurements of loads, deflections, wall and slab rotations. Crack measurements were made at critical positions at or close to the joint.

A theoretical relationship for wall moment-rotation behavior developed on the basis of the column deflection curve (CDC) technique and a bilinear stress-strain relationship for masonry shows fair agreement with test results. Interaction curves based on a straight line stress-strain relationship for masonry with modification factors on prism ultimate strength, f'_m , also satisfactorily predict test results.

An effective stiffness method suitable for use in analysing concrete masonry walls of practical proportion is proposed. Wall stiffnesses obtained from this method can be used in existing rigid frame analysis programs.

ACKNOWLEDGEMENTS

This investigation was made possible through financial assistance and material donations provided by the Natural Sciences and Engineering Research Council of Canada and Genstar Concrete Ltd., Edmonton. The authors would like to thank the Department of Civil Engineering for providing testing facilities for this research.

Appreciation is also expressed to Mr. L. Burden and Mr. R. Helfrich whose assistance during the testing program proved invaluable.

This report is based on a doctoral thesis prepared by the senior author.

Table of Contents

Chapter	Page
1. INTRODUCTION	1
1.1 General Remarks	1
1.2 Object and Scope	4
1.3 Layout of Thesis	5
2. REVIEW OF LITERATURE	7
2.1 Introductory Remarks	7
2.2 Prior Research	7
2.3 Current Design Practices and Proposals	17
2.4 Joint Behavior	18
3. WALL/SLAB JOINT BEHAVIOR AND STRENGTH	21
3.1 Wall Behavior and Strength	21
3.1.1 Column Deflection Curve Technique	21
3.1.1.1 Construction of Column Deflection Curves	24
3.1.1.2 Construction of the Moment-Curvature-Load ($M-\phi-P$) Curves	28
3.1.1.3 Application of CDC Technique to Masonry Walls	29
3.1.1.4 Computer Codings	36
3.1.2 Interaction Curves	40
3.1.3 Equilibrium Failure Theory	41
3.2 Strength of a Wall/Slab Joint	45
4. EXPERIMENTAL PROGRAM	47
4.1 Introduction	47
4.2 Materials and Material Properties	47
4.2.1 Concrete Block Units	50
4.2.2 Mortar	50

4.2.3 Grout	54
4.2.4 Concrete	54
4.2.5 Reinforcing Steel	54
4.2.6 Prisms	57
4.3 Masonry Properties	62
4.3.1 Compressive Strength	62
4.3.1.1 Unit-Mortar Method	62
4.3.1.2 Prism Test Method	62
4.3.2 Stress-Strain Relationship	62
4.4 Construction of Full-Scale Specimens	65
4.5 Test Set-Up	70
4.6 Instrumentation	73
4.6.1 Prisms	73
4.6.2 Full-Scale Specimens	73
4.7 Testing Procedure	80
4.7.1 Prisms	80
4.7.2 Full-Scale Specimens	81
4.7.2.1 Placement of Specimens	81
4.7.2.2 Load Application	82
5. TEST RESULTS	87
5.1 Introduction	87
5.2 General Behavior of Type I Specimens	87
5.2.1 Specimen WSA100	87
5.2.2 Specimen WSA400	88
5.2.3 Specimen WSB100	88
5.2.4 Specimen WSB400	93
5.3 General Behavior of Type II Specimens	97

5.3.1 Specimen FRA150	97
5.3.2 Specimen FRB100	97
5.4 Deflected Shapes	105
5.4.1 Type I Specimens	105
5.4.2 Type II Specimens	105
5.5 Load-Rotation Characteristics	115
5.5.1 Type I Specimens	115
5.5.2 Type II Specimens	120
5.6 Wall Strain Distribution	120
6. DISCUSSION AND ANALYSIS OF TEST RESULTS	125
6.1 Introduction	125
6.2 Comparison of Test Results with Proposed Theories	126
6.2.1 Typical Behavior and Failure Modes	126
6.2.2 Ultimate Strength	137
6.3 Effective Wall Stiffness Approach	142
6.3.1 Limitations of Proposed Effective Stiffnesses	159
6.4 Comparison of Wall Ultimate Strengths	159
7. CONCLUSIONS AND RECOMMENDATIONS	162
7.1 Conclusions	162
7.2 Recommended Design Procedure	164
7.3 Recommendations for Future Work	165
Bibliography	166
APPENDIX A - DESIGN EXAMPLE	172
APPENDIX B - CDC PROGRAM	180
APPENDIX C - OTHER EXAMPLES	223

List of Tables

Table	Page
4.1 Properties of Concrete Masonry Units	51
4.2 Mortar Test results	52
4.3 Grout Test results	55
4.4 Concrete Test results	56
4.5 Properties of Reinforcing Bars	58
4.6 Prism Test Results	59
4.7 Details of Full-Scale Specimens	66
4.8 Out-of-Plumb Measurements	83
5.1 Moment-Rotation Data for Specimen WSA100	89
5.2 Moment-Rotation Data for Specimen WSA400	90
5.3 Moment-Rotation Data for Specimen WSB100	94
5.4 Moment-Rotation Data for Specimen WSB400	95
5.5 Moment-Rotation Data for Specimen FRA150 (North Wall)	98
5.6 Moment-Rotation Data for Specimen FRA150 (South Wall)	99
5.7 Moment Rotation Data for Specimen FRB100 (North Wall)	106
5.8 Moment-Rotation Data for Specimen FRB100 (South Wall)	107
6.1 Measured and Computed Deflections and Rotations for Specimen WSA100	144
6.2 Measured and Computed Deflections and Rotations for Specimen WSA400	144
6.3 Measured and Computed Deflections and Rotations for Specimen FRA150 (North Wall)	145
6.4 Measured and Computed Deflections and Rotations for Specimen FRA150 (South Wall)	145
6.5 Measured and Computed Deflections and Rotations for Specimen WSB100	146

Table	Page
6.6 Measured and Computed Deflections and Rotations for Specimen WSB400	146
6.7 Measured and Computed Deflections and Rotations for Specimen FRB100 (North Wall)	147
6.8 Measured and Computed Deflections and Rotations for Specimen FRB100 (South Wall)	147
6.9 Stiffness Distribution at Failure for Unreinforced Walls	157
6.10 Stiffness Distribution at Failure for Reinforced Walls	158
6.11 Comparison of Ultimate Strength Values for Upper Walls	160
A.1 Design Example	178

List of Figures

Figure	Page
1.1 Wall/Slab Frame Showing Problem Areas	2
1.2 Wall/Slab Joint Distortions	3
2.1 Joint and Idealized Moment Rotation Relationship (Sahlin, 1959)	8
2.2 Various Joints Tested by Sahlin (1969)	10
2.3 Joint Failure Modes	19
3.1 Wall Model	22
3.2 Column Deflection Curve	23
3.3 Use of Column Deflection Curves	25
3.4 Various Beam Column Solutions	26
3.5 Graphical Technique for Drawing Moment-Curvature-Load Curves (Pfrang et al., 1964)	30
3.6 Single Curvature Bending with Equal End Eccentricities (Furler, 1981)	31
3.7 Single Curvature Bending with Unequal End Eccentricities (Furler, 1981)	32
3.8 Double Curvature Bending (Furler, 1981)	33
3.9 Simplified Building with Load Carrying Walls and Loaded Slabs (Sahlin, 1971)	35
3.10 Stress-Strain Relations for Masonry	37
3.11 Wall Moment-Rotation Curves for Unreinforced Concrete Masonry	38
3.12 Wall Moment-Rotation Curves for Reinforced Concrete Masonry	39
3.13 Interaction Curves for Unreinforced 200mm Walls	42
3.14 Interaction Curves for Reinforced Partially Grouted 200mm Walls	43
3.15 Interaction Curves for Reinforced Fully Grouted 200mm Walls	44
4.1 Type I Specimen	48

Figure	Page
4.2 Type II Specimen	49
4.3 Concrete Block Units	53
4.4 Type I Prism	60
4.5 Type II Prism	60
4.6 Stress-Strain Relationship for Ungrouted Concrete Masonry Prisms	63
4.7 Stress-Strain Relationship for Grouted Concrete Masonry Prisms	64
4.8 Typical Joint Reinforcement Details	68
4.9 Slab Reinforcement Details for Type II Specimens	69
4.10 Loading Arrangement for Type I Specimens	71
4.11 Slab Loading Apparatus for Type I Specimens	72
4.12 Elevation View of Loading Arrangement for Type II Specimens	74
4.13 Location of Demec Points on Prisms	75
4.14 Instrumentation of Type I Specimens	76
4.15 Instrumentation of Type II Specimens	79
5.1 Crack Distribution at Failure on Specimen WSA100	91
5.2 Crack Distribution at Failure on Specimen WSA400	92
5.3 Crack Distribution at Failure of Specimen WSB100	96
5.4 Deflected Shape for Specimen WSA100	108
5.5 Deflected Shape for Specimen WSB100	109
5.6 Deflected Shape for Specimen WSB400	110
5.7 Deflected Shape for Specimen FRA150	111
5.8 Deflected Shape for Specimen FRB100	112
5.9 Load-Rotation Curves for Specimen WSA100	116

Figure	Page
5.10 Load-Rotation Curves for Specimen WSA400	117
5.11 Load-Rotation Curves for Specimen WSB100	118
5.12 Load-Rotation Curves for Specimen WSB400	119
5.13 Load-Rotation Curves for Specimen FRA150 (North Wall)	121
5.14 Load-Rotation Curves for Specimen FRA150 (South Wall)	122
5.15 Load-Rotation Curves for Specimen FRB100 (North Wall)	123
5.16 Load-Rotation Curves for Specimen FRB100 (South Wall)	124
6.1 Internal Stress Distribution on a Wall Cross-Section Having a Balanced Failure (Ferguson, 1979)	128
6.2 Internal Stress Distribution on a Wall Cross-Section Having a Compression Failure (Ferguson, 1979)	128
6.3 Internal Stress Distribution on a Wall Cross-Section Having a Tension Failure (Ferguson, 1979)	129
6.4 Comparison of Moment-Rotation Behavior of Upper Wall of Specimen WSA100	131
6.5 Comparison of Moment-Rotation Behavior of Upper Wall of Specimen WSA400	132
6.6 Comparison of Moment-Rotation Behavior of Upper Wall of Specimen FRA150	133
6.7 Comparison of Moment-Rotation Behavior of Upper Wall of Specimen WSB100	134
6.8 Comparison of Moment-Rotation Behavior of Upper Wall of Specimen WSB400	135
6.9 Comparison of Moment-Rotation Behavior of Upper Wall of Specimen FRB100	136
6.10 Ultimate Strengths Using Interaction Curves for Unreinforced 200 mm Walls	139

Figure	Page
6.11 Ultimate Strengths Using Interaction Curves for Reinforced Fully Grouted 200 mm Walls	140
6.12 Ultimate Strengths Using Interaction Curves for Reinforced Partially Grouted 200 mm Walls	141
6.13 PFT Model for Type I Specimens	148
6.14 PFT Model for Type II Specimens	149
6.15 I_e/I_n Versus P/P_b for All Walls	151
6.16 I_e/I_n Versus P/P_b For Unreinforced Upper Walls	152
6.17 I_e/I_n Versus P/P_b For Reinforced Upper Walls	153
6.18 I_e/I_n Versus P/P_b For Unreinforced Lower Walls	154
6.19 I_e/I_n Versus P/P_b For Reinforced Lower Walls	155
A.1 External Wall of a 8-Storey Building	174
B.1 Cross-Sections	184
B.2 Stress-Strain Relations for Masonry	184
B.3 Stress-Strain Relations for Steel	185
B.4 Cases 1 and 4: Constant Modulus between any Two Strain Values except ϵ_2 and ϵ_3	185
B.5 Cases 2A and 2B: Change in Modulus between ϵ_1 and ϵ_2	186
B.6 Case 3: Change in Modulus between ϵ_3 and ϵ_4	187
B.7 Cases 5A and 5B: Tension and Constant/Change in Modulus between ϵ_3 and ϵ_4	188
B.8 Cases 6A and 6B: Large amount of tension on Cross-Section	189

List of Plates

Plate	Page
4.1 Typical Failure of Ungrouted Prism	61
4.2 Test Set-Up for Type II Specimens	77
4.3 Temporary Adjustable Slab Support for Type I Specimens	84
5.1 Wall Crushing Failure of Specimen WSB400	100
5.2 Side View of Crack Distribution at Failure on Specimen WSB400	101
5.3 Back View of Crack Distribution at Failure on Specimen WSB400	102
5.4 Side View of Crack Distribution at Failure on Specimen FRA150	103
5.5 Back View of Crack Distribution at Failure on Specimen FRA150	104
5.6 Side View of Crack Distribution at Failure on Specimen FRB100	113
5.7 Back View of Crack Distribution at Failure on Specimen FRB100	114

List of Symbols

a	= modification factor on prism strength
A	= cross sectional area
b	= width of wall cross-section
D_b	= PFT node at lower wall midheight
D_j	= PFT node at wall/slab joint
D_t	= PFT node at upper wall midheight
e	= eccentricity of wall loading
e_f	= eccentricity at failure
e_r	= relative eccentricity, e/t
e_{rf}	= relative eccentricity at failure
e_{rtest}	= test relative eccentricity
E	= modulus of elasticity
E_c	= modulus of elasticity of concrete
E_i	= tangent modulus of elasticity of masonry
EI	= rigidity modulus
E_m	= modulus of elasticity of masonry
$(EI)_s$	= rigidity modulus of slab
$(EI)_m$	= rigidity modulus of masonry
f'_m	= masonry ultimate strength
g	= $1 + d/2h$
h	= slab depth
H	= wall height
H_c	= height of equivalent column (short)
H/t	= slenderness ratio
I	= moment of inertia

I_{eu}	= effective moment of Inertia of upper wall
I_{el}	= effective moment of Inertia of lower wall
I_n	= net moment of Inertia of wall
I_s	= moment of Inertia of slab
I_w	= moment of inertia of wall
K	= stiffness = $(EI)/L$
K_l	= lower wall stiffness $(EI)_L/H$
K_s	= slab stiffness = $(EI)_s/L$
K_t	= total wall stiffness, $(EI)_T/L$
K_u	= upper wall stiffness, $(EI)_s/L$
K_w	= wall stiffness = $(EI)_w/H$
L	= distance from centre to centre of wall
L_c	= height of equivalent column (long)
L_{cq}	= quarter wavelength of CDC
m	= M/M_b
M	= moment at any point
M_o	= end moment
M_b	= maximum elastic moment = $f'_m bt^2/6$
M_F	= fixed end moment
M_R	= rigid frame moment
M_{lw}	= lower wall moment
M_{pL}	= plastification moment
M_{sl}	= slab moment
M_{smax}	= maximum slab moment
M_t	= total wall moment
M_{uw}	= upper wall moment
P	= wall axial load or precompression

P_b	= short wall cross sectional capacity
P_{bal}	= balanced load
P_L	= lower wall axial load
P_s	= applied slab load
P_u	= upper wall axial load
S	= standard deviation
t	= wall thickness
V	= coefficient of variation
w_D	= design load
w_{eq}	= equivalent uniformly distributed load
x	= distance along thrust line
\bar{X}	= mean value
y	= displacement of wall from thrust line
α	= ratio of effective wall thickness to half wall thickness
β	$= \frac{(EI)_s H}{(EI)_w L}$
δ	= H/t
Δx	= incremental wall/column height
ϵ	= strain
ϵ_p	= compression yield strain
ϵ_{ub}	= ultimate compression strain
γ	= angle between column chord and thrust line
θ	= rotation at any point on CDC
ψ	= P_u/P_L
ψ_1	= $1 + P_u/P_L$
σ	= stress at any point
σ_f	= failure stress
σ_{ub}	= ultimate compression stress

θ_o	= end rotation of CDC
θ_j	= joint rotation
θ_{lw}	= rotation of lower wall
θ_{sl}	= rotation of slab
θ_{uw}	= rotation of upper wall
θ_{ult}	= ultimate joint rotation
θ_w	= wall rotation
ν	= wall end actual rotation
ϕ	= curvature at any point
ϕ_b	= yield curvature = $2\epsilon_{ub}/t$

1. INTRODUCTION

1.1 General Remarks

The subject of the behavior and strength of the joint between masonry walls and concrete floor slabs has been of significant interest to researchers for over the last decade and a half. The developments have followed the original work of Sahlin in 1959. Recent research efforts (Colville, 1977; Awni and Hendry, 1979) have been concentrated on simplified procedures for estimating the eccentricity of load at the wall/slab joint. Figure 1.1 shows the places in a structure where estimating the joint eccentricity may be a problem.

Figure 1.1(a) shows a roof joint where there is no precompression on the slab. The slab can be assumed to be simply supported, based on the fact that cracking and yielding at the joint may occur to relief the moment developed under slab loading. Alternatively, the slab load may be assumed to result in a triangular distribution of loading on the wall, leading to a known eccentricity as shown in the figure.

Below the roof joint (Figure 1.1(b)), the situation may be fairly complex as shown in Figure 1.2. In this case, the rotation of all the individual elements meeting at the joint may be different from one another. This problem is a direct result of the the low tensile strength of the jointing material. Awni (1980), Chandrakeerthy and Hendry (1983) reported that substantial loss in rigidity at the joint may

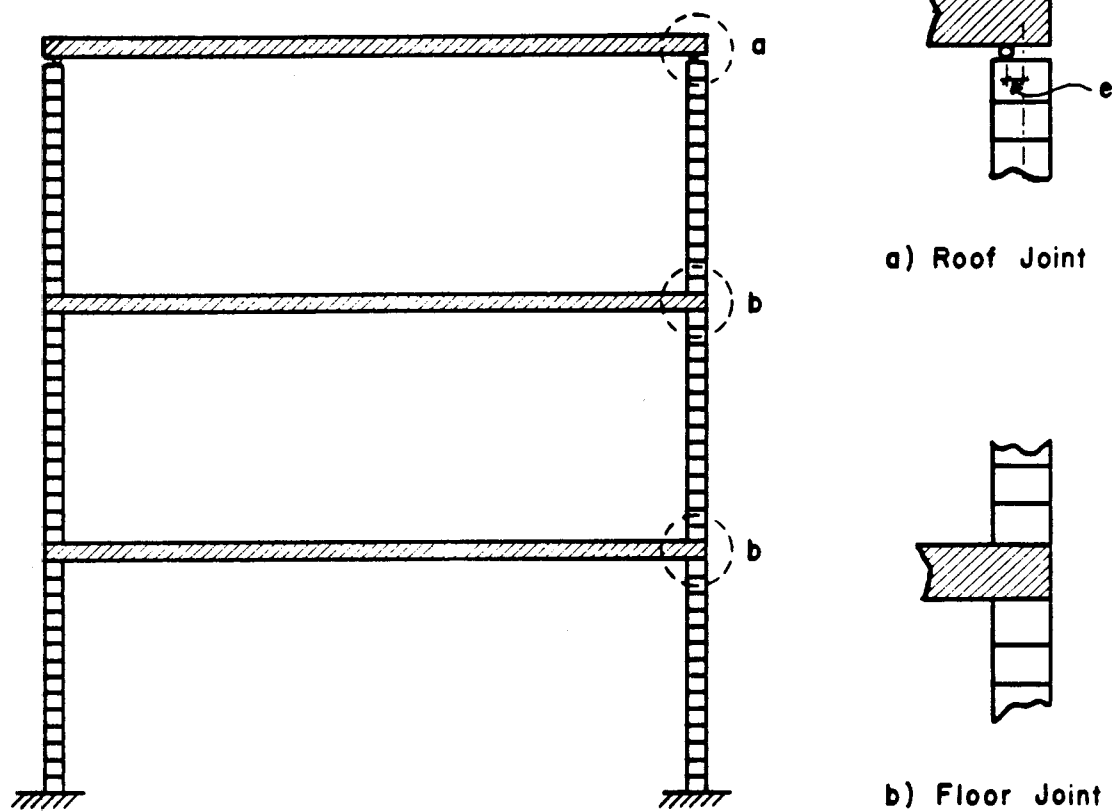


Figure 1.1 Wall/Slab Frame Showing Problem Areas

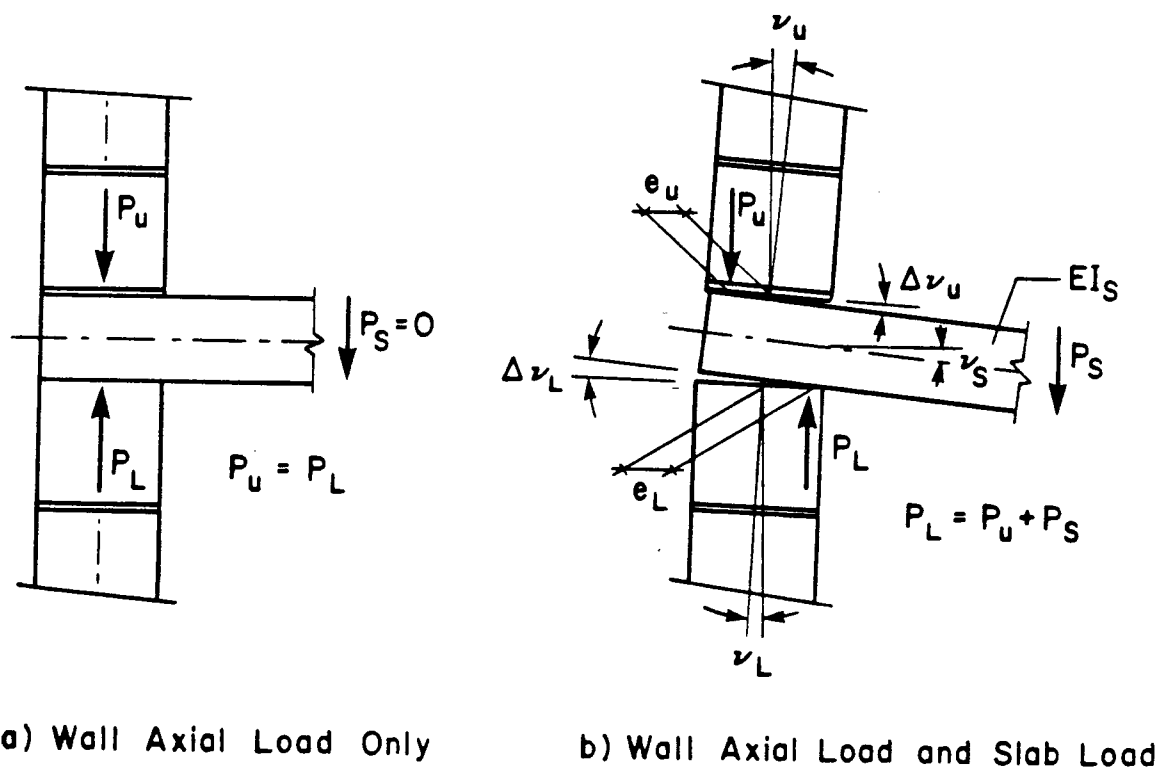


Figure 1.2 Wall/Slab Joint Distortions

result, depending on the relative stiffness of the slab to the wall.

Various tests (Sahlin, 1959 and 1969; Maurenbrecher, 1972; Colville, 1977; Ferguson, 1979; Awni, 1980; Pacholok, 1980) have been conducted to identify the variables affecting the behavior and strength of the joint. The major variables known to affect the strength of the walls at the wall/slab joint are:

1. the degree of fixity at the joint,
2. the level of precompression on the wall,
3. the slenderness ratio of the wall and
4. the relative stiffnesses of the slab and wall.

Most analytical efforts have been concentrated on unreinforced masonry. Availability of tests on full-scale masonry wall/slab joints tested to ultimate conditions will provide further insights for a rational estimation of the joint capacity of both reinforced and unreinforced masonry wall construction.

1.2 Object and Scope

The main objectives of this research are:

1. to further study the behavior of concrete masonry walls at a wall/slab joint at ultimate conditions
 - a. by providing additional data, especially at low wall axial loading.
 - b. by studying the effect of cracking at the joint on ultimate strength development of the walls

2. to provide design guidance at ultimate strength of the walls from experimental and analytical studies.

1.3 Layout of Thesis

A review of the existing literature on the subject of masonry walls and wall/slab joints is presented in Chapter 2. The purpose of this review is to establish the scope of the available work on the major variables, so as to indentify the gaps therein. Chapter 3 presents the column deflection curve (CDC) analysis of masonry walls using a bi-linear stress-strain relation for masonry. Also presented is the interaction diagram approach based on effective wall thickness. Straight line stress-strain relations for masonry and modification factors on prism ultimate strength, f'_m , were used.

An experimental program designed to provide data at low wall axial load in simple wall/slab joints and frames is presented in Chapter 4. In Chapter 5, results of the test program are presented and typical behavior during testing described.

Chapter 6 discusses the behavior of the walls in relation to the CDC analysis. Ultimate strength of the walls are compared with predictions from CDC analysis and various interaction diagrams. Using a computer-based analytical studies, effective stiffnesses for the upper and lower walls at a concrete masonry wall/slab joint of practical dimensions are proposed in this chapter. A design proposal

is presented in this chapter, with its limitations clearly spelt out.

Chapter 7 contains the major conclusions of the study, with recommendations for the design of concrete masonry walls at a wall/slab joint and proposals for future work.

A design example of an 8-storey masonry wall structure based on the proposed effective stiffnesses in this study is given in Appendix A.

2. REVIEW OF LITERATURE

2.1 Introductory Remarks

This Chapter reviews the existing literature on wall/slab joint behavior and design. The first part contains a summary of previous theoretical and experimental studies. The next section discusses the design procedures that evolved from the various studies. The final section examines the various failure patterns at a wall/slab joint.

2.2 Prior Research

The first reported investigation into the behavior of the joint between a masonry wall and floor slab was by Sahlin in 1959. Sahlin carried out tests on frame structures of brick masonry walls typical of top and intermediate storeys at a constant ratio of wall precompression to floor slab load. From the results of these tests, Sahlin proposed a rigid, perfectly plastic moment rotation relationship as an approximation of the true behavior of the joint. In Sahlin's presentation, the joint distortion, θ_j , remains at zero until a 'plastification moment', M_{pl} , is attained. The moment then remains constant at M_{pl} until the ultimate joint rotation, θ_{ult} , is reached (Fig. 2.1). Sahlin utilized the continuity condition at the joint requiring that the slab rotation θ_{sl} be equal to the wall rotation θ_w plus the joint distortion θ_j to derive expressions for calculating the load carrying capacity of the wall.

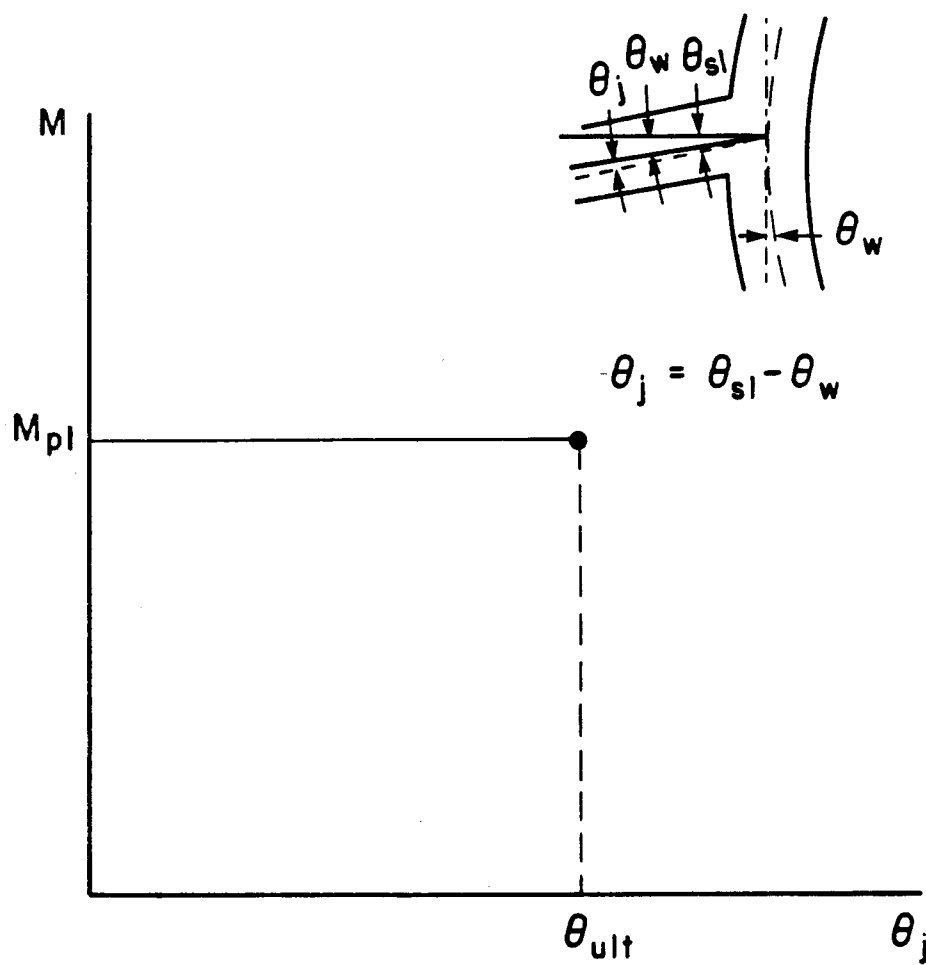
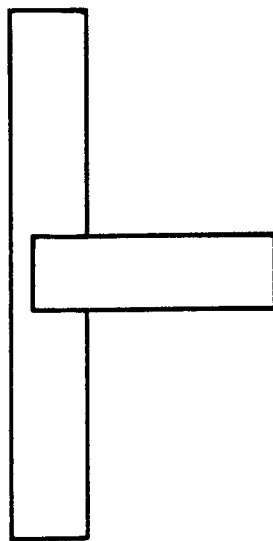


Figure 2.1 Joint and Idealized Moment Rotation Relationship
(Sahlin, 1959)

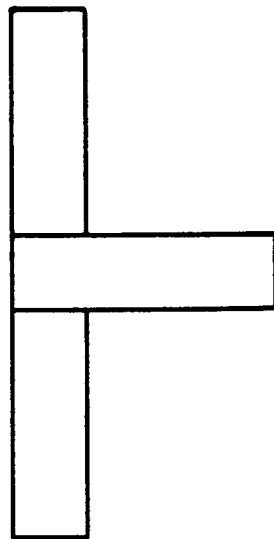
In 1969, Sahlin reported results of tests on full-scale statically indeterminate masonry wall/floor slab joints with full and partial penetration of slab, as well as attic type joints (Fig. 2.2). Sahlin found that the behavior of attic type joints and joints with partial penetration compared closely with his proposed moment-rotation behavior. Joints with full penetration slabs were found to exhibit limited plasticity in their behavior. Sahlin (1971) later presented approximate procedures for wall design based on his previous studies. However, his expressions are complex and require experimental determination of moment-rotation behavior of various joint details before they can be utilized.

Risager (1969) developed equations for evaluating the bearing capacity of linear elastic walls with no tensile strength. A parabolic approximation of the deflection curve with equal angles of rotation at the ends of an 'equivalent column' was assumed. Bearing capacity and eccentricity of the compressive force at the ends of the walls were determined and illustrated graphically for walls with no sidesway. Cracked and uncracked wall conditions with failure by ultimate stress or buckling were considered. The angle of rotation at the ends of the wall must however be known to utilize Risager's curves.

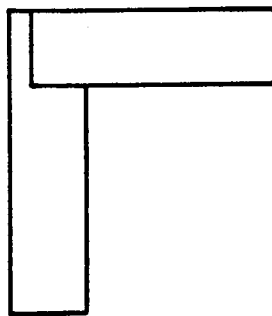
Colville (1977, 1979) extended Risager's analysis to include walls with different end eccentricities, bent in single or double curvature. The curvature of the wall obtained from the assumed parabolic deflected shape was



(a) Partial Slab Penetration



(b) Full Slab Penetration



(c) Attic Type

Figure 2.2 Various Joints Tested by Sahlin (1969)

approximated in order to obtain expressions for the relationships between load, end eccentricity and end rotation for stress and buckling failure conditions. These expressions were used to derive wall rotation factors depending on the wall eccentricity, slenderness and type of curvature. The ultimate joint eccentricity was then derived by considering compatibility at the joint using elastic slab rotation and elastic wall rotation modified by a wall rotation factor. A major assumption in the analysis was that the ratio of wall to slab stiffness remained constant throughout the loading range. A simplified design procedure was presented from the analysis assuming infinite joint stiffness for obtaining ultimate joint eccentricity. Stress reduction factors depending on the calculated wall load eccentricity and the slenderness ratio were presented for design.

Colville and Hendry (1977) carried out a series of tests on a two storey single bay load-bearing brick masonry structure to study the effects of wall precompression, magnitude of floor live load and the sequence of loading the wall and floor on wall/slab joint capacity. The results indicated that a significant restraining moment could be developed at the joint even at relatively low precompression levels. It was also found that the degree of joint fixity was not significantly affected by the magnitude of the floor live load, particularly if the compressive stress was at least 0.293 MPa. Increasing joint precompression was found to

increase the joint rigidity in a non-linear fashion; but the sequence of loading was not found to greatly influence joint restraining moment. Strength capacities of walls tested in Colville's program and those from tests conducted by the Brick Institute of America (Gross et al., 1969) were found to correlate well with predictions based on Colville's design procedure for precompression stress greater than 0.293 MPa.

Awni and Hendry (1979), Awni (1980) modified Colville's expressions for the ultimate eccentricity at a wall/slab joint to reflect further effects of joint precompression based on test results. Awni and Hendry also extended the semi-empirical relationship on ultimate eccentricity to the case of masonry walls supporting two-way slabs, using moment coefficients from ACI Standard 318-1963. A suggestion for assuming two-thirds of total width as effective in two-way hollow brick walls was also made. Results of tests on a half-scale model of Colville's two-storey frame and a full-scale three-storey two-bay structure earlier constructed by Sinha (1977) were compared with values determined from Awni's expressions. Good correlation of predicted eccentricities with test results was reported. However, Awni noted that in the full-scale structure, with ratio of floor/wall stiffness greater than 3, only about 30 percent of the maximum joint fixity could be developed irrespective of the amount of wall precompression.

Furler and Thurliman (1977), Furler(1980, 1981) presented a technique based on a numerical analysis of the wall system for predicting the behavior and strength of a masonry wall/floor slab joint. The procedure was used to obtain moment-rotation characteristics of the wall using a tri-linear stress-strain relationship for masonry and a column deflection curve (CDC) technique. The masonry wall was modelled as a series of rigid units and springy mortar joints. A straight line moment-rotation relationship was then proposed for the slab, the simplest of which joined the point at full fixity to that at zero fixity. The moment based on compatibility of rotation was then taken as the failure moment of the joint. Furler and Thurliman tested 44 clay block walls under two different levels of axial load and with enforced end rotation at one end to simulate slab action on the wall. It was found that with increased axial load, the angle of rotation of the wall increased at cracking, but decreased at failure. Comparison of theoretical and experimental relationships between end eccentricity and end rotation was reported to be in fair agreement.

Maurenbrecher and Hendry (1970, 1972) studied the effect of wall precompression and mortar strength on the behavior of masonry wall/floor slab joints. Their test results showed that, within the elastic range, precompression level had little effect on the degree of fixity of the joint. In addition, it was observed that walls

with lower strength mortar allowed more rotation of the slab and had lesser ultimate joint moment. Analyses using ultimate strength interaction curves were used to compare information obtained from tests. Satisfactory comparisons between analytical and experimental values were reported.

Sinha and Hendry (1977) investigated strains, deflections and rotations resulting from loading a full-scale, two-bay three-storey brick structure. The test results indicated that for particular loading conditions a brick structure could be idealized as a frame for the purpose of calculating effective eccentricities and effective heights. The effective eccentricities resulting from floor loading were found to vary throughout the height of the structure, and were lower than the theoretical values calculated on the basis of uniform strain distribution and full joint fixity. It was also found that the effective height of a wall was related to its disposition in the structure and the type of floor loading to which it was subjected.

Carlsen (1969) (through Maurenbrecher, 1972) studied the effect of length of bearing of slabs on the bearing capacity of the joint and ultimate slab restraining moment. The test results showed that the bearing capacity of the wall was not affected by the bearing length of the slabs; but a reduction in bearing length reduced the ultimate slab moment.

Germanino and Macchi (1977) carried out an experimental study on ceramic block wall/concrete slab structures to investigate the reliability of a frame analysis using suitable values of stiffness and idealizations of the joints. From the test results and trial analyses, it was suggested that suitable strength and stiffness of members could be deduced from tests on specimens of reduced size. It was also suggested that models with reduced stiffnesses in floors and walls or assumption of hinges in the critical sections of floors could be used for practical analysis at cracked stages or collapse.

Ferguson (1979), Pacholok (1980) and Tenende (1983) tested full-scale wall/slab specimens of both block and brick masonry, with cast-in-place and precast concrete slabs. The effects of magnitude of wall precompression, amount and details of wall and joint reinforcement, tie-back and degree of slab penetration in the wall on the behavior and strength of the joint were investigated. Both Ferguson and Pacholok reported that the joint behaved as observed by Sahlin. Ferguson classified the failure modes as compression and tension types depending on the amount of joint precompression, P . A balanced load P_{bal} was defined as that load which produced maximum compression stress on one edge and zero stress on the other edge. Both Ferguson and Pacholok reported no significant change in failure mode for reinforced or unreinforced walls, except for an increase in joint capacity when reinforcement was present. Comparison of

the test results with interaction diagrams derived from a computer program developed by Hatzinikolas (1978) was found to be satisfactory. The PFT program (Beaufait et al., 1970) for a general purpose frame analysis was also used to compare measured and theoretical rotations. Trial and error techniques were used to obtain the cracked section properties used in the computer analysis. Fair agreement between theoretical and experimentally measured rotations was reported.

Tenende reported increased ultimate joint strength when walls made of brick or block masonry contained slab reinforcement anchored into the wall rather than being terminated in a U-bend in the slab. However, this detail tended to make shear failure at the end of the slab predominant.

Chandrakeerthy and Hendry (1983) reported tests on a single bay, two-storey structure built of cavity wall construction, with one set of cavity walls later replaced by a single leaf wall. Results indicated that full fixity was unobtainable in single leaf walls at any precompression, but a high degree of fixity was initially developed in the cavity wall. Also, reported eccentricities in the single leaf wall were found to be small at all precompression levels because of high slab to wall stiffness ratio.

Rerup, Karuks and Huggins (1972) investigated strength and relative rotations of the connection between reinforced concrete walls and precast concrete floor panels which were

loaded in bending and shear. The results showed that with adequate prestressing applied at the joint, full structural continuity can be obtained without providing poured-in-place concrete for jointing.

2.3 Current Design Practices and Proposals

Present North American design procedure provides a means of estimating the load bearing capacity of a masonry wall provided the eccentricity of loading and the slenderness ratio of the wall are known. In order to calculate the eccentricity of floor loading, Gross, Dikkers and Grogan (1969) suggest the use of a triangular stress distribution on the bearing area of the wall for a 'hinged' joint, or complete restraint when the floor is 'clamped' into position. What constitutes clamping is, however, not well defined. Current British practice (Hendry et al., 1981; Curtin et al., 1982) recommends assuming a triangular stress distribution on the bearing area for lightly loaded walls; but recommends a partial frame analysis for cases in which walls carry high precompression. Again, the distinction between high and low axial load remains a matter of judgement of the designer.

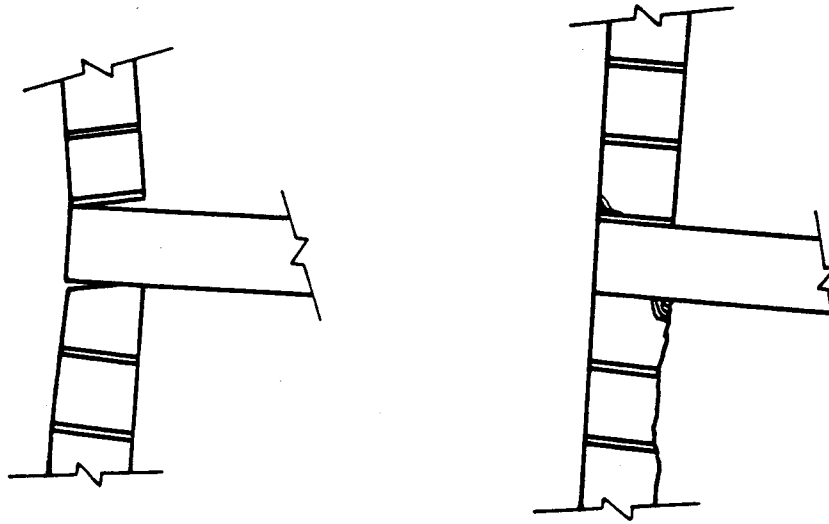
The Swiss Code (through Furler, 1981) provides wall moment-rotation curves related to the wall axial load. Slab interaction is simulated by drawing a straight line which assumes full fixity of the slab at one end and full rotation at the other end. The joint strength is obtained on the

basis of the compatibility of rotation between the wall and the slab.

2.4 Joint Behavior

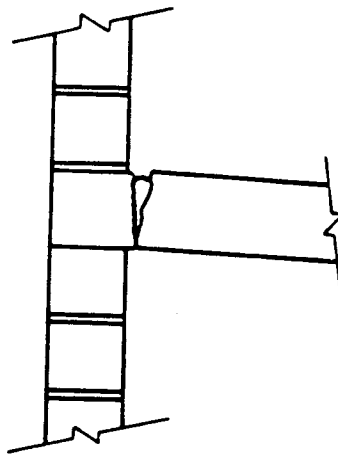
Using statically determinate joint tests, various Researchers (Maurenbrecher, 1972; Ferguson, 1979; Pacholok, 1980) have identified three main failure modes at the joint as shown in Figure 2.3. Fig. 2.3(a) depicts an 'equilibrium' failure mode typical of walls carrying low axial load. The tendency is for both upper and lower walls to rotate away from the slab as the joint opens up. With intermediate to high axial loads, local crushing near the joint accompanied by splitting along the face of the wall may produce the failure mode shown in Figure 2.3(b). A combination of the above two failure modes may also occur within this range of axial loading. The third failure mode shown in Figure 2.3(c) is due to extensive tensile cracking in the slab with the wall remaining relatively intact; or a combination of wall splitting and slab tensile failure.

Ferguson and Pacholok have observed that these failure modes are the same for reinforced and unreinforced walls. The only difference is in the axial and moment capacities at the joint. These researchers and others have also noted the differential rotation between the walls and the slab at the joint during inelastic deformation stages. It is the effect of this differential rotation on the strength the joint that needs to be examined further.



(a) Equilibrium Failure

(b) Splitting and Local Crushing



(c) Slab Failure

Figure 2.3 Joint Failure Modes

Colville (1977) has noted that the assumption of a triangular stress distribution in the wall is an oversimplification, and that there is little indication that the resulting errors are on the conservative side if this assumption is used for design. Awni(1980), Chandrakeerthy and Hendry (1983) have also observed that full fixity at the joint cannot be attained however high the axial load may be. Colville's design procedure is valid for unreinforced walls only and has not been tested extensively.

The CDC procedure presented by Furler and Thurliman seems to give good insight into the behavior of the wall under different levels of axial load. However, the interaction of the slab and the wall needs to be investigated further in order to adequately predict ultimate strength at the joint.

The research efforts in this thesis will be directed at further verification of available procedures through tests to ultimate strength. This is with a view to evolving a design procedure capable of predicting ultimate strength of both reinforced and unreinforced walls at the wall/slab joint.

3. WALL/SLAB JOINT BEHAVIOR AND STRENGTH

3.1 Wall Behavior and Strength

In this chapter, the behavior and strength of masonry walls are examined using a numerical analysis procedure and strength interaction diagrams. The effect of the interaction between the walls and the slab on the limiting strength at the joint is also examined.

3.1.1 Column Deflection Curve Technique

The rotations of a masonry wall can be considered as concentrated at the mortar joints, with the masonry units acting as rigid members. A numerical analysis procedure using the column deflection curve (CDC) approach can then be used to study the behavior of the wall under combined axial load and bending moment. This procedure is similar to that proposed by Furler (1981). This representation of the wall is shown in Figure 3.1.

The CDC technique has been applied to steel and reinforced concrete respectively by Galambos (1965) and Nathan (1972). The procedure takes into consideration the geometric and material non-linearity of the element under consideration.

A column of an arbitrary length under the action of a given axial load P may occupy an infinite number of equilibrium configurations as shown in Figure 3.2. A particular configuration is uniquely defined by the load and

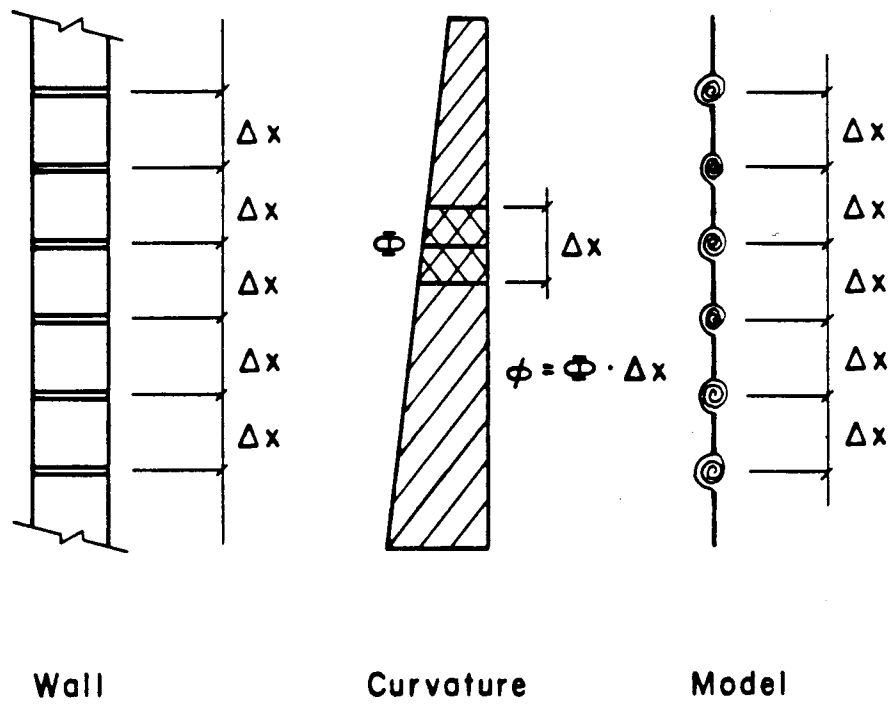


Figure 3.1 Wall Model

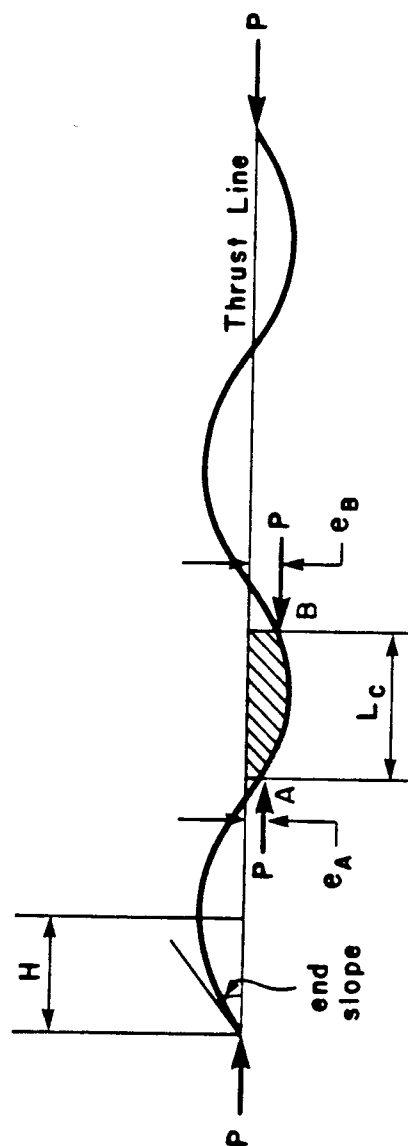


Figure 3.2 Column Deflection Curve

some parameter such as the end slope. Such a configuration is termed a column deflection curve (CDC). The shape of a quarter wavelength L_{cq} is representative of the entire configuration of each CDC.

Considering any two points A and B as shown in Figure 3.2, the moments in the column are Pe_A and Pe_B , where e_A and e_B are measured from the thrust line. Thus for any column of length L_c (the distance between points A and B measured along the thrust line) carrying the given load P and end moments Pe_A and Pe_B , the segment of the CDC between points A and B represents a possible equilibrium configuration of that column.

Now consider a column of length L_c with fixed load P and increasing equal end moments as shown in Figure 3.3. To obtain the value of maximum end moment, a number of CDC half-waves for load P are located on a common centre line as shown in the figure. Depending on whether the length of the column is L_c or H_c , the limiting end moment could be a stability criterion for column length H_c or material failure criterion for column length L_c .

3.1.1.1 Construction of Column Deflection Curves

CDC's are usually constructed numerically. Any one CDC can give information about an infinite combination of end moments, some of which are shown in Figure 3.4.

The method of construction as given by Galambos (1965) is briefly described below:

1. Let the displacement of a CDC from the thrust line

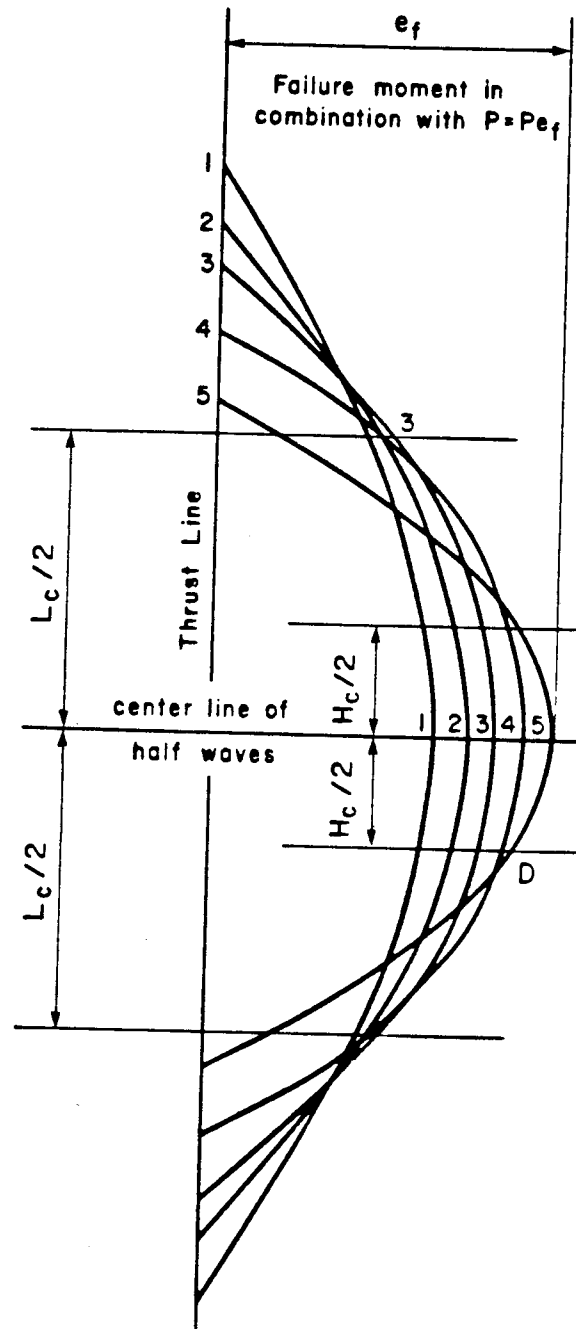


Figure 3.3 Use of Column Deflection Curves

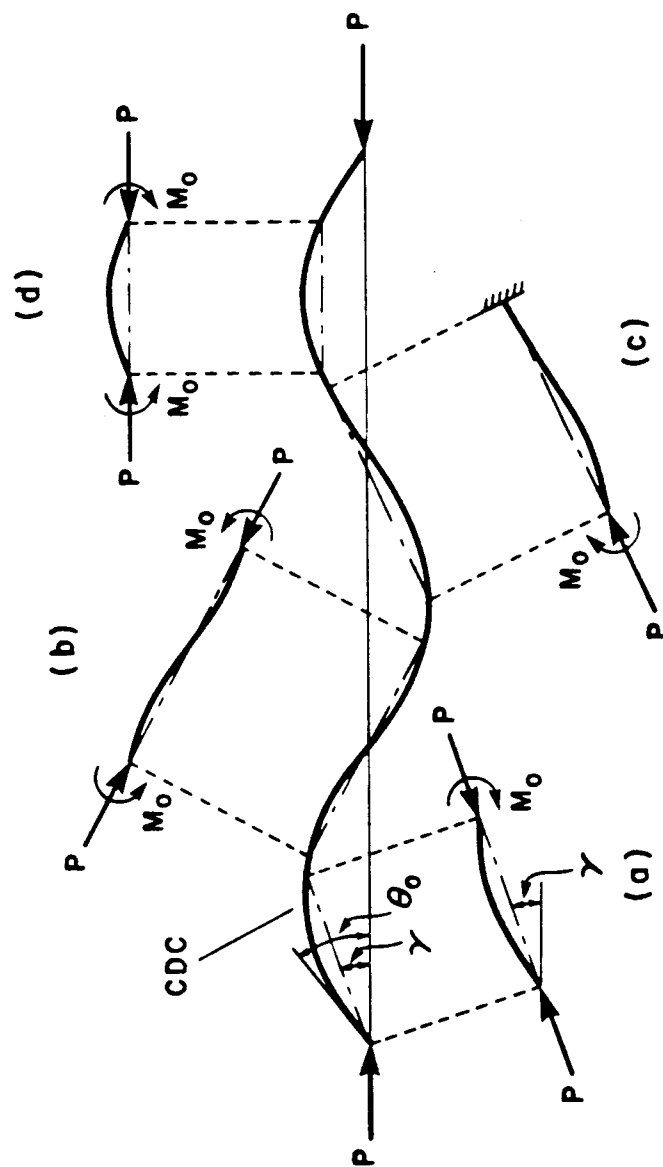


Figure 3.4 Various Beam Column Solutions

be y , and the distance along the thrust line be x . Then expanding $y(x)$ in a Taylor's series about some point x_0 leads to:

$$y(x_0 + \Delta x) = y(x_0) + y'(x_0)(\Delta x) + \\ (1/2)y''(x_0)(\Delta x)^2 + \dots$$

where primes indicate differentiation with respect to x . But y' is the slope θ of the CDC, and y'' is an acceptable approximation of the curvature ϕ . Thus, if we truncate the series after three terms (equivalent to assuming constant or circular curvature within Δx), we obtain:

$$y(x_0 + \Delta x) = y(x_0) + \theta(x_0)(\Delta x) + \\ (1/2)\phi(x_0)(\Delta x)^2 \quad (3.1)$$

2. Similarly, expanding the slope $y'(x)$ in a Taylor series about x_0 we have:

$$y'(x_0 + \Delta x) = y'(x_0) + y''(x_0)(\Delta x) + \\ (1/2)y'''(x_0)(\Delta x)^2 + \dots$$

And, introducing the same notation, and truncating at a corresponding point after the y'' term, we obtain:

$$\theta(x_0 + \Delta x) = \theta(x_0) + \phi(x_0)(\Delta x) \quad (3.2)$$

3. For a given value of P , it is possible to construct a curve of moment M versus curvature ϕ for a

particular cross section. Then, if x_0 is a point of zero displacement and therefore of zero moment and curvature ϕ , a selected value of $\theta(x_0)$ may be inserted into Equations 3.1 and 3.2 to yield y_1 and θ_1 at $x_1 = x_0 + \Delta x$.

4. The moment curvature relation for the cross-section and material may then be used to obtain ϕ_1 from $M_1 = Py_1$, and we then have all the necessary information to use Equations 3.1 and 3.2 to proceed from x_1 to $x_2 = x_1 + \Delta x$.
5. By repeating this process for successive stations along the thrust line until the slope θ reduces to zero, we obtain the configuration of a quarter wavelength of the CDC for the particular selected values of end slope and thrust for the given column cross section.

3.1.1.2 Construction of the Moment-Curvature-Load (M- ϕ -P) Curves

M- ϕ -P curves are constructed using a numerical analysis procedure (Pfrang et al., 1964), based on an assumed stress-strain relationship for masonry. The procedure is outlined as follows:

1. A value of P is selected
2. A value of the curvature ϕ is chosen
3. A series of compression strain values are then studied, beginning from the assumed maximum strain on the cross-section. This then determines the neutral axis and the strain distribution throughout

the depth of the member.

4. The stress distribution across the depth of the wall is determined from the assumed stress-strain curve for masonry.
5. The axial load corresponding to each stress distribution is evaluated.
6. The calculated axial load is compared with the selected axial load, and agreement is sought within 0.1% error.
7. When the selected value of axial load is bracketed, the moment corresponding to this particular stress distribution is then evaluated by integration.
8. The above procedure is then repeated for another value of ϕ to trace a complete M- ϕ -P curve.
9. Another value of P is selected and the entire procedure is repeated for this new axial load.

Figure 3.5 illustrates the technique of obtaining the M- ϕ -P curves graphically.

3.1.1.3 Application of CDC Technique to Masonry Walls

In applying Equations 3.1 and 3.2 to masonry walls in this study, segment length, Δx , is defined as the distance centre-to-centre of mortar joints.

Figures 3.6 to 3.8 show the graphical application of CDC's to the solution of combined axial load and end moments for walls of various curvatures (single and double curvature bending, with equal or unequal end eccentricities) when spanning between floor slabs. The wall is used to fit the CDC curves depending on its

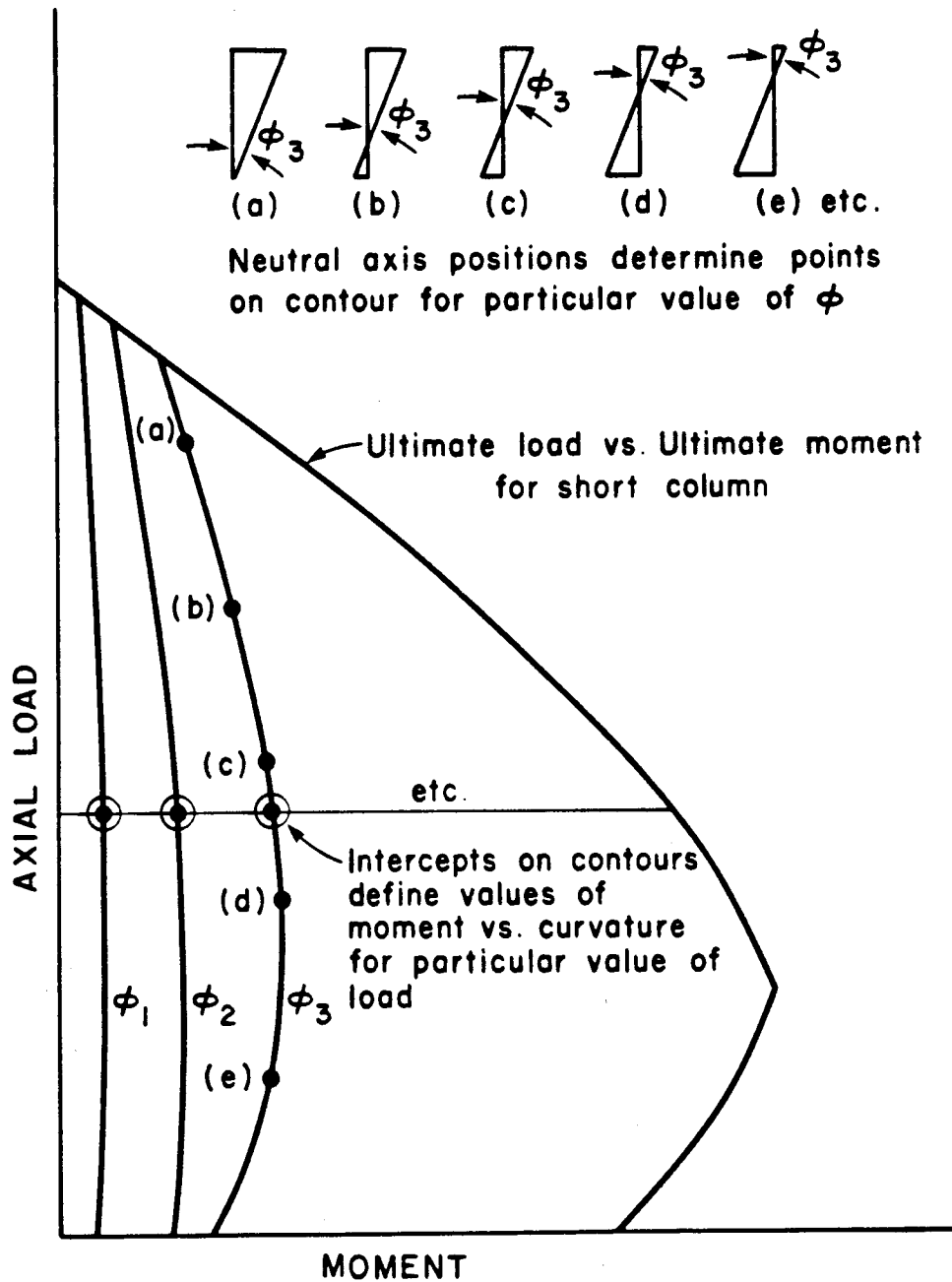


Figure 3.5 Graphical Technique for Drawing Moment-Curvature-Load Curves (Pfrang et al., 1964)

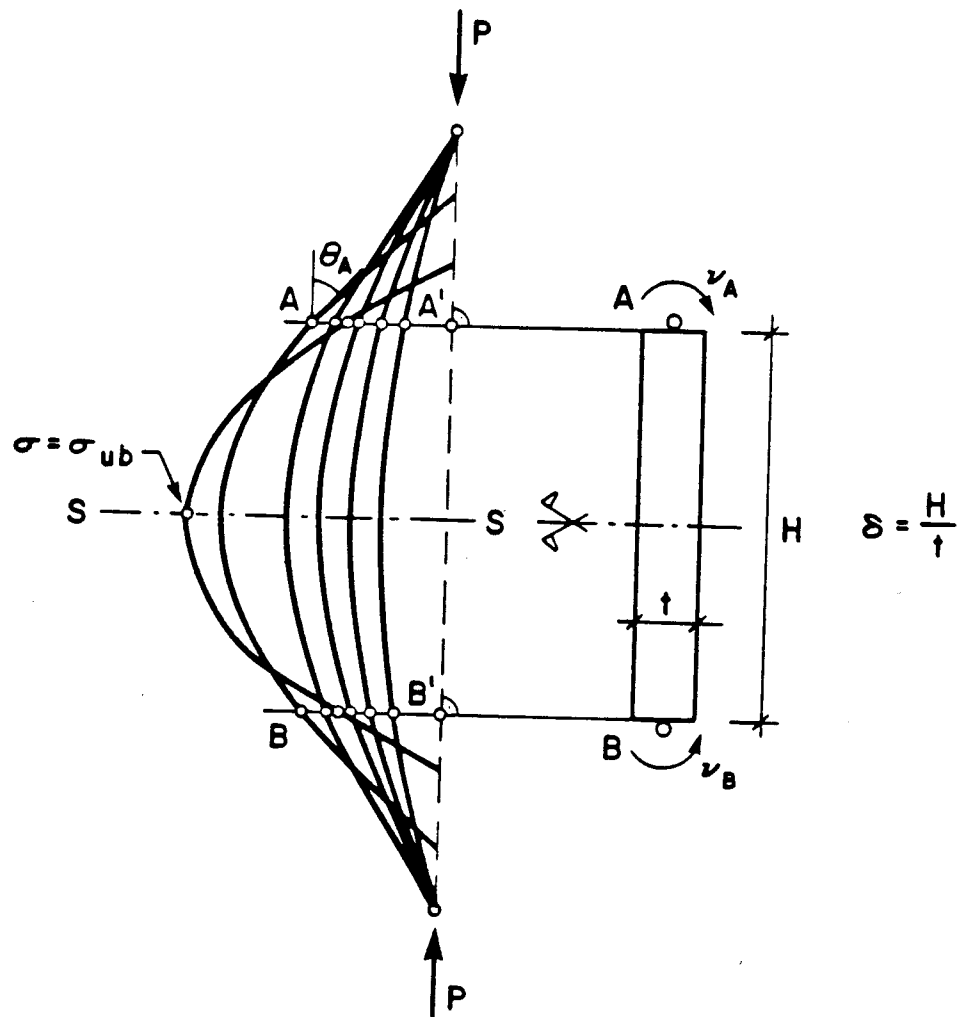


Figure 3.6 Single Curvature Bending with Equal End Eccentricities (Furler, 1981)

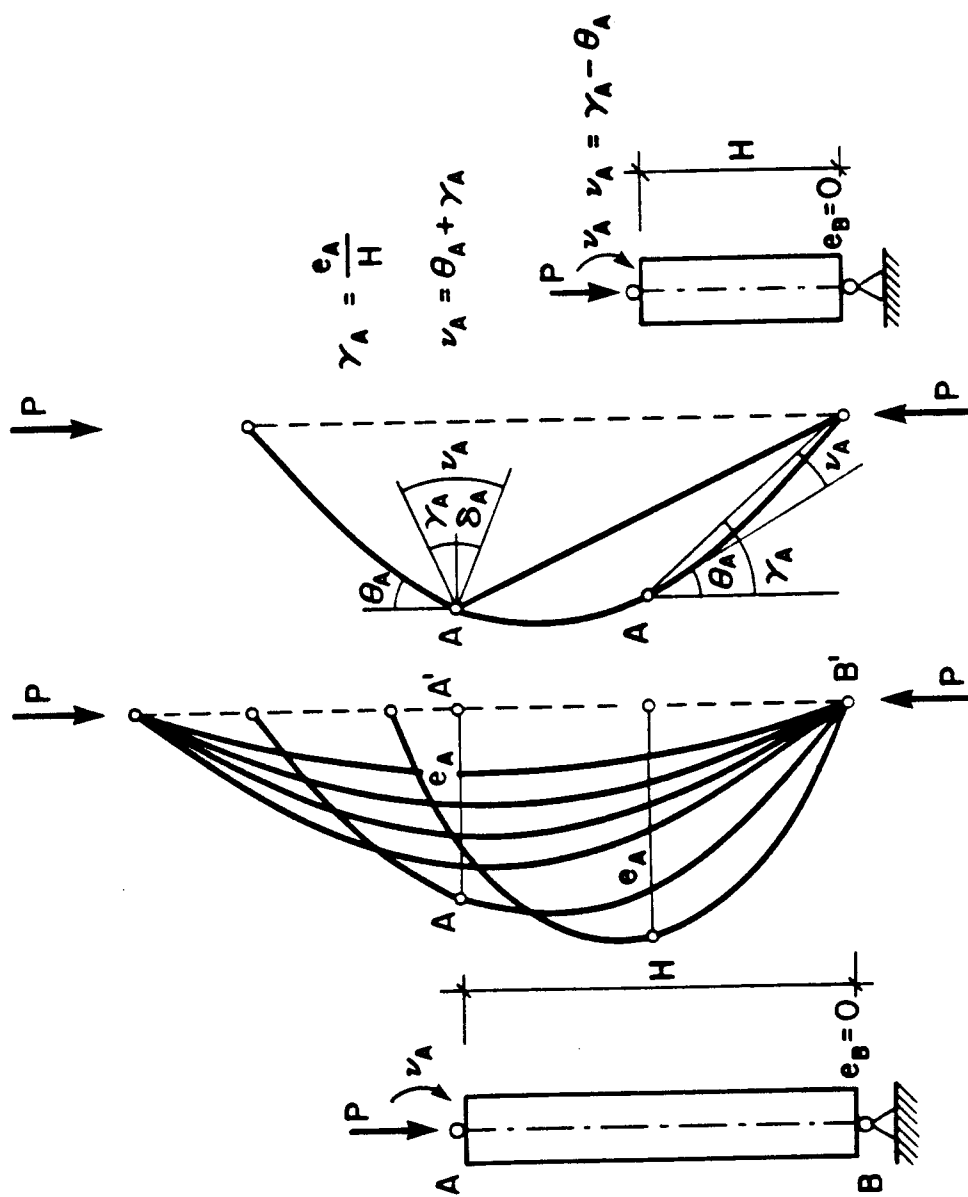


Figure 3.7 Single Curvature Bending with Unequal End Eccentricities (Furler, 1981)

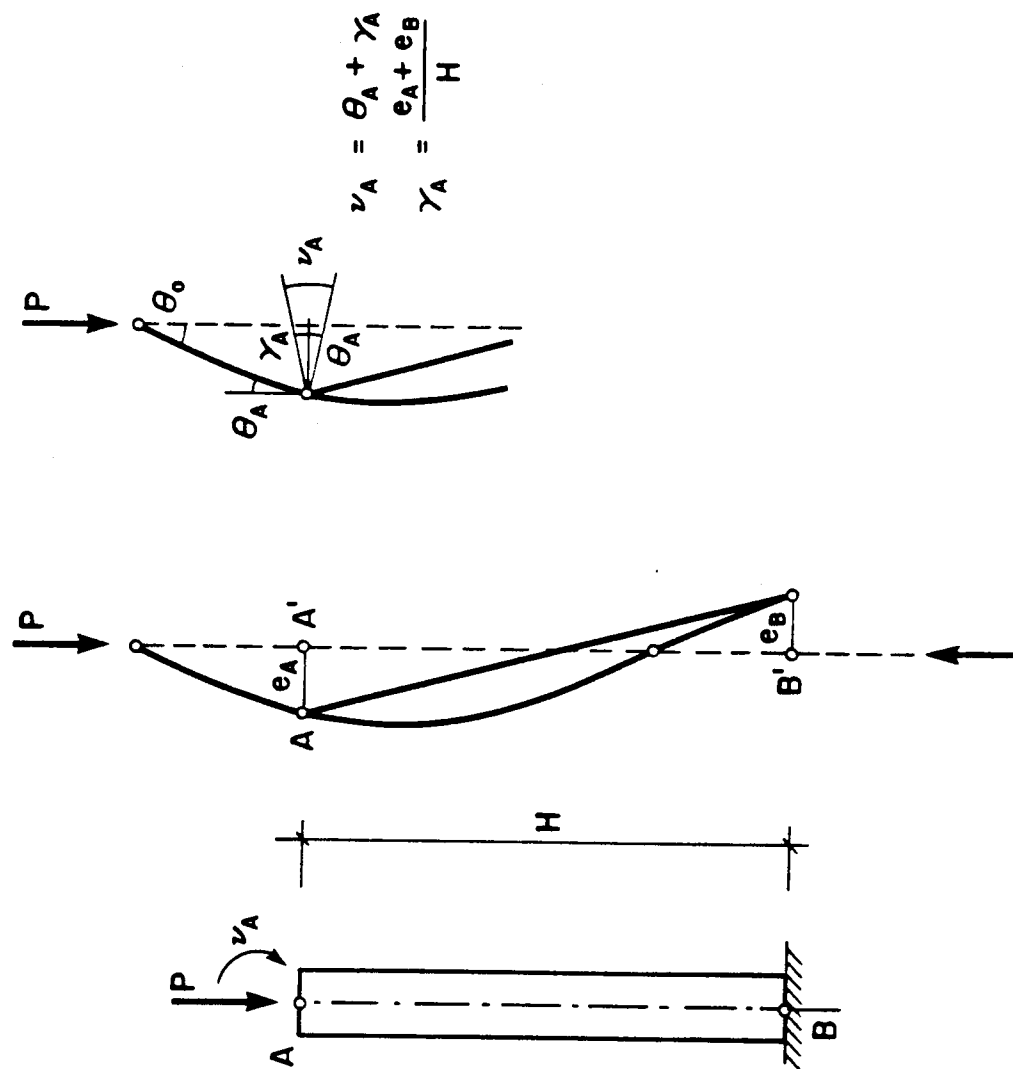


Figure 3.8 Double Curvature Bending (Furler, 1981)

boundary conditions and height. The actual rotation at the end of the wall ν can then be determined geometrically as:

$$\nu_A = \gamma_A + \theta_A = \nu_B \quad (3.3)$$

or

$$\nu_A = \gamma_A - \theta_A = \nu_B \quad (3.4)$$

where $\gamma_A = (e_A - e_B)/H$ or e_A/H depending on the type of curvature; θ_A is the end rotation from the numerical analysis, e_A and e_B are the end eccentricities and H is the height of the wall.

In a simplified building with load carrying walls and loaded slabs, an external wall can usually be divided into two parts separated at the point of inflection as illustrated schematically in Figure 3.9 (Sahlin, 1971). The moment-rotation relationship can thus be obtained for one part consisting of a wall centrally loaded at one end (at the inflection point) and eccentrically loaded at the other end (at the slab end). This configuration corresponds to that shown in Figure 3.7. The masonry walls analysed in this study have similar CDC's but the walls fit below the maximum moment point of the CDCs as shown. Hence, the actual end rotation of each wall is

$$\nu_A = \gamma_A - \theta_A \quad (3.5)$$

and:

$$\gamma_A = \frac{e_A}{H}$$

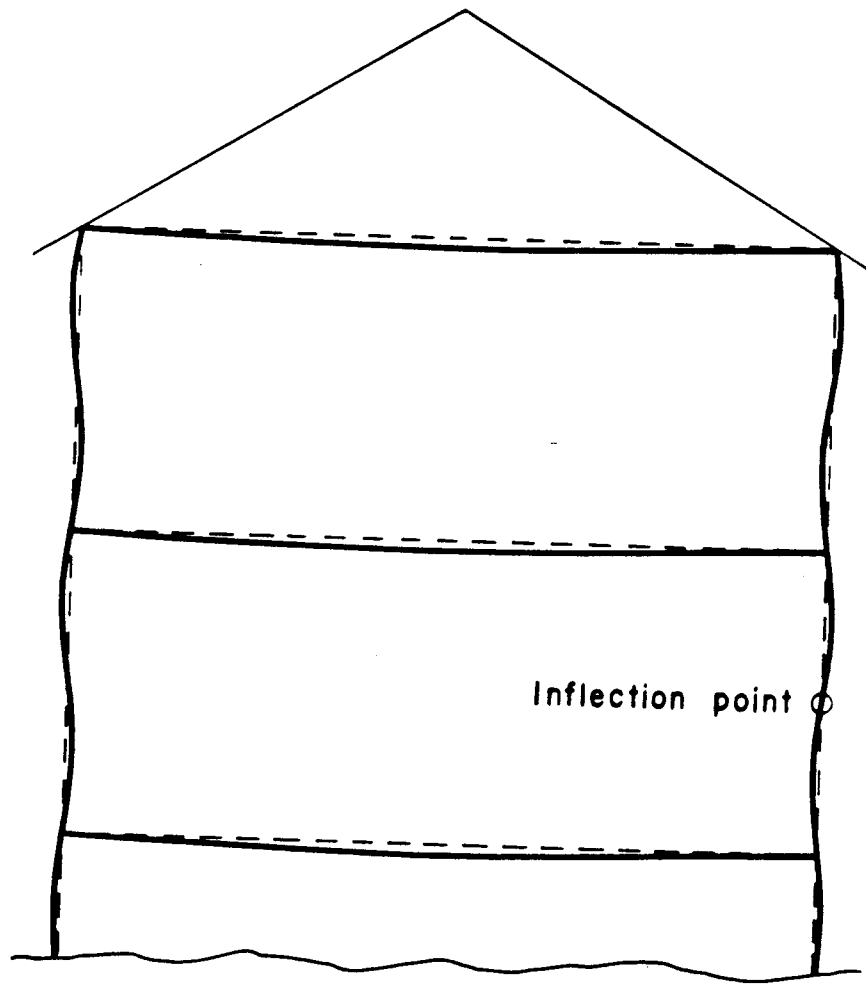
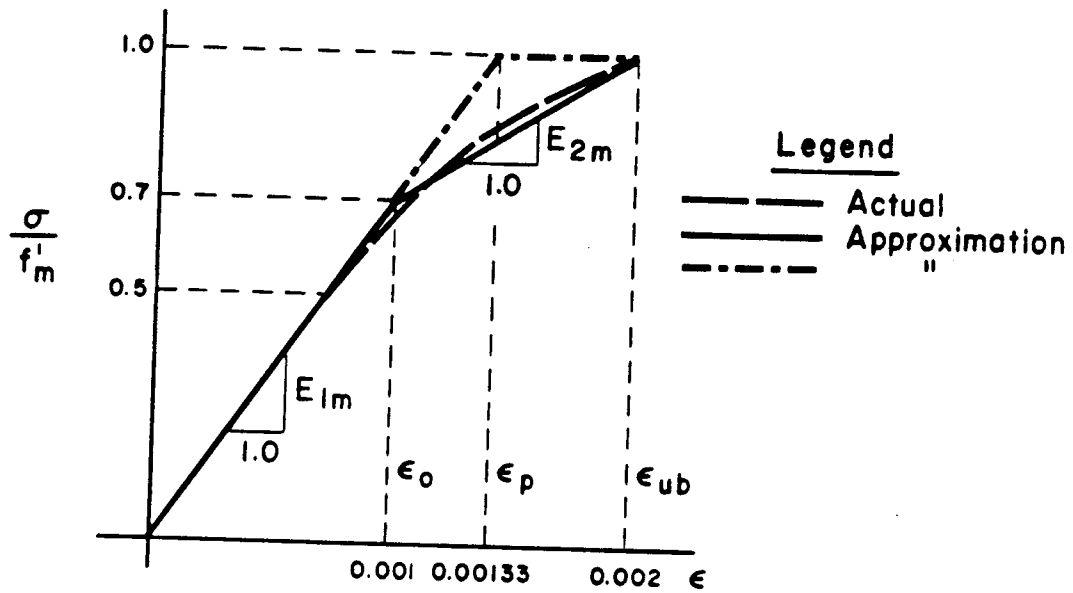


Figure 3.9 Simplified Building with Load Carrying Walls and Loaded Slabs (Sahlin, 1971)

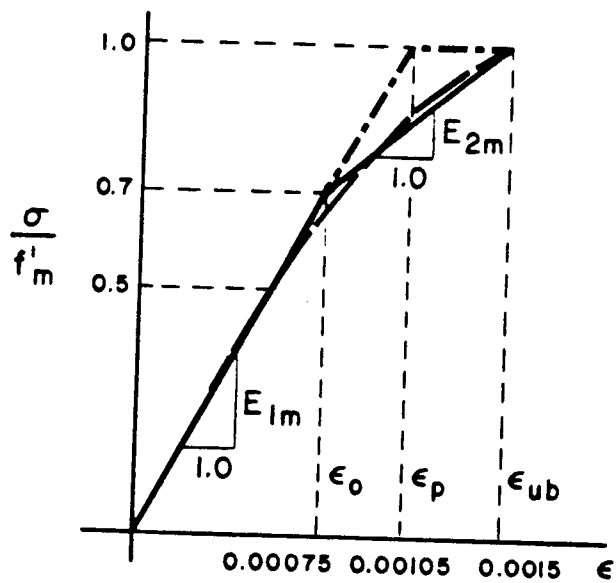
3.1.1.4 Computer Codings

The CDC technique has been coded for computer analysis of the masonry walls as described above. The program contains a $M-\phi t-P$ subroutine that generates an $M-\phi t$ curve for a particular axial load, P , by iterating to convergence at 0.1% error in P . This subroutine is called by a main program which uses one $M-\phi t-P$ curve at a time to generate a series of CDC's for chosen parameters until material failure or instability is reached. Bilinear inelastic stress-strain relations are used to approximate the actual stress-strain relationships for grouted and ungrouted concrete masonry prisms (Yokel et al., 1971; Hamid, 1978). The strain on the cross-section is limited to 0.002 for ungrouted masonry and 0.0015 for grouted masonry. The assumed stress-strain relations for the analysis are shown in Figure 3.10. The cross-sections, nomenclatures and flow charts for the computer program are detailed in Appendix B1. The listing of the program is given in Appendix B2.

Figures 3.11 and 3.12 show the relationship between wall moment and end-rotation obtained using the CDC technique for unreinforced and reinforced walls. The parameter a is the effective wall thickness factor. The total thickness of the hollow cross section is equivalent to $2at$, where t is the total solid section thickness.



(a) Ungrouted Masonry



(b) Grouted Masonry

Figure 3.10 Stress-Strain Relations for Masonry

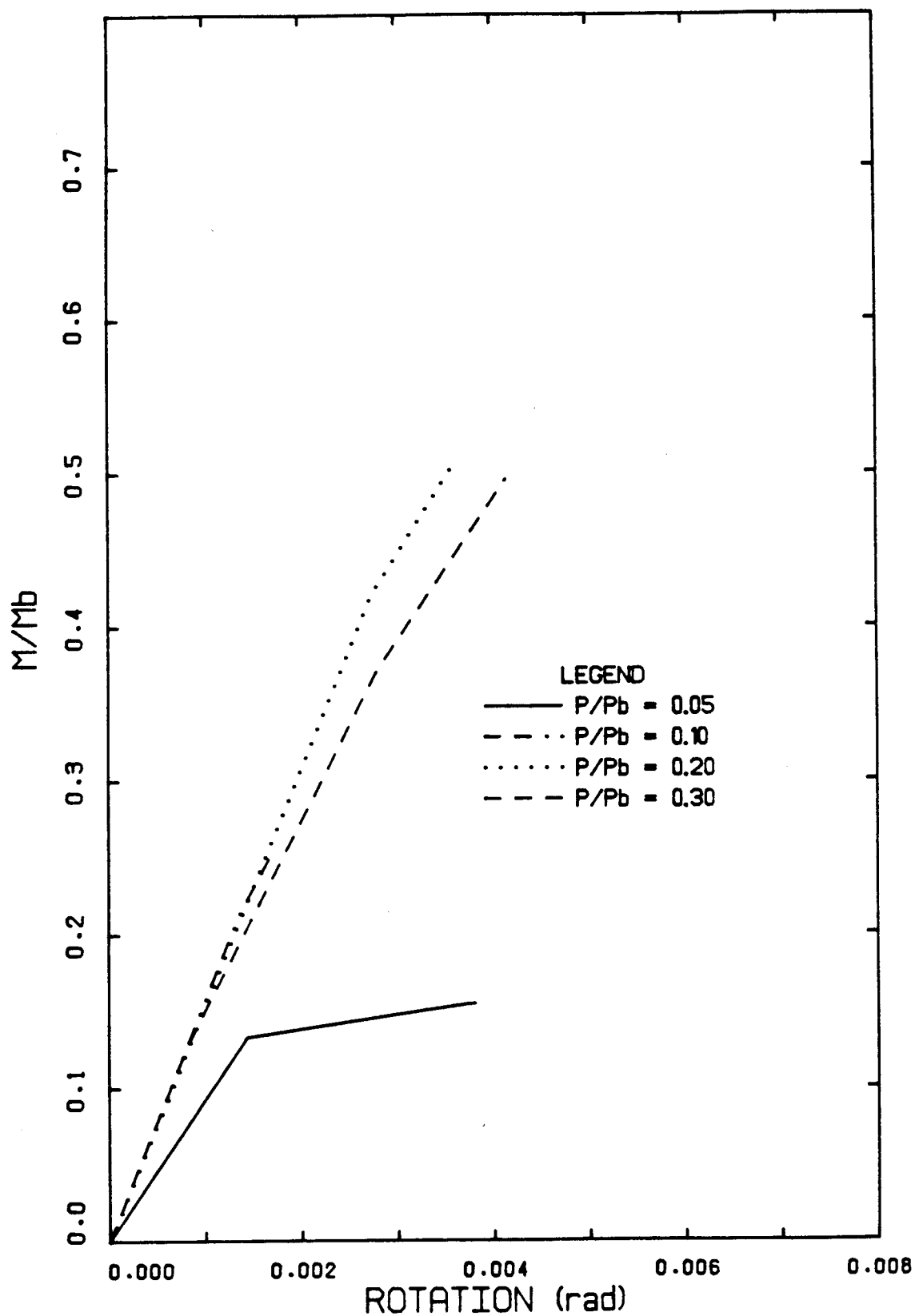


Figure 3.11 Wall Moment-Rotation Curves for Unreinforced Concrete Masonry

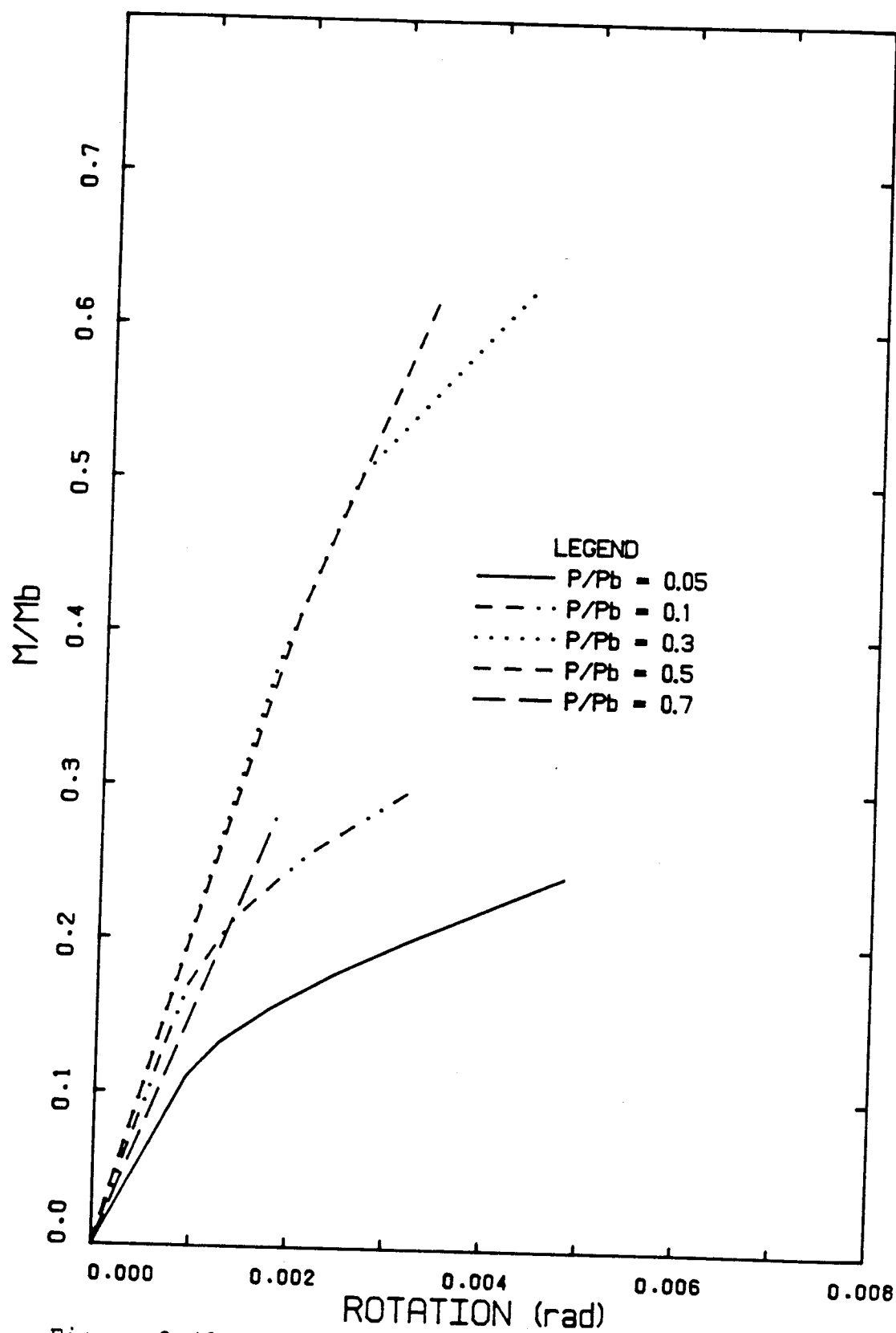


Figure 3.12 Wall Moment-Rotation Curves for Reinforced Concrete Masonry

3.1.2 Interaction Curves

The use of interaction diagrams to predict failure loads for masonry walls under combined axial load and moment is well documented in the literature. The use of a straight line stress-strain diagram gives a simple approach to predicting the lower limit of strength of concrete masonry or brick walls when appropriate parameters from small scale tests are used. To predict strength when significant bending moment is involved (e/t greater than $1/6$), Yokel et al. (1971) observed that the use of a straight line stress-strain diagram with a modification factor, a , applied to masonry ultimate strength, f'_m , correlated better with test results than the use of a rectangular stress block. The term a is a coefficient which depends on the strain gradient in the cross-section at failure. Based on experimental observations (Yokel et al. (1971); Fattal and Cattaneo, 1976), the compressive strength in flexure, af'_m , derived from linear stress distribution in the cross-section at failure exceeded the compressive strength, f'_m , developed in axial compression by a significant margin. The modification factor for f'_m depends on load eccentricity, and Yokel et al. found that it varied between 1.4 and 2.4 at e/t of $1/3$. An average modification factor of 1.54 was suggested by Yokel et al. when e/t exceeds $1/6$. Yokel et al. recommended that the interaction diagram drawn on the basis of af'_m can be completed by a straight line connecting the intersection of the curve with the $e/t=1/6$ line and the maximum value of the axial load on the load axis.

Figure 3.13 shows interaction diagrams for unreinforced 200mm thick walls, using values of modification factor, a , of 1.0, 1.5 and 2.0 applied to prism f'_m . The value of a for hollow masonry wall is taken as 0.28. Figures 3.14 and 3.15 show the interaction diagrams for values of a equal to 0.41 and 0.50 for reinforced walls with three voids and five voids grouted per metre width of wall. Values of gross area vertical reinforcement ratio, ρ_g , of 0.00108 and 0.00374 are assumed with modification factors of 1.0, 1.5 and 2.0 applied to prism f'_m in each case.

3.1.3 Equilibrium Failure Theory

Maurenbrecher (1972) described an 'equilibrium failure' at an unreinforced wall/slab joint as failure resulting in simultaneous separation of the upper and lower walls from the slab (Figure 2.3(a)). Using simple mechanics and assuming equal moments in the upper and lower walls at the joint at failure, the following expression for maximum slab load was derived:

$$\frac{P_{smax}}{P_u} = \frac{t/g}{L + t/(2g)} \quad (3.6)$$

where P_u is the upper wall axial load; P_{smax} is the maximum slab load; L is the distance from the slab load to the center of the wall; t is the wall thickness; h is the slab depth; $g = 1/(1+h/2H)$ and H is the wall height.

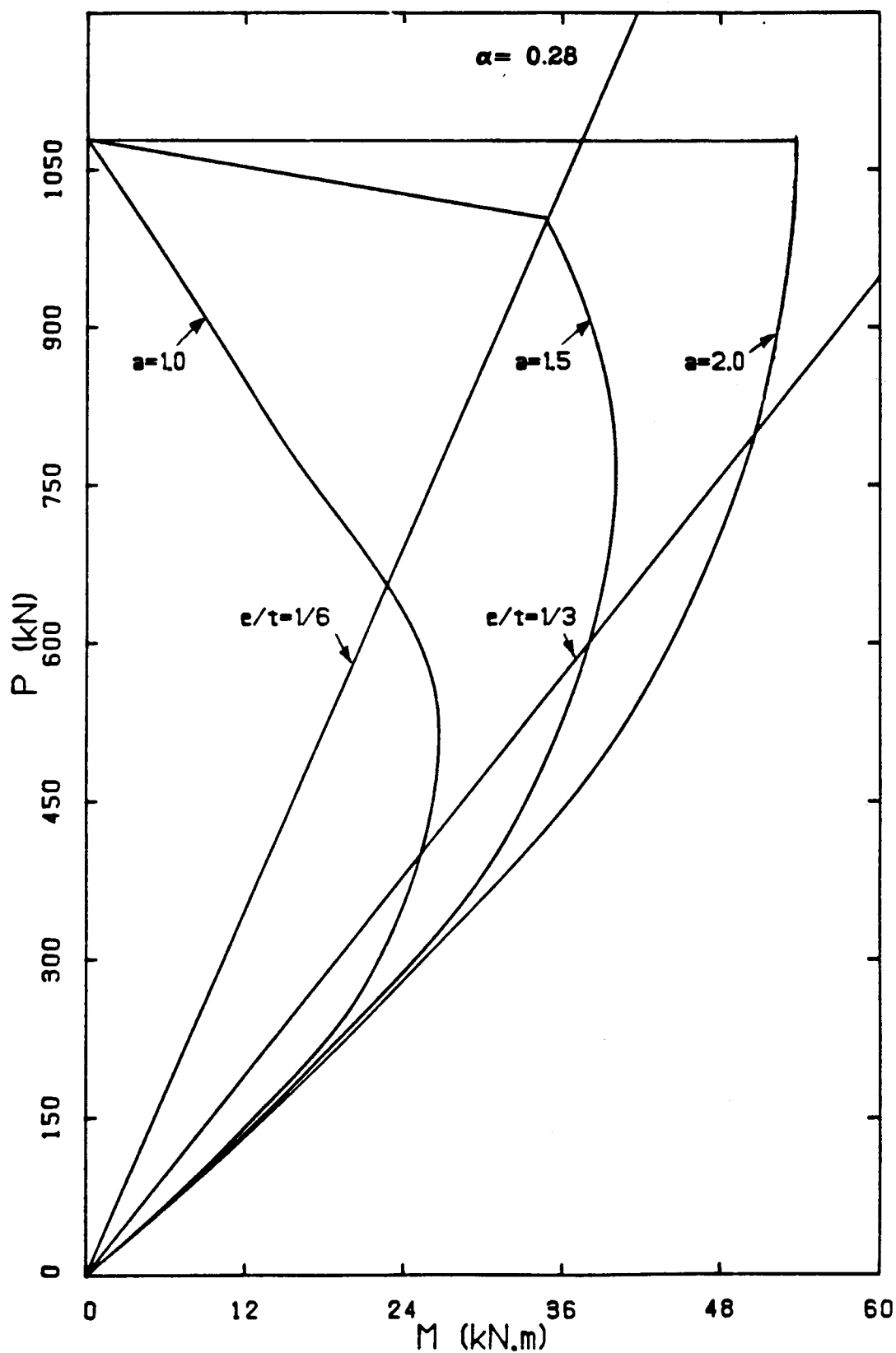


Figure 3.13 Interaction Curves for Unreinforced 200mm Walls

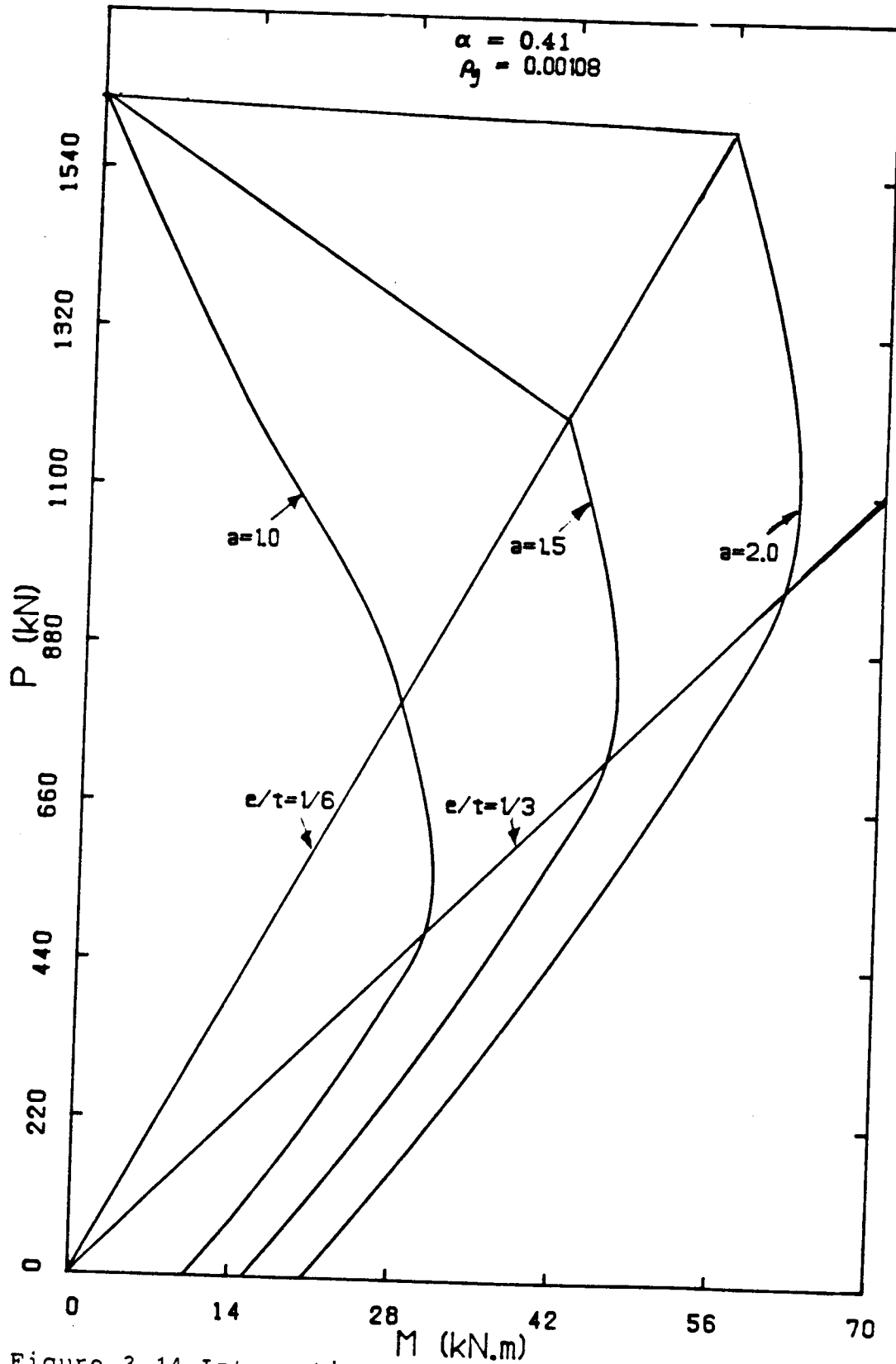


Figure 3.14 Interaction Curves for Reinforced Partially Grouted 200mm Walls

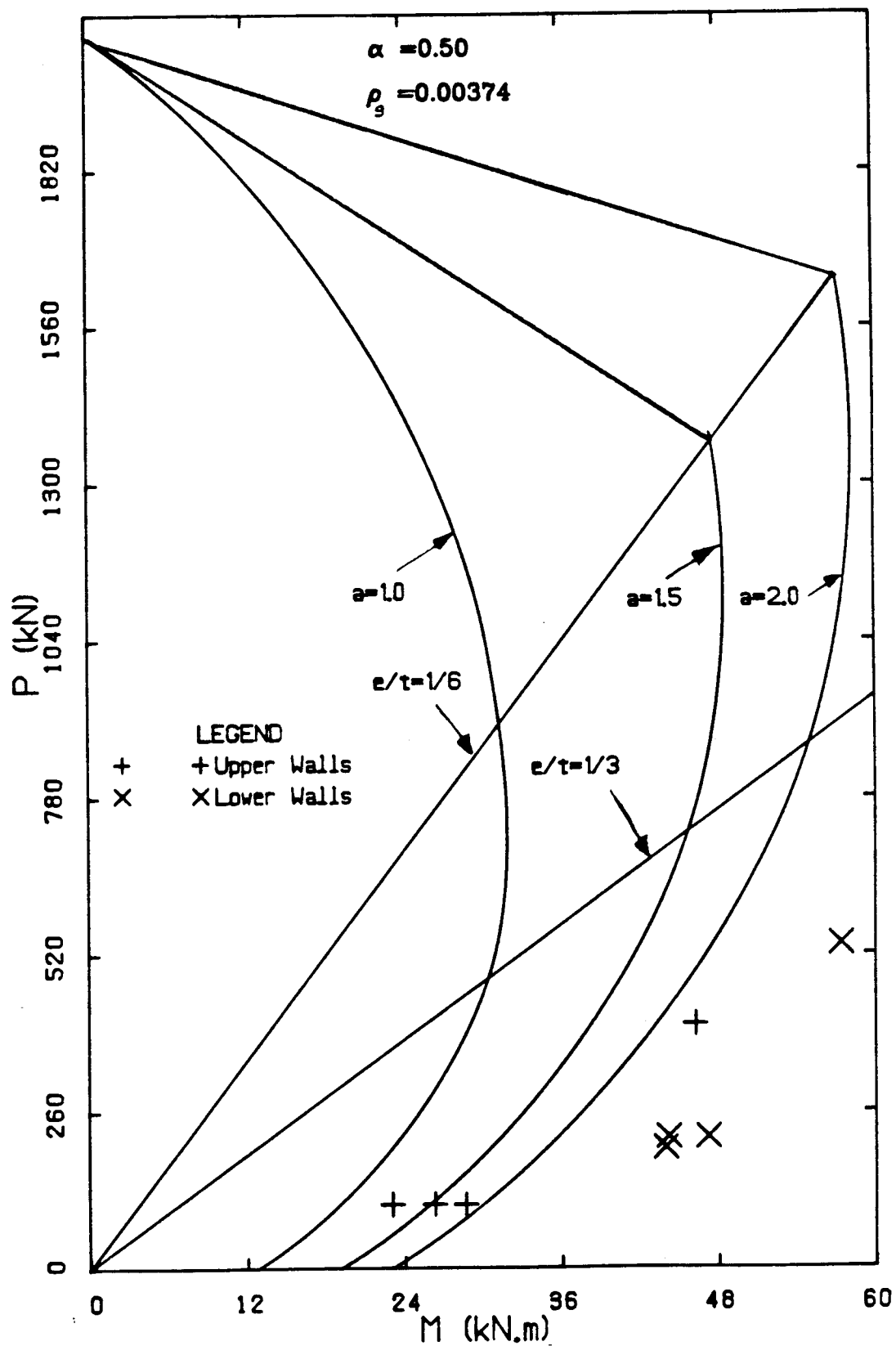


Figure 3.15 Interaction Curves for Reinforced Fully Grouted 200mm Walls

3.2 Strength of a Wall/Slab Joint

Studies of masonry wall/slab joints indicate that the stiffness of a wall at the joint is significantly influenced by the level of axial load on the wall. In fact, the extent of cracking in the wall, which further influences the stiffness, is also influenced by the level of axial load. Another major factor influencing joint strength is the ratio of slab to wall stiffness at the joint.

For estimating stiffness, EI , of a slender masonry wall, Yokel et al. (1971) proposed the following approximate relations:

$$EI = \frac{E_i I_n}{3} \quad (3.7)$$

when section cracking is not a very significant factor.

or

$$EI = E_i I_n (0.2 + P/P_b) \leq 0.7 E_i I_n \quad (3.8)$$

when section cracking is significant.

E_i is the initial tangent modulus of elasticity; I_n is the moment of inertia of the uncracked net section; P is the axial load on the wall; and P_b is the short wall axial compressive load capacity. Fattal and Cattaneo (1976) reported that Equation 3.8 in the region of $P/P_b > 0.50$ was a good approximation for brick prisms, but underestimated the EI for eccentrically loaded block prisms.

In a study of buckling loads of concrete masonry walls Hatzinikolas in 1978 proposed that for eccentrically loaded

reinforced or unreinforced concrete masonry the following equation may be used for estimating wall stiffness, EI:

$$EI = 2E_m I_n (1/2 - e/t) \quad (3.9)$$

where E_m is the modulus of elasticity of masonry, recommended by Hatzinikolas as $750f'_m$; e is the eccentricity of loading; and t is the wall thickness. Equation 3.9 is found to give conservative estimates of EI when e/t is large (Ferguson, 1979 and Pacholok, 1980).

The effect of the ratio of slab to wall stiffness, β , on the maximum joint moment can be determined from standard structural analysis or approximated by the following equation (Salvadori and Levy, 1967):

$$M_R = \frac{3M_F}{3 + 2\beta} \quad (3.10)$$

where M_R is the rigid frame moment and M_F is the fixed end moment resulting from the applied loads.

The problem of wall limit strength at the joint is then reduced to that of finding the effect of wall axial load on upper and lower wall stiffnesses, provided the joint precompression is adequate. A rational determination of the upper and lower wall effective stiffnesses at the limit of joint moment can lead to provisions for design of the walls at a wall/slab joint. This aspect is further discussed in Chapter 6.

4. EXPERIMENTAL PROGRAM

4.1 Introduction

The experimental program was designed to provide additional data on concrete masonry simple wall/slab joints at lower wall precompression. Frame type specimens were designed to provide some replicates, and also to provide the additional benefit of testing full span slabs. For these reasons, four full-scale wall/slab joints (Type I Specimens) and two H-type wall/slab frames (Type II Specimens) were tested. Axial load on the walls varied from a low of 100 kN/m to a high of 400 kN/m, corresponding to two-and-half to ten storeys of gravity loads in usual loadings and spans.

The specimen dimensions were chosen so as to simulate half-storey walls above and below a slab based on the assumption of a point of inflection at mid-height of wall in double curvature bending. Elevation views and dimensions of the specimens are shown in Figures 4.1 and 4.2.

All slabs were 200 mm thick and 1000 mm wide. The total length of the cantilever slabs was 1000 mm, giving a distance of 850 mm from slab load application to the center of the wall. The slabs of Type II specimens had a total length of 5075 mm with a distance center-to-center of walls of 4675 mm.

4.2 Materials and Material Properties

All test specimens were built from commercially available materials, typical of those commonly used in masonry building construction in Edmonton.

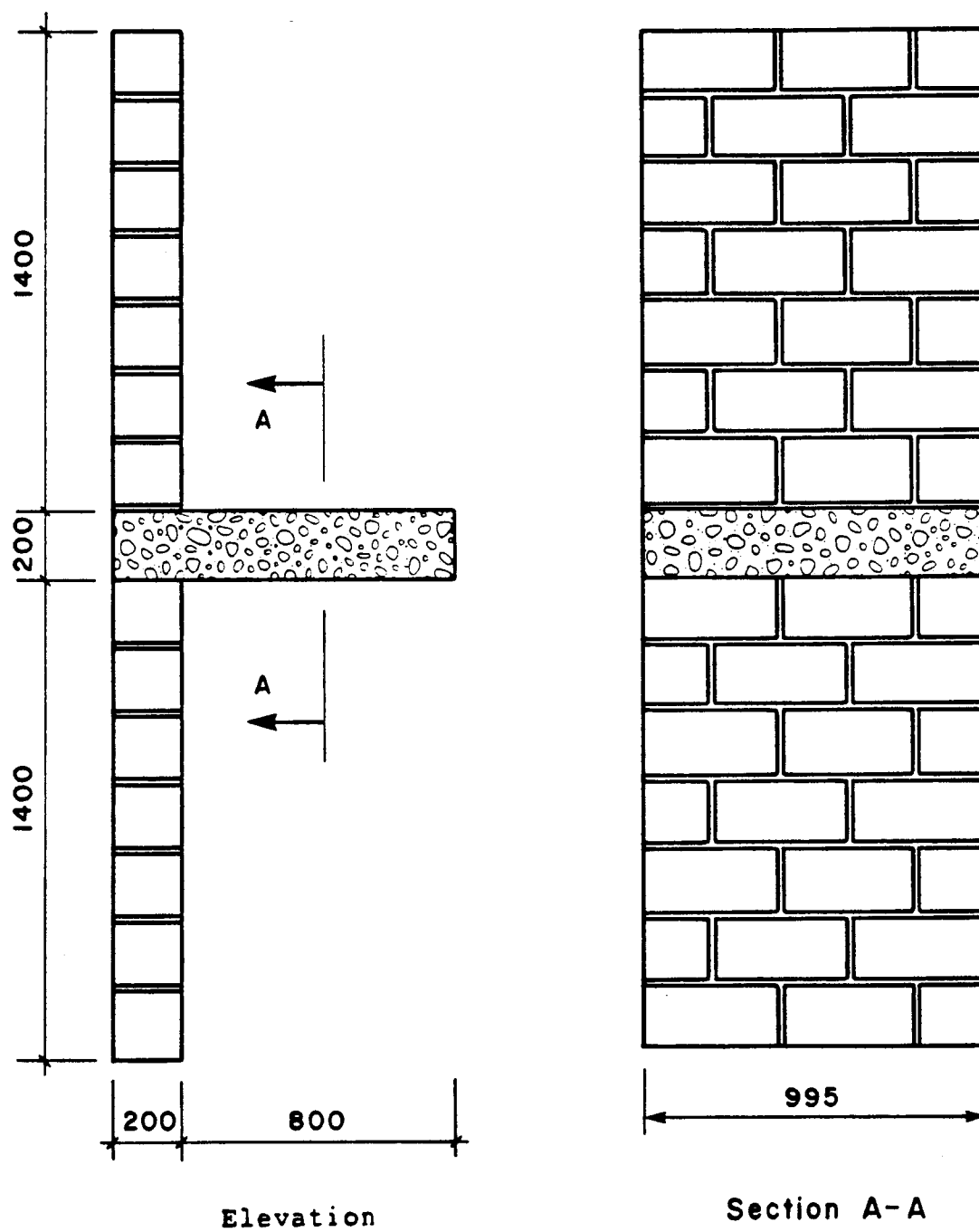


Figure 4.1 Type I Specimen

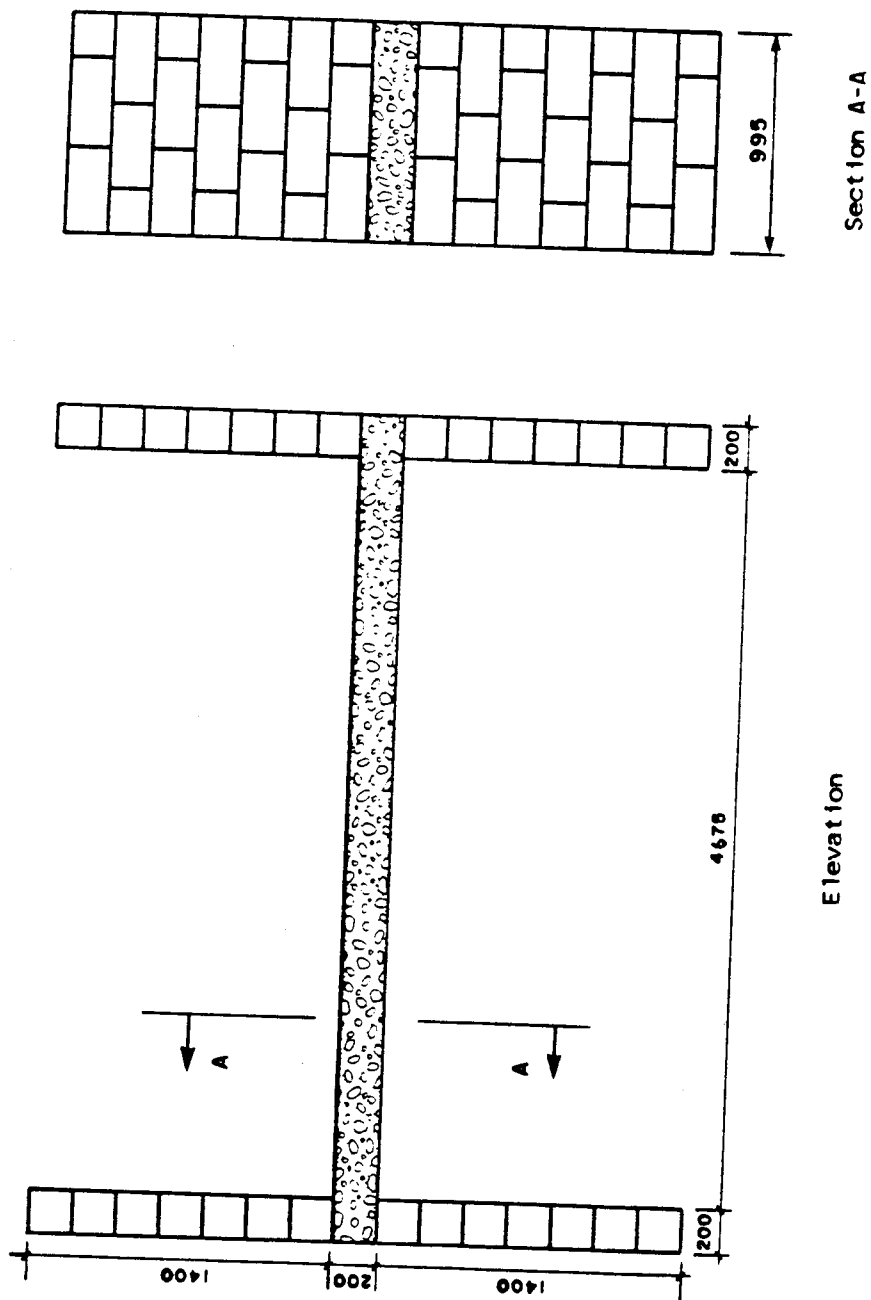


Figure 4.2 Type II Specimen

4.2.1 Concrete Block Units

The standard units used in the construction of all specimens were nominally 200 mm x 200 mm x 400 mm stretcher blocks, 200 mm x 200 mm x 400 mm corner blocks, and 200 mm x 200 mm x 200 mm half blocks. The units are shown schematically in Figure 4.3. Five of each unit type were measured and tested in compression in the MTS machine. Some standard-corner units (standard format at one end, corner format at the other) were mixed with the normal standard and corner units. The results showed that strength variation from one unit type to the other could be significant. The average compressive strength of all the 15 units are summarized in Table 4.1.

4.2.2 Mortar

Type S mortar mixed in accordance with CSA standard A179M - 1976 was used in all specimens. The mix proportions by volume were 1 part normal Portland cement, 1/2 part hydrated lime and 4 parts masonry sand. The mortar was mixed in an electric mixer to a job site consistency, with water added as necessary. A total of 34 - 50 mm mortar cubes were made during construction of the test specimens. Eleven cubes were soaked in lime until tested, in accordance with CSA Standard A179M-1976. The remaining 23 were cured similarly to the wall specimens i.e. air-dried. All mortar cubes were tested at 28 days. Table 4.2 shows the results of the lime-soaked mortar tests.

Table 4.1 Properties of Concrete Masonry Units

Masonry Unit	Actual Dimensions		Minimum Face Shell thickness mm	Gross Area mm	Net Solid %	Compressive Strength		Moisture Content %
	Width mm	Length Height mm				Gross Area MPa	Net Area MPa	
200mm Standard	190.6	392.3	191.3	74760	56	7.53	13.94	1.10
200mm Corner	191.2	392.5	190.9	75050	56	10.61	19.64	0.49
200mm Half	191.4	191.1	192.0	36512	56	7.84	14.51	0.99
						X		15.46
						S		3.03
						V		0.20

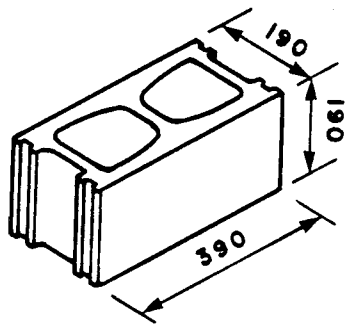
Table 4.2 Mortar Test results

Mortar ID	Crushing Load	Compressive Strength	Type
	KN	MPa	
MC01	23.50	9.40	Lime Saturated
MC02	23.20	9.28	Lime Saturated
MC03	23.75	9.50	Lime Saturated
MC04	32.60	13.04	Lime Saturated
MC05	29.00	11.60	Lime Saturated
MC06	27.50	11.00	Lime Saturated
MC07	25.00	10.00	Lime Saturated
MC08	27.00	10.80	Lime Saturated
MC09	28.50	11.40	Lime Saturated
MC10	29.00	11.60	Lime Saturated
MC11	21.00	8.40	Lime Saturated

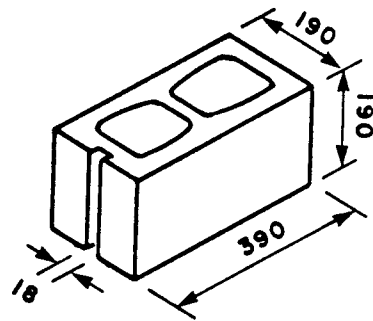
\bar{X} 10.54

S 1.35

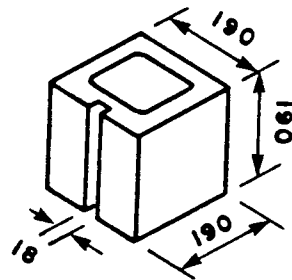
V 0.13



20 cm Standard



20 cm Corner



20 cm Half

Figure 4.3 Concrete Block Units

4.2.3 Grout

The grout mixture was proportioned using 10 mm pea gravel, normal Portland cement and concrete sand. The mix proportions by weight were 1 part Portland cement, 3.92 parts sand, 2.78 parts pea gravel, and a water cement ratio of 1. These proportions are in accordance with CSA-A179M-1976. Ten grout cylinders were cast and tested at 28 days to determine the grout strength. The specimens were grouted in two batches, with 5 grout specimens taken from each batch. The results from the grout tests are shown in Table 4.3. The lower strength of the grout, compared to the unit strength, may be attributed to the non-absorbent moulds used in grout sampling.

4.2.4 Concrete

All slabs were cast on the same day using the same batch of ready mixed concrete with a specified slump of 100 mm to 150 mm and a specified minimum 28 day strength of 25 MPa. The maximum aggregate size was 20 mm. A total of 12 - 150 mm concrete test cylinders were also cast and were tested in accordance with CSA Standard CAN3-A23.2-M77. Results of the concrete tests are given in Table 4.4.

4.2.5 Reinforcing Steel

20M deformed bars were used as tension reinforcement in the slabs. 10M bars were used as stirrups and as slab distribution steel. 15M bars were used as vertical reinforcement in the walls. All reinforcing bars were from the same heat and had a minimum specified yield strength of

Table 4.3 Grout Test results

Grout ID	Crushing Load	Compressive Strength	Type
	kN	MPa	
GL01	177.50	10.04	First Batch
GL02	190.25	10.77	First Batch
GL03	175.00	9.90	First Batch
GL04	167.50	9.48	First Batch
GL05	172.50	9.76	First Batch
GL06	215.00	12.16	Second Batch
GL07	260.00	14.71	Second Batch
GL08	250.00	14.14	Second Batch
GL09	205.00	11.60	Second Batch
GL10	205.00	11.60	Second Batch

\bar{X} 11.42

S 1.82

V 0.16

Table 4.4 Concrete Test results

Concrete ID	Crushing Load kN	Compressive strength MPa
CS01	507.50	28.71
CS02	510.00	28.86
CS03	490.00	27.72
CS04	508.00	28.75
CS05	505.00	28.58
CS06	455.00	25.75
CS07	490.00	27.72
CS08	505.00	28.58
CS09	520.00	29.42
CS10	526.00	29.77
CS11	507.50	28.72
CS12	510.00	28.86

\bar{X} 28.44

S 1.03

V 0.04

400 MPa. No joint reinforcement was used in any of the walls. Table 4.5 shows the average properties of the reinforcing bars.

4.2.6 Prisms

Eight single block prisms and eight one-and-half block prisms, each three blocks high as shown in Figures 4.4 and 4.5, were built at the same time as the full-scale specimens using the same techniques as for the walls. Four fully grouted prisms and four ungrouted prisms were built and tested for each type of wall specimen.

The ungrouted prisms generally failed by tensile splitting occurring first on the sides, and then spalling of the face shell. The grouted prisms failed by splitting initially at the faces followed by complete separation of the grout from the units at failure. Plate 4.1 shows the typical failure of an ungrouted prism.

The ungrouted prisms which were $1\frac{1}{2}$ blocks wide produced the lowest average net compressive strength of 7.4 MPa while the highest average net compressive strength of 10.7 MPa was attained by the grouted single block prisms. The overall average compressive strength of all prisms was 8.8 MPa. Table 4.6 gives a summary of the prism test results.

Table 4.5 Properties of Reinforcing Bars

Reinforcing Bar	Yield Stress MPa	Yield Strain mm/mm	Ultimate Stress MPa	Young's Modulus MPa
10M	425	0.00261	640	192 300
15M	400	0.00208	665	194 200
20M	400	0.00210	677	195 000

Table 4.6 Prism Test Results

Prism ID	Crushing Load kN	Net Area Compressive Strength MPa	Type
PA101	369.1	9.20	UngROUTed, Type I
PA102	419.3	10.45	UngROUTed, Type I
PA103	351.2	8.73	UngROUTed, Type I
PA104	246.3	6.14	UngROUTed, Type I
PA201	481.2	7.92	UngROUTed, Type II
PA202	451.9	7.44	UngROUTed, Type II
PA203	421.6	6.89	UngROUTed, Type II
PA204	450.0	7.41	UngROUTed, Type II
PB101	855.3	11.48	Grouted, Type I
PB102	640.3	8.62	Grouted, Type I
PB103	887.3	11.94	Grouted, Type I
PB104	807.4	10.87	Grouted, Type I
PE201	1040.7	9.24	Grouted, Type II
PE202	851.4	7.59	Grouted, Type II
PE203	1002.3	8.90	Grouted, Type II
PE204	893.4	7.94	Grouted, Type II

\bar{X} 8.80
 S 1.67
 V 0.19

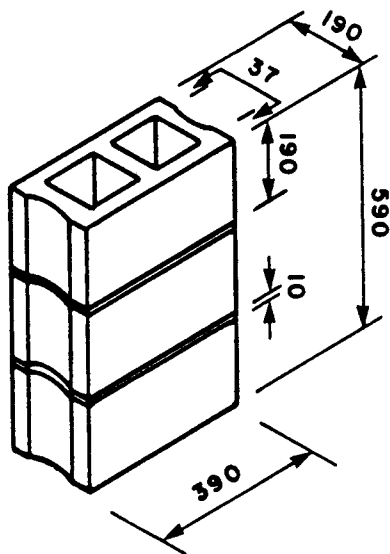


Figure 4.4 Type I Prism

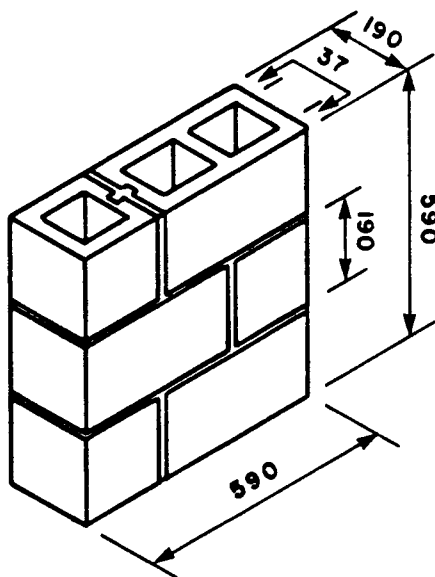


Figure 4.5 Type II Prism



Plate 4.1 Typical Failure of Ungrouted Prism

4.3 Masonry Properties

4.3.1 Compressive Strength

4.3.1.1 Unit-Mortar Method

The ultimate compressive strength of the concrete block masonry at 28 days, f'_m , was determined by the Unit-Mortar method described in Clause 4.3.3 of CSA Standard S304-M78. Using the average compressive strength of 15.5MPa for the 15 units tested and Type M mortar, the value of f'_m obtained from Table 3 of CSA Standard S304 was 10.2 MPa.

4.3.1.2 Prism Test Method

The Prism Test method for determining f'_m is described in Clause 4.3.4 of CSA Standard S304-M78. The h/t value for all prisms was 3.16. Using the overall average compressive strength of 8.80 MPa for the prisms and a correction factor of 1.2 for h/t of 3 from Table 1 of CSA S304-M78, the compressive strength of masonry was found to be equal to 10.5 MPa.

It is observed that the values of f'_m obtained here correlates very closely with that obtained by the Unit and Mortar method, despite the difference in the grout and unit strengths.

4.3.2 Stress-Strain Relationship

Figures 4.6 and 4.7 show the stress-strain relationship obtained for ungrouted and grouted concrete masonry prisms. Strain measurements indicated high lateral expansion on both

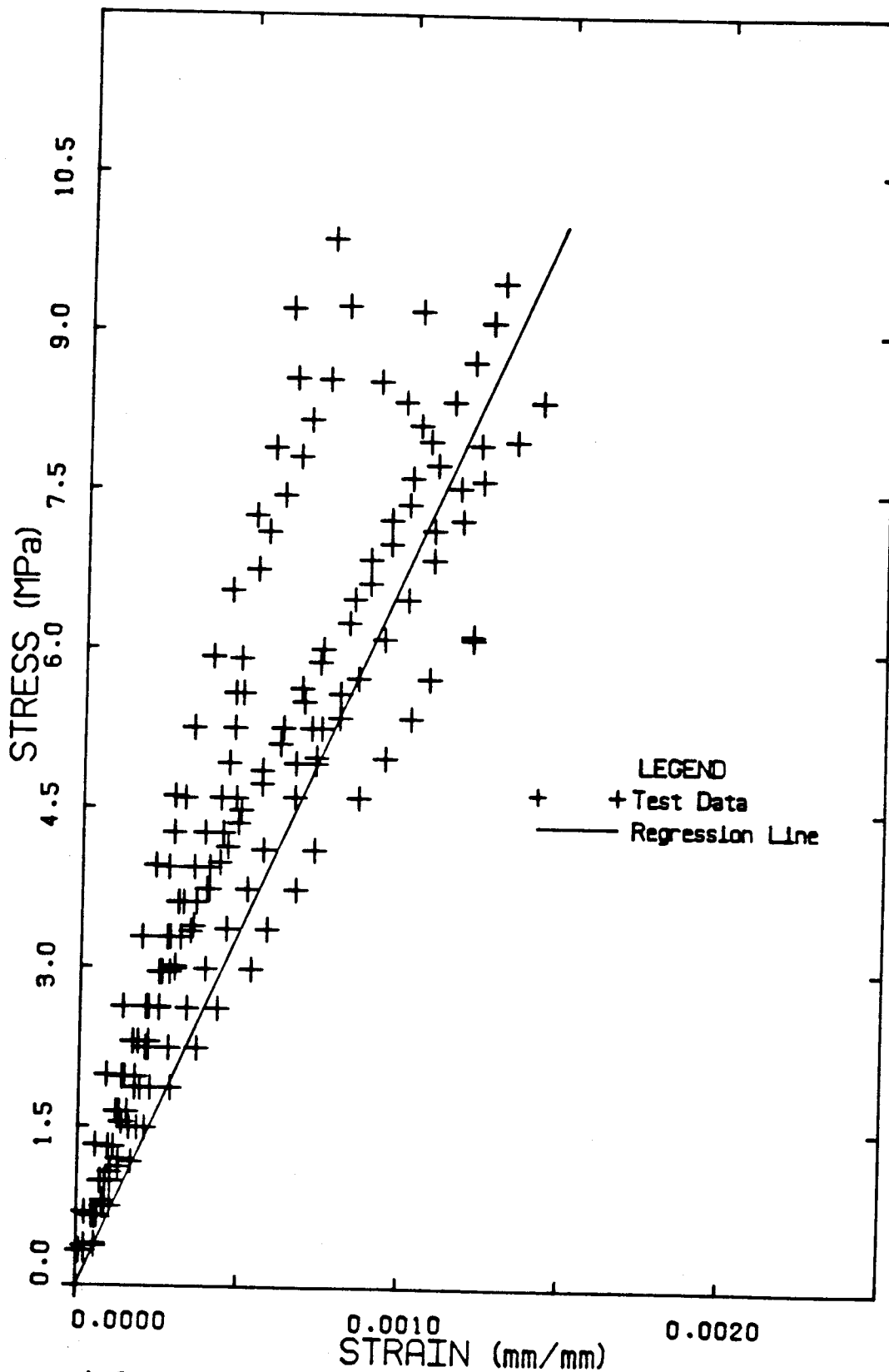


Figure 4.6 Stress-Strain Relationship for UngROUTED Concrete Masonry Prisms

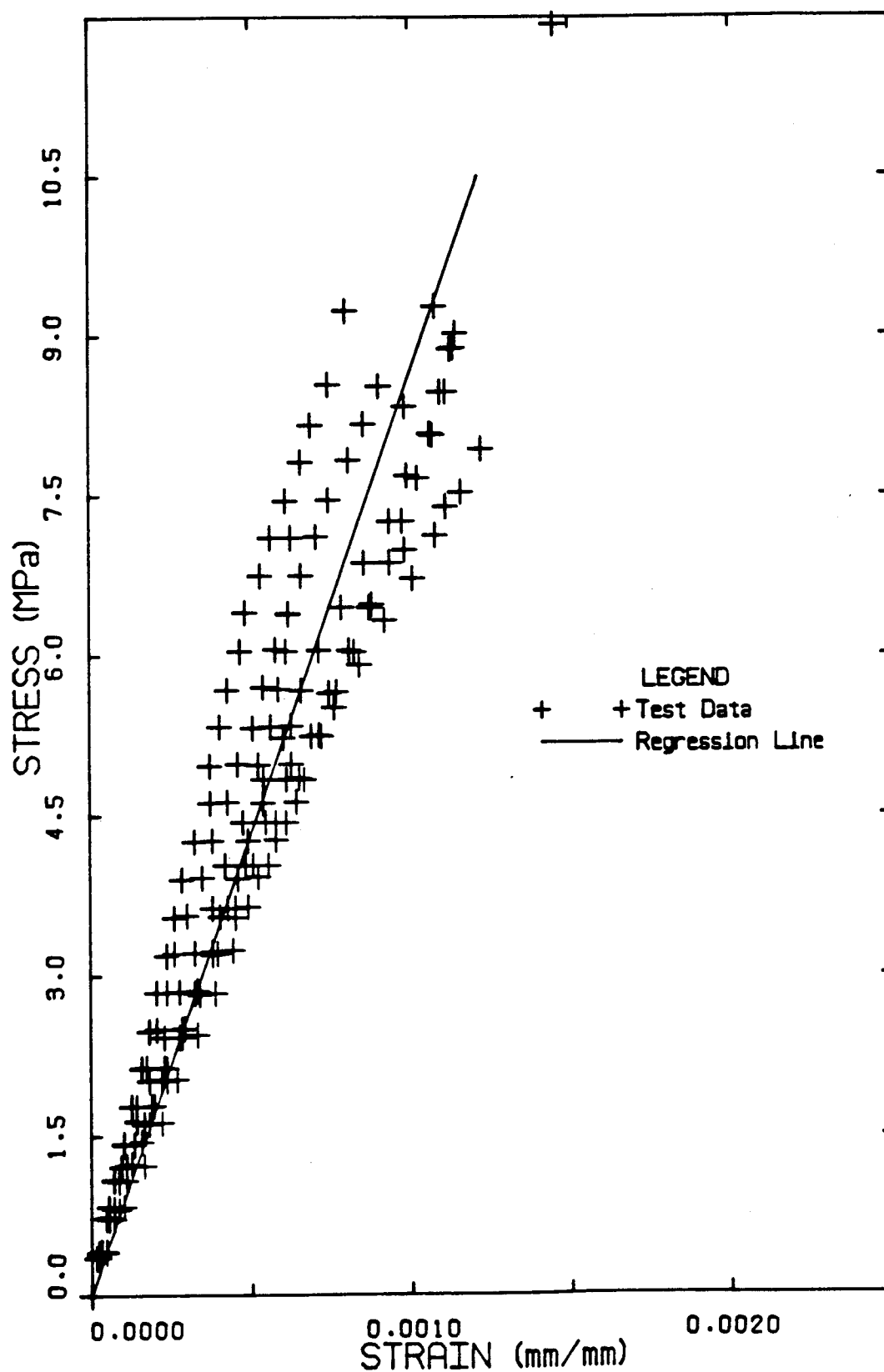


Figure 4.7 Stress-Strain Relationship for Grouted Concrete Masonry Prisms

sides of the ungrouted prisms. Strain measurements could only be taken up to approximately 70% maximum load for the ungrouted prisms, whereas measurements could be taken up to 90% maximum load or more for the grouted prisms. This difference was due to the more sudden failure of ungrouted prisms. From a linear regression analysis of the data, the modulus of elasticity was $770f'_m$ for the ungrouted prisms and $960f'_m$ for the grouted prisms.

4.4 Construction of Full-Scale Specimens

The full-scale specimens were constructed and cured in the laboratory for a duration of approximately two months before testing.

All walls were constructed by an experienced mason using techniques typical of good workmanship with supervision. Each course of the wall consisted of one standard, one corner block and one half block in running bond. The bed and head joints were of 10 mm face shell mortar cut flush and then tooled. The mason kept the outer face of the wall in alignment using horizontal line and level. Two Type I and one Type II specimens had reinforcement in the walls with all cores fully grouted. The specimen details are given in Table 4.7.

The construction procedure for a typical Type I specimen was as follows:

1. The first course was laid on fresh mortar placed on paper on the laboratory floor. This course included clean out holes for the reinforced walls or was fully grouted for the unreinforced walls.

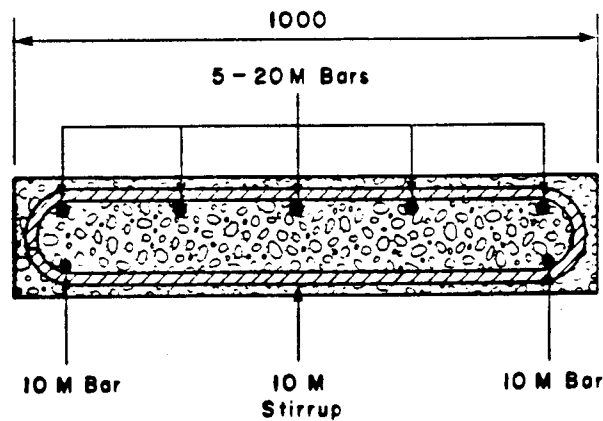
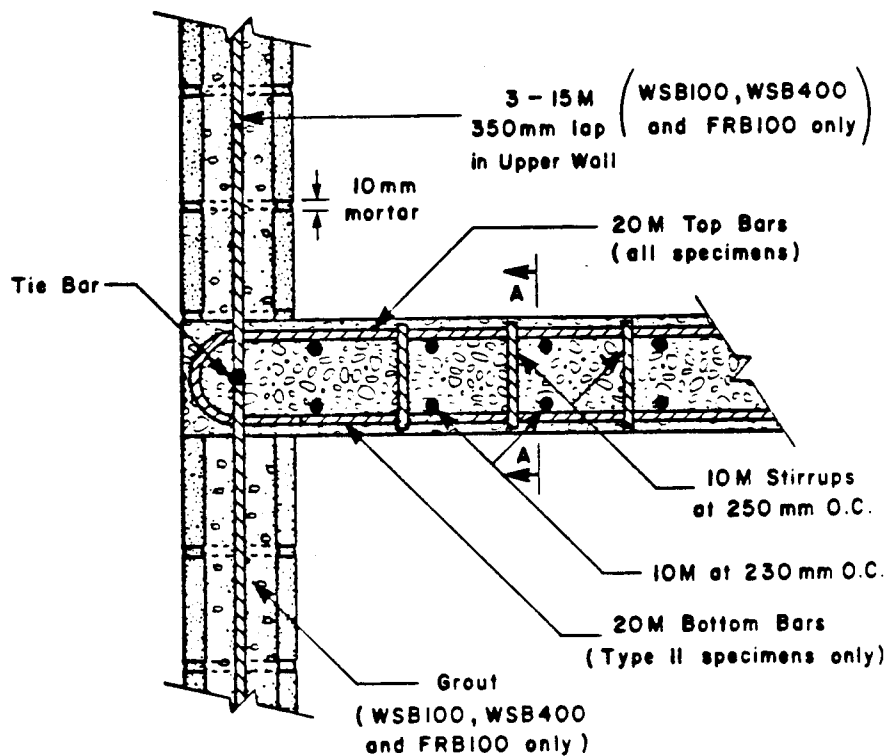
Table 4.7 Details of Full-Scale Specimens

Specimen	Grouting	Reinforcement		
		Wall	Slab	Stirrups
WSA100	UngROUTed	None	4-20M	3-10M
WSA400	UngROUTed	None	6-20M	3-10M
FRA150	UngROUTed	None	3-20M T 4-20M B	12-10M
WSB100	Grouted	3-15M	5-20M	3-10M
WSB400	Grouted	3-15M	8-20M	3-10M
FRB100	Grouted	3-15M	4-20M T 7-20M B	12-10M

2. The next six courses were then constructed. For the unreinforced walls, styrofoam pieces were placed in the sixth course from the bottom of the wall to allow only one course to be filled with slab concrete. The reinforced walls had reinforcement placed in three alternate cores before grouting all cores solid up to the sixth course from the bottom of the wall.
3. The slab forms were erected 7 days after the lower walls were constructed.
4. The slab reinforcement was placed; slab concrete was poured and vibrated, then covered with polyethylene sheets for 7 days.
5. The top seven courses were laid on the slab after 24 hours of curing and reinforcement was placed in those walls designated for reinforcement.
6. All seven courses in the reinforced walls were grouted solid, but only the top and bottom courses in the unreinforced walls were grouted.

The only difference in the construction of Type II specimens was that the walls were built on the end fixtures used in the test set-up.

All slabs were reinforced so as to ensure failure in the wall prior to slab failure. The reinforcing bars were terminated with U-bends providing minimum cover in the slab to prevent slab end shearing during testing. Nominal stirrups were placed in the slabs to act as shear reinforcement. The reinforcement details at a typical joint and in the slabs of Type II specimens are shown in Figures 4.8 and 4.9 respectively.



Section A - A (WSB100)

Figure 4.8 Typical Joint Reinforcement Details

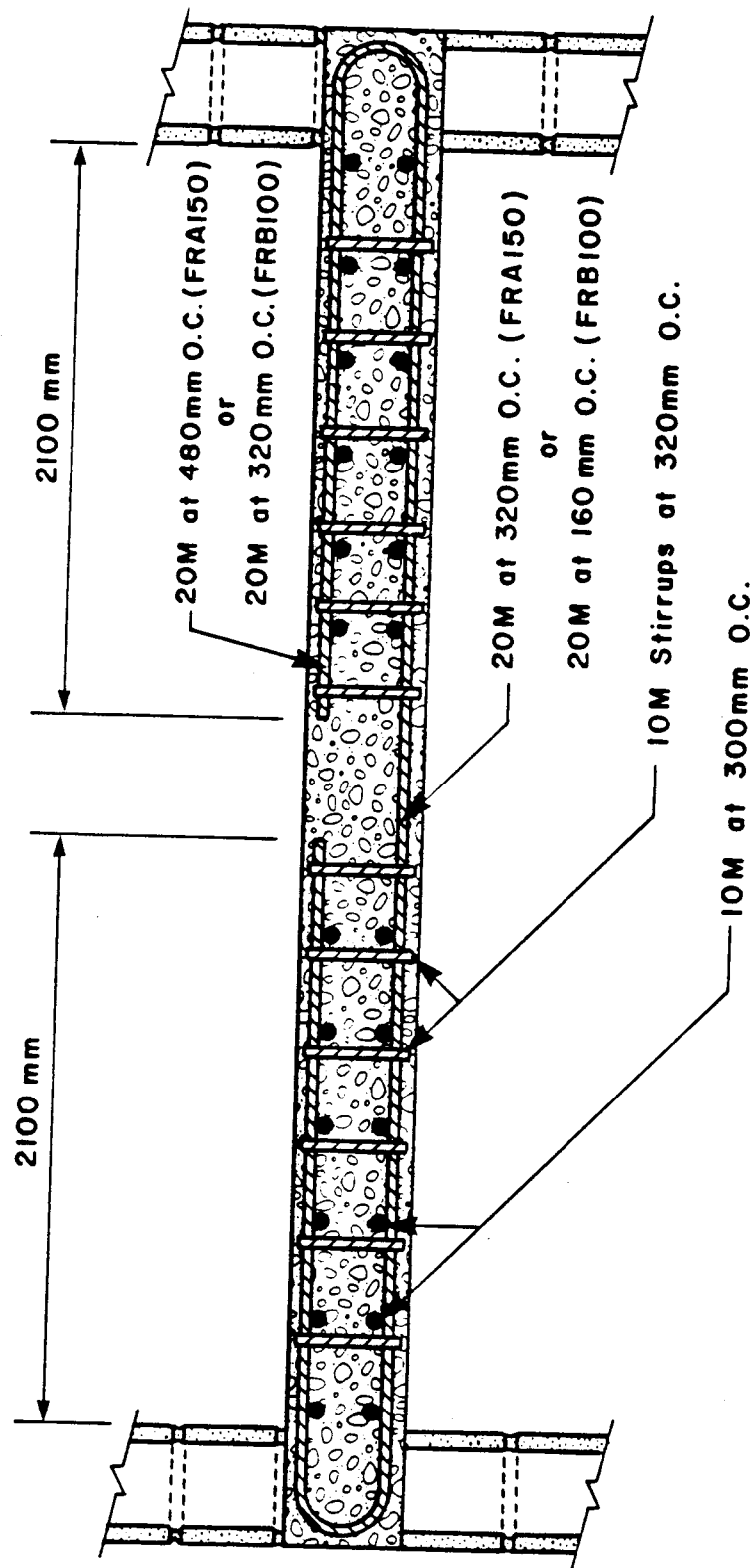


Figure 4.9 Slab Reinforcement Details for Type II Specimens

4.5 Test Set-Up

The MTS hydraulic testing machine with a capacity of about 6.7×10^4 N in compression, and capable of maintaining a preset load to ± 40 N was used for applying compression load to the prisms and the walls of Type I specimens. The compression load on the full-scale specimens was applied through a channel-roller system weighing 2.1 kN. Figure 4.10 shows the loading arrangement for Type I specimens.

The vertical load on the cantilevered slabs was applied through two jacks, each having a capacity of 100 kN. for Type I specimens. The jacks were anchored to the laboratory strong floor and load was applied through an assembly below the slab. The assembly consisted of two channels transmitting the load through 4 high tensile rods to two HSS sections placed at the edge of the slab. The slab load was applied at a distance of 850 mm from the centerline of the wall. Two tension load cells of 90 kN capacity each were placed between the jacks and the Channels below the slab. Figure 4.11 shows the slab loading details. Steel angles at the top of the wall and at the wall/slab joint provided lateral restraint perpendicular to the plane of the wall.

Type II specimens were tested in the location where they were constructed. A test frame consisting of steel columns and built-up beams was constructed for the purpose of applying precompression load to the walls and preventing sidesway movement of the wall/slab frame. The wall loads were applied by two 1800 kN capacity hydraulic jacks. The air driven motor hydraulic system used to operate the jacks for applying wall loads to Type II specimens and all the

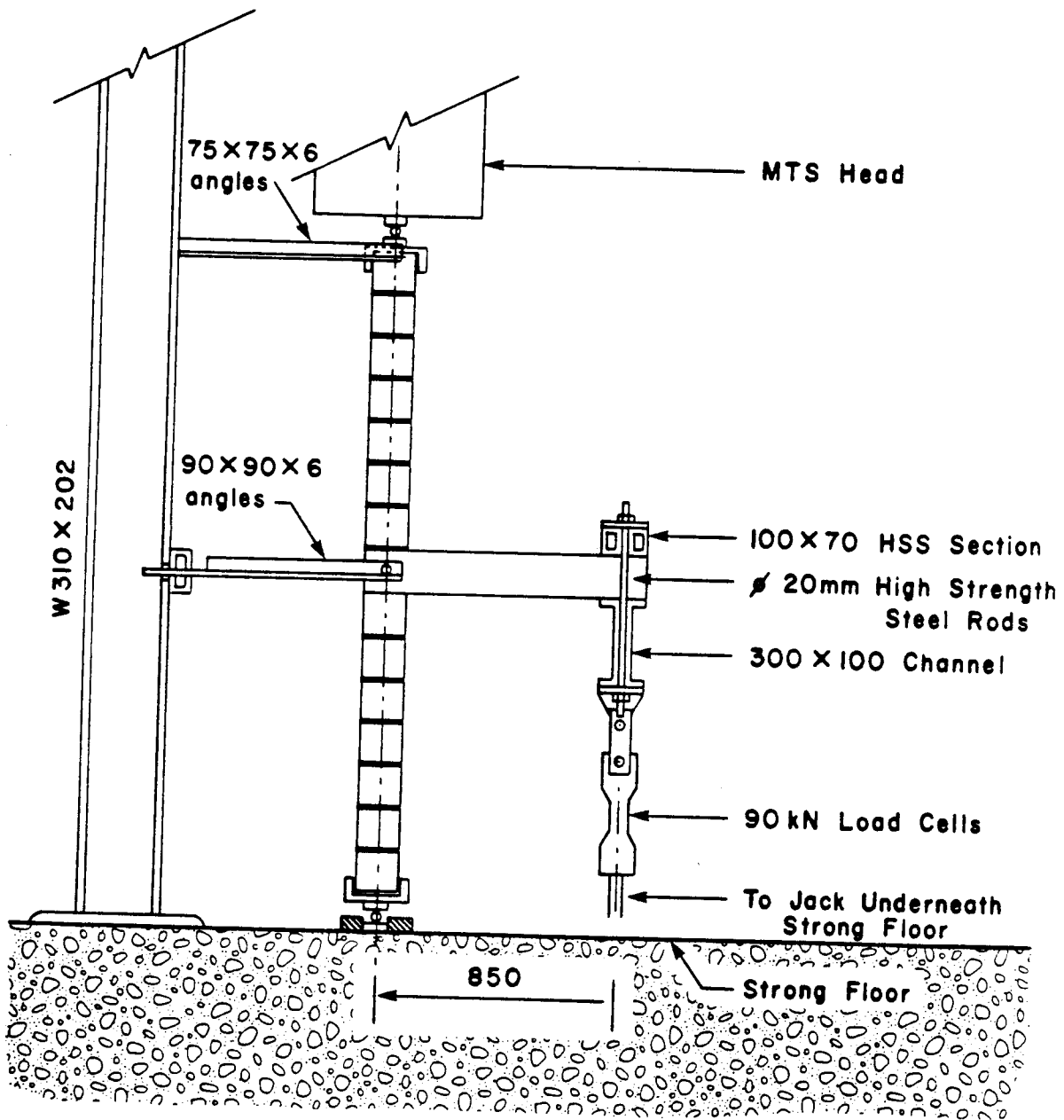


Figure 4.10 Loading Arrangement for Type I Specimens

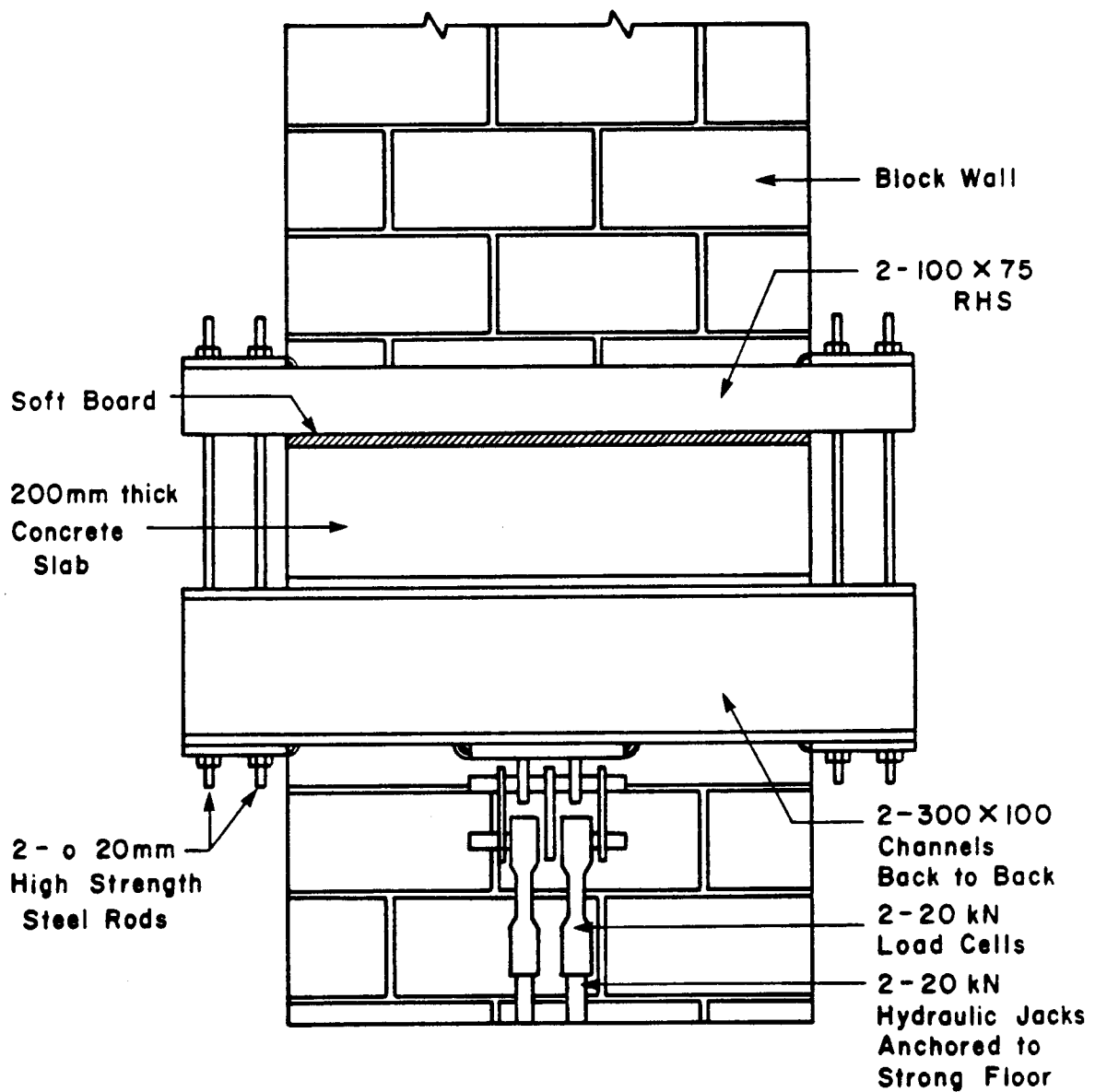


Figure 4.11 Slab Loading Apparatus for Type I Specimens

slab loads was accurate to $\pm 1\%$. The slab was line loaded at two points spaced 1200 mm apart and symmetrical about the centerline of the slab. The line loads were applied through two 270 kN hydraulic center pull rams. The line loading arrangement was similar to that used for Type I specimens. A 45 kN capacity jack was positioned at each end of Type II specimens to prevent sideways. Load cells were attached to these jacks to measure the sideways forces. Figure 4.12 shows the elevation view of the loading arrangement. Plate 4.2 shows a partial view of the test set-up.

4.6 Instrumentation

4.6.1 Prisms

Vertical deformations were monitored by the movement of the MTS machine head. For a more accurate vertical strain measurement, a Demec gauge was used to measure strains across two mortar joints. Measurements were made on each face of the prisms over a length of 254 mm between a pair of Demec points. Figure 4.13 shows the instrumentation of the prisms.

4.6.2 Full-Scale Specimens

Instrumentation for Type I specimens is as shown in Figure 4.14. Vertical deformations of the walls were monitored using the MTS machine. Horizontal deflections were measured at each of the two courses above and below the slab, at the mid-height and on the top and bottom courses of the wall. LVDT's measuring to an accuracy of $1/40$ mm or $1/80$

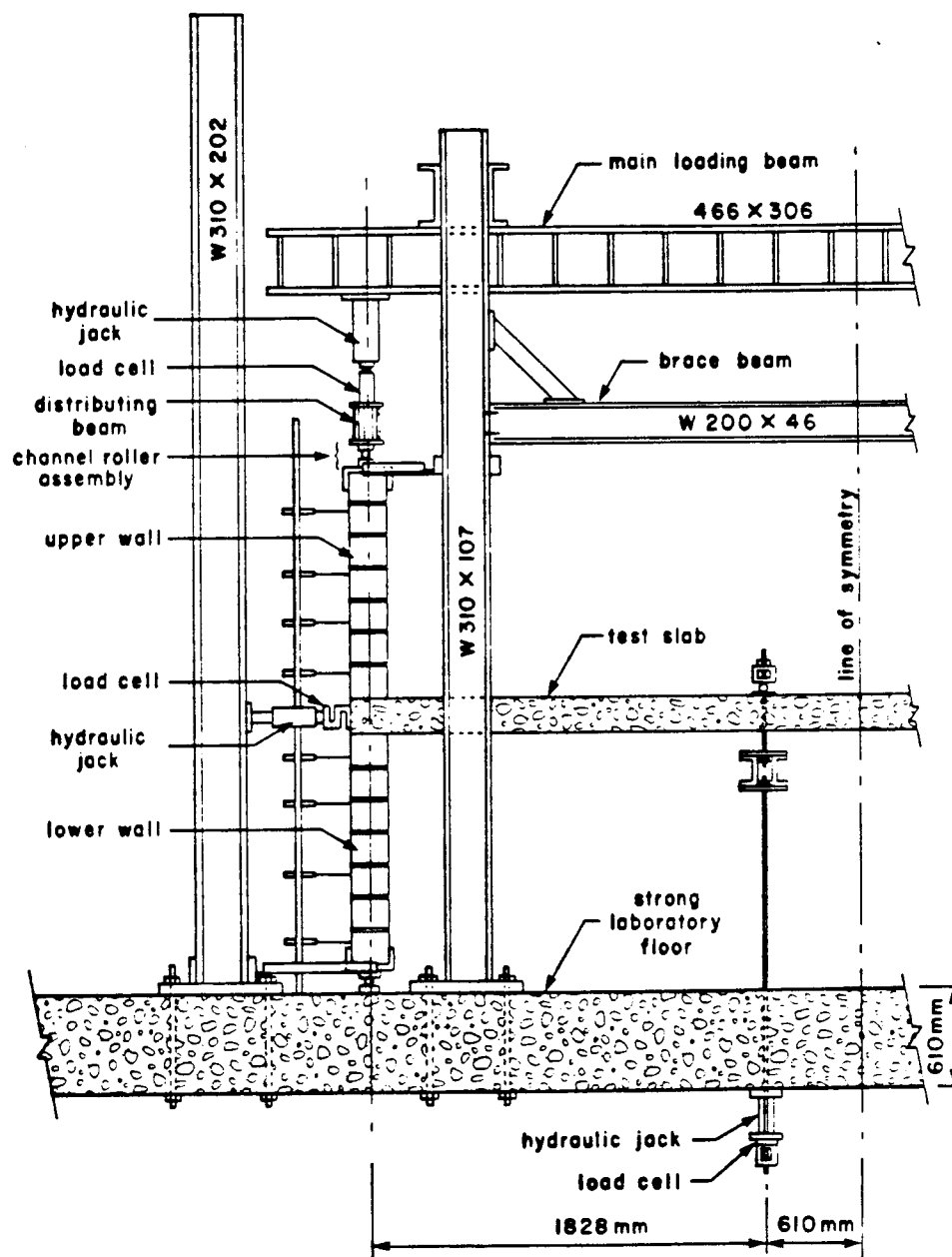
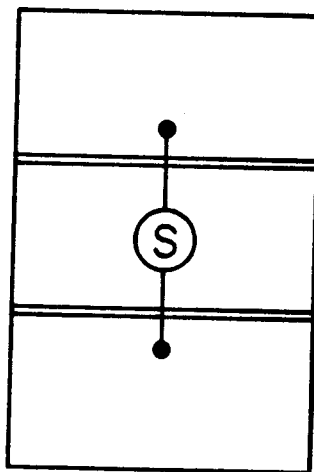
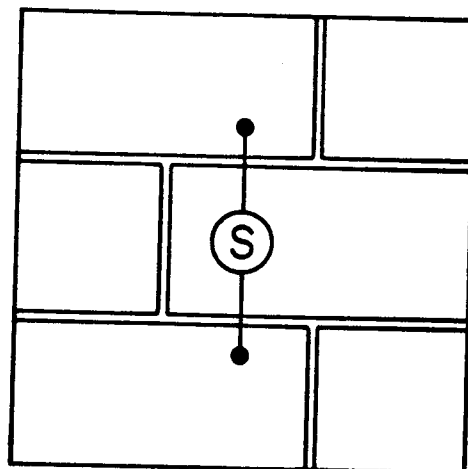


Figure 4.12 Elevation View of Loading Arrangement for Type II Specimens



(a) Type I Prism



(b) Type II Prism

Figure 4.13 Location of Demec Points on Prisms

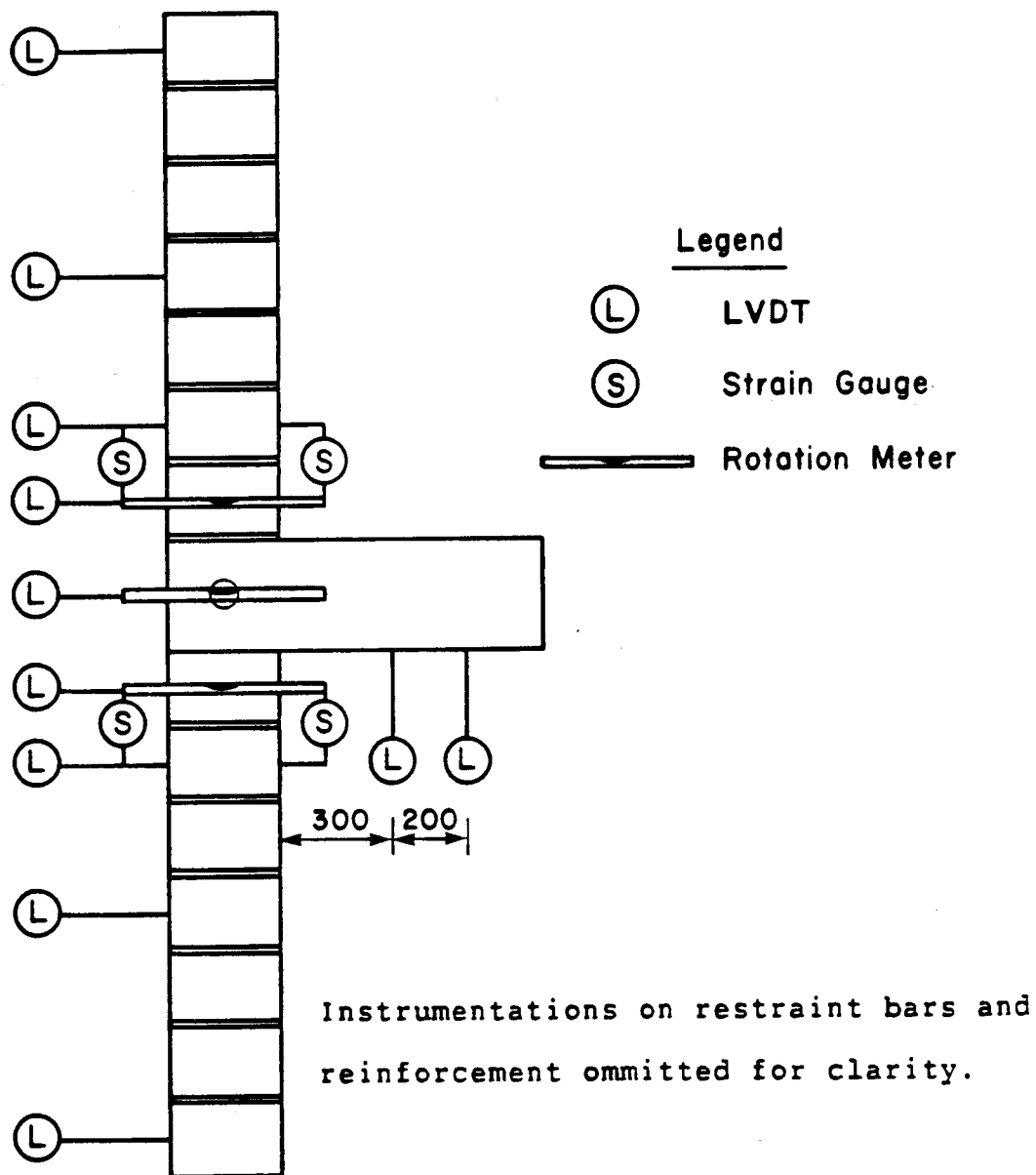


Figure 4.14 Instrumentation of Type I Specimens

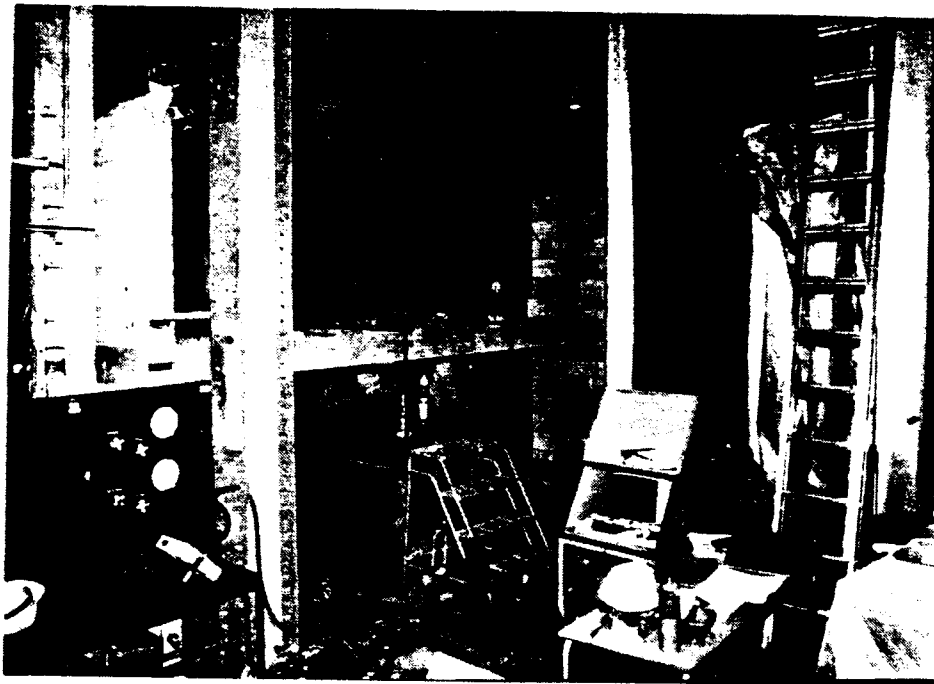
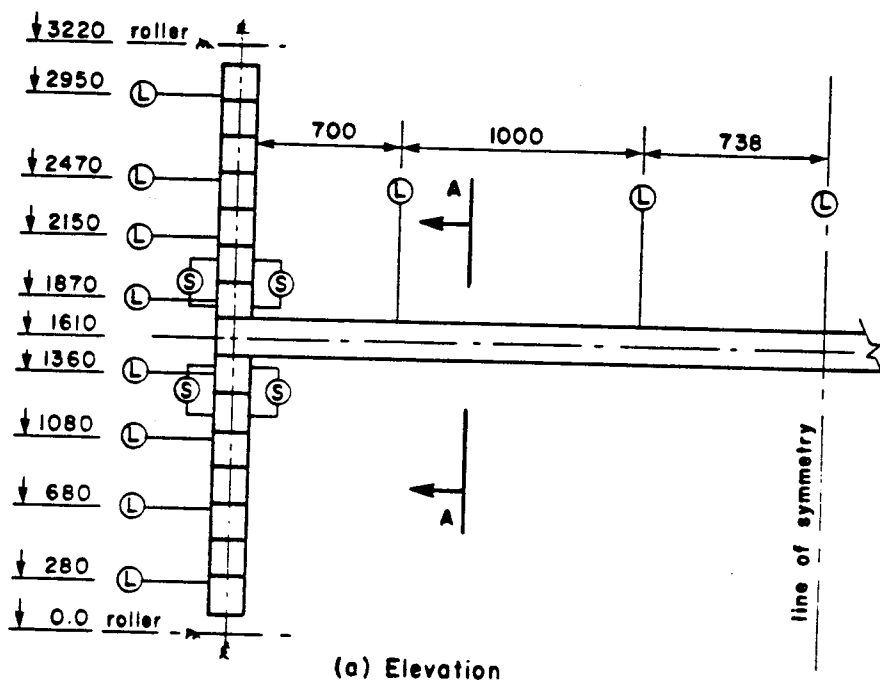


Plate 4.2 Test Set-Up for Type II Specimens

mm were placed at the end of the slab, at each of the end courses, and at the courses immediately above and below the slab for monitoring rotations and joint displacements. LVDT's measuring to 1/12 mm were used at the other locations on the wall. LVDT's on the walls of Type II specimens were placed closer to the mortar joints where rotations tended to concentrate. This slightly different arrangement is shown in Figure 4.15. LVDT's were also placed on the slab (2 on Type I and 5 on Type II specimens) to monitor slab deflection as well as to act as a check on the rotation of the slab. The LVDT's were attached to the wall or slab with thin wires.

Rotations of the walls and the slabs at the joint were measured by means of mechanical rotation gauges or determined indirectly from deflection measurements obtained from LVDT's. The rotation gauges employed a bubble centering mechanism on a lever arm of 381 mm for the walls and 470 mm for the slab in Type I specimens. A constant lever arm of 610 mm was used in connection with the LVDTs for measuring rotations in Type II specimens. Strains on the both faces of the wall one course above and below the slab, across the mortar joints, were measured using a Demec strain gauge with a gauge length of 204 mm. Strains in the middle reinforcing bar in the wall and in one bar at the top or bottom position in the slab were measured using electrical resistance strain gauges mounted on the bars. The position of the strain gauges on the wall steel coincided with the mortar joints across which strains were being measured on the both faces of the wall. Also, electrical resistance strain gauges were mounted on the restraint angles at the wall/slab joint in

Instrumentations on restraint bars and
reinforcement omitted for clarity.



- Legend**
- (L) LVDT
 - (S) Strain Gauge
 - (R) Rotation Gauge

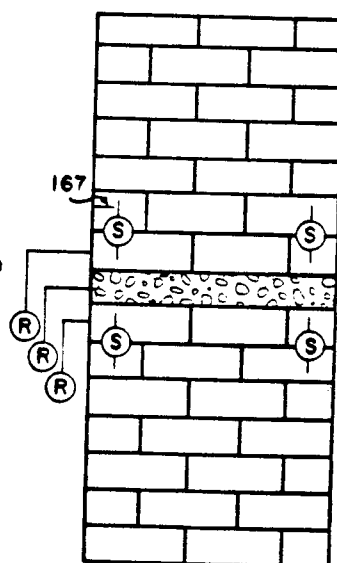


Figure 4.15 Instrumentation of Type II Specimens

Type I specimens, and the end restraints of the walls of Type II specimens.

Vertical loads on the walls were read directly on the MTS machine for Type I specimens. For Type II specimens, 450 kN capacity load cells were used for measuring the wall load and 225 kN capacity load cells were used for measuring the line loads applied to the slab.

The strain gauges and LVDTs were powered by a common power supply producing output in the range of ± 6 volts. The load cells were powered by a 10 volt source. The analog signals from the devices were converted into digital form by a digital voltmeter controlled by an interactive Fortran program in the Data General computer in the Structures Laboratory. This allowed measurements to be monitored and read into storage during testing. At any particular load level, all output was measured and recorded automatically with the exception of the manual readings. The interactive Fortran program allowed for monitoring the deformation and control of loading during the test. After completion of a test, the data were printed on a hard copy terminal, stored on a magnetic disk and later transferred to the Amdahl 470 computer for further processing.

4.7 Testing Procedure

4.7.1 Prisms

All prisms were tested in axial compression. Soft fiber boards were placed at the top and bottom of the prism to distribute the load over the total area. Load was applied in

increments of approximately one-twentieth of the estimated failure load for each prism. At each increment, strain readings were taken and recorded on both faces of the prism using a 254 mm Demec gauge. Loading and measurements were continued until crushing occurred.

4.7.2 Full-Scale Specimens

4.7.2.1 Placement of Specimens

Type I specimens were transported to the MTS machine in a clamping device consisting of two frames connected by steel rods. The frames, constructed of C180x15 sections, had a shape identical to the shape of the wall profile. The frames were placed on two sides of the wall and a compressive force applied by tightening nuts on the rods. Rubber pads were placed between the channels and the specimen at various locations to prevent damage to the wall. The specimens were then lifted by a 100 kN overhead crane by means of four chains located at the top of the wall and the end of the slab on each side of the specimen. The lengths of the chain were adjusted prior to lifting to maintain the slab in a horizontal position when the wall was lifted.

The specimen was guided into the testing machine using the overhead crane and two 10 kN chain hoists. The bottom plate of the channel-roller assembly was placed on a 10 mm layer of plaster of Paris to ensure that loading was distributed evenly. The wall was set on plaster in the bottom channel-roller assembly in a plumb

configuration while the plaster was allowed to set.

A temporary support was placed under the slab to provide stability. The clamping frames were then removed and the top channel-roller assembly plastered into place. A 10 kN load was applied to the channel to provide an even set of the plaster and overall stability of the specimen. Out-of-plumb readings were taken and the slab loading apparatus, the joint restraining assembly and the measuring devices were connected.

For Type II specimens, the bottom walls were cast into the bottom channel roller assembly. After stripping the slab form, a temporary line support was placed at the midspan of the slab to prevent rotation due to slab dead load. Out-of-plumb readings were then taken. Table 4.8 shows the out-of-plumb readings measured on the full scale specimens. When it was time to test the specimen, the top channel-roller assemblies for both walls were plastered into place.

4.7.2.2 Load Application

The same procedure was followed for load application on both Type I and Type II specimens. With a 10 kN load applied to the walls, the temporary slab support was replaced by a 45 kN capacity jack and load cell as shown in Plate 4.3. The load cell was connected to a strain indicator so that the jack supported the weight of slab plus the loading assembly. This was an attempt to keep the slab level during the application of the axial load. Bolts were then removed from the

Table 4.8 Out-of-Plumb Measurements

Specimen	Axial Load kN	Maximum Out of Plumb*	
		Upper Wall mm	Lower Wall mm
FRA150**		+5 SE 0 SW	0 SE 0 SW
FRB100	100	+15 SE +10 NW +5 SE 0 SW	+3 NE -5 NW +6 SE +4 SW
WSA100***	100	+3 N +5 S	+3 N +6 S
WSA400	400	+12 N +6 S	+13 N +8 S
WSB100	100	-2 N +3 S	-2 N +3 S
WSB400	400	-2 N +7 S	-5 N +7 S

* A positive out-of-plumb indicates that the top wall leans towards the slab.

** FR implies frame specimen (Type II)
 A implies unreinforced walls
 B implies reinforced walls

*** WS implies single joint specimen (Type I)

N implies north wall
 S implies south wall

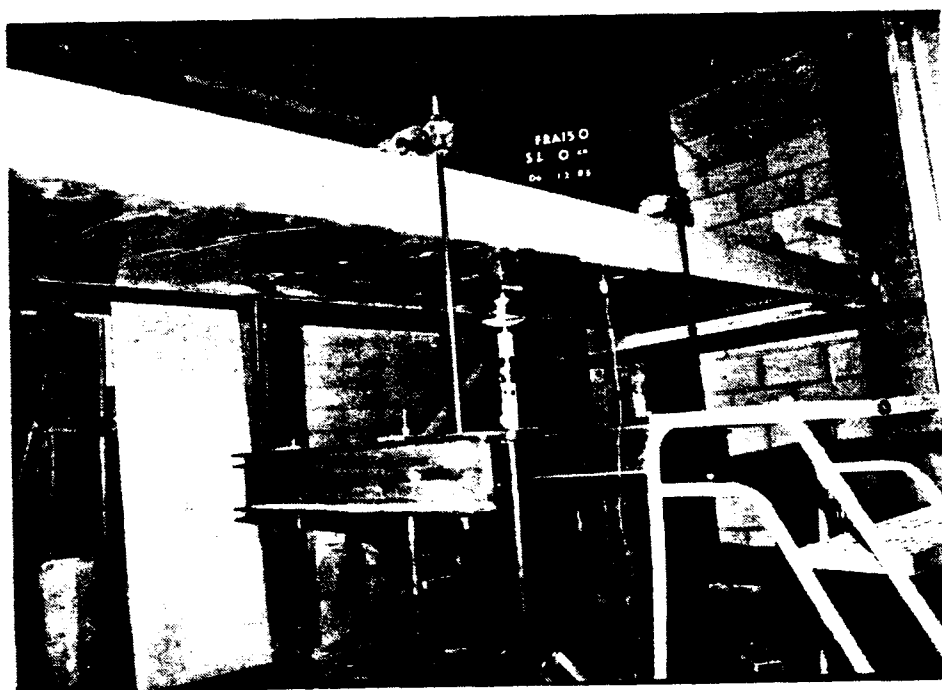


Plate 4.3 Temporary Adjustable Slab Support for Type I Specimens

channel-roller assemblies to produce in them pin-ended joints. All initial readings were taken at this time. The wall axial load was then applied in 5 increments up to the predetermined level, with instrumentation readings being taken at each increment. As the axial load was increased on the wall, efforts were made to keep the slab level by controlling the readings of the load cell of the temporary support. After the required axial wall load was reached, the temporary slab support was removed and all readings were taken again. The wall axial loading was continuously monitored and kept constant throughout the test of each specimen. The slab loading was then applied in approximately 20 increments to the estimated maximum load. At each slab load increment, all instruments except Demec gauges were read. The Demec readings were taken at every third load increment. Attempts were made to keep the slab load constant during reading which took approximately five minutes. Slab load versus end rotation was plotted during each test to indicate possible inelastic behavior and imminent failure. This procedure was continued until failure appeared to be imminent, at which point only automatic readings were taken at more frequent intervals until failure of the specimen.

During the loading of the specimens, crack inspection and crack measurements were carried out. Photographs were taken and sketches made to help interpret the test results. Testing time for Type I specimen was between two to three hours. testing of Type

II specimens took between three to four hours.

5. TEST RESULTS

5.1 Introduction

In this chapter the results of tests of small and full-scale specimens are presented, and typical behavior during tests is described.

5.2 General Behavior of Type I Specimens

5.2.1 Specimen WSA100

As the slab load was increased, the specimen continued to deform until the load reached 72% of the maximum value at which load a 0.15 mm horizontal tensile crack was observed at the first mortar joint below the slab. As the slab loading was increased further, this crack widened and another horizontal crack developed at the joint between the upper wall and the slab. When the slab load reached 92% of the maximum value, the width of the crack in the lower wall was 2.6 mm. Further slab load continued to widen the cracks already developed, and the rotation of the upper wall began to decrease due to the separation of the upper wall from the slab and the lower wall. When the test was discontinued for instability reasons, the crack in the lower wall was approximately 4 mm wide and the crack at the joint between the upper wall and the slab was approximately 2.5 mm wide. It was observed that the first course of the lower wall held rigidly to the slab, while the remainder of the upper and lower walls did not show any visible signs of distress. The mortar joint bonded partially to the first and second

courses below the slab in the lower wall, and fully to the slab at the joint between the upper wall and the slab. Figure 5.1 is a sketch of the crack distribution at failure of the specimen. The moment-rotation data is given in Table 5.1.

5.2.2 Specimen WSA400

No noticeable cracks were detected in either the top or bottom wall of Specimen WSA400 until 92% of the maximum slab load was reached when a horizontal crack at the first mortar joint below the slab was observed. At a slab load of 98% maximum load, this lower wall crack extended into the course above and measured 1.4 mm. Immediately after the next increment, the walls exploded, and the bottom wall was prevented from falling by the tie-backs and the safety chain on the slab. The sketch of the crack distribution just prior to failure is shown in Figure 5.2. Table 5.2 gives the moment -rotation data for the specimen.

5.2.3 Specimen WSB100

The first noticeable crack occurred along the first mortar joint below the slab at a slab load equal to 45% of the maximum value. At 64% maximum slab load, this crack had widened and the first three joints above the slab were also beginning to open up. When the slab load reached 80% of its maximum, the horizontal crack initiated in the first mortar joint below the slab was climbing vertically into the course above on the side of the wall. Also, vertical cracks were developing independently on both faces of the upper wall and

Table 5.1 Moment-Rotation Data for Specimen WSA100

Inc.	Tie Force kN	Moment, M (kN.m)			Max. Axial Load P _L (kN)	Rotation, θ (radians)				Applied Slab Load, P _s (kN)
		M _{SI}	M _{UW}	M _{LW}		θ_{SI}	θ_{UW}	θ_{LW}	θ_J	
5	1.20	0.0	0.0	0.0	100.0	0.00	0.0000	0.0000	0.0000	0.00
6	1.58	1.89	-0.07	-0.79	110.0	0.00011	0.00013	0.00020	-0.00002	2.22
8	1.97	3.42	0.35	3.32	111.8	0.00043	0.00040	0.00053	0.00003	4.02
9	2.42	6.98	1.68	5.33	116.0	0.00060	0.00067	0.00060	0.0000	8.21
10	2.50	8.92	2.53	6.30	118.3	0.00086	0.00073	0.00087	0.00013	10.49
12	2.87	12.01	3.72	5.33	122.0	0.00120	0.00031	0.00120	0.00027	14.17
15	2.86	16.99	6.05	10.35	127.8	0.00195	0.00153	0.00200	0.00042	19.99
16	2.81	18.81	6.94	11.17	129.9	0.00232	0.00180	0.00233	0.00052	22.13
18	3.88	21.71	7.48	13.34	133.3	0.00530	0.00227	0.00533	0.00303	25.54*
20	3.18	22.90	8.57	13.37	134.7	0.01400	0.00193	0.01421	0.01210	26.94
22	3.29	23.90	8.83	14.05	135.9	0.01390	0.00193	0.01420	0.01210	28.12
31	3.37	22.00	8.92	14.01	135.9	0.01400	0.00193	0.01420	0.01210	25.88

* Trend in reversed curvature of upper wall

Table 5.2 Moment-Rotation Data for Specimen WSA400

Inc.	Tie Force kN	Moment, M (kN.m)			Max. Axial Load P _L (kN)	Rotation, θ (radians)				Applied Slab Load, P _s (kN)
		M _{s1}	M _{uw}	M _{lw}		θ_{s1}	θ_{uw}	θ_{lw}	θ_j	
8	0.63	0.0	0.0	0.0	403.9	0.000216	0.0010	0.00027	-0.00078	0.00
11	0.26	10.11	4.78	5.16	413.9	0.00038	0.00113	0.00067	-0.00075	11.89
14	0.46	21.78	10.10	10.79	432.6	0.00168	0.00213	0.00180	-0.00045	25.62
15	0.80	27.53	12.54	13.74	439.4	0.00205	0.00240	0.00213	-0.00035	32.39
17	1.46	34.52	15.32	17.52	447.6	0.00265	0.00280	0.00267	-0.00015	40.61
18	1.67	39.15	17.33	19.85	453.0	0.00292	0.00307	0.00293	-0.00015	46.06
20	1.99	47.26	20.90	23.90	462.6	0.00346	0.00353	0.00353	-0.00007	55.60
23	2.12	60.15	26.83	30.04	477.8	0.00476	0.00433	0.00460	0.00043	70.76
26	2.01	72.17	32.56	35.60	491.9	0.00751	0.00527	0.00673	0.00246	84.90
27	5.91	73.78	30.37	39.29	493.8	0.00870	0.00560	0.00760	0.00310	86.80
28	2.30	76.81	34.52	37.98	497.32	0.00968	0.00587	0.00847	0.00381	90.36
29	1.97	78.62	35.61	38.58	499.4	0.01081	0.00600	0.00953	0.00481	92.45

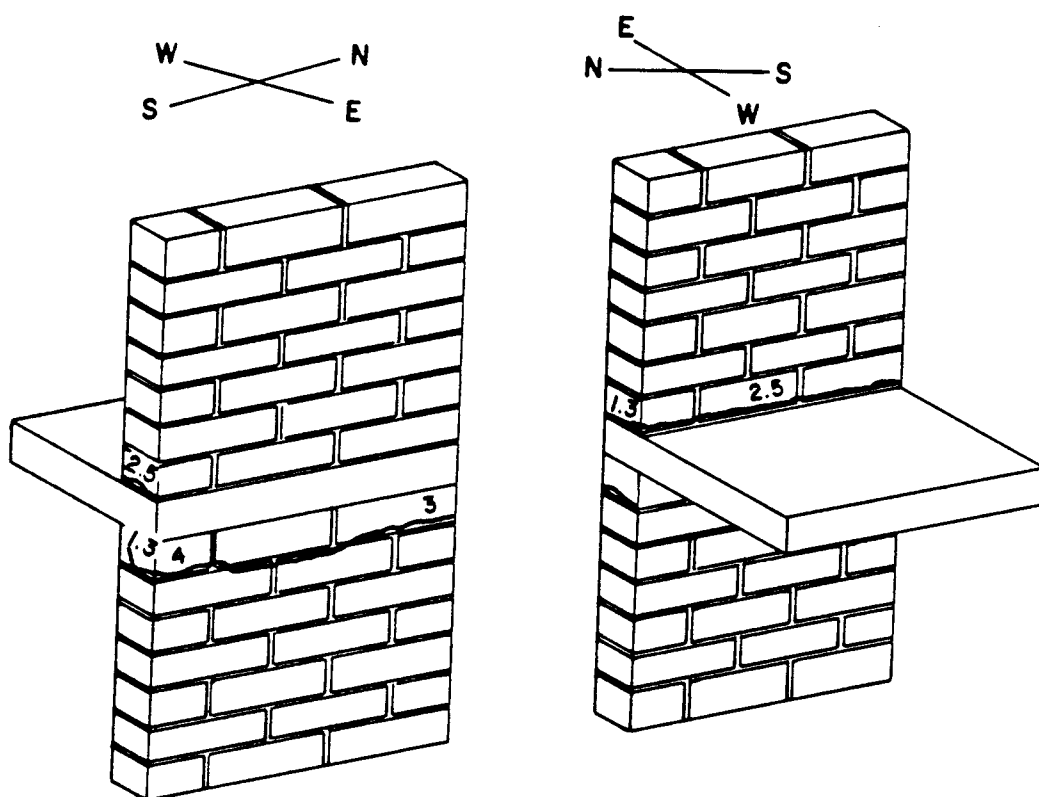


Figure 5.1 Crack Distribution at Failure on Specimen WSA100

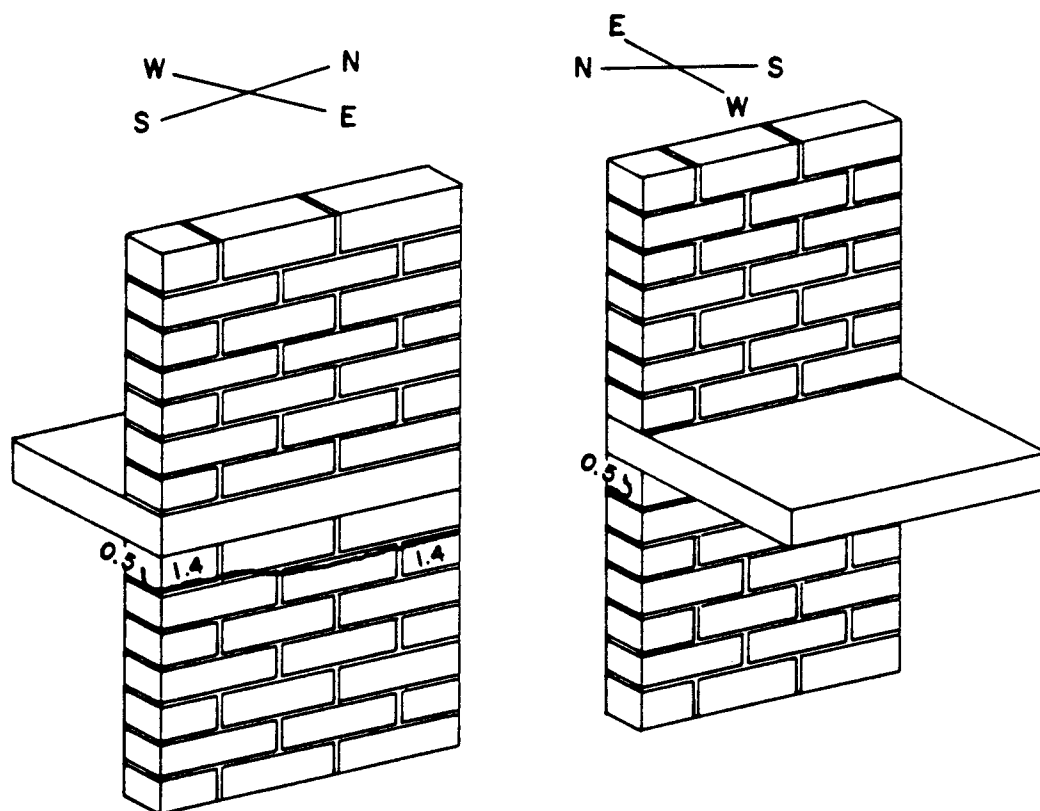


Figure 5.2 Crack Distribution at Failure on Specimen WSA400

on the sides. As the maximum load was approached, crushing of the first course below the slab began to develop from the north end of the lower wall. At maximum load, crushing had extended to approximately 50% of the width of the wall, at a distance of one-quarter to half the depth of the course from the slab beginning at the north end. Maximum crack widths were 2.5 mm at the joint between the upper wall and the slab and 4.5 mm at the first mortar joint below the slab. Fig 5.3 is a sketch of the crack distribution on the walls at failure. Table 5.3 gives the moment-rotation data for the specimen.

5.2.4 Specimen WSB400

A hairline horizontal tensile crack was detected in the first mortar joint below the slab at 63% maximum slab load. At 73% maximum slab load, vertical cracks developing through the slab into the upper wall were 0.38 mm wide. Meanwhile, a hairline tension crack was also observed at the back of the lower wall just below the slab, spreading throughout the width of the specimen. When the slab load reached 84% of the maximum value, the crack in the first mortar joint below the slab started to extend vertically into the course above, and cracks were developing in the first joint above the slab. At maximum load, the specimen crushed in a manner similar to that observed for specimen WSB100 as shown in Plate 5.1. At failure, the maximum crack width was 1 mm in the first mortar joint below slab, and 0.5 mm in the joint between the upper wall and the slab. Plates 5.2 and 5.3 show the distribution of cracks in the wall at failure and Table 5.4

Table 5.3 Moment-Rotation Data for Specimen WSB100

Inc.	Tie Force kN	Moment, M (kN.m)			Max. Axial Load P _L (kN)	Rotation, θ (radians)				Applied Slab Load, Ps (kN)
		M _{s1}	M _{uw}	M _{lw}		θ_{s1}	θ_{uw}	θ_{lw}	θ_j	
5	1.77	0.00	-0.22	2.46	111.6	0.000	0.00027	0.00020	-0.000270	0.00
10	2.41	6.90	1.65	5.29	117.5	0.00043	0.00073	0.00067	-0.00030	8.12
14	3.37	11.89	3.27	8.35	123.4	0.00113	0.00107	0.00107	0.00007	13.99
18	3.56	20.04	6.95	12.31	133.0	0.00189	0.00180	0.00187	0.00010	23.58
24	3.37	29.10	11.34	16.42	143.6	0.00314	0.00253	0.00313	0.00060	34.24
28	5.17	37.25	13.80	21.60	153.2	0.00514	0.00353	0.00507	0.00160	43.82
34	7.93	47.28	16.42	28.39	165.0	0.00897	0.00580	0.00887	0.00317	55.62
38	8.91	55.85	19.70	33.14	175.1	0.01324	0.00860	0.01313	0.00464	65.70
42	9.28	62.34	22.46	36.47	182.7	0.01692	0.01100	0.01680	0.00593	73.34
45	10.05	66.90	24.01	39.20	188.1	0.02011	0.01300	0.02007	0.00711	78.70
50	10.31	72.86	26.62	42.18	195.1	0.02503	0.01633	0.02513	0.00870	85.72
53	10.14	77.03	28.70	44.01	200.0	0.03216	0.02080	0.03173	0.01502	90.62
56	12.80	75.02	25.75	45.07	197.7	0.03796	0.02293	0.03640	0.01502	88.26

Table 5.4 Moment-Rotation Data for Specimen WSB400

Inc.	Tie Force kN	Moment, M (kN.m)			Max. Axial Load P _L (kN)	Rotation, θ (radians)				Applied Slab Load, P _s (kN)
		M _{sl}	M _{uw}	M _{lw}		θ_{sl}	θ_{uw}	θ_{lw}	θ_j	
9	-2.94	0.00	3.34	-1.10	410.2	0.00032	0.00047	0.00033	-0.000140	0.00
13	2.54	13.26	4.54	8.37	423.4	0.001027	0.00107	0.00093	-0.000044	13.38
15	2.80	22.36	8.61	12.84	431.1	0.001622	0.00147	0.00147	0.00016	24.09
17	6.34	30.79	9.89	19.46	444.0	0.00200	0.00180	0.00187	0.00020	34.00
19	6.90	39.35	13.48	25.90	454.1	0.00249	0.00220	0.00227	0.00029	44.09
21	7.76	47.98	16.88	28.59	464.2	0.00308	0.002533	0.00287	0.000550	54.23
24	7.95	59.94	22.34	34.35	478.3	0.00416	0.00313	0.00373	0.00103	68.30
27	5.06	72.08	30.22	37.86	492.6	0.00568	0.00380	0.00540	0.00188	82.58
30	7.43	83.80	33.92	45.14	506.4	0.00838	0.00473	0.00827	0.00365	96.37
32	7.56	92.91	38.09	49.51	517.1	0.01141	0.00580	0.01080	0.00561	107.08
37	7.25	05.22	44.11	55.04	531.6	0.01746	0.00740	0.01453	0.01006	121.57
40	7.33	10.08	46.33	57.38	537.3	0.02206	0.00727	0.01800	0.01511	127.28
41	5.83	04.35	45.65	54.45	532.8	0.02568	0.00687	0.02087	0.019132	122.76

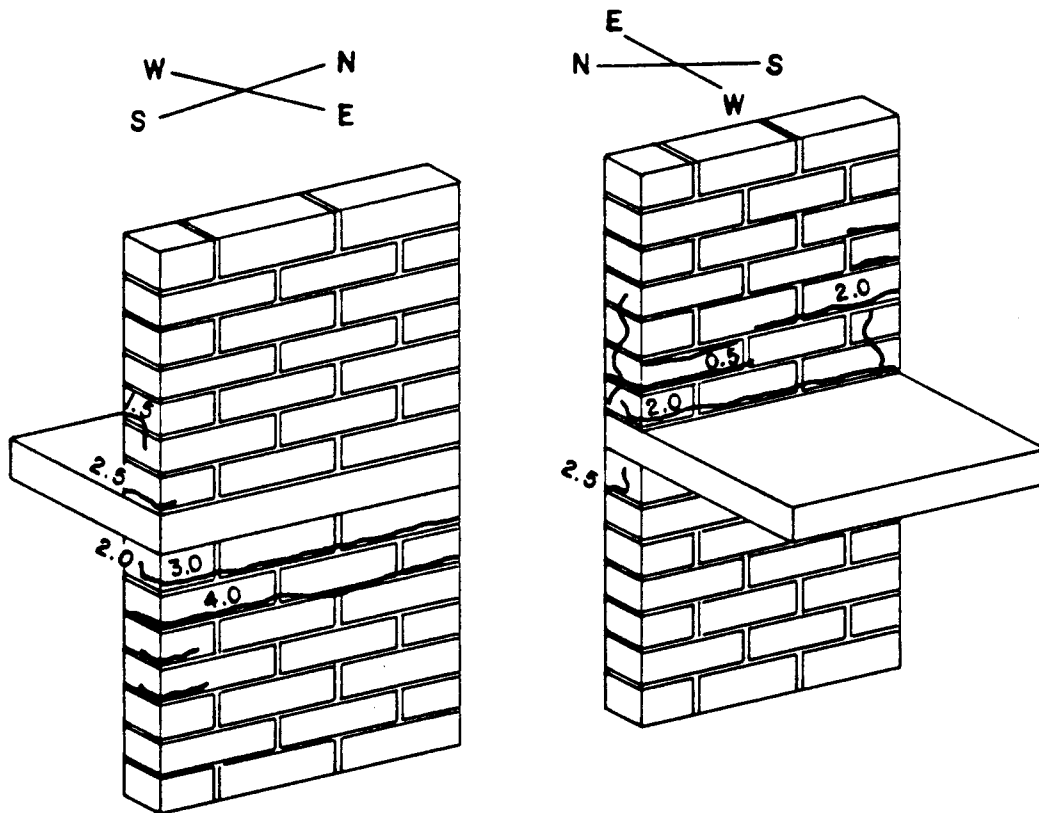


Figure 5.3 Crack Distribution at Failure of Specimen WSB100

gives the moment-rotation data for the specimen.

5.3 General Behavior of Type II Specimens

5.3.1 Specimen FRA150

North and south walls in the frame exhibited similar behavior during testing. Hairline horizontal tensile cracks were observed one joint below the slab in both walls at 49% maximum slab load. At 70% maximum load, these cracks were 2.3 mm wide, and the cracks in the joints between the upper wall and the slab were 1.5 mm wide. At this stage, the horizontal cracks in the bottom walls started to extend vertically into the course below the slab on the sides of the wall. At the onset of instability behavior of the frame, maximum crack widths were 7.0 mm at the back of the bottom wall and 5.0 mm at the joint between the upper wall and the slab. The vertical crack in the first course below the slab was 4 mm wide and extended upwards 70 mm. Plates 5.4 and 5.5 show the crack distribution in the walls and Tables 5.5 and 5.6 give the moment-rotation data for the north and south walls of the specimen, respectively.

5.3.2 Specimen FRB100

The behaviors of the north and south walls were also quite similar for this specimen. Hairline horizontal cracks in the first mortar joint below the slab were noted in both bottom walls at 28% maximum slab load. At 50% maximum slab load, horizontal cracks started developing in the second joint below the slab and at the joint between the upper wall

Table 5.5 Moment-Rotation Data for Specimen FRA150 (North Wall)

Inc.	Tie Force kN	Moment, M (kN.m)			Max. Axial Load P _u (kN)	Rotation, θ (radians)				Applied Slab Load, P _s (kN)
		M _{SI}	M _{UW}	M _{LW}		θ_{SI}	θ_{UW}	θ_{LW}	θ_j	
6	-0.07	0.00	0.00	0.00	155.5	0.00102	0.00107	0.00102	-0.000050	0.00
10	-0.47				178.1	0.00217	0.00215	0.00213	0.00002	11.05
12	-0.20	18.73	6.19	12.53	181.1	0.00154	0.00140	0.00255	0.00009	14.07
14	-0.14				184.0	0.00277	0.00262	0.00276	0.00014	17.03
16	-0.37	24.58	7.23	17.14	187.0	0.00307	0.00286	0.00309	0.00021	20.03
18	-0.68	26.44	9.17	17.27	190.2	0.00352	0.00312	0.00356	0.00040	23.15
22	-0.97	29.80	10.25	19.55	196.3	0.00464	0.00317	0.00523	0.00207	29.36*
32	-1.82				204.6	0.00877	0.00210	0.00902	0.00667	37.58
41	-2.77				214.0	0.01276	0.00078	0.01372	0.01198	47.00
48	-3.99				227.1	0.02248		0.02080		60.10**
50	-4.61				229.9	0.02532		0.02372		62.90
55	-5.89				230.6	0.03162		0.03035		63.62
56	-5.88				230.4	0.03162		0.03035		63.40

* Trend in reversal of curvature of upper wall

** Excessive widening of joint cracks begins

Table 5.6 Moment-Rotation Data for Specimen FRA150 (South Wall)

Inc.	Tie Force kN	Moment, M (kN.m)			Max. Axial Load P _L (kN)	Rotation, θ (radians)				Applied Slab Load, P _s (kN)
		M _{sl}	M _{uw}	M _{lw}		θ_{sl}	θ_{uw}	θ_{lw}	θ_j	
6	-0.15	0.00	0.00	0.00	154.5	0.00040	0.00280	0.00032	-0.002370	0.00
10	0.00				177.0	0.00188	0.00153	0.00161	0.00035	
12	0.00	18.77	6.07	12.70	180.1	0.00239	0.00194	0.00209	0.00045	13.04
14	-0.06	24.32	7.32	17.05	184.1	0.00274	0.00220	0.00241	0.00054	17.14
16	-0.48	26.48	9.16	17.32	187.3	0.00313	0.00255	0.00278	0.00058	20.28
18	-0.64				190.4	0.00353	0.00270	0.00316	0.00083	23.40
22	-1.68	29.77	10.89	18.94	197.0	0.00523	0.00296	0.00486	0.00227	30.00*
32	-2.48				205.6	0.00899	0.00191	0.00866	0.00708	38.60
41	-3.49				215.3	0.01292	0.00042	0.01261	0.01250	48.30
48	-4.72				228.2	0.02268		0.01732		61.20**
50	-5.35				231.1	0.02572		0.01932		64.10
55	-6.63				231.8	0.03232		0.02374		64.80
56	-6.63				231.3	0.03234		0.02375		64.30

* Trend in reversal of curvature of upper wall

** Excessive widening of joint crack begins



Plate 5.1 Wall Crushing Failure of Specimen WSB400

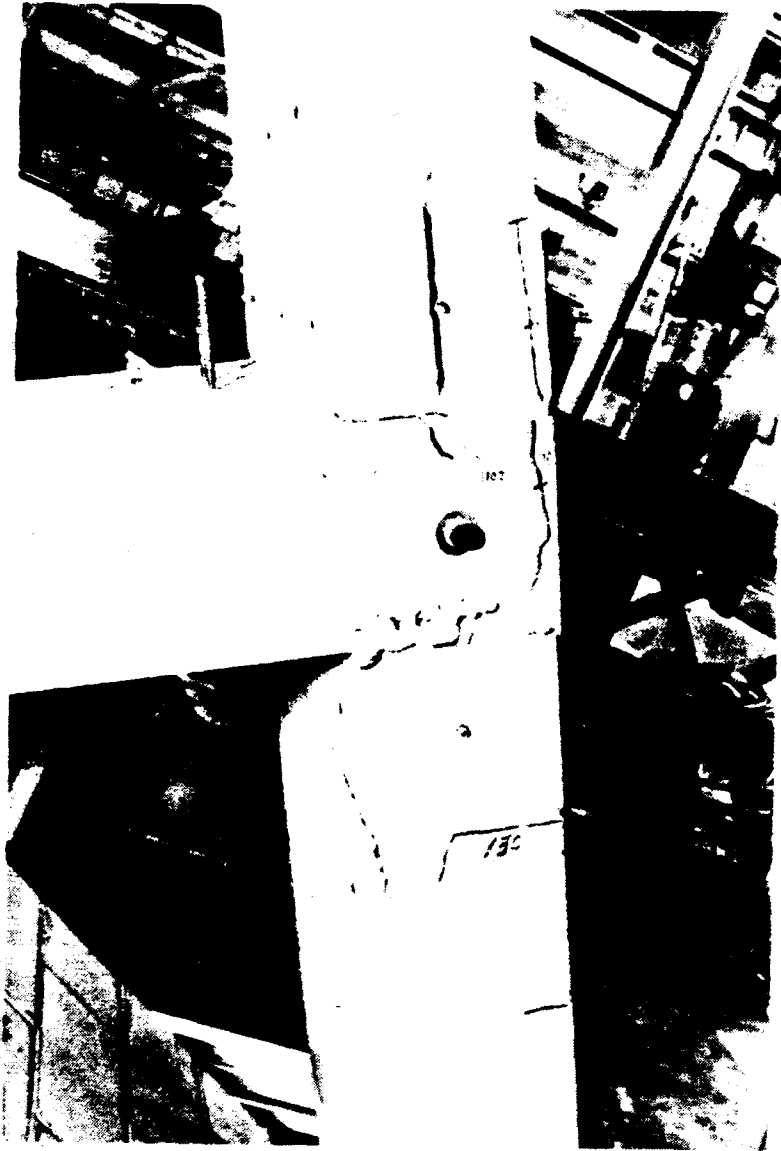


Plate 5.2 Side View of Crack Distribution at Failure on Specimen WSB400

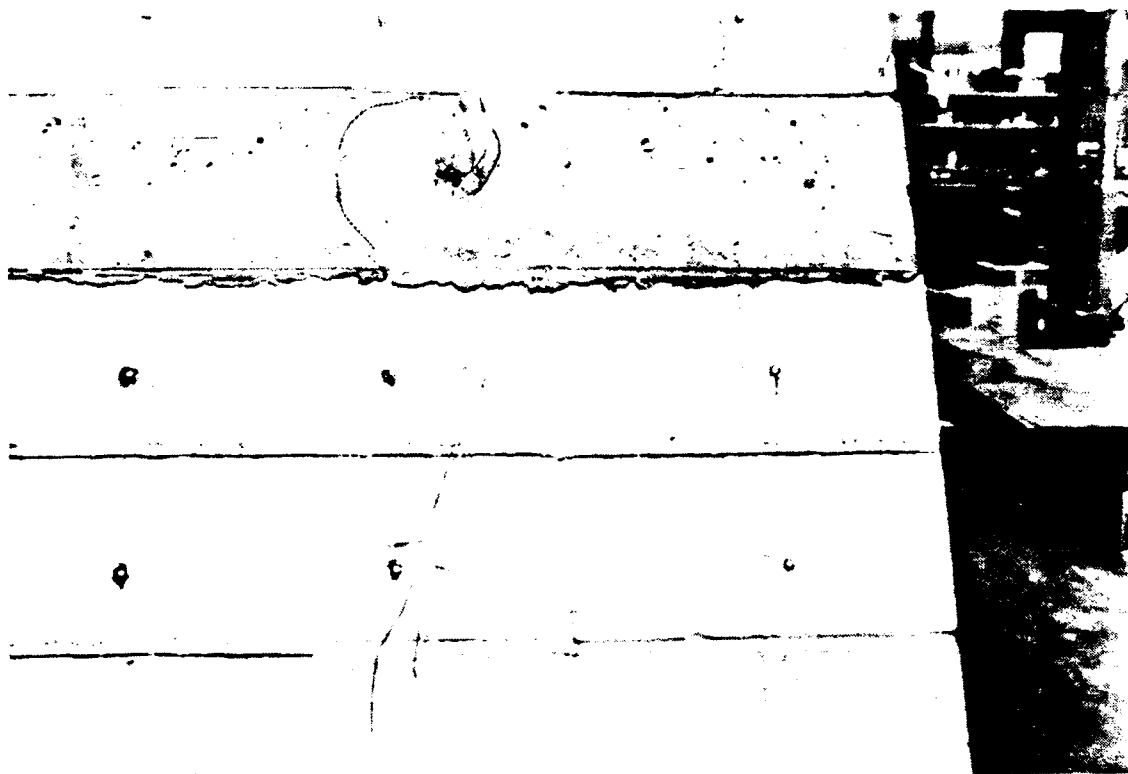


Plate 5.3 Back View of Crack Distribution at Failure on
Specimen WSB400

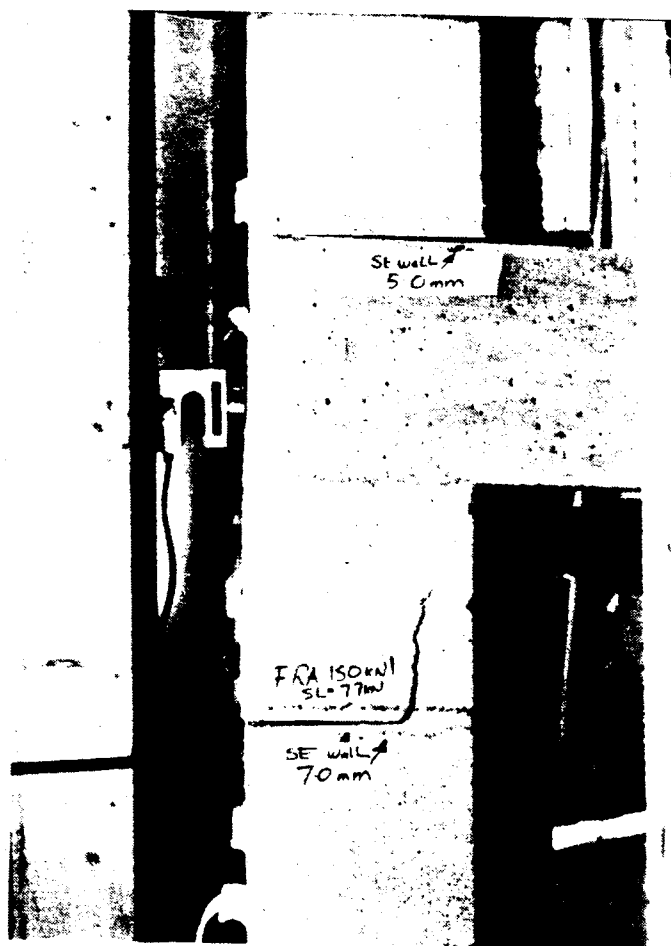


Plate 5.4 Side View of Crack Distribution at Failure on Specimen FRA150

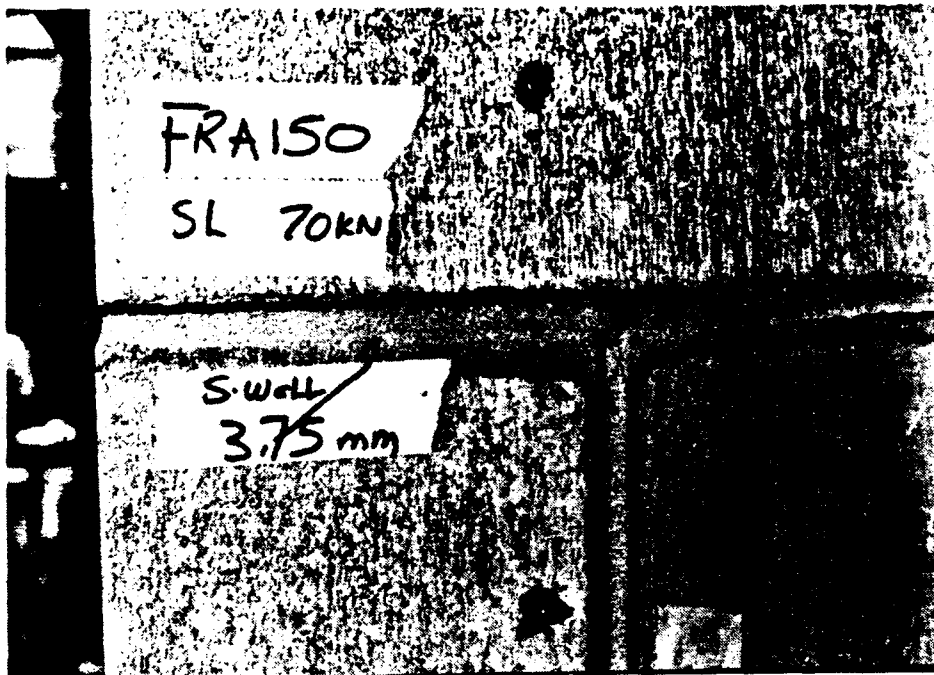


Plate 5.5 Back View of Crack Distribution at Failure on Specimen FRA150

and the slab. At 70% maximum slab load, vertical cracks were developing in the slab at the joint. When the load reached 88% maximum value, these vertical cracks were developing into the wall courses above and below the slab, and connecting some of the existing cracks in the top and bottom walls. Cracks were also beginning to develop in the joint between the upper wall and the slab in the second and third joints of the lower wall and in the second joint of the upper walls. When the specimen finally crushed locally in the lower south wall just below the slab, maximum crack width had reached 3.5 mm in the lower walls, 1.5 mm in the joint between the upper wall and the slab, and 1.0 mm between the lower wall and the slab. Plates 5.6 and 5.7 show typical crack distribution at maximum load. Tables 5.7 and 5.8 give the moment-rotation data of the north and south walls of the specimen, respectively.

5.4 Deflected Shapes

5.4.1 Type I Specimens

The deflected shapes of Type I specimens are shown in Figures 5.4 to 5.6. The lateral restraint system at the wall/slab joint appears to have kept joint translation at a minimum in all the tests. The LVDT's on Specimen WSA400 did not register any significant deflection.

5.4.2 Type II Specimens

The deflected shapes of the frame specimens are shown in Figures 5.7 and 5.8. The deflection measurements were

Table 5.7 Moment Rotation Data for Specimen FRB100 (North Wall)

Inc.	Restraint kN	Moment, M (kN.m)			Max. Axial Load P _u (kN)	Rotation, θ (radians)			Applied Slab Load, P _s (kN)
		M _{s1}	M _{uw}	M _{lw}		θ_{s1}	θ_{uw}	θ_{lw}	
6	-0.36	0.00	0.00	0.00	106.3	0.00029	0.00061	0.00030	0.00
10	-0.78				145.0	0.00220	0.00182	0.00209	27.20
13	-1.56	32.13	12.35	19.79	159.3	0.00587	0.00320	0.00569	41.54
18	-2.02	46.00	20.55	25.46	168.6	0.00722	0.00401	0.00744	50.80
24	-2.79				193.9	0.01200	0.00570	0.01247	76.10
27	-3.04	66.89	29.95	36.94	200.5	0.01313	0.00607	0.01359	82.70
31	-3.27				208.4	0.01514	0.00619	0.01501	90.60
37	-3.44	70.38	28.27	42.11	217.8	0.01859	0.00620	0.00866	100.00*
42	-3.54				218.9	0.02171	0.00457	0.01840	101.10
49	-3.61				231.3	0.02931	0.00137	0.02189	103.50
52	-3.32				219.4	0.03113	-0.00052	0.02223	101.60

* Trend in reversal of curvature of upper wall

Table 5.8 Moment-Rotation Data for Specimen FRB100 (South Wall)

Inc.	Restraint kN	Moment, M (kN.m)			Max. Axial Load P _L (kN)	Rotation, θ (radians)				Applied Slab Load, P _s (kN)
		Ms1	M1w	M1w		θ s1	θ uw	θ 1w	θ j	
6	-0.00	0.00	0.00	0.00	106.3	0.00029	0.00026	0.00020	0.00004	0.00
10	-0.00				148.9	0.00205	0.00151	0.00192	0.00013	31.11
13	-0.63	32.07	11.81	20.25	160.6	0.00592	0.00338	0.00580	0.00255	42.80
18	-0.97	46.31	26.46	19.85	170.1	0.00752	0.00425	0.00739	0.00327	52.30
24	-2.30				195.6	0.01174	0.00639	0.01049	0.00535	77.80
27	-2.48	67.17	29.64	37.53	202.6	0.01271	0.00682	0.01135	0.00589	84.80
31	-2.69				210.4	0.01486	0.00696	0.01241	0.00790	92.60
37	-3.15	70.57	28.13	42.45	219.2	0.01838	0.00724	0.01411	0.01114	101.40*
42	-4.64				220.5	0.02114	0.00656	0.01477	0.01458	102.70
49	-6.75				232.6	0.02718	0.00344	0.01515		104.80
52	-7.61				220.8	0.02899	0.00278	0.01499	0.02621	103.00

* Trend in reversal of curvature of upper wall.

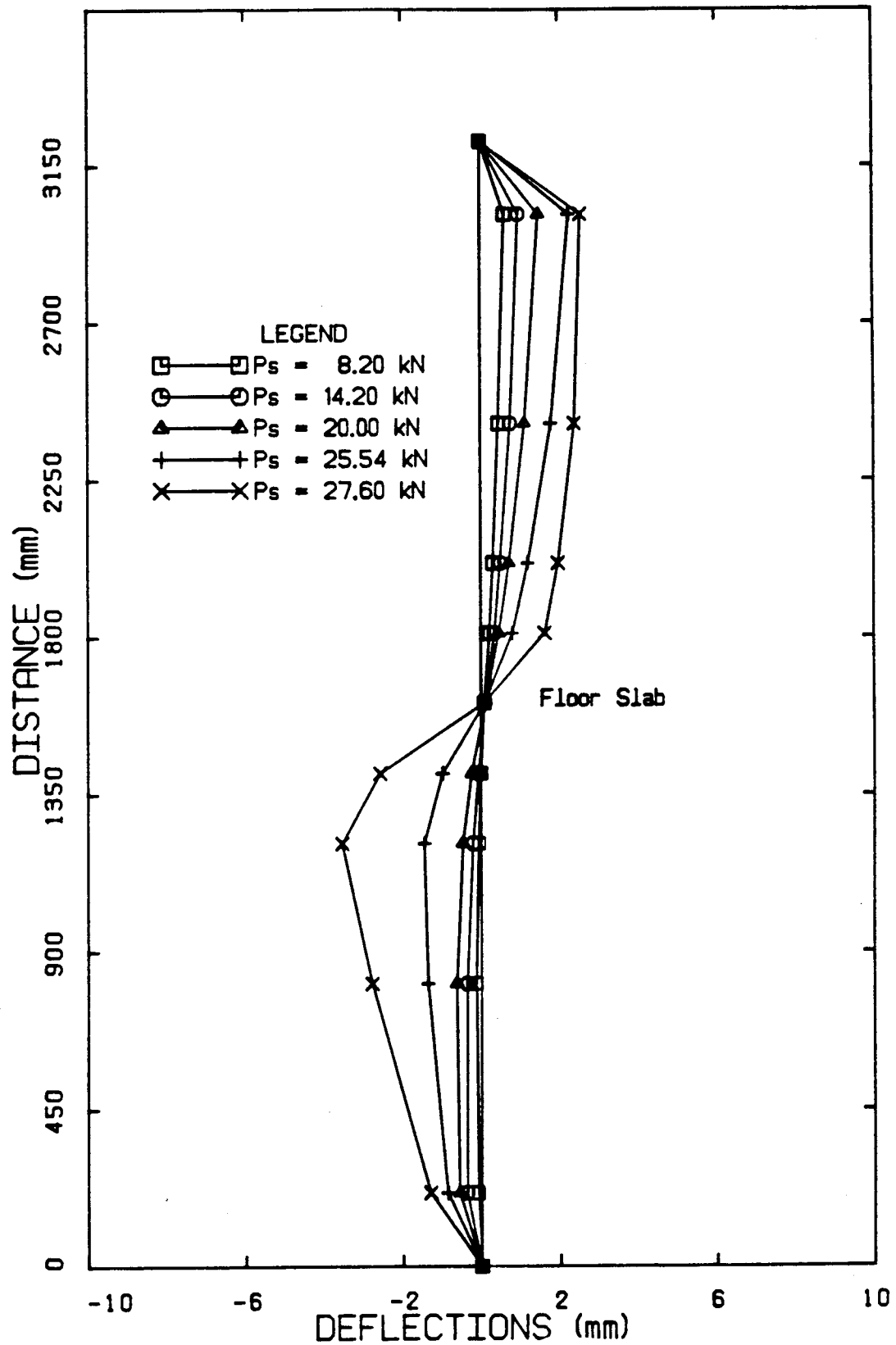


Figure 5.4 Deflected Shape for Specimen WSA100

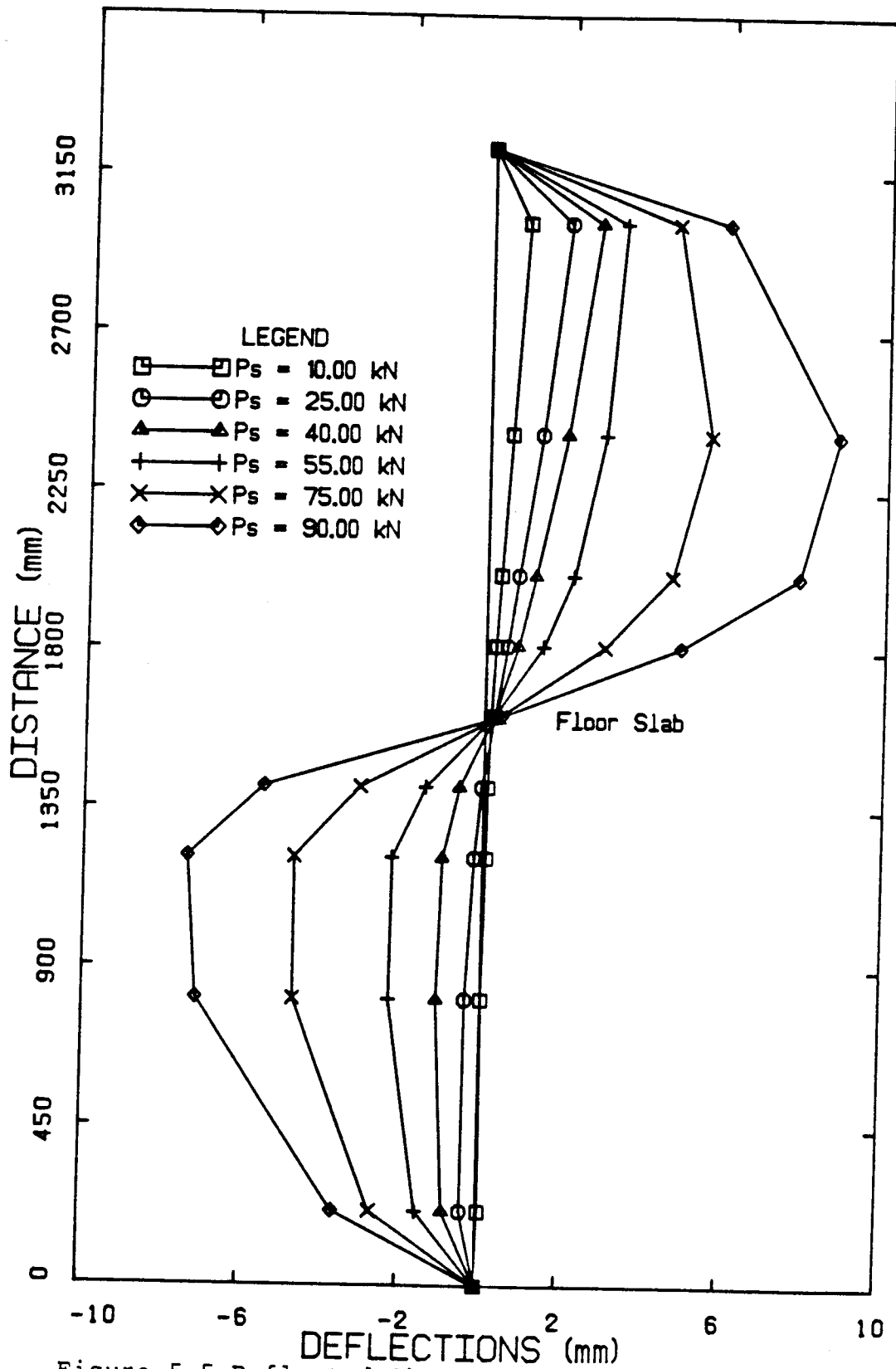
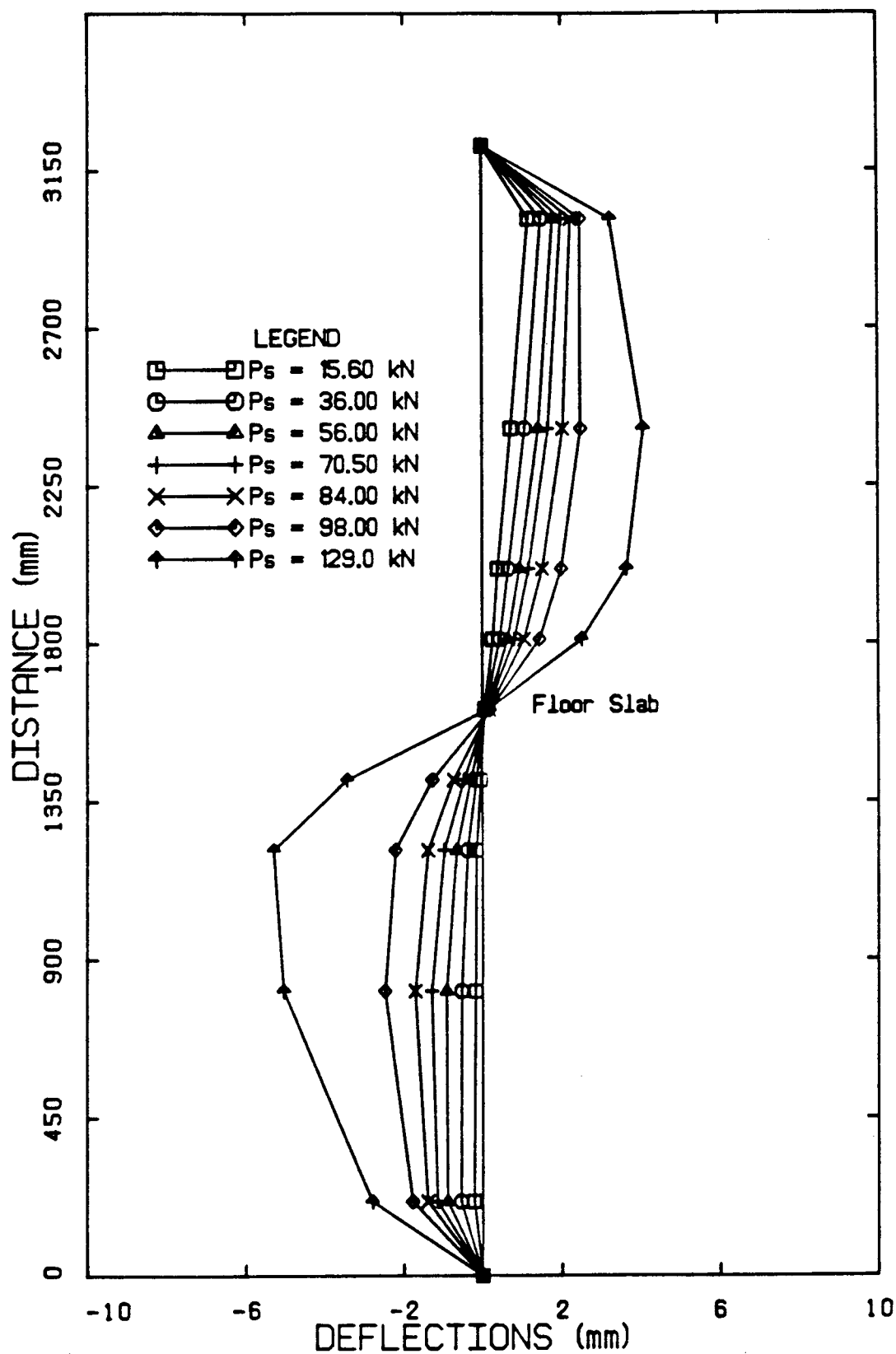


Figure 5.5 Deflected Shape for Specimen WSB100



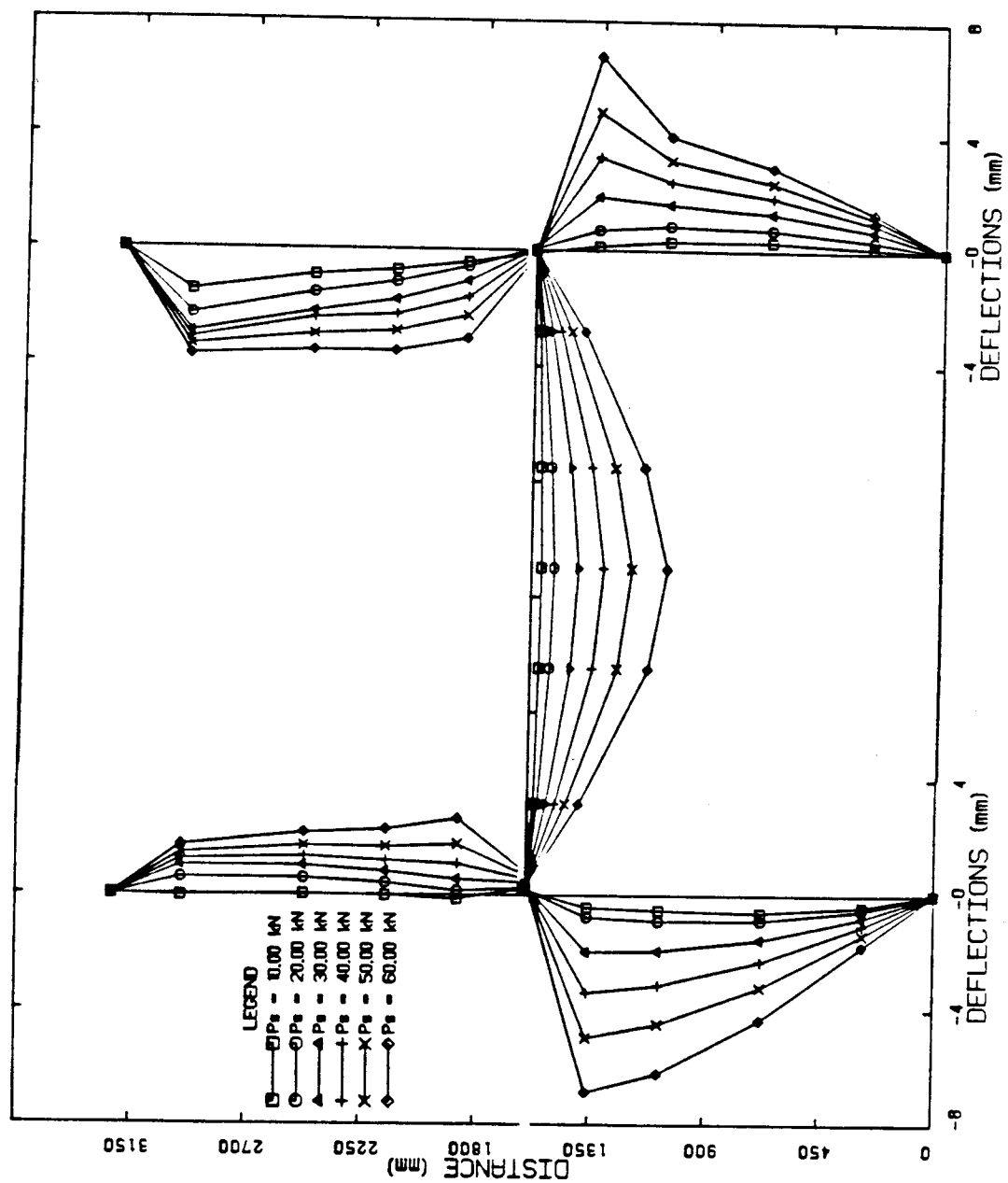


Figure 5.7 Deflected Shape for Specimen FRA150

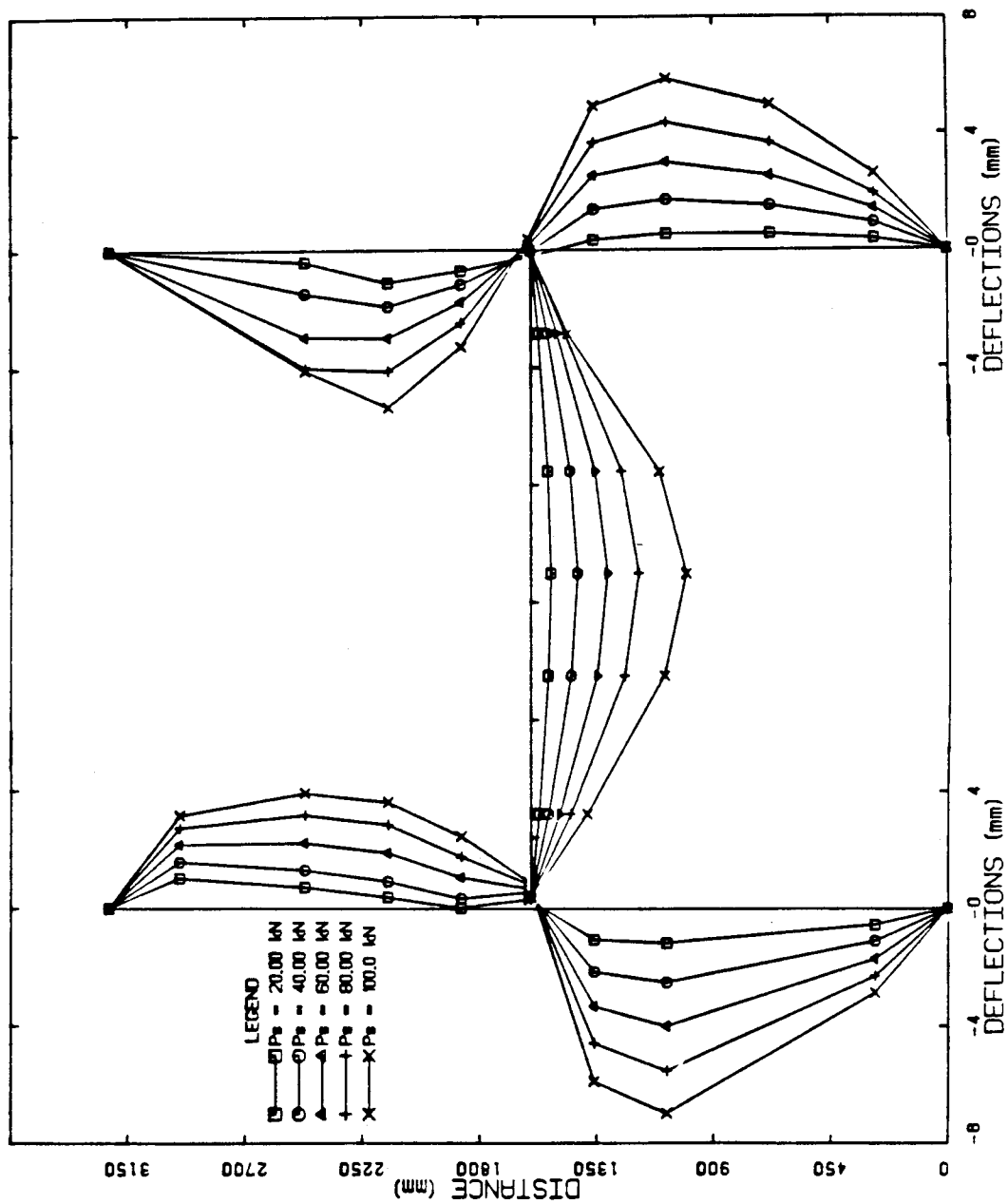


Figure 5.8 Deflected Shape for Specimen FRB100



Plate 5.6 Side View of Crack Distribution at Failure on Specimen FRB100

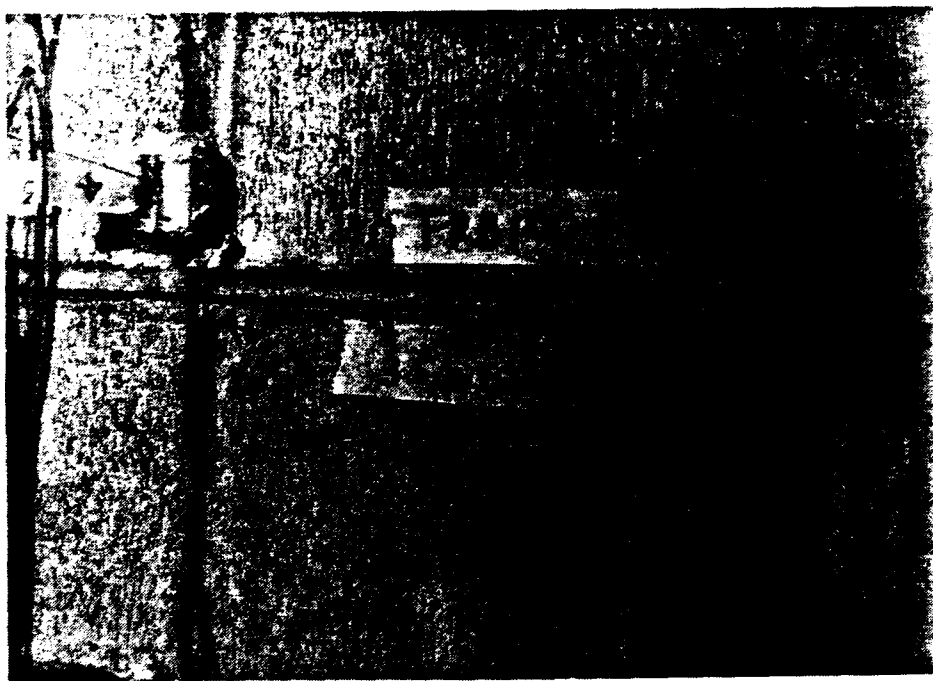


Plate 5.7 Back View of Crack Distribution at Failure on
Specimen FRB100

taken quite close to the joints where rotation was concentrated. The lateral restraint system at slab level kept joint displacement to a minimum, and the frames retained their symmetrical configuration during the tests.

5.5 Load-Rotation Characteristics

5.5.1 Type I Specimens

The load-rotation characteristics of the slab, lower wall and upper wall for Type I specimens are shown in Figures 5.9 to 5.12. The technique for attempting to prevent the slab from rotating until full axial load was applied (Plate 4.3) worked quite well for specimens with low axial load. However, it was more difficult to prevent the slab from rotating as high wall axial loads were applied. This difficulty accounts for the residual rotation in the slab at zero slab load in some of the curves. The construction technique of concreting the first course of the lower wall with the slab resulted in the slab and lower wall having similar rotations, especially for low slab load and low axial wall load. The upper wall, upon significant separation from the slab tended to reverse its rotational trend as further loading was applied. Generally, as the wall axial load increased, less ductility was observed in the behavior of the wall, as shown by comparing Figures 5.9 and 5.10. The unreinforced walls subjected to low axial load exhibited instability at failure.

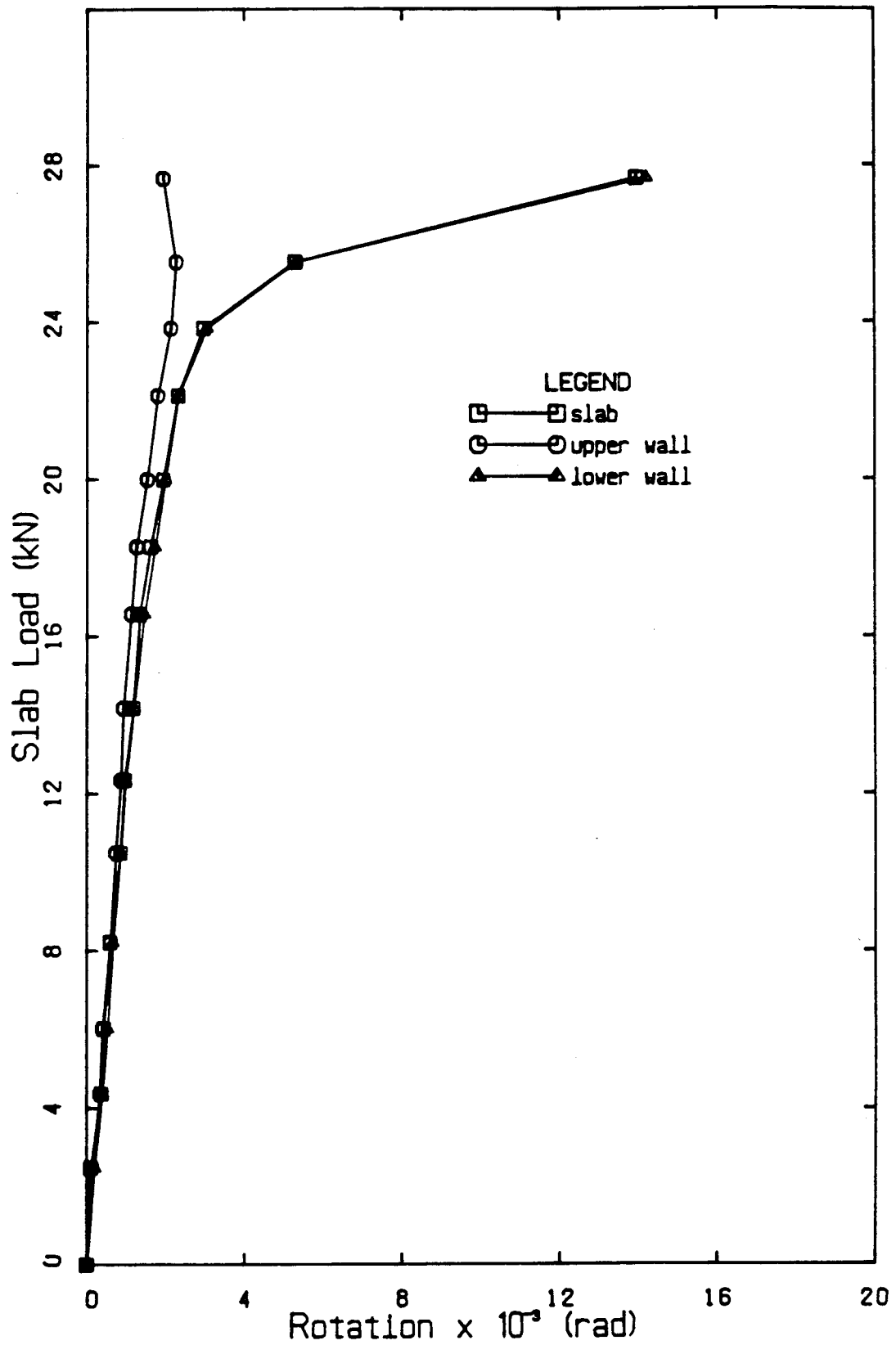


Figure 5.9 Load-Rotation Curves for Specimen WSA100

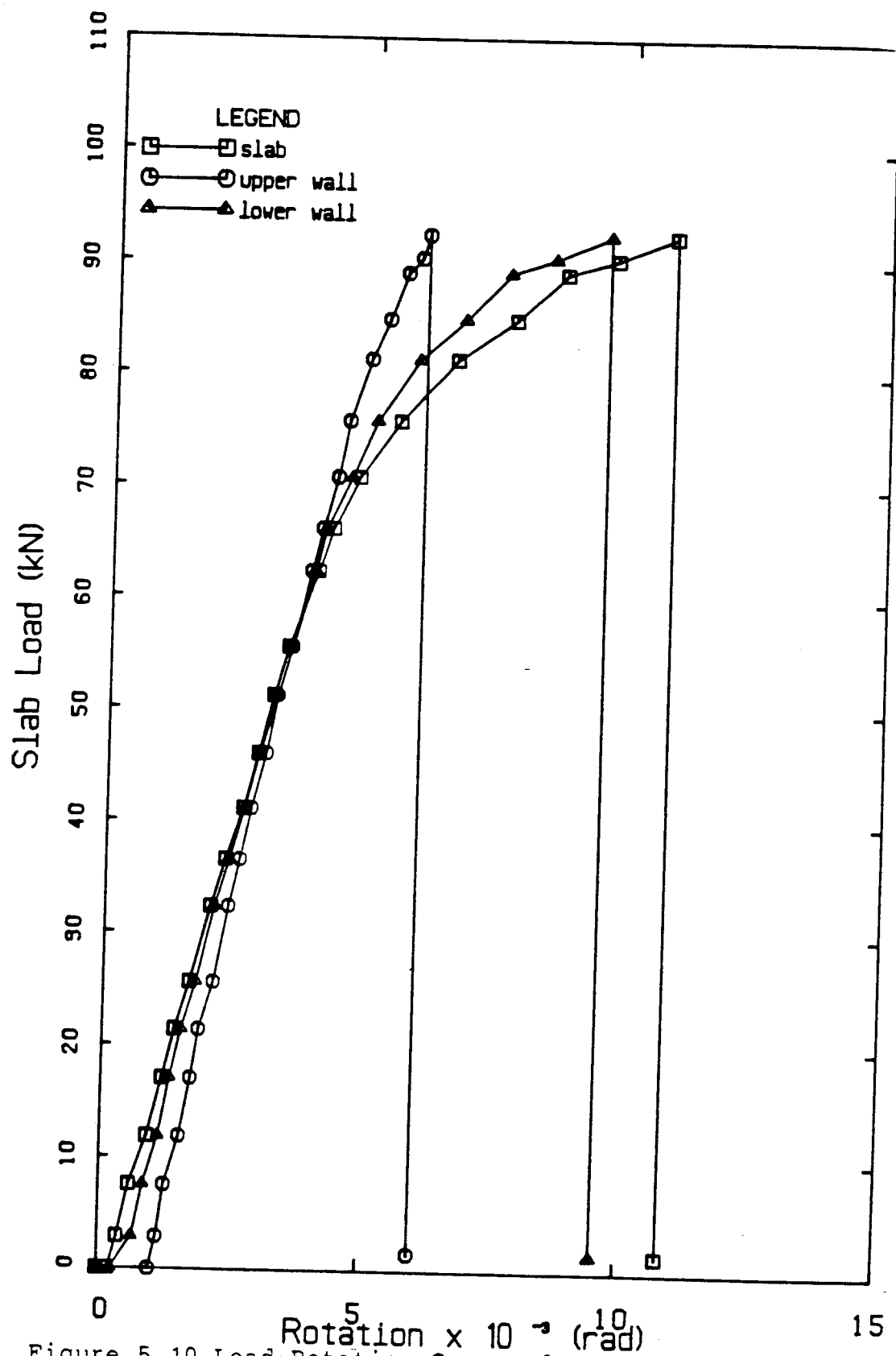


Figure 5.10 Load-Rotation Curves for Specimen WSA400

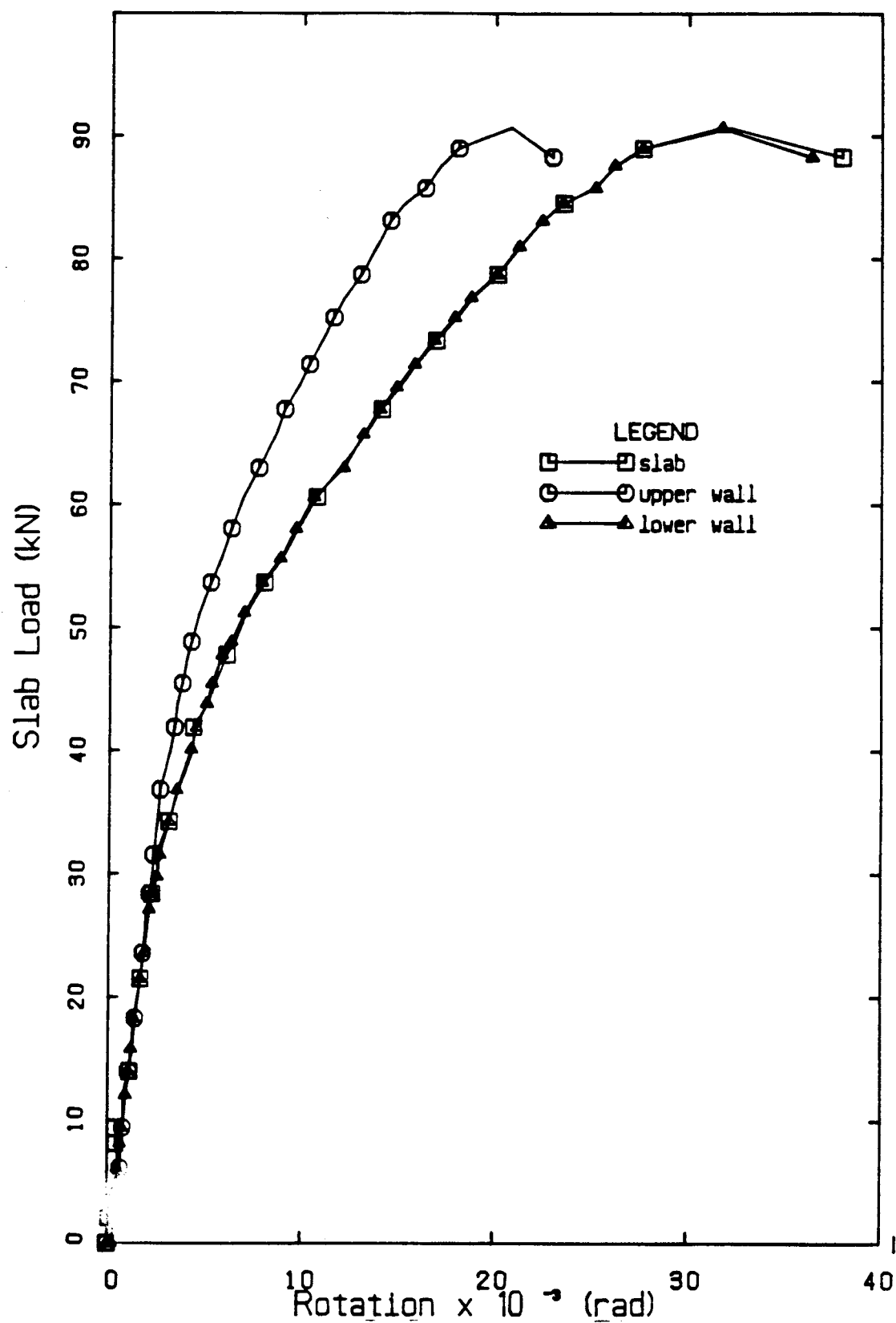


Figure 5.11 Load-Rotation Curves for Specimen WSB100

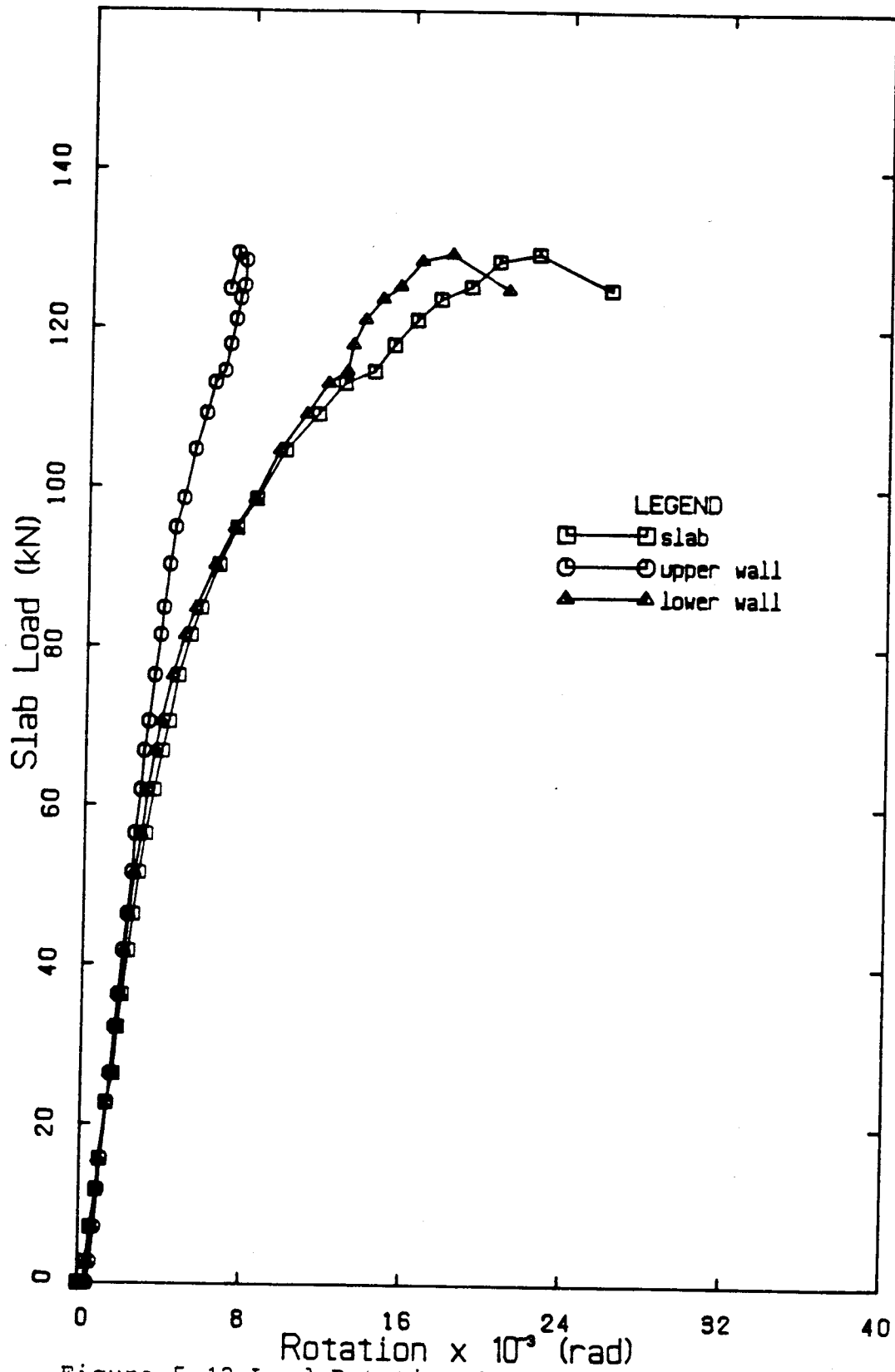


Figure 5.12 Load-Rotation Curves for Specimen WSB400

5.5.2 Type II Specimens

The load-rotation curves for Type II specimens are shown in Figures 5.13 to 5.16. These curves show similar characteristics to those of the Type I specimens, except for comparatively earlier reversal of curvature of the upper wall.

5.6 Wall Strain Distribution

Strain measurements obtained by means of a Demec gauge across the mortar joints on the face of the wall were not reliable when there was any significant amount of tension. This makes interpretation of these measurements difficult. Compression strain measurements were fairly close across the width of the wall, and strains of up to 0.0019 close to the failure of the full-scale specimens were measured. Some strain variation across the width of the wall as reported by Colville (1977) was also observed in this study.

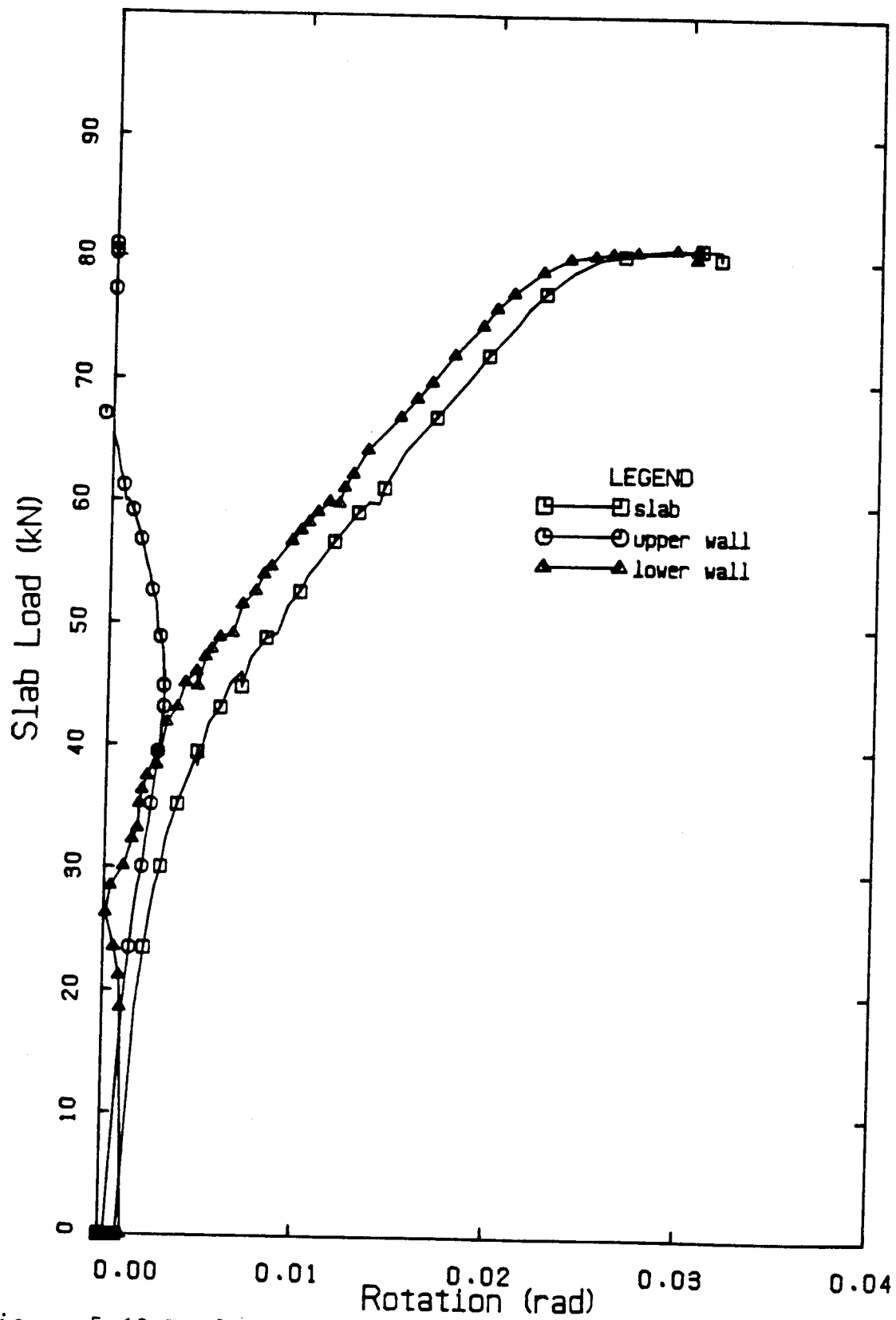


Figure 5.13 Load-Rotation Curves for Specimen FRA150 (North Wall)

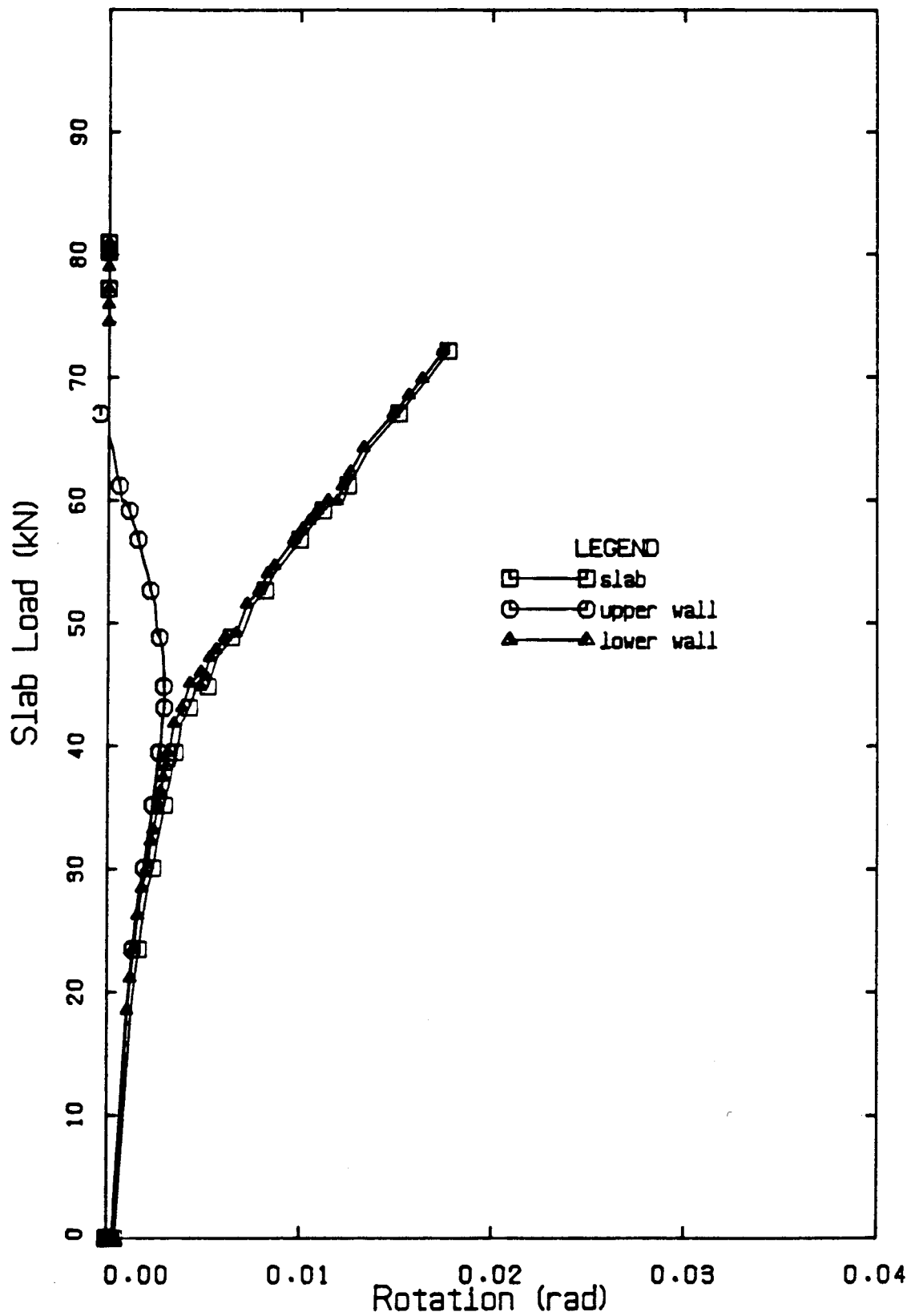


Figure 5.14 Load-Rotation Curves for Specimen FRA150 (South Wall)

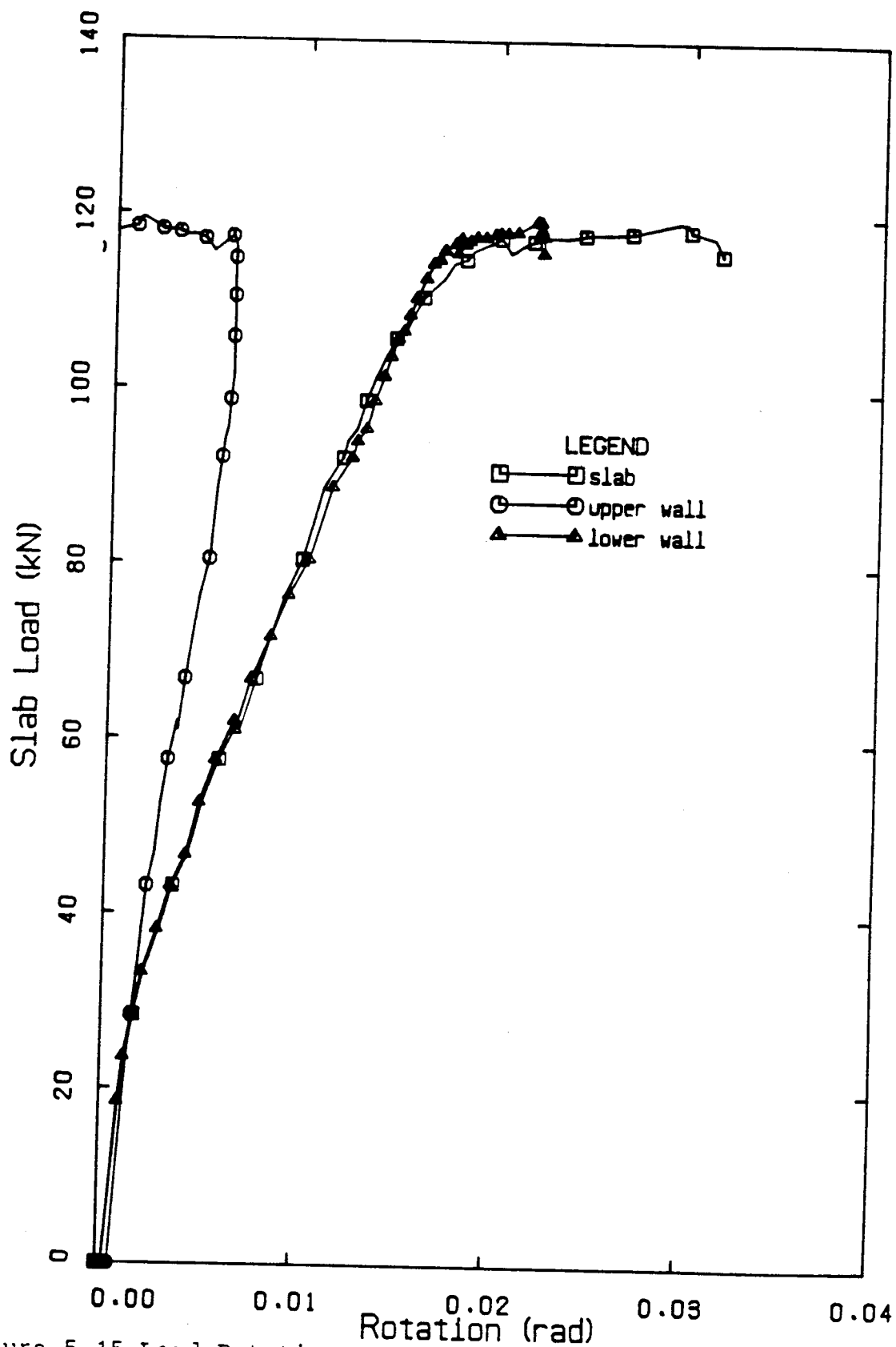


Figure 5.15 Load-Rotation Curves for Specimen FRB100 (North Wall)

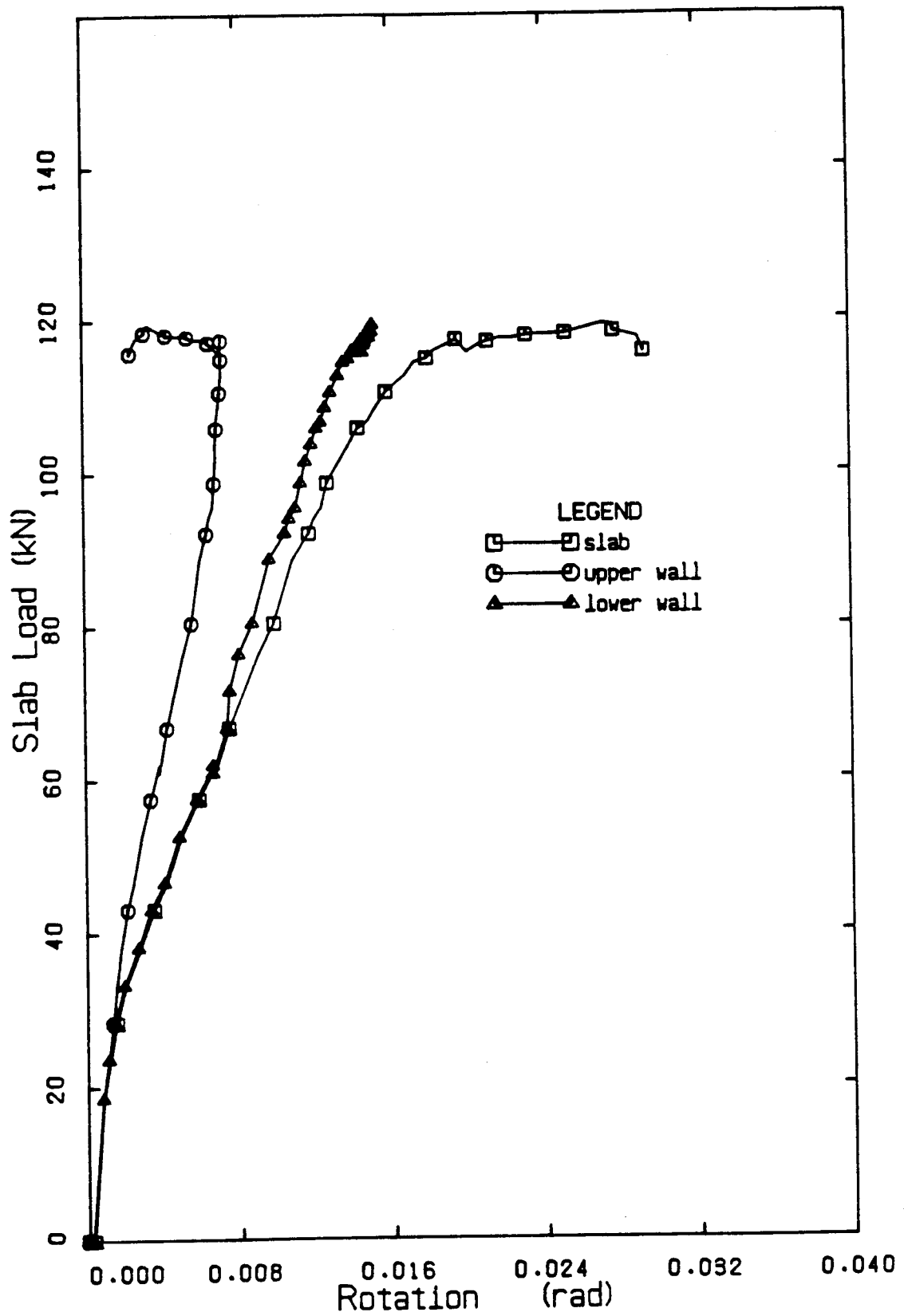


Figure 5.16 Load-Rotation Curves for Specimen FRB100 (South Wall)

6. DISCUSSION AND ANALYSIS OF TEST RESULTS

6.1 Introduction

In this chapter, test results are discussed in relation to proposed and existing theories for behavior and strength of masonry walls and masonry wall/slab joints. The first part discusses typical behavior and failure modes. Comparisons are made with theories proposed by Sahlin and with the CDC technique described in Chapter 3. Similarities and differences in the behavior of Type I and Type II specimens are examined in relation to these theories.

The second section examines various limit theories for assessing the ultimate strength of the walls at the wall/slab joint. The use of a simplified stress-strain diagram for masonry, with modifications for the effect of strain gradient, is employed in the interaction diagram approach. Colville's (1977) and Awni's (1980) method of estimating the ultimate joint eccentricity of a wall/slab frame are used to compare with test results obtained for the frame with unreinforced walls.

Finally, the relationship between the stiffness of the walls at the joint and the level of axial load on the walls is determined from frame model analysis of test specimens using a standard computer program. The results of the modelling compared with interaction curves and CDC predictions lead to proposed equations for estimating stiffnesses at failure for reinforced and unreinforced concrete masonry walls, within the limits of the investigations. An example of a design of a typical external

wall in a 8-storey masonry building illustrates the applicability of the design procedure.

6.2 Comparison of Test Results with Proposed Theories

6.2.1 Typical Behavior and Failure Modes

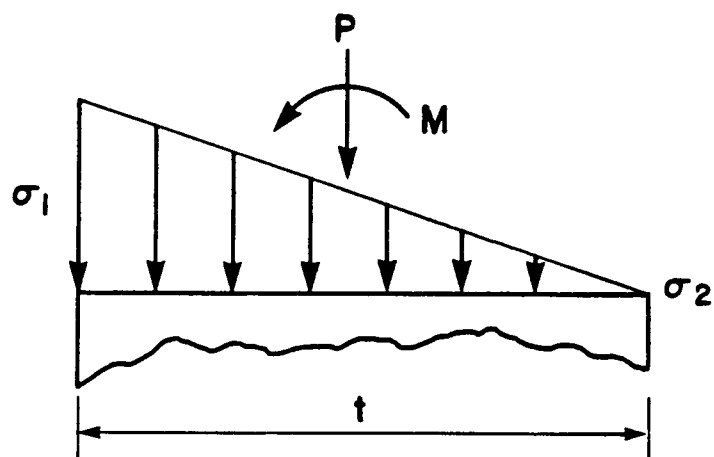
The behavior at a wall/slab joint has been described by Sahlin (1959) and further verified by Ferguson (1979) and Pacholok (1980). Ferguson classified Sahlin's description of failure modes into tension and compression types, and a possible combination of both. The tension type failure mode is characterized by wide cracking at the joint between the slab and the upper and lower walls, usually leading to instability. This type of failure was observed in both Type I and Type II specimens with unreinforced walls subjected to wall axial loads of 100 kN and 150 kN respectively. Type I and Type II specimens with reinforced walls behaved similarly, but with lesser crack width at the joint because of the restraint offered by continuous reinforcement. It will be recalled that the construction procedure for the specimens allowed the slab concrete to fill the top course in the lower wall. Thus the joint opening in the lower wall occurred between the first and second courses in the lower walls. As loading progressed, joint cracking progressed upwards into the first course. This failure mode is recognized by Sahlin as occurring when the limiting joint rotation is reached or approached.

The compression type failure mode in unreinforced wall specimens is characterized by a crushing failure of the

walls when the limiting edge stress is reached in the upper or lower wall. Type I specimens with reinforced walls exhibited this type of behavior in combination with significant cracks at critical joints in the upper and lower walls. Specimen WSA400 failed suddenly in crushing of the walls after the crack width measured at the critical location in the lower wall was more than 1.40 mm. Sahlin recognizes these failure modes as the attainment of ultimate edge stress before or after the limiting slab restraining moment is attained. Specimens WSB100 and WSB400 had obvious edge crushing in the course immediately below the slab on the compression side as shown in Plate 5.2. Frame FRB100 exhibited this type of behavior by local crushing at one edge of the lower wall.

Ferguson's classification based on relating axial wall load to the balanced load, P_{bal} , and the stress distribution on the cross section of the wall, as shown in Figures 6.1 to 6.3, was also examined in relation to the behavior of the test specimens. Calculations based on an effective solid thickness of 56% for the unreinforced walls give balanced loads of 540 kN and 1023 kN for the unreinforced and reinforced walls respectively. Based on these calculations, a tensile mode of failure would be expected in all the specimens. However, as discussed earlier, combination type failure modes were observed in the specimens with reinforced walls, even at a 100 kN wall axial load.

In all specimens, no relative rotation was recorded at the joint until the slab load reached 30 to 50% of its maximum value, depending on the wall axial load. Slight



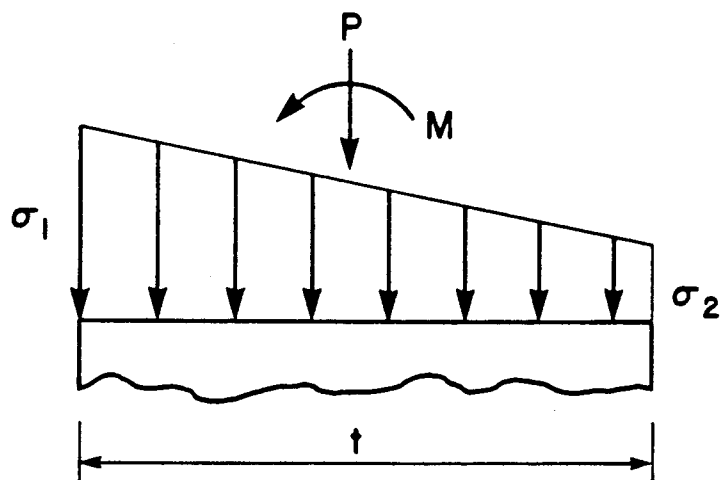
$$P = P_{bal}$$

$$M = M_{PL}$$

$$\sigma_1 = f'_m$$

$$\sigma_2 = 0 \quad \theta = 0$$

Figure 6.1 Internal Stress Distribution on a Wall Cross-Section Having a Balanced Failure (Ferguson, 1979)



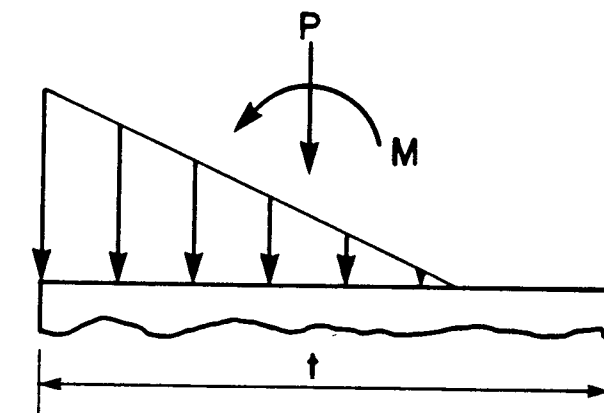
$$P > P_{bal}$$

$$M = M_{PL}$$

$$\sigma_1 = f'_m$$

$$\sigma_2 > 0$$

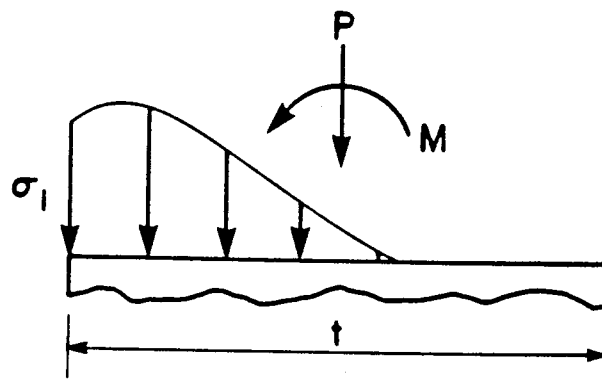
Figure 6.2 Internal Stress Distribution on a Wall Cross-Section Having a Compression Failure (Ferguson, 1979)



$$P < P_{bal} \quad M = M_{PL}$$

$$\sigma_l = f'_m \quad 0 < \theta < \theta_{ult}$$

(a) Stresses when $\theta < \theta_{ult}$



$$P < P_{bal} \quad M = M_{PL}$$

$$\sigma_l < f'_m \quad 0 < \theta = \theta_{ult}$$

(b) Stresses when $\theta = \theta_{ult}$

Figure 6.3 Internal Stress Distribution on a Wall Cross-Section Having a Tension Failure (Ferguson, 1979)

differences in rotation then became noticeable between the upper wall and the slab (Figures 5.11 to 5.19). Again, because of the construction procedure, the lower wall rotation at the joint was quite similar to that of the slab.

The CDC technique described in Chapter 3 was used to calculate upper wall rotations for comparison with measured values. Figures 6.4 to 6.9 show the theoretical moment rotation curves based on bi-linear stress-strain relationships for masonry as described in Chapter 3. Maximum strains of 0.002 and 0.0015 obtained from prism tests were employed for unreinforced and reinforced walls, respectively.

The moments in the upper and lower walls of the Type I specimens were derived from the strain measurements on the joint restraint angles and considerations of equilibrium of the structure. The strain measurements on the end restraint of the north upper wall of specimen FRA150 showed significant difference from each other. The maximum moment in the upper wall as calculated from the strain measurements was therefore quite low compared to all other upper wall measurements, and could therefore be regarded as unrepresentative. This result is therefore omitted in the plots of Figure 6.8. The lower wall moments of the frame specimens were estimated from the computer frame model analysis described in Section 6.3 and the measured upper wall moments. This was because of the unreliable nature of the strains measured on the reaction angles on the lower walls.

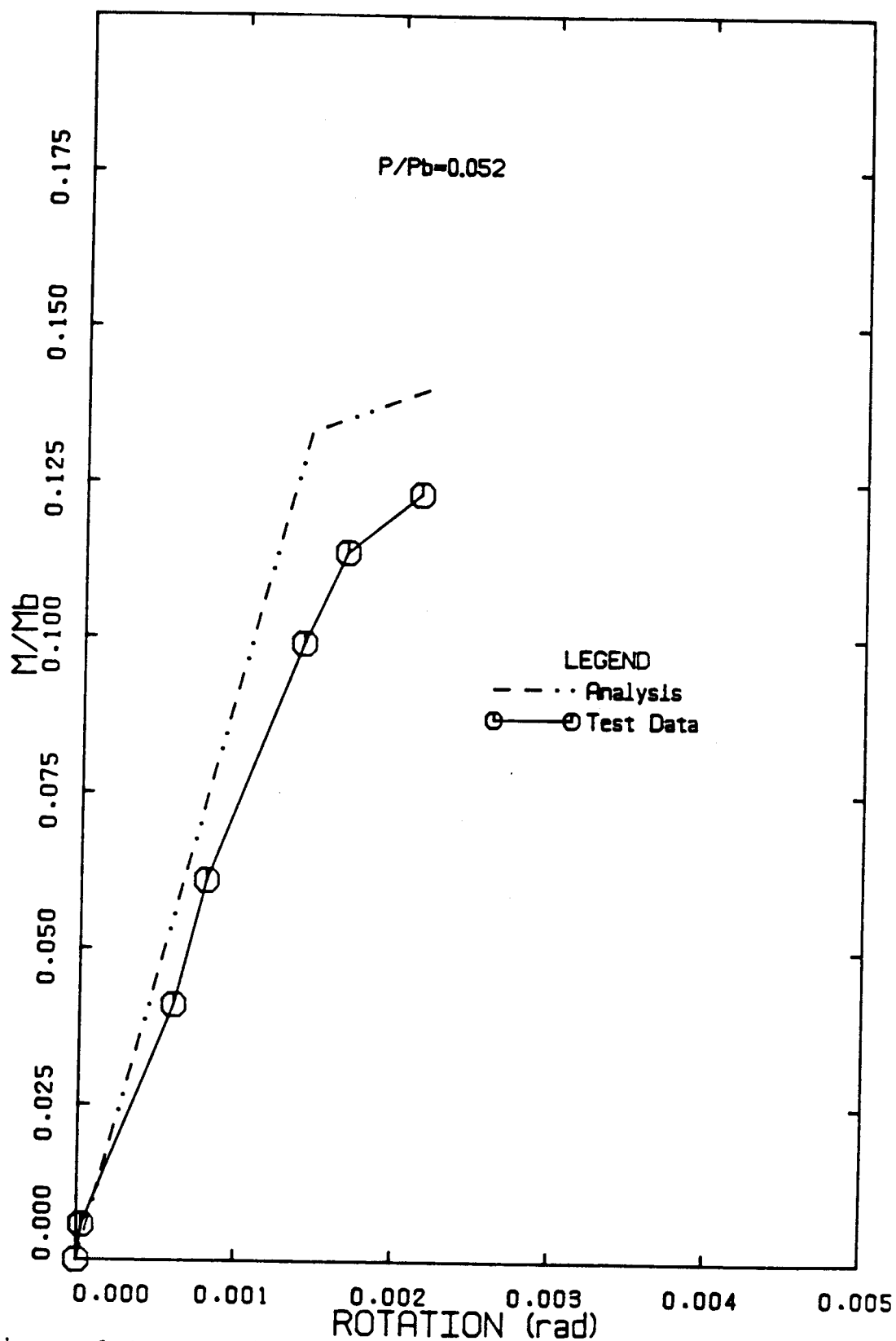


Figure 6.4 Comparison of Moment-Rotation Behavior of Upper Wall of Specimen WSA100

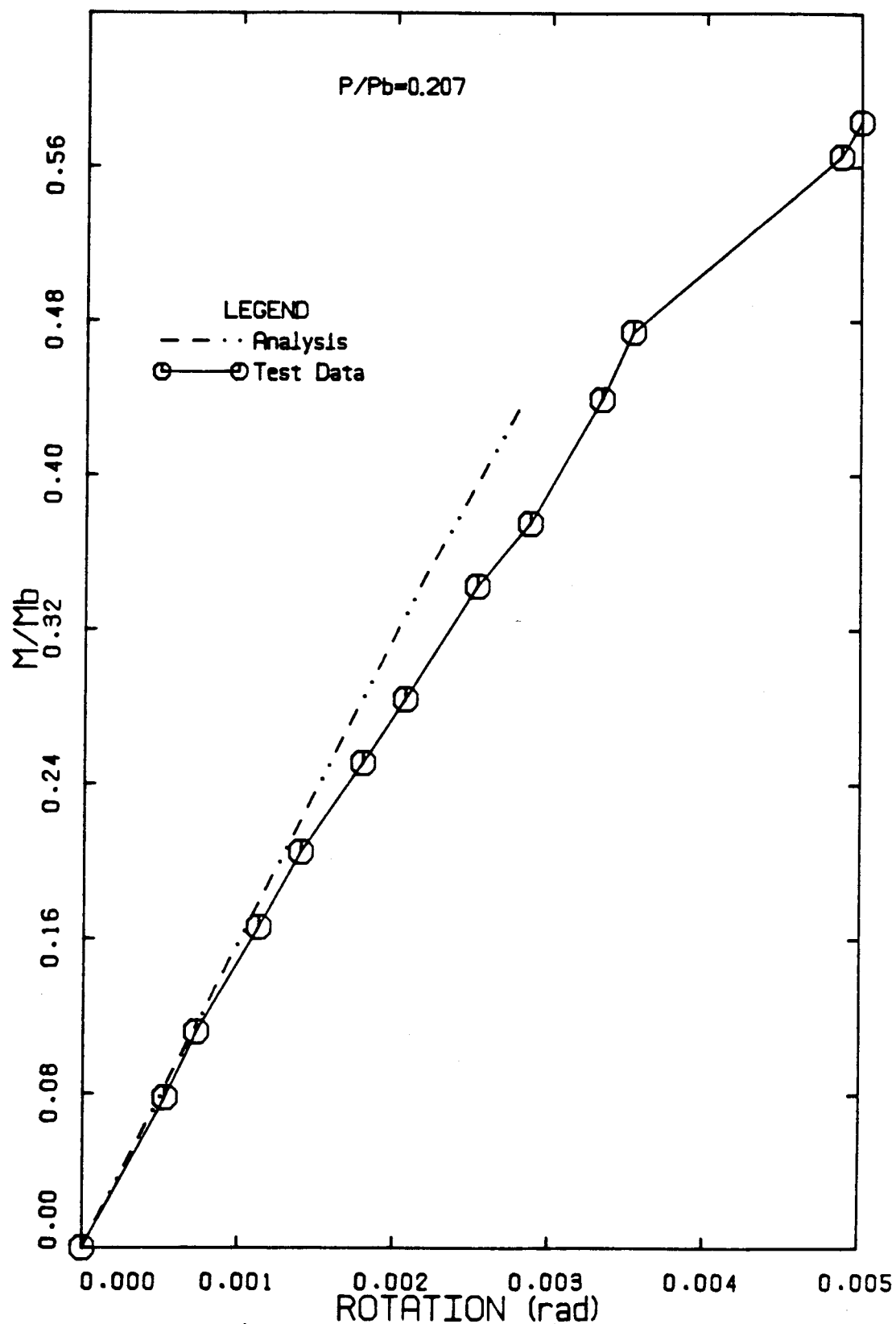


Figure 6.5 Comparison of Moment-Rotation Behavior of Upper Wall of Specimen WSA400

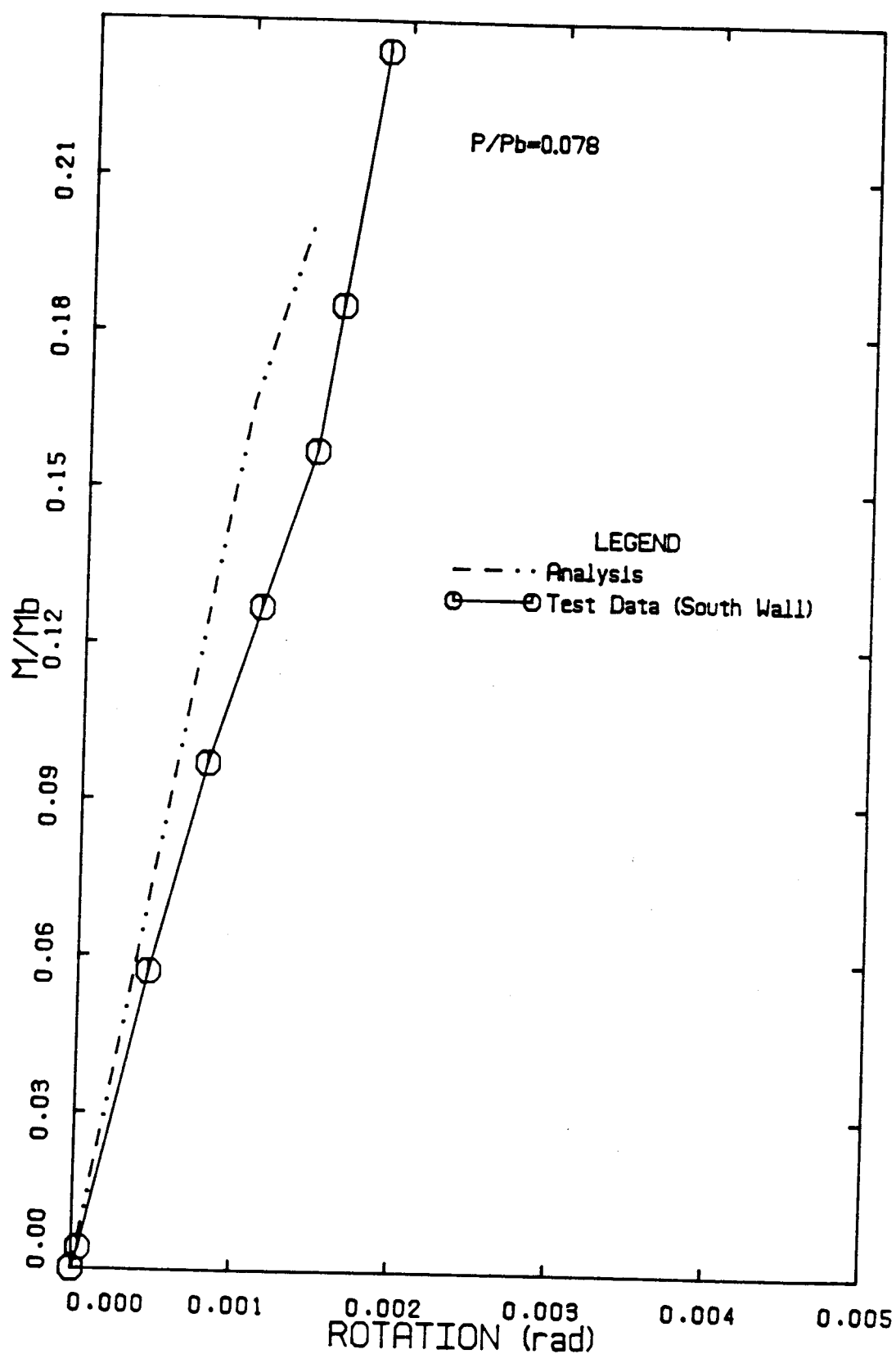


Figure 6.6 Comparison of Moment-Rotation Behavior of Upper Wall of Specimen FRA150

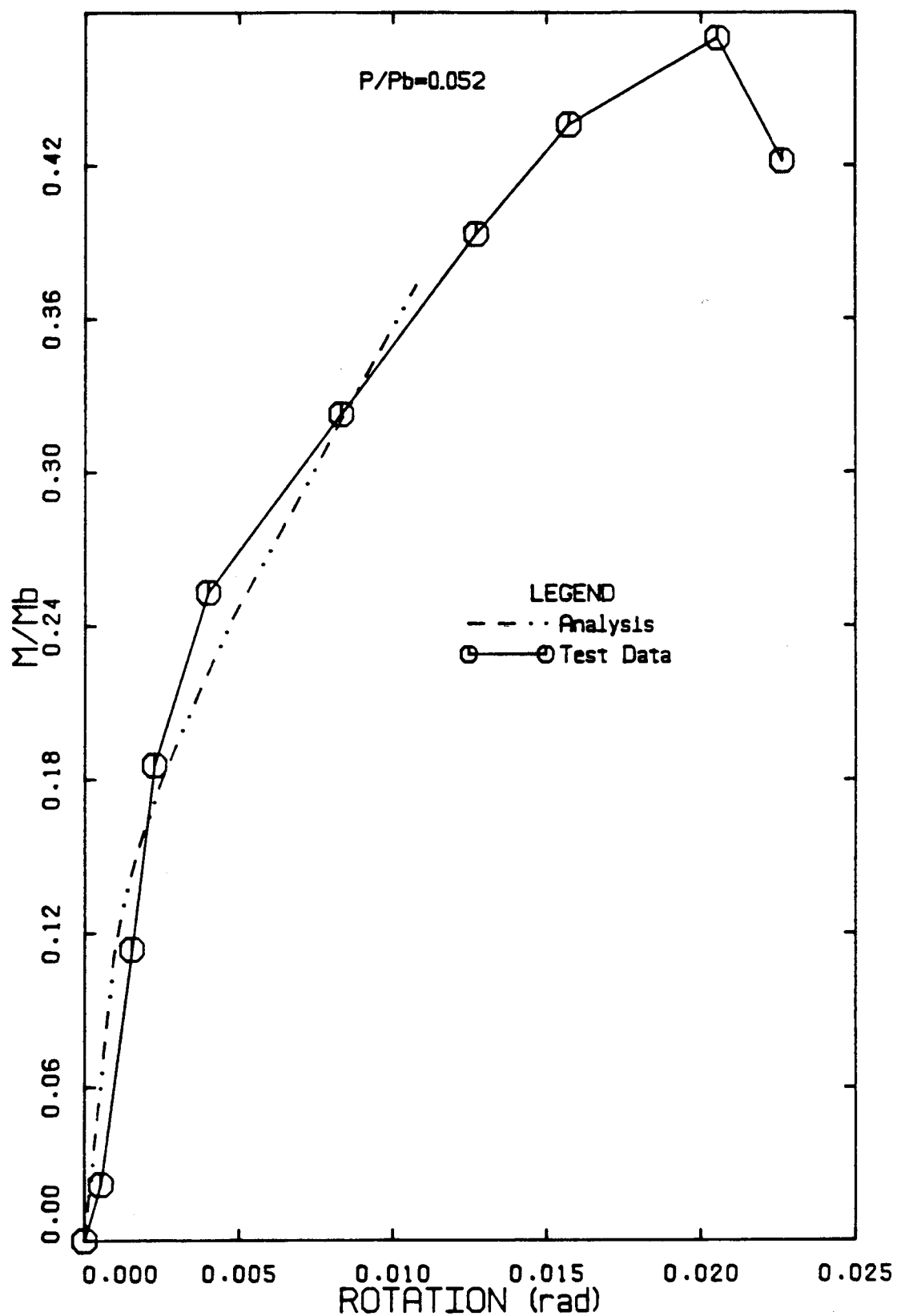


Figure 6.7 Comparison of Moment-Rotation Behavior of Upper Wall of Specimen WSB100

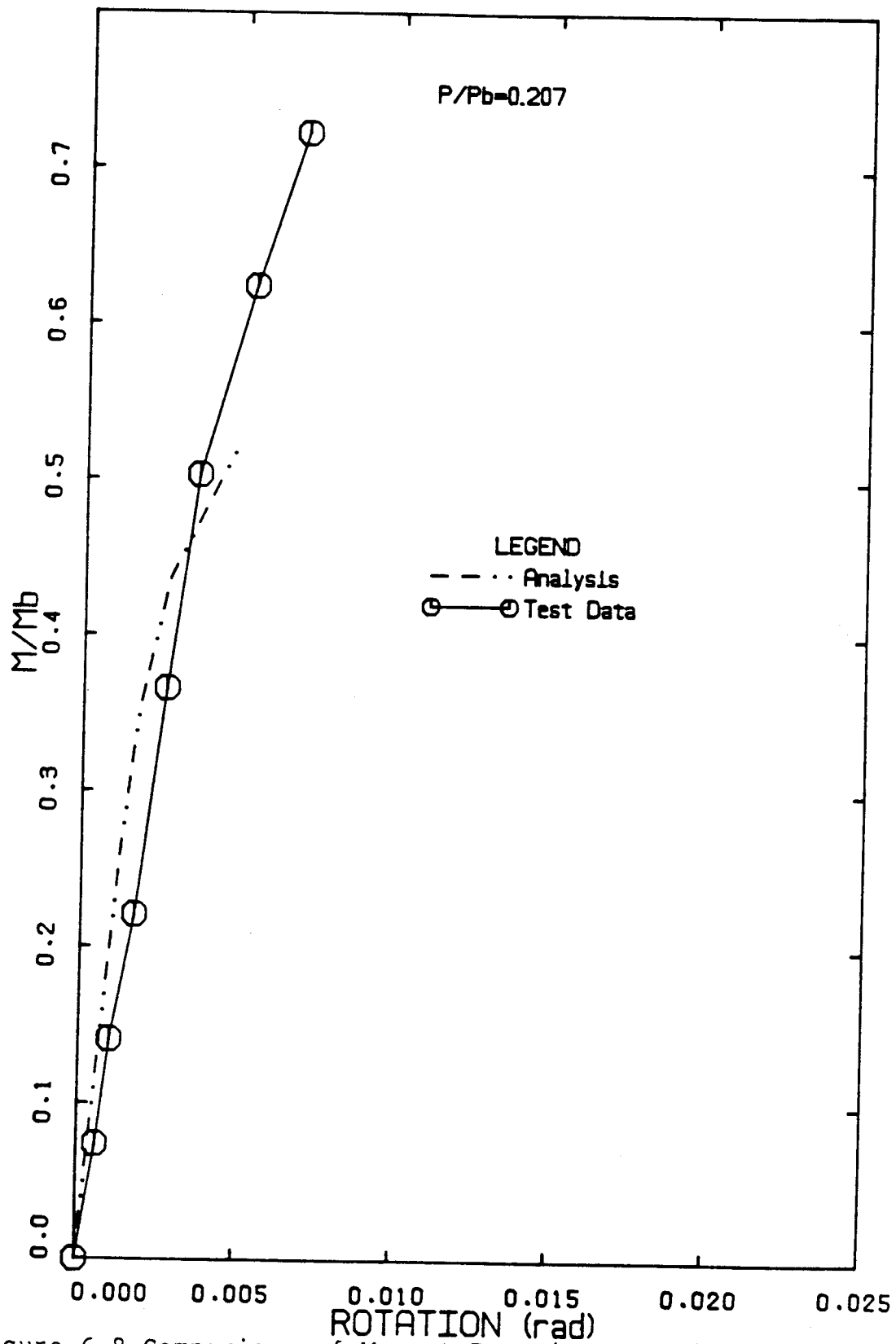


Figure 6.8 Comparison of Moment-Rotation Behavior of Upper Wall of Specimen WSB400

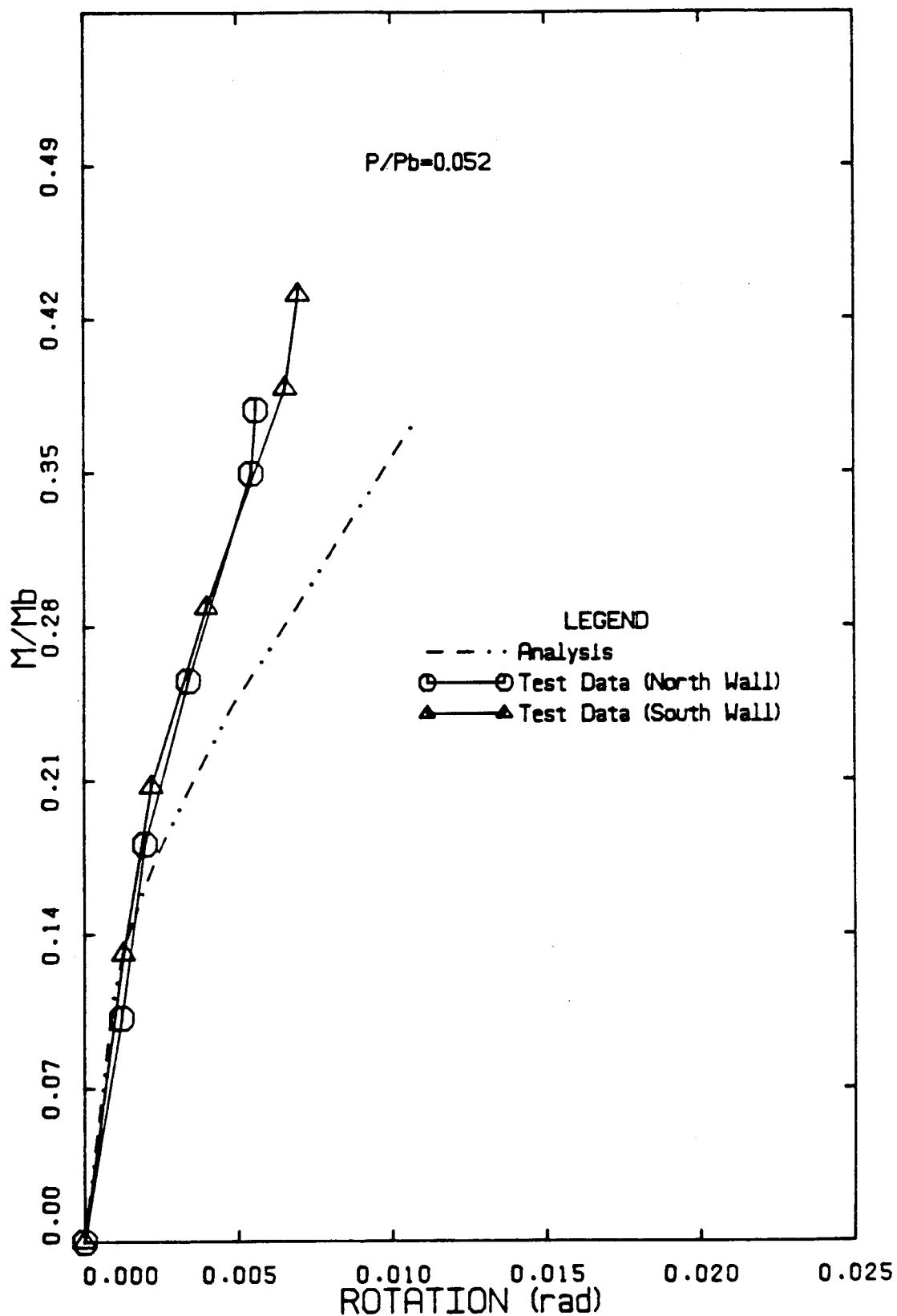


Figure 6.9 Comparison of Moment-Rotation Behavior of Upper Wall of Specimen FRB100

It is observed that the analysis prediction of initial stiffness for all the specimens is fairly satisfactory. Comparison of cracked wall stiffnesses indicated that the unreinforced walls had lower stiffnesses while the reinforced walls showed somewhat higher stiffnesses than predicted by theory. Also, as the wall axial load increased, closer correlation with theory was observed for all specimens. It should be noted that the wall axial load acting on an accidental eccentricity on the wall usually resulted in some initial rotation in the wall which could result in some loss of stiffness. This might be especially so in unreinforced walls carrying low axial load, before application of slab load. As the upper wall separated from the slab at the joint, reversed curvature trend of the upper wall was observed in most cases at the joint. This was likely due to some yielding and movement at the joint, as the limiting joint cracking at which the upper wall separated from the slab was reached.

Measured maximum rotation was close to predicted in specimens with with low wall axial load showing this phenomenon of trend of reversal in curvature. For specimens with higher wall axial load, measured rotations were higher than predicted by the CDC technique. This is probably due to the enhancement of the tensile strength of masonry because of the higher precompression.

6.2.2 Ultimate Strength

Interaction curves based on values of α of 0.28 and 0.50 were used to compare wall maximum moment in specimens

with unreinforced and reinforced walls, respectively. These values of α correspond to ungrouted and fully grouted wall cross sections. Figure 6.10 compares wall ultimate strengths using interaction curves drawn for unreinforced 200 mm thick walls, with modification factors, α , of 1.0, 1.5 and 2.0 applied to prism f'_m . In the case of the lower walls, moment capacity is plotted against total axial load at failure. The figure shows results from the present study together with those from the tests conducted by Ferguson (1979) and Pacholok (1980). The results of Ferguson and Pacholok are adjusted to the value of f'_m in the present study. Figure 6.11 shows test results for reinforced 200 mm thick walls compared with interaction curves based on a value of α equal to 0.50 and gross area reinforcement ratio of 0.00374. Test results of Ferguson and Pacholok are shown on interaction curves in Figure 6.12 based on a value of α equal to 0.41 and gross area reinforcement ratio of 0.00108. In general, it is observed that interaction curves based on α equal to 1 is a good lower limit for strength when eccentricity to thickness ratio, e/t , exceeds $1/3$, but is conservative for e/t ratios between $1/6$ and $1/3$ for unreinforced and reinforced walls.

Maurenbrecher's 'equilibrium failure' theory was used to calculate maximum slab loads on Type I specimens with unreinforced walls. There is good correlation between calculated and measured loads. Details of this application are given in Appendix C.1.

The method proposed by Colville (1979) and later modified by Awni (1980) for estimating ultimate joint

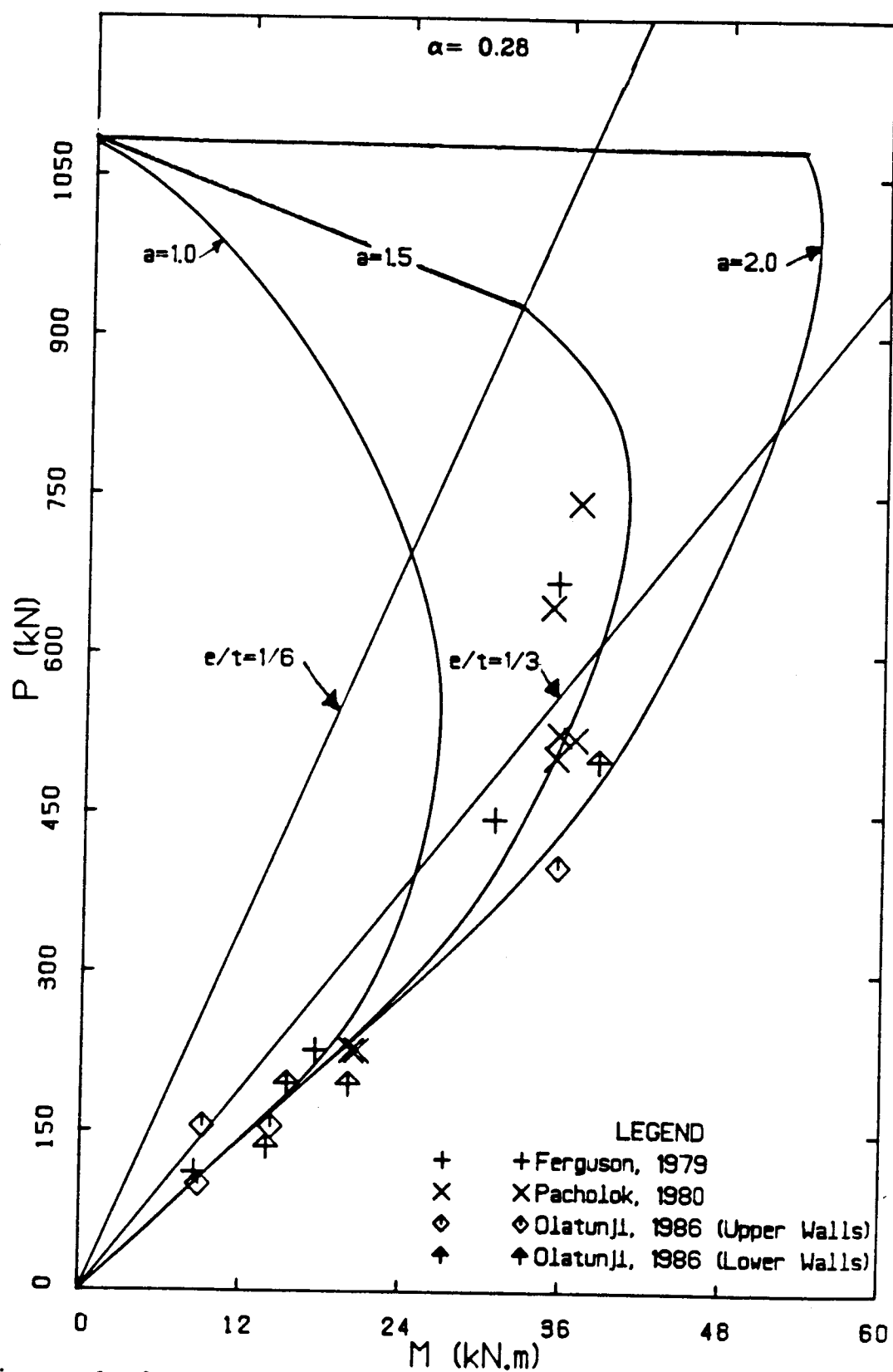


Figure 6.10 Ultimate Strengths Using Interaction Curves for Unreinforced 200 mm Walls

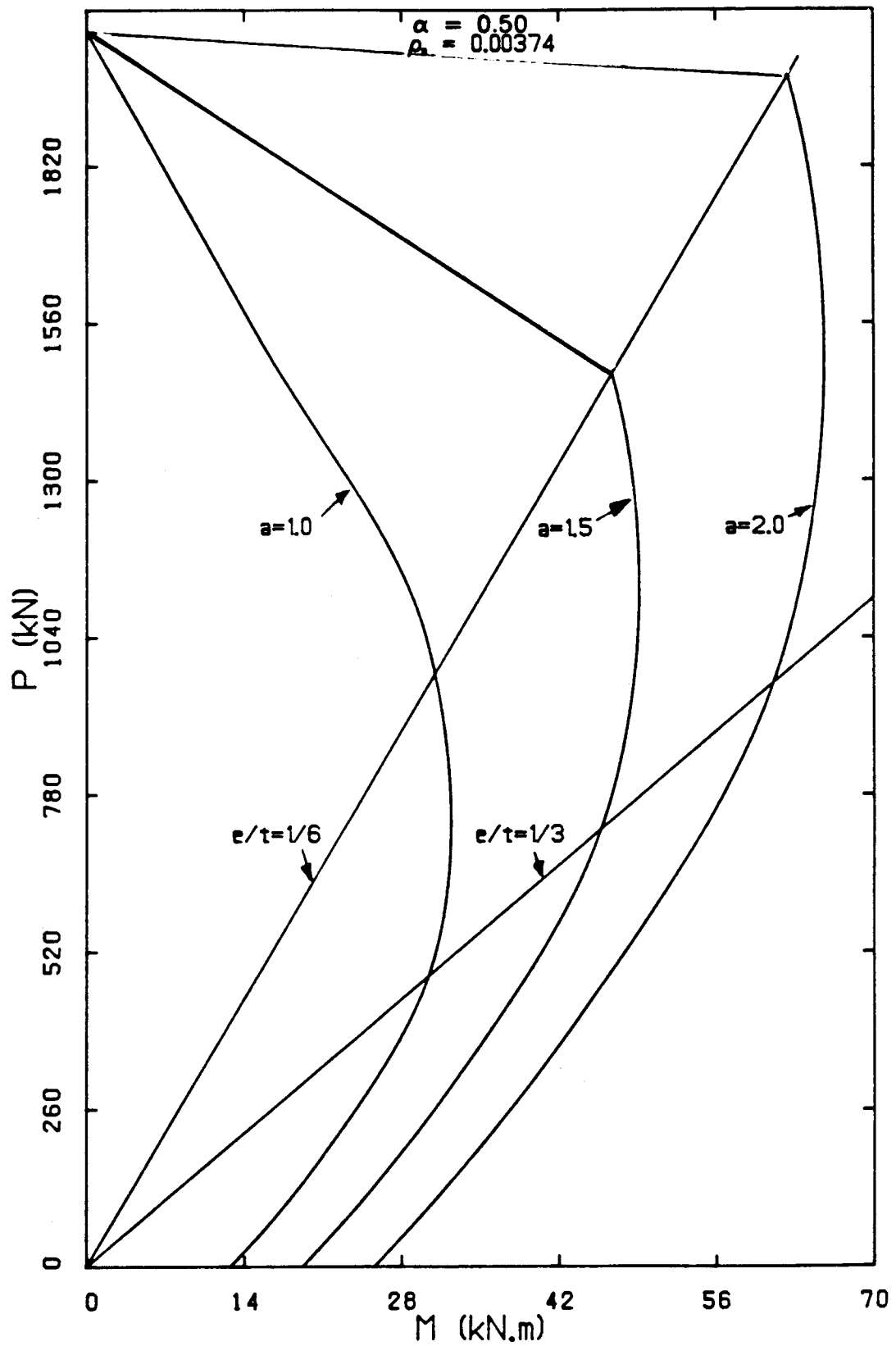


Figure 6.11 Ultimate Strengths Using Interaction Curves for Reinforced Fully Grouted 200 mm Walls

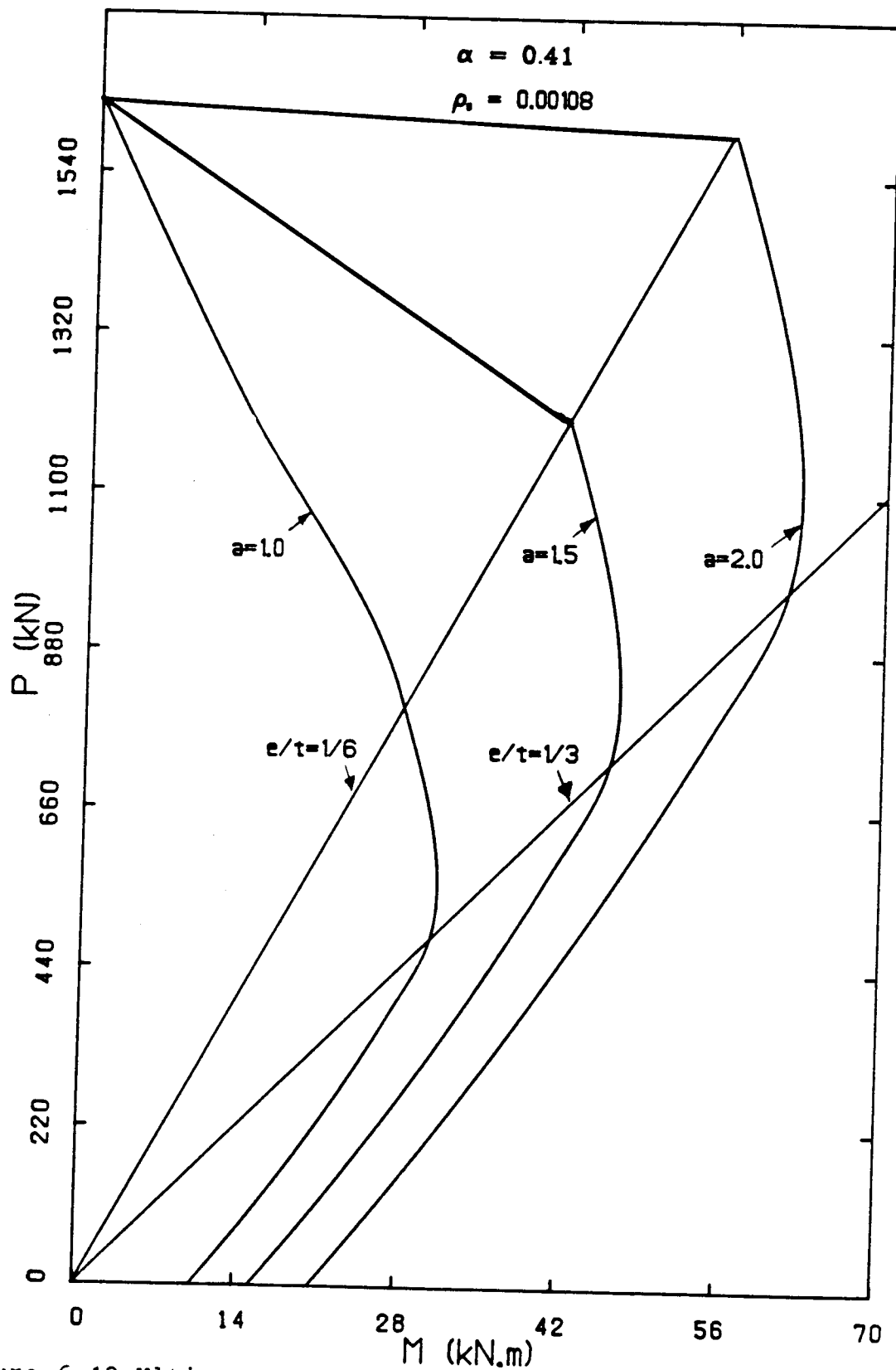


Figure 6.12 Ultimate Strengths Using Interaction Curves for Reinforced Partially Grouted 200 mm Walls

eccentricity at a wall/slab joint for frames with unreinforced walls was used to compare test results obtained for Specimen FRA150. Awni's equation gives ultimate joint eccentricity of about 40% of that measured in the test. Colville's method gives a closer result in this case. Details of application of this methods are given in Appendix C.2.

The CDC method gives maximum moments in the upper wall lower than measured in most of the tests. Comparison of ultimate strength predictions is discussed in Section 6.4

6.3 Effective Wall Stiffness Approach

Masonry wall/slab frames can be analysed by means of a standard frame analysis program using appropriate values of stiffnesses for the upper and lower walls at failure of a wall/slab joint. A model analysis was carried out on the test specimens using a standard computer program, PFT, program for analysing rigid frames. This program is the version of the "Plane Frame and Truss Program" (Beaufait et al., 1970), available at the University of Alberta. The program computes end moments, end shears and end axial forces for each member in a frame. It also computes horizontal deflection, vertical deflection and rotation at each joint.

The specimens were modelled to output the rotation and deflection at the wall/slab joint and horizontal deflections at or near the centres of the upper and lower walls. The forces measured at the joint during testing were applied as external loads. Figures 6.13 and 6.14 show the PFT models

for Types I and II specimens.

The major variables in the analysis were the modulus of elasticity, E_m , the effective moment of inertia of the upper wall, I_{eu} , and the effective moment of inertia of the lower wall, I_{el} . E_m was obtained from a regression analysis of values obtained from tests on three-block prisms as discussed in Chapter 5. The resulting value of E_m used was $750f'_m$ (7650 MPa) for unreinforced walls, and $950f'_m$ (9690 MPa) for reinforced walls. The cracked stiffness of the slab was used in the analysis. The values of I_{eu} and I_{el} were obtained by a trial and error procedure relating the deflected shape and rotations given by the program to the measured values. The nodes D_t , D_j , and D_b at which the deflections and rotations were computed are as shown in Figures 6.13 and 6.14. Tables 6.1 to 6.8 show the comparison of values predicted by PFT with those actually measured.

Relative rotation between the upper wall and the slab increased more rapidly when the crack width at the critical location in the lower wall varied between 0.13 mm and 0.38 mm, depending on the wall axial load in specimens with unreinforced walls. This crack width was up to 0.5 mm or more when the walls were reinforced. It appeared that the trend of curvature reversal of the upper wall coincided with this crack limit, which signified the attainment of maximum moment at the wall/slab joint.

Awni(1980), Chandrakeerthy and Hendry (1983) reported that when the ratio of two times slab to wall stiffness, K , greatly exceeded 1, the maximum joint moment at an unreinforced masonry wall/slab joint might not be greater

Table 6.1 Measured and Computed Deflections and Rotations
for Specimen WSA100

Incr	P _u kN	P _L kN	M _{s1} kN.m	M _{uw} kN.m	M _{lw} kN.m	I _{eu} $\times 10^8$ mm ⁴	I _{el} $\times 10^8$ mm ⁴	θ_{s1} radians	Dt ⁺ mm	Dj ⁺ mm	Db ⁺ mm	Comments
12	105.5	119.9	12.04 12.20	3.72 3.88	8.33 8.41	2.70	4.70	0.00093 0.00111	0.45 0.20	0.75 -0.20	0.11 -0.47	measured computed
15	105.5	125.5	16.99 15.10	6.05 5.20	10.35 9.90	1.55	3.75	0.00195 0.00210	1.12 0.93	0.11 0.43	-0.47 -0.34	measured computed
18	105.5	133.2	21.74 19.82	7.48 6.79	13.34 13.03	0.90	1.85	0.00530 0.00512	1.78 1.73	-0.09 0.28	-1.44 -1.35	measured computed
22	105.5	135.9	23.90 22.00	8.92 8.36	14.01 13.66	0.56	0.89	0.01400 0.01050	3.44 3.30	-0.37 -0.24	-3.96 -3.37	measured computed

* PFT nodes

Table 6.2 Measured and Computed Deflections and Rotations
for Specimen WSA400

Incr	P _u kN	P _L kN	M _{s1} kN.m	M _{uw} kN.m	M _{lw} kN.m	I _{eu} $\times 10^8$ mm ⁴	I _{el} $\times 10^8$ mm ⁴	θ_{s1} radians	Dt ⁺ mm	Dj ⁺⁺ mm	Db ⁺⁺ mm	Comments
14	404.7	432.6	21.80 19.90	10.1 9.6	10.80 10.30	4.00	4.40	0.00168 0.00166	0.52	0.03	-0.48	measured computed
18	404.7	453.0	39.20 37.30	17.3 17.3	19.90 20.00	4.00	4.60	0.00292 0.00304	0.91	-0.01	-0.92	measured computed
23	404.7	477.7	60.10 58.20	26.8 27.4	30.00 30.8	4.20	4.40	0.00476 0.00475	1.24	-0.27	-1.62	measured computed
29	404.7	499.5	78.60 76.80	35.6 36.8	38.60 40.06	0.56	0.89	0.01080 0.01080	3.23	-0.02	-3.27	measured computed

* LVDTs did not register deflections

Table 6.3 Measured and Computed Deflections and Rotations
for Specimen FRA150 (North Wall)

Incr	P _u kN	P _L kN	M _{sl} kN.m	M _{uw} kN.m	M _{tw} kN.m	I _{eu} $\times 10^9$ mm ⁴	I _{el} $\times 10^9$ mm ⁴	θ_{sl} radians	D _t mm	D _j mm	D _b mm	Comments
12	155.5	181.0	18.73	6.19	12.53	1.70	3.50	0.00257 0.00252	0.15 0.76	0.20 0.03	-0.64 -0.69	measured computed
16	155.5	187.0	24.58	4.64 7.23	17.14	1.70	1.00	0.00300 0.00290	0.43 0.83	0.18 -0.03	-0.75 -0.83	measured computed
18	155.5	190.2	26.44	6.86 9.17	17.27	1.80	3.40	0.00352 0.00357	0.60 1.05	0.25 0.01	-0.90 -0.99	measured computed
22	155.3	195.6	29.32	9.16 10.47	18.84	1.45	2.50	0.00514 0.00518	0.87 1.41	0.34 -0.18	-1.51 -1.55	measured computed

Table 6.4 Measured and Computed Deflections and Rotations
for Specimen FRA150 (South Wall)

Incr	P _u kN	P _L kN	M _{sl} kN.m	M _{uw} kN.m	M _{tw} kN.m	I _{eu} $\times 10^9$ mm ⁴	I _{el} $\times 10^9$ mm ⁴	θ_{sl} radians	D _t mm	D _j mm	D _b mm	Comments
12	155.5	181.1	18.77	5.92 6.07	12.70	1.70	3.50	0.00239 0.00253	-1.04 -0.72	-0.05 0.03	0.45 0.73	measured computed
16	155.5	187.1	24.37	9.58 7.32	17.05	1.70	4.00	0.00313 0.00301	-1.38 -0.90	0.03 -0.02	0.67 0.83	measured computed
18	155.3	190.3	26.48	11.32 9.16	17.32	1.80	3.40	0.00753 0.00357	-1.57 -1.05	0.03 0.00	0.78 1.00	measured computed
22	155.3	195.6	29.77	14.30 10.89	18.94	1.45	2.65	0.00523 0.00513	-1.90 -1.62	0.04 -0.18	1.16 1.32	measured computed

Table 6.5 Measured and Computed Deflections and Rotations
for Specimen WSB100

Incr	P _u kN	P _L kN	M _{s1} kN.m	M _{uw} kN.m	M _{lw} kN.m	I _{eu} $\times 10^9$ mm ⁴	I _{el} $\times 10^9$ mm ⁴	θ_{s1} radians	D _t mm	D _j mm	D _b mm	Comments
1R	106.3	129.9	20.04 20.04	6.95 7.16	12.31 12.89	2.00	4.40	0.00187 0.00185	1.26 0.89	0.24 0.30	-0.35 -0.36	measured computed
2R	106.3	150.1	37.25 37.25	13.80 14.46	21.60 22.79	1.40	2.40	0.00513 0.00521	2.08 1.81	0.21 0.35	-1.34 -1.33	measured computed
42	106.3	179.6	62.34 62.34	22.46 23.69	36.47 38.64	0.75	1.30	0.01690 0.01610	5.27 5.40	0.33 0.79	-4.46 -4.32	measured computed
53	106.3	196.9	77.03 77.03	28.70 30.35	44.01 46.68	0.54	0.85	0.03220 0.03080	9.15 9.83	0.39 0.80	-7.31 -8.75	measured computed

Table 6.6 Measured and Computed Deflections and Rotations
for Specimen WSB400

Incr	P _u kN	P _L kN	M _{s1} kN.m	M _{uw} kN.m	M _{lw} kN.m	I _{eu} $\times 10^9$ mm ⁴	I _{el} $\times 10^9$ mm ⁴	θ_{s1} radians	D _t mm	D _j mm	D _b mm	Comments
19	402.8	449.1	39.36 39.36	13.48 14.13	25.90 25.24	2.10	4.80	0.00249 0.00296	1.25 1.04	0.08 0.22	-0.72 -0.74	measured computed
24	402.8	473.3	59.94 59.94	22.34 23.57	34.35 36.37	2.50	4.10	0.00116 0.00481	1.67 1.61	0.13 0.24	-1.29 -1.29	measured computed
32	402.8	512.1	92.91 92.91	38.09 40.37	49.51 52.54	2.10	2.70	0.01140 0.01020	2.95 3.00	0.20 -0.10	-3.15 -3.14	measured computed
40	402.8	532.1	110.1 110.1	46.33 49.11	57.38 60.96	1.60	1.95	0.02240 0.01630	4.17 4.75	0.15 -0.24	-5.24 -5.09	measured computed

Table 6.7 Measured and Computed Deflections and Rotations
for Specimen FRB100 (North Wall)

Incr	P _u kN	P _L kN	M _{s1} kN.m	M _{uw} kN.m	M _{lw} kN.m	I _{eu} $\times 10^8$ mm ⁴	I _{e1} $\times 10^8$ mm ⁴	θ_{s1} radians	D _t mm	D _j mm	D _b mm	Comments
13	106.3	148.5	32.13	11.08 12.35	19.79	1.55	2.55	0.00435 0.00425	1.03 1.33	0.46 0.13	-1.86 -1.15	measured computed
18	106.3	169.1	46.00	15.59 20.55	25.46	1.40	1.80	0.00772 0.00758	1.76 2.37	0.64 0.22	-3.29 -2.06	measured computed
27	106.3	201.2	66.89	21.35 29.95	36.94	1.20	1.50	0.01313 0.01336	3.24 4.02	0.84 0.15	-5.62 -3.84	measured computed
37	106.3	218.2	70.38	23.13 28.27	42.11	0.84	1.26	0.01860 0.01858	3.83 5.50	0.89 0.10	-6.79 -5.41	measured computed

Table 6.8 Measured and Computed Deflections and Rotations
for Specimen FRB100 (South Wall)

Incr	P _u kN	P _L kN	M _{s1} kN.m	M _{uw} kN.m	M _{lw} kN.m	I _{eu} $\times 10^8$ mm ⁴	I _{e1} $\times 10^8$ mm ⁴	θ_{s1} radians	D _t mm	D _j mm	D _b mm	Comments
13	106.3	148.6	32.07	12.65 11.81	20.25	1.55	2.55	0.00421 0.00431	-1.50 -1.20	-0.20 0.14	1.03 1.40	measured computed
18	106.3	169.1	46.31	17.63 26.46	19.85	1.40	1.80	0.00752 0.00759	-2.41 -2.09	-0.05 0.22	2.43 2.44	measured computed
27	106.3	201.2	67.17	23.73 29.64	37.53	1.20	1.50	0.01271 0.01308	-4.08 -3.75	0.30 0.13	4.46 4.00	measured computed
37	106.3	218.2	70.57	26.34 28.13	42.45	0.84	1.26	0.01838 0.01855	-4.10 -5.39	0.68 0.09	7.12 5.59	measured computed

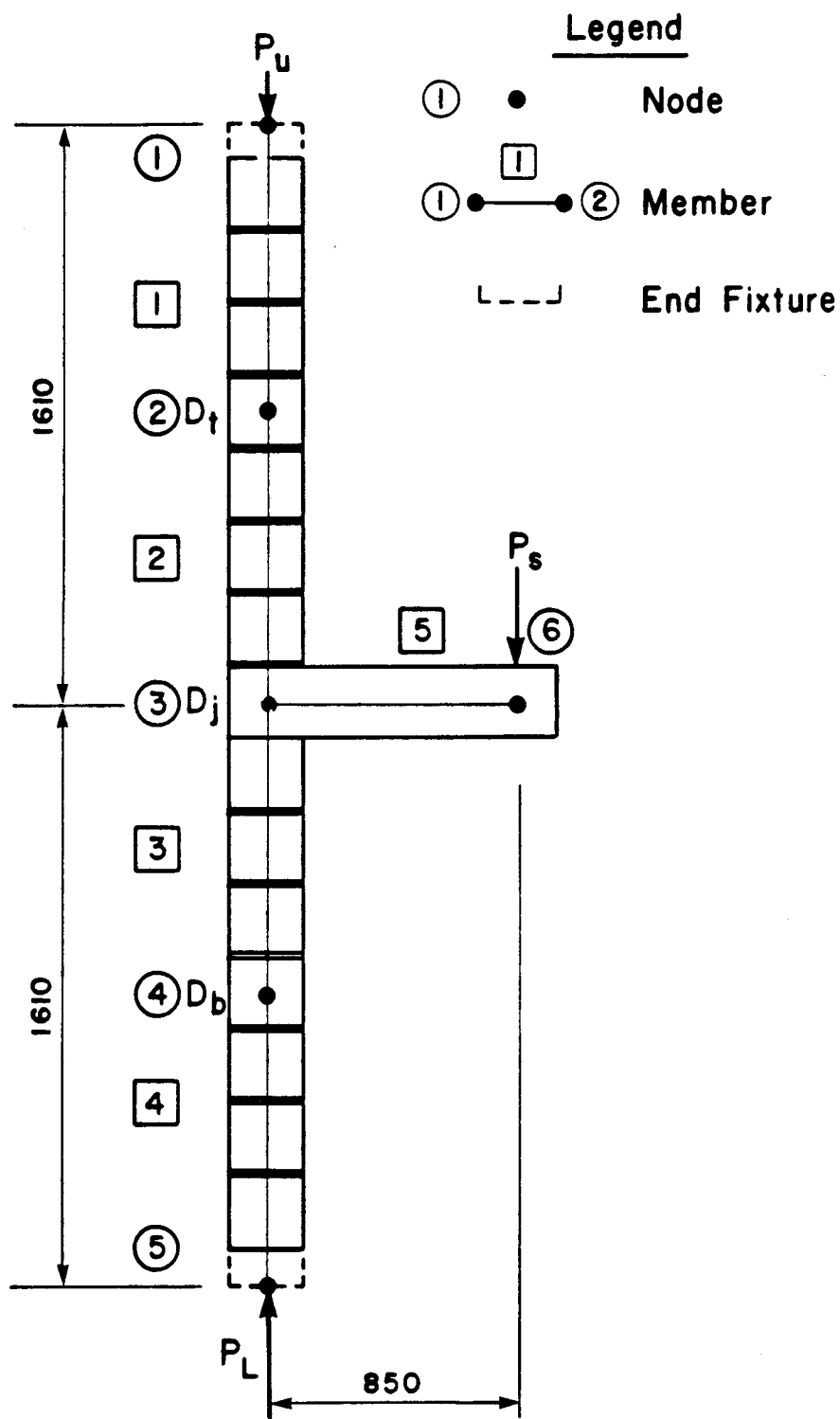


Figure 6.13 PFT Model for Type I Specimens

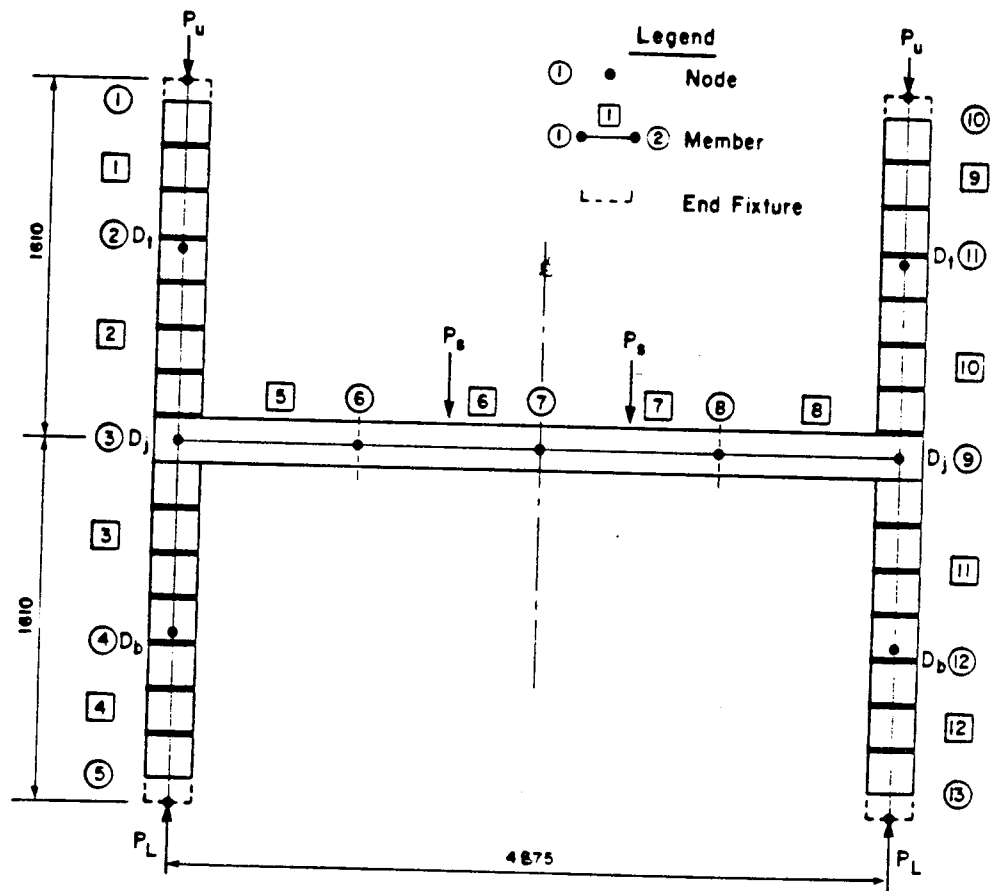


Figure 6.14 PFT Model for Type II Specimens

than 30% of the fixed end moment. Specimen FRA150 had a value of $K = 3.34$ ($\beta = 1.67$) and values of moments of 67% and 68% of the fixed end moment at the north and south wall/slab joints respectively, at the attainment of maximum moment in the walls. These values were obtained from the model analysis which predicted the slab mid-span deflection to within 5% accuracy. The slab end-rotation was predicted to within 1% accuracy. Equation 3.10 predicted a rigid frame moment of 64% of the fixed end moment at this instance. This is an indication that the value of $K = 3.34$ has not lowered the rigid frame moment, and Equation 3.10 gives a very good estimate in this case.

In the tests, slab loading was usually continued until the slab rotation indicated unstable behavior or edge crushing occurred in the lower wall. At this stage, the maximum crack width, usually occurring in the lower wall, was more than 1.5 mm and in some cases as great as 2.5 mm in the upper wall and 3.5 mm in the lower wall. It appears that the major difference between the behavior of the upper walls in Type II specimens and Type I specimens was the ability of the frame specimens in specimens with unreinforced walls to carry substantially more slab load after the limiting joint moment was reached. For reinforced wall specimens, edge crushing of the wall was the consistent mode of failure. This was after substantial cracking was tolerated at the wall/slab joint.

Figures 6.15 to 6.19 are plots of I_e/I_n versus P/P_b from model analysis studies of specimens tested in this study together with those tested by Pacholok. Ferguson's

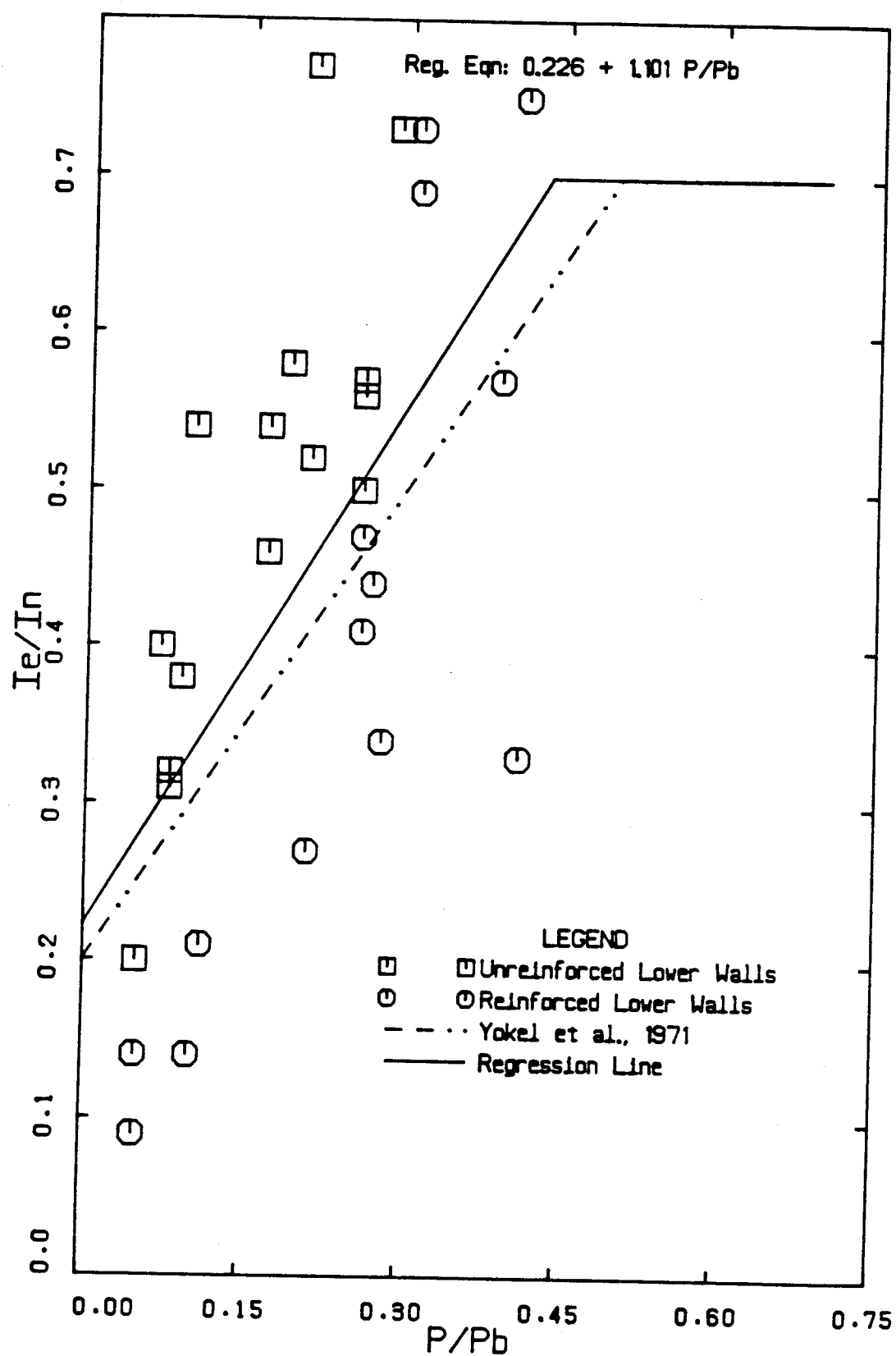


Figure 6.15 I_e/I_n Versus P/P_b for All Walls

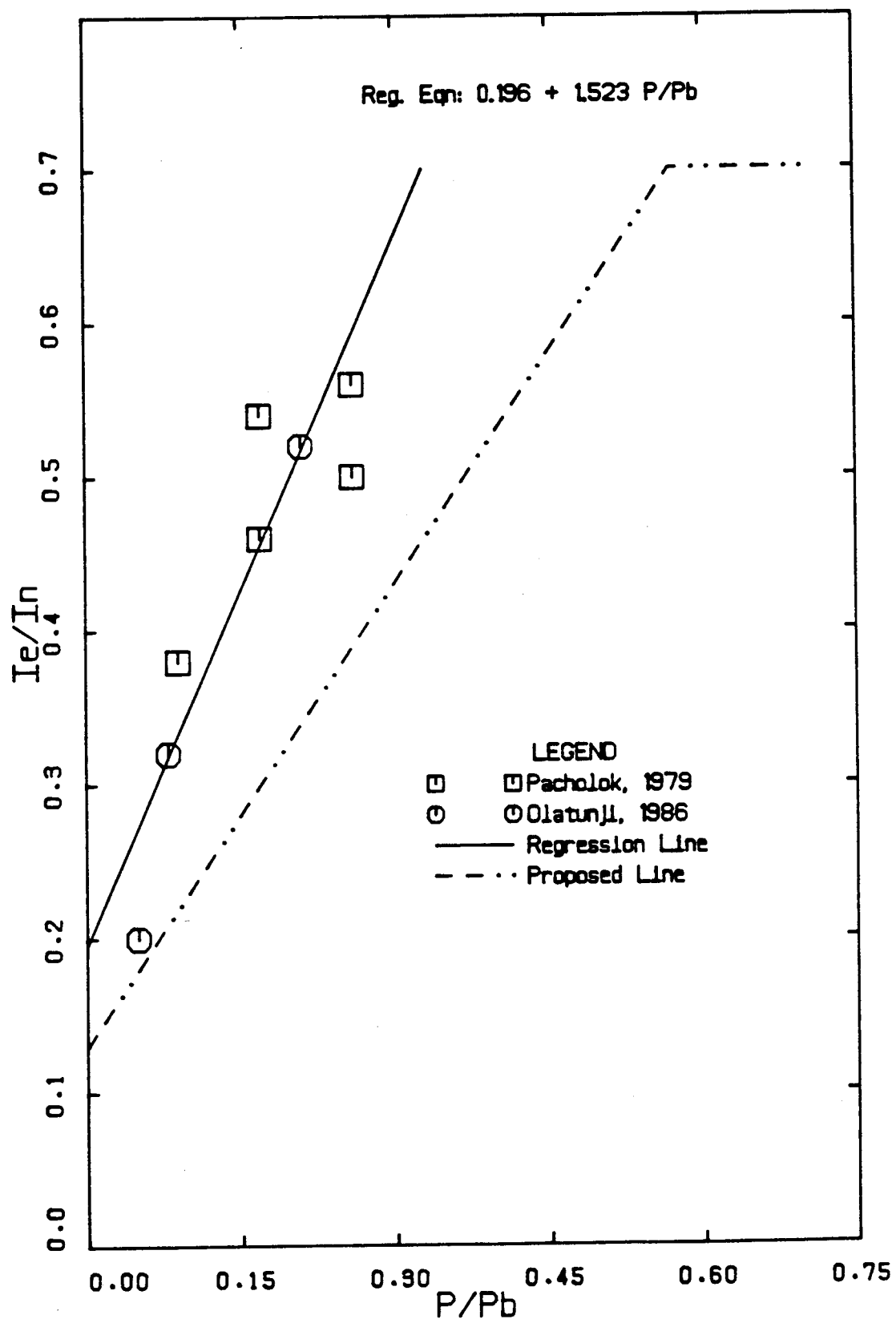


Figure 6.16 I_e/I_n Versus P/P_b For Unreinforced Upper Walls

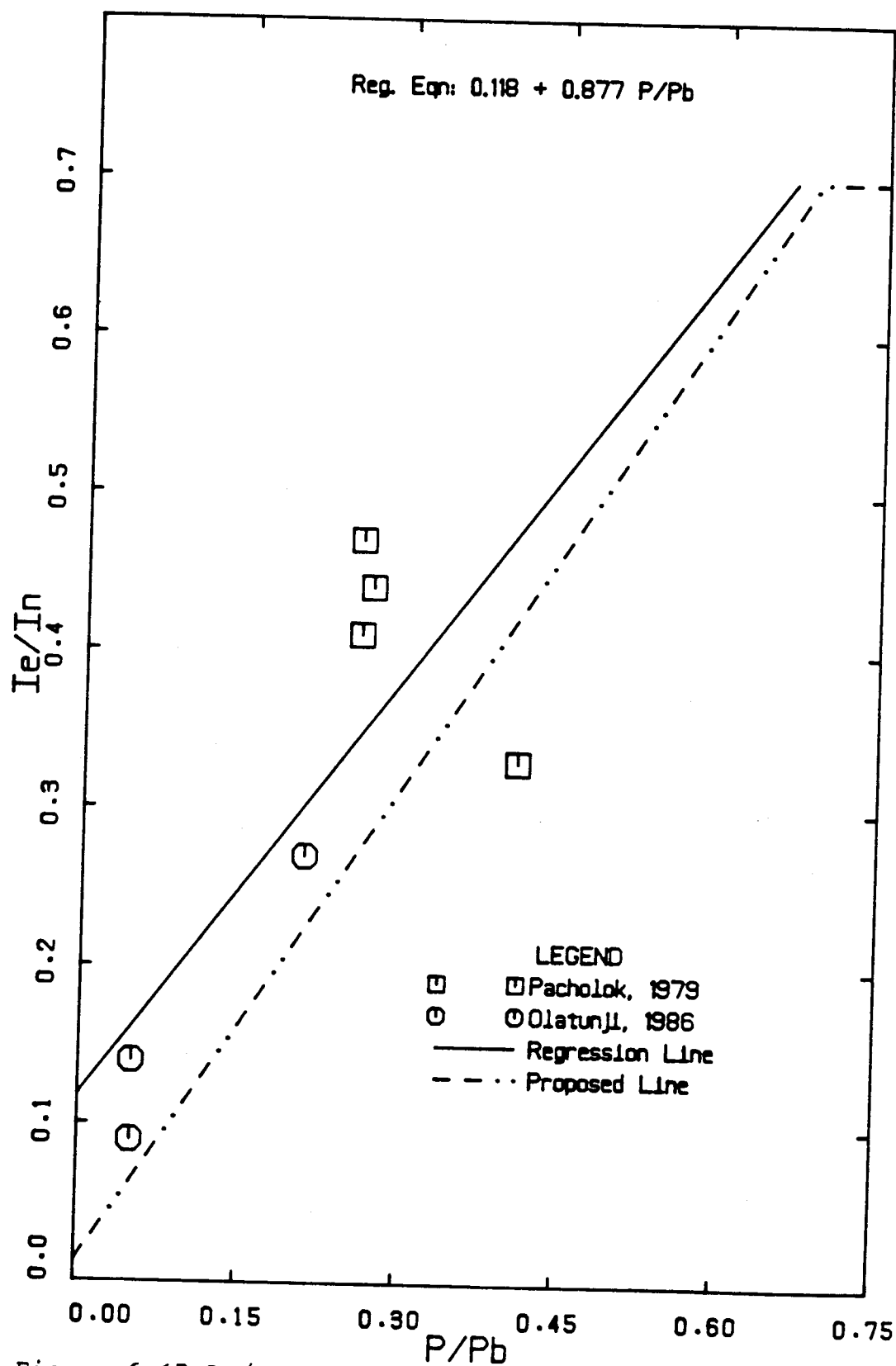


Figure 6.17 I_e/I_n Versus P/P_b For Reinforced Upper Walls

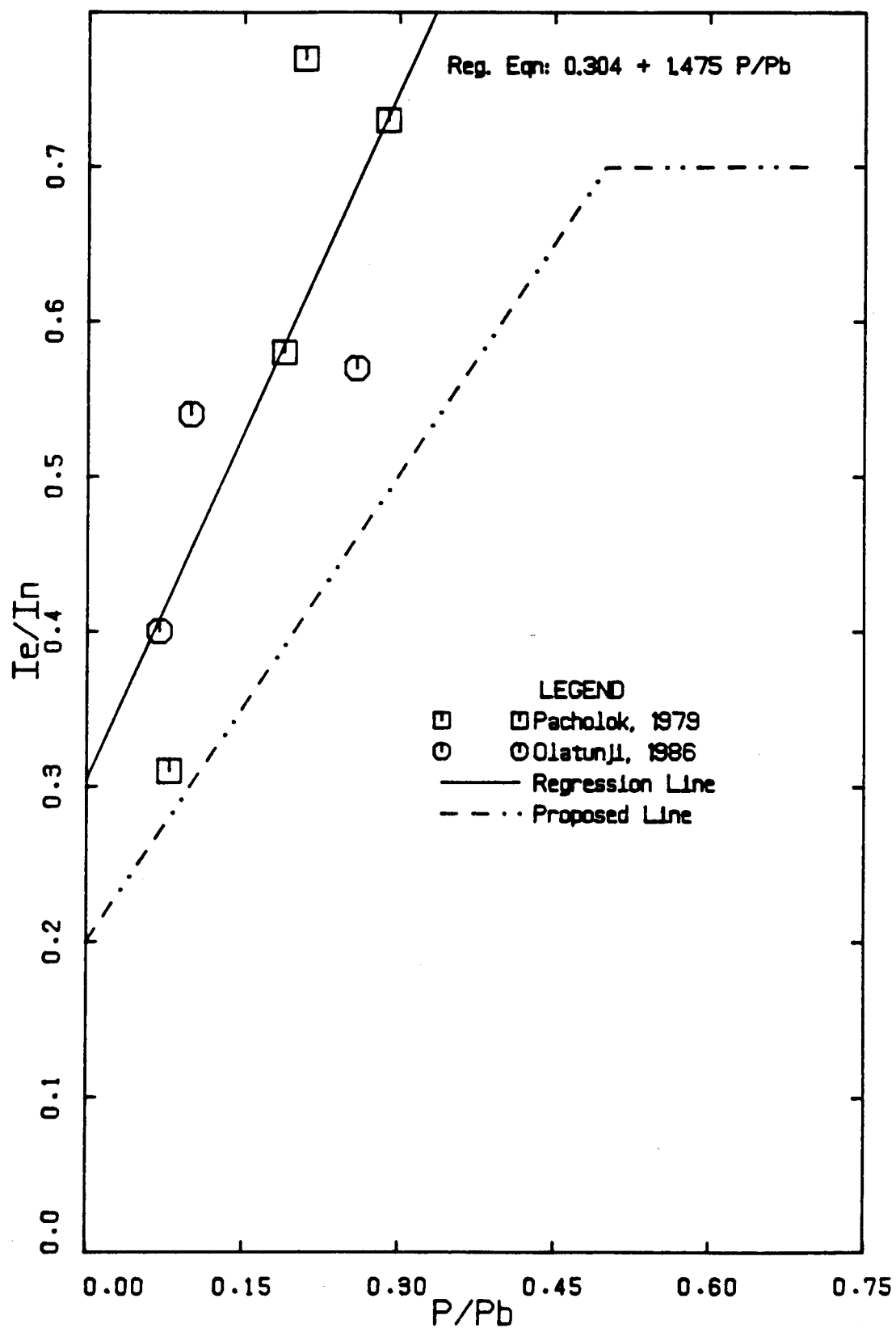


Figure 6.18 I_e/I_n Versus P/P_b For Unreinforced Lower Walls

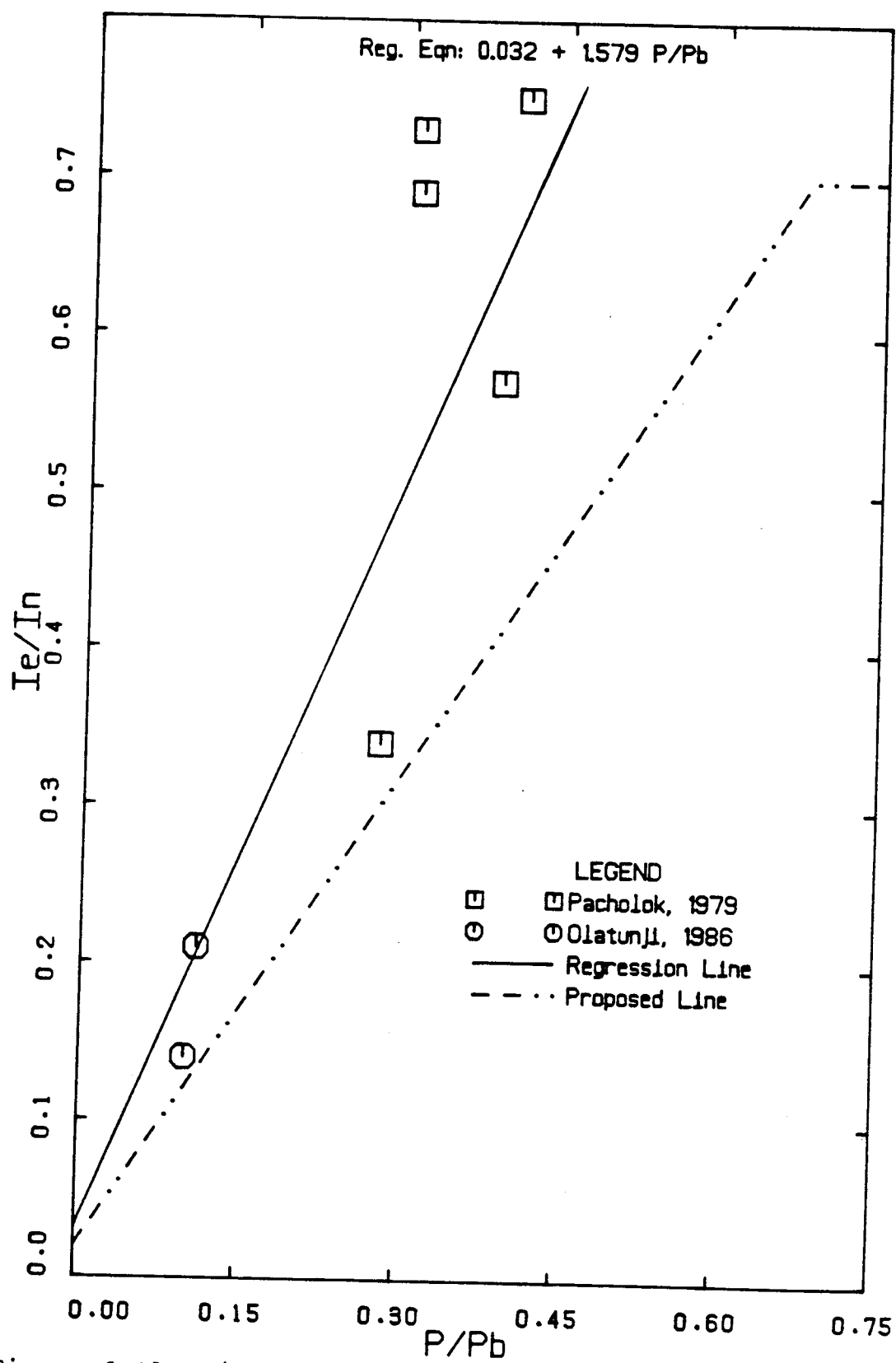


Figure 6.19 I_e/I_n Versus P/P_b For Reinforced Lower Walls

results were excluded because of the high P-Δ moments developed in his tests due to lack of horizontal restraints at the wall/slab joints. The regression lines and equations for relating stiffnesses to P/P_b for unreinforced and reinforced upper and lower walls are shown in the figures. The confidence level on the the regression lines for the rather limited number of data is at least 95% in all cases. Based on the observation of stiffness distribution between the upper and lower walls as shown in Tables 6.9 and 6.10, and the fact that the regression line for the total data has a slope of 1.10 on 1.0 for P/P_b as shown in Figure 6.15, proposed design lines are drawn for each case based on the following equations:

For unreinforced upper walls:

$$EI = E_m I_n (0.13 + P/P_b) \leq 0.7 E_m I_n \quad (6.1)$$

For unreinforced lower walls:

$$EI = E_m I_n (0.20 + P/P_b) \leq 0.7 E_m I_n \quad (6.2)$$

For reinforced upper walls:

$$EI = E_m I_n (0.013 + P/P_b) \leq 0.7 E_m I_n \quad (6.3)$$

For reinforced lower walls:

$$EI = E_m I_n (0.02 + P/P_b) \leq 0.7 E_m I_n \quad (6.4)$$

Considering the cluster of test data in Figures 6.18 and 6.19, Yokel et al.'s limit of $0.7 E_m I_n$ is adopted in these proposals.

Table 6.9 Stiffness Distribution at Failure for Unreinforced Walls

Specimen	I_{eu} $\times 10^8$ mm^4	P_u/P_b	I_{el} $\times 10^8$ mm^4	P/P_b	I_T $\times 10^8$ mm^4	I_{eu}/I_T	I_{el}/I_T
WSA100*	0.20	0.05	0.40	0.07	0.60	0.33	0.67
WSA400*	0.52	0.21	0.57	0.26	1.09	0.48	0.52
FRA150*	0.32	0.08	0.55	0.10	0.87	0.37	0.63
E50**	0.38	0.09	0.31	0.11	0.69	0.55	0.45
E100**	0.54	0.17	0.58	0.19	1.12	0.48	0.52
A101**	0.46	0.17	0.77	0.21	1.23	0.37	0.63
A150**	0.56	0.26	0.73	0.29	1.29	0.43	0.57
E150**	0.50	0.26	0.69	0.29	1.19	0.42	0.58

\bar{X} 0.41
 \bar{S} 0.05
 \bar{V} 0.13

* Bin. walls; loads in kN (Olatunji, 1986)
 ** Bin. walls; loads in kips (Pacholok, 1979)

Table 6.10 Stiffness Distribution at Failure for Reinforced Walls

Specimen	I_{eu} $\times 10$ mm	P_u/P_b	I_{e1} $\times 10^5$ mm ⁴	P_L/P_b	I_{τ} $\times 10^5$ mm ⁴	I_{eu}/I	I_{e1}/I_{τ}
WSB100*	0.09	0.05	0.14	0.10	0.23	0.39	0.61
FRB100*	0.14	0.05	0.21	0.11	0.35	0.40	0.60
WSB400*	0.27	0.21	0.34	0.28	0.61	0.44	0.56
B150**	0.41	0.26	0.69	0.31	1.10	0.37	0.63
B200**	0.47	0.35	0.57	0.40	1.04	0.45	0.55
C200***	0.44	0.27	0.73	0.31	1.17	0.38	0.62
C300***	0.33	0.41	0.75	0.49	1.08	0.31	0.69

\bar{x} 0.39
 S 0.05
 V 0.12

* 8in. walls, fully grouted; loads in kN (Olatunji, 1986)

** 8in. walls, partially grouted; loads in kips (Pacholok, 1979)

*** 10in. walls, partially grouted; loads in kips (Pacholok, 1979)

6.3.1 Limitations of Proposed Effective Stiffnesses

It should be noted that these equations are limited by the following peculiarities of the studies from which they were derived:

1. Limited test results and the usual scatter in masonry tests.
2. Walls built of concrete masonry units.
3. The use of E_m of $750f'_m$ for unreinforced walls and $950f'_m$ for reinforced walls
4. Slab to wall stiffness ratio β of 1.70. This restriction may not be necessary if the wall precompression is greater than 0.50 MPa.
5. Gross area reinforcement ratio in the walls not greater than 0.00374.
6. Eccentricity to thickness ratio, e/t , greater than 0.2.
7. Wall of usual storey height in double curvature. Very slender walls should be checked for moment magnification at mid-height using the appropriate procedure.

A design example showing the application of the proposed procedure for an 8-storey structure is given in Appendix A.

6.4 Comparison of Wall Ultimate Strengths

Table 6.11 shows the comparison between measured values of upper wall moments with values predicted by the various methods described above. With the exception of the result of upper wall of Specimen FRA150 which was questioned, the ratio of test to predicted moment is 1.0 or greater. The effective stiffness model results predict test results

Table 6.11 Comparison of Ultimate Strength Values for Upper Walls

Specimen	M/Mb				Measured to Predicted Ratio		
	Measured	Predicted					
		Interaction	CDC	PFT	Interaction	CDC	PFT
WSA100	0.145	0.131	0.140	0.111	1.10	1.04	1.31
WSA400	0.583	0.409	0.451	0.603	1.54	1.29	0.97
FRA150 N	0.150	0.204	0.195	0.171	0.74	0.77	0.88
FRA150 S	0.234	0.204	0.195	0.178	1.15	1.20	1.31
WSB100	0.470	0.303	0.371	0.497	1.56	1.27	0.95
WSB400	0.759	0.475	0.512	0.789	1.60	1.49	0.96
FRB100 N	0.380	0.303	0.371	0.463	1.25	1.03	0.82
FRB100 S	0.431	0.303	0.371	0.461	1.42	1.16	0.93
				\bar{X}	1.30	1.16	1.02
				S	0.29	0.21	0.19
				V	0.23	0.19	0.18

N implies north wall
S implies south wall

within the usual scatter in masonry tests. Using the results obtained from an interaction curve for a value of a equal to 1.0, a safe limit on the maximum moment in the wall can be imposed.

7. CONCLUSIONS AND RECOMMENDATIONS

7.1 Conclusions

The following are the major conclusions derived from an investigation into the behavior and strength of concrete masonry wall/slab joints:

1. Concrete masonry walls major mode of failure at a wall/slab joint is either by tension cracking at the mortar joint or edge crushing, or a combination of both. The particular failure mode depends on the level of axial load on the wall and whether reinforcement is present in the wall or not.
2. The moment defined as the plastification moment by Sahlin, M_{pL} , can occur between 80% and 100% of the maximum ultimate moment of the wall depending on the level of wall axial load and whether or not reinforcement is present in the wall.
3. Based on limited prism tests in this study, the moduli of elasticity of grouted and ungrouted concrete masonry are $770f'_m$ and $960f'_m$ respectively. There is relatively more scatter in test results for ungrouted prisms than for grouted prisms.
4. The column deflection curve (CDC) technique of analysing the walls, based on the assumption that rotation is concentrated at the mortar joints and using a bi-linear stress-strain relationship approximation for concrete masonry gives a fair prediction of rotation behavior and ultimate strength for unreinforced and reinforced walls.
5. The ultimate strength of unreinforced and reinforced

concrete masonry walls at a wall/slab joint can be satisfactorily estimated using theoretical load-moment interaction diagrams based on prism ultimate strength, f'_m , and a straight line stress-strain relationship. This estimate is conservative for wall e/t ratios between $1/6$ and $1/3$.

6. Rigid frame action can be assumed at a masonry wall/slab joint if the precompression stress on the wall is greater than 0.54 MPa and ratio of slab to wall stiffness, β , is not greater than 1.70.
7. Within the scope of the limitations of this investigation, effective stiffness of unreinforced and reinforced concrete masonry walls of practical construction dimensions can be satisfactorily estimated using the following equations:

For unreinforced upper walls:

$$EI = E_m I_n (0.13 + P/P_b) \leq 0.7 E_m I_n \quad (6.1)$$

For unreinforced lower walls:

$$EI = E_m I_n (0.20 + P/P_b) \leq 0.7 E_m I_n \quad (6.2)$$

For reinforced upper walls:

$$EI = E_m I_n (0.013 + P/P_b) \leq 0.7 E_m I_n \quad (6.3)$$

For reinforced lower walls:

$$EI = E_m I_n (0.020 + P/P_b) \leq 0.7 E_m I_n \quad (6.4)$$

8. A structure consisting of load bearing concrete masonry walls and cast-in-place concrete slabs can be satisfactorily analysed by means of existing rigid frame analysis methods based on effective stiffness values

proposed in this study.

9. Interaction diagrams based on straight line stress-strain diagram to prism ultimate strength and a modification factor α of 1 is recommended for design.

7.2 Recommended Design Procedure

The following steps are recommended for the design of walls at a concrete masonry wall/slab joint:

1. Obtain masonry f'_m from prism tests or unit and mortar tests.
2. Compute modulus of elasticity as $750f'_m$ for unreinforced walls or $950f'_m$ for reinforced walls.
3. Compute net moment of inertia of masonry wall, I_n
4. Compute short wall axial load capacity, P_b
5. Compute minimum effective EI according to Equations 6.1 to 6.4 given above.
6. Use the estimated stiffness values obtained in Step 5 in a standard structural analysis program to obtain moments, axial and shear forces for design. Load factors of 1.4 and 1.7 on dead and live loads as recommended in CSA Standard A23.3-M77 Code for Design of Concrete Structures may be employed.
7. Check ultimate strength limits by using an appropriate interaction curve based on a straight line stress-strain relationship for masonry and prism f'_m . An undercapacity factor such as 0.8 recommended for good workmanship (Amrhein et al., (1983); Suter and Fenton, 1986) employed in the design example in appendix A may be applied to ultimate strength values obtained from the

interaction curve for the value of a equal to 1.

7.3 Recommendations for Future Work

In order to further verify and extend the effective stiffness procedure, it is recommended that:

1. More tests on simple wall/slab joint specimens of concrete masonry with joint precompression less than 0.54 MPa be undertaken.
2. Tests using brick masonry walls be undertaken
3. Tests on slab to stiffness ratio less than 1.70
4. Effect of partial penetration of slab on joint fixity be investigated.

Bibliography

1. Amrhein, J.E., Simpson, S.E., Selna, L.G. and Tobin, R.E. Slender Masonry Walls Test. *Proc., 3rd Canadian Masonry Symposium*, Edmonton, Jan., pp. 11-1 to 11-15.
2. Awni, A and Hendry A.W. 1979. A simplified Method for Eccentricity Calculations. 1979 *Proc., 5th International Brick masonry Conference*, Washington D.C.
3. Awni, A. 1980. *The Compressive Strength of Brick Masonry Walls with Reference to Wall/Floor Slab Interaction*. Ph.D thesis, University of Edinburgh, Scotland.
4. Beaufait, F.W. and Rowan, W.L. 1970. *Computer Methods of Structural Analysis*. Prentice Hall, Inc., Englewood Cliffs, N.J.
5. Carlsen, B.E. 1969. On Bearing Capacity of Joints Between Precast Slabs and Brickwalls. *Proc., CIB International Symposium on Bearing Walls*, Warsaw.
6. Chandrakeerthy, S.R. De S. and Hendry A.W. 1983. Behaviour of Wall-Floor Slab Joints in Single Leaf and Cavity Walls. *International Journal of Masonry Construction*, Vol. 3, No. 1, pp. 10-13.
7. Colville, J. 1977. *Analysis and Design of Brick Masonry Walls*. Research Report, University of Edinburgh, Scotland.
8. Colville, J. 1979. Stress Reduction Design Factors for Masonry Walls. *Proc., ASCE*, Vol. 105, No. ST10, Oct., pp. 2035-2051

9. CSA Standard A179M-76. 1976. *Mortar and Grout for Unit Masonry*. Canadian Standards Association, Rexdale, Ontario.
10. CSA Standard CAN3-A23.2-M77. 1977. *Methods for Test for Concrete*. Canadian Standards Association, Rexdale, Ontario.
11. CSA Standard CAN3-A23.3-M77. 1977. *Code for the Design of Concrete Structures*. Canadian Standards Association, Rexdale, Ontario.
12. CSA Standard CAN3-S304-M78. 1978. *Masonry Design and Construction for Buildings*. Canadian Standards Association, Rexdale, Ontario.
13. Curtin W.G., Shaw, G., Beck J.K. and Bray, W.A. 1982. *Structural Masonry Designers' Manual*. Granada Publishing Ltd., London.
14. Drysdale, R.G. and Suter G.T. 1981. *Modern Engineered Masonry*, A 2-Day Practice Oriented Course.
15. Fattal, S.G. and Cattaneo, L.E. Structural Performance of Masonry Walls Under Compression and Flexure. *Building Science Series No. 33*, National Bureau of Standards.
16. Ferguson, S.N. 1979. *Interaction of Brick Masonry Walls and Concrete Floor Slabs*. M.Sc. Thesis, Univ. of Alberta, Edmonton, Canada.
17. Furler, R. and Thurliman, B. 1977. Strength of Brickwalls Under Enforced End Rotations. *Proc., 6th International Symposium on Load Bearing Brickwork*, London.

18. Furler, R. 1980. *Versuche über die Rotationsfähigkeit von Kalksandsteinmauerwerk*. Institut für Baustatik und Konstruktion, Eidgenössische Technische Hochschule, Zurich.
19. Furler, R. 1981. *Tragverhalten von Mauerwerkswänden unter Druck und Biegung*. Institut für Baustatik und Konstruktion, Eidgenössische Technische Hochschule, Zurich.
20. Galambos, T.V. 1965. Column Deflection Curves. Lecture No. 9, *Plastic Design of Multi-Storey Frames*, Fritz Engineering Laboratory Report No. 273-20, Lehigh University, pp. 9.1-9.25.
21. Germanino, G. and Macchi, G. 1977. Experimental Research of a Frame-Idealization for a Bearing Wall Multistorey Structure. *Proc., 6th International Symposium on Load Bearing Brickwork*, London, pp. 353-366.
22. Gregory, A.H., Hartley, J.R. and Lewis, D.G. 1969. *Basic Statistics*. Methuen Educational Limited, London.
23. Gross, J.G., Dikkers, R.D. and Grogan J.C. 1969. *Recommended Practice for Engineered Brick Masonry*. Structural Clay Products Institute, Virginia, November, 1969.
24. Hamid, A.A.A. 1978. *Behaviour Characteristics of Concrete Masonry*. Ph.D. Thesis, McMaster University.
25. Hatzinikolas, M. 1978. *Concrete Masonry Walls*. Ph.D. Thesis, The University of Alberta, Edmonton, Canada.

26. Hendry A.W., Sinha, B.P. and Davies S.R. 1982. *An Introduction to Load Bearing Brickwork Design*. Ellis Horwood Ltd., London.
27. Lenczner, D. 1972. *Elements of Loadbearing Brickwork*. International Series of Monographs in Civil Engineering, Vol. 5, Edited by D.J. Silverleaf and J.L. Rankes.
28. Maurenbrecher, A.H.P. and Hendry A.W. 1970. Aspects of the Strength and Fixity of the Joint between a Brickwall and Floor Slab. *Proc., 2nd international Brick Masonry Conference*. Stoke-on-Trent, England.
29. Maurenbrecher, A.H.P. 1972. *Wall/Floor Slab Joint Behavior in Brickwork*. Ph.D. Thesis, University of Edinburgh, Scotland.
30. Nathan, N.D. 1972. Slenderness of Prestressed Concrete Columns. *PCI Journal* Vol.17, No. 6, pp. 45-47.
31. Pacholok, R.M. 1980. *An Investigation of Concrete Masonry Walls and Concrete Slab Interaction*. M.Sc. Thesis, Univ. of Alberta, Edmonton.
32. Pfrang, E.O., Siess, C.P. and Sozen, M.A. 1964. Load-Moment-Curvature Characteristics of Reinforced Concrete Cross Sections. *Proc., ACI Journal*, Vol. 61, No. 44, Jul., pp. 763-777.
33. Rerup, H.J., Karuks, E. and Huggins M.W. 1972. *An Investigation of A Floor to Wall Connection for Precast Concrete Panel Construction*. Systems Building Centre, University of Toronto, Publication No. 72-1.

34. Risager, S. 1969. Structural Behavior of Linear Elastic walls Having No Tensile Strength. *Designing, Engineering and Constructing With Masonry Products*. Gulf Publishing Co., pp 257-266
35. Sahlin, S. 1959. *Structural Interaction of Walls and Floor Slabs*. National Swedish Council for Building Research, Report No. 35.
36. Sahlin, S. 1969. Interaction of Brick Masonry Walls and Floor Slabs. *Designing, Engineering and Constructing With Masonry Products*. Gulf Publishing Co., pp. 266-277.
37. Sahlin, S. 1971. *Structural Masonry*. Prentice Hall, Inc., Englewood Cliffs, N.J.
38. Salvadori, M and Levy M. 1967. *Structural Design in Architecture*. Prentice Hall, Inc., Englewood Cliffs, N.J.
39. Sinha, P.B. and Hendry A.W. 1977. An Investigation into Behavior of A Brick Cross-Wall Structure. *Proc., 6th International Symposium on Load Bearing Brickwork*, London, pp. 67-76.
40. Suter, G.T. and Fenton, G. A. 1986. Flexural Capacity of Reinforced Masonry Materials. *Proc., ACI Journal* Vol.83, No. 1, Jan.-Feb., pp. 127-136.
41. Tenende, L.M. 1983. Unpublished report. Dept. of Civil Engineering, Univ. of Alberta, Edmonton.
42. Yokel, F.Y., Mathey, R.G. Dijkers, R.D. 1970. Compressive Strength of Slender Concrete Masonry Walls. *Building Science Series No. 33*, National Bureau of Standards.

43. Yokel, F.Y., Mathey, R.G. Dikkers, R.D. 1971. Strength of Masonry Walls Under Compressive and Transverse Loads. *Building Science Series No. 34*, National Bureau of Standards.
44. Yokel, F.Y. and Dikkers, R.D. 1971. Strength of Load Bearing Masonry Walls. *Proc., ASCE*, Vol. 97, No. ST5, May, pp. 1593-1609.

APPENDIX A - DESIGN EXAMPLE

APPENDIX A.1

DESIGN EXAMPLE FOR A TYPICAL EXTERNAL WALL

Consider the design of a 200mm outer wall in a 8-storey building as shown in Figure A.1. It is assumed that the slabs are simultaneously loaded at all floor levels. The wall are assumed fully grouted. Design is based on vertical loads only.

Floor Span : 6.5 metres

Storey Height: 3.0 metres.

Walls are bent in double curvature at all storeys above ground floor. Ground floor walls are bent in single curvature.

Loadings	: Slab Dead load = 0.15×23.5	
		= 3.5 kN/m^2
	Topping	= 0.2
	Partitions	= 1.0
	Total	= 4.7 kN/m^2
	Live Load	= 2.0 kN/m^2
	Wall Self-Weight = 2.1×3	
		= 6.3 kN/m
	Parapet	= 2.0 kN/m

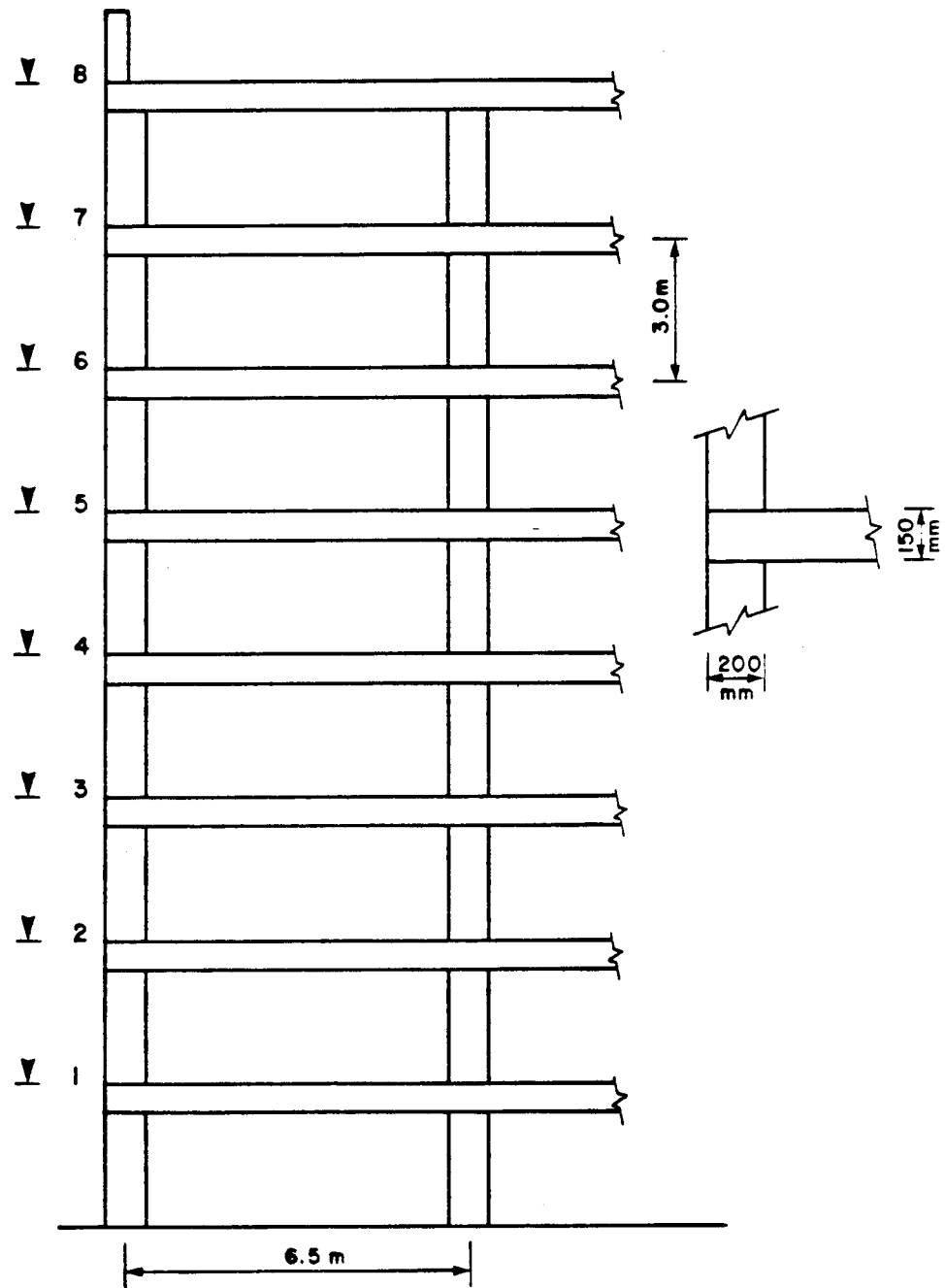


Figure A.1 External Wall of a 8-Storey Building

Design Loads: (assuming factors of 1.4 and 1.7 for dead and live loads respectively)

$$\text{Slab D.L./wall} = 4.7 \times 3.3 \times 1.4 = 21.7 \text{ kN/m}$$

$$\text{Slab L.L./wall} = 2.0 \times 3.3 \times 1.7 = 11.2 \text{ kN/m}$$

$$\text{Total Load/wall} = 32.9 \text{ kN/m}$$

$$\text{Wall Dead Load} = 6.3 \times 1.4 = 8.8 \text{ kN/m}$$

Slab Design Load, w_D :

$$w_D = 4.7 \times 1.4 + 2.0 \times 1.7 = 9.98 \text{ kN/m}^2$$

Stiffness Parameters:

$$\text{Masonry } f'_m = 10 \text{ MPa}$$

$$\text{Concrete } f'_c = 20 \text{ MPa}$$

$$\text{Walls: } E_m = 950f'_m = 9690 \text{ MPa}$$

$$I_n = 1/12 \times 1000 \times 190^3 = 5.72 \times 10^8$$

$$E_m I_n = 5.54 \times 10^{12} \text{ N.mm}^2$$

$$P_b = f'_m b t = 10 \times 1000 \times 190 = 1900 \text{ kN}$$

$$\text{Slab: } E_s = 5000\sqrt{f'_c} = 22360 \text{ MPa}$$

$$I_s = 1/12 \times 1000 \times 150^3 = 2.81 \times 10^8 \text{ mm}^4$$

$$E_s I_s = 6.28 \times 10^{12} \text{ N.mm}^2$$

$$\beta = \frac{E_s I_s H}{E_m I_n L} \quad (\text{Double Curvature})$$

$$= \frac{6.29 \times 3.0/2}{5.54 \times 6.5} = 0.26$$

At all floors except the first;

$$\begin{aligned} \text{Rigid Frame Moment, } M_R &= \frac{3w_D L^2}{12(3 + \beta)} \quad (\text{Double Curvature}) \\ &= 9.98 \times 6.5^2 / 12 \times 3 / 3.26 \\ &= 32.33 \text{ kN.m/m} \end{aligned}$$

At first floor

$$\begin{aligned} \text{Rigid Frame Moment, } M_R &= \frac{3w_D L^2}{12(3 + 2\beta)} \quad (\text{Single Curvature}) \\ &= 9.98 \times 6.5^2 / 12 \times 3 / 3.52 \\ &= 29.95 \text{ kN.m/m} \end{aligned}$$

Effective EI:

Unreinforced Walls:

$$(EI)_{uu} = E_m I_n (0.130 + P/P_b)$$

$$(EI)_{ul} = E_m I_n (0.200 + P/P_b)$$

Reinforced Walls:

$$(EI)_{ru} = E_m I_n (0.013 + P/P_b)$$

$$(EI)_{rl} = E_m I_n (0.020 + P/P_b)$$

The design is laid out in Table A.1, where:

$$K = \frac{EI}{H}$$

K_u = upper wall stiffness at the joint

K_l = lower wall stiffness at the joint

K_t = total stiffness at the joint

M_t = total moment at the joint

Table A.1 Design Example

Level	Load		Load Ratio		Stiffness		Moment				Interaction with $\phi = 0.8$				Reinforcement Required	
	Pu	P	Pu/Pb	P/Pb	KuH	KfH	KtH	KuMt	KfMt	KtMt	Upper Wall	Lower Wall	UR	R***	Upper Wall	Lower Wall
	kN	kN			Emin	Emin	Emin	kN.m	kN.m	kN.m	UR	R***	UR	R***		
8	3.53	36.43	0.0019	0.019	0.015	0.039				30.03	0	10.2	2.80	11.80		****
7	45.23	78.13	0.024	0.041	0.037	0.061	0.098	12.21	20.12		3.6	12.0	5.60	13.40	Reinf. 3-15M	Reinf. 5-20M
6	86.93	119.8	0.046	0.063	0.059	0.083	0.142	13.43	18.90		6.4	13.6	8.40	14.80	Reinf. 3-15M	Reinf. 5-20M
5	128.6	161.5	0.068	0.085	0.081	0.105	0.183	14.31	18.02		8.8	14.4	10.80	16.20	Reinf. 3-15M	Reinf. 5-15M
4	170.3	203.2	0.090	0.107	0.103	0.127	0.230	14.47	17.85		11.6	16.4	13.60	17.20	Reinf. 3-15M	Reinf. 5-15M
3	212.0	244.9	0.112	0.129	0.125	0.149	0.274	14.75	17.60		14.0	17.6	15.50	18.40	Reinf. 3-15M	Reinf. 3-15M
2	253.7	286.6	0.134	0.151	0.147	0.171	0.318	14.95	17.40		16.0	18.8	17.20	19.60	Reinf. 3-15M	Reinf. 3-15M
1	295.4	328.3	0.155	0.173	0.168	0.098	0.266	18.92	11.03	**	17.2	20.4	18.40	21.20	Reinf. 3-15M	Reinf. 3-15M

* Assuming parapet height of 1.2 metres

** Assuming single curvature, using total height, H

*** Fully grouted and reinforced with 3-15M bars

**** Only mortar connection here to relief moment development

Notes on Design Example

The following should be noted concerning Table A.1:

1. Only vertical loading is considered. Lateral loading effects may be considered additionally.
2. An undercapacity factor of 0.8 has been used on the appropriate interaction curve drawn on the basis of α equal to 1 to check the wall capacity.
3. This example has a fairly large slab span, resulting in significant moment at the external wall.
4. Continuity requirements for reinforcement detailing may mean reinforcing the walls when reinforcement is not required, or increasing the number or amount of reinforcing bars at a particular level.

APPENDIX B - CDC PROGRAM

APPENDIX B1

PROGRAM NOMENCLATURES
AND
FLOW CHARTS

B1.1 Cross-Section

The cross-sections considered are shown in Figure B.1, together with the nomenclatures. Only rectangular cross-sections are considered. The stress-strain curves for masonry and steel are shown in Figures B.2 and B.3.

The strains on the cross-section are designated ϵ_1 , ϵ_2 , ϵ_3 , ϵ_R , ϵ_4 beginning at the least compressed or tensile face respectively. The positive value of ϵ_1 shows compression on the tensile face whereas negative value shows tension. Figures B.4 to B.8 show the strain and stress distribution on the cross-section considered for various cases in the generating of the moment-load-curvature data theoretically. For any of the cases shown, the following is true:

The curvature, ϕ , is given by:

$$\phi = \frac{\epsilon_4 - \epsilon_1}{t}$$

or $\phi t = \epsilon_4 - \epsilon_1$ (B.1)

The strain values are given as:

$$\begin{aligned}\epsilon_1 &= \epsilon_4 - \phi t \\ \epsilon_2 &= \epsilon_1 - a\phi t \\ \epsilon_R &= \epsilon_1 - \lambda\phi t \\ \epsilon_3 &= \epsilon_1 - (1 - a)\phi t\end{aligned}$$

(B.2)

The stress corresponding to the strain in masonry, ϵ , is given as:

$$\text{or } a_i = \sigma_i = \epsilon_i E_{1m} \text{ for } \epsilon_i \leq \epsilon_0 \quad (\text{B.3})$$

$$a_i = \sigma_i = \epsilon_0 E_{1m} + (\epsilon - \epsilon_0) E_{2m} \text{ for } \epsilon_i \geq \epsilon_0 \quad (\text{B.4})$$

where i refers to a particular point on the cross-section.

for reinforced masonry, f_s becomes an additional term as given below:

$$f_s = \epsilon_R E_s \quad (B.5)$$

where

$$-f_y \leq f_s \leq f_y$$

It should be noted that tension contribution of masonry is neglected in the analysis, thus:

$$a_i = 0 \text{ whenever } \epsilon_i \text{ is negative.}$$

Depending on the stress distribution on the cross-section, axial load and moment about center line of the cross-section are evaluated according to the following equations (the bracket term is added only for reinforced walls):

$$P/P_b = \frac{P}{f_m b} = \int_c^t a h + \left(\frac{\rho f_s}{f_m} \right) \quad (B.6)$$

$$M/M_b = \frac{M}{f_m b/6} = \int_c^t a h^2 \quad (B.7)$$

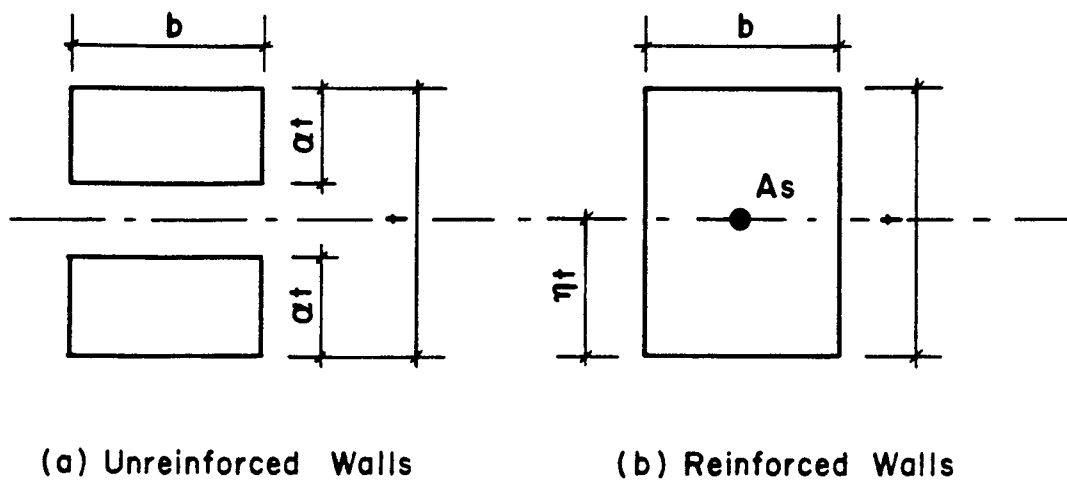


Figure B.1 Cross-Sections

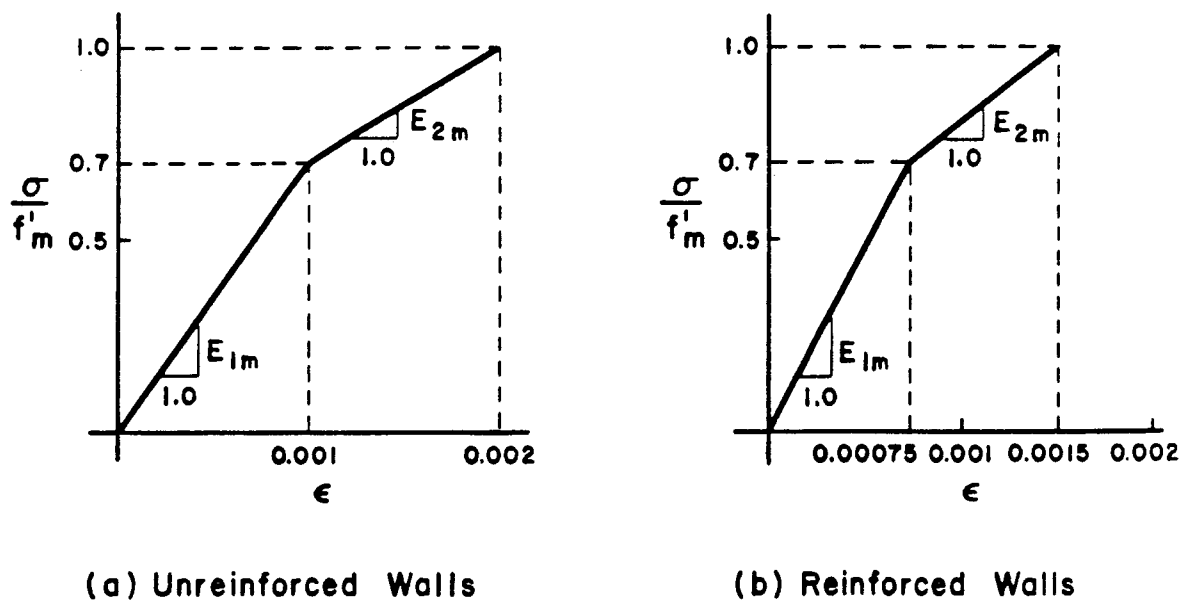


Figure B.2 Stress-Strain Relations for Masonry

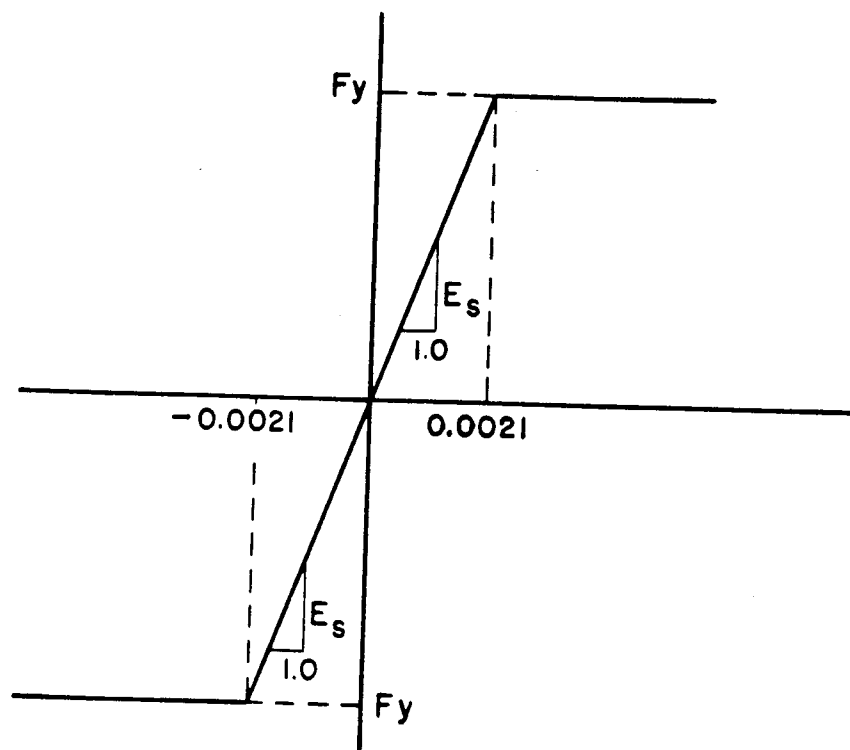


Figure B.3 Stress-Strain Relations for Steel

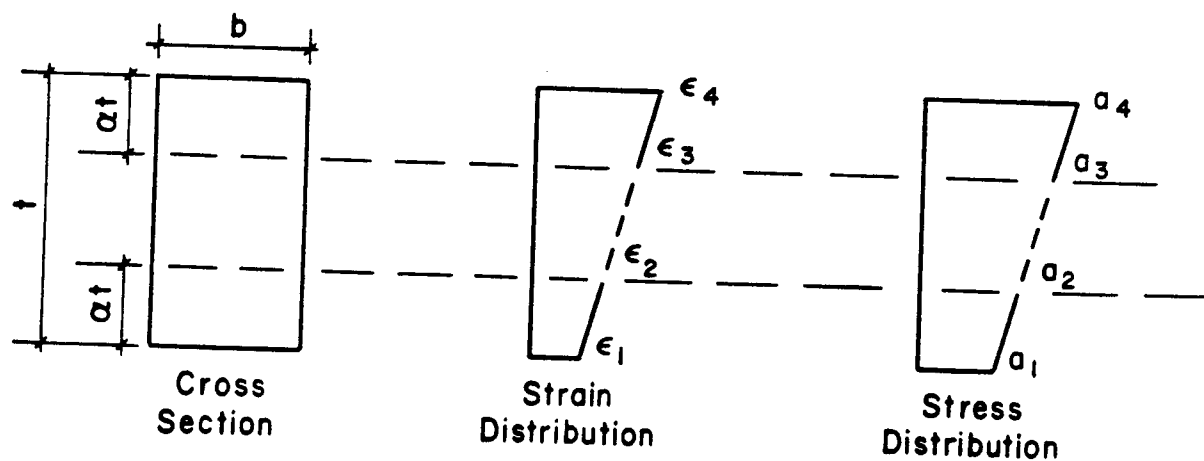
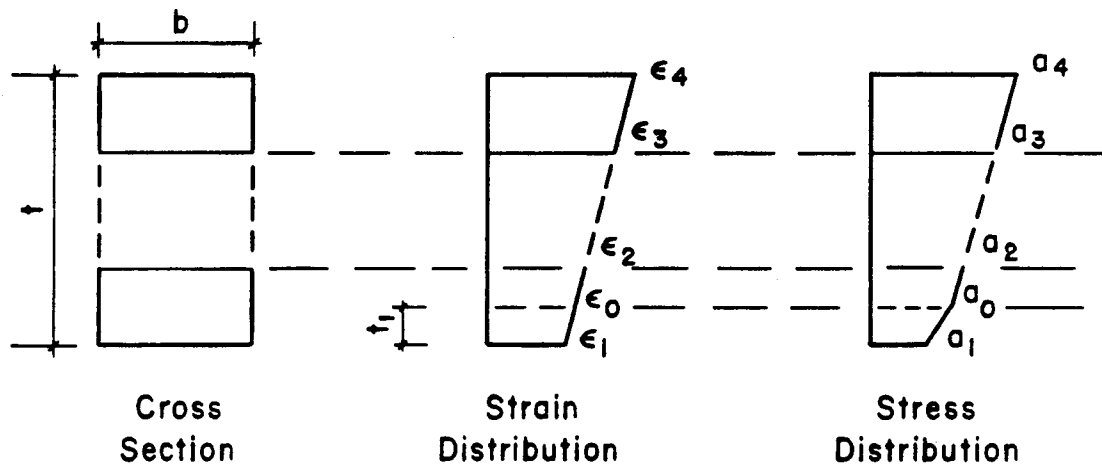
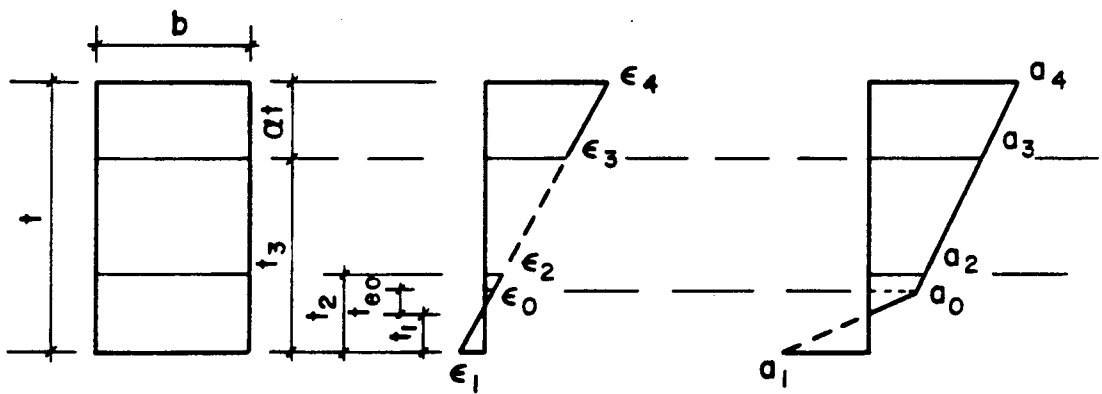


Figure B.4 Cases 1 and 4: Constant Modulus between any Two Strain Values except ϵ_2 and ϵ_3



CASE 2A



CASE 2B

Figure B.5 Cases 2A and 2B: Change in Modulus between ϵ_1 and ϵ_2

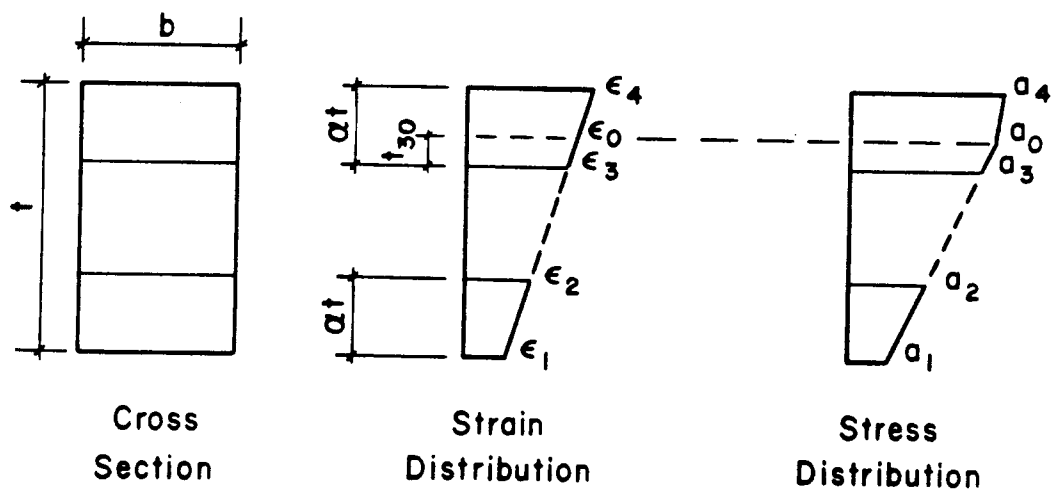
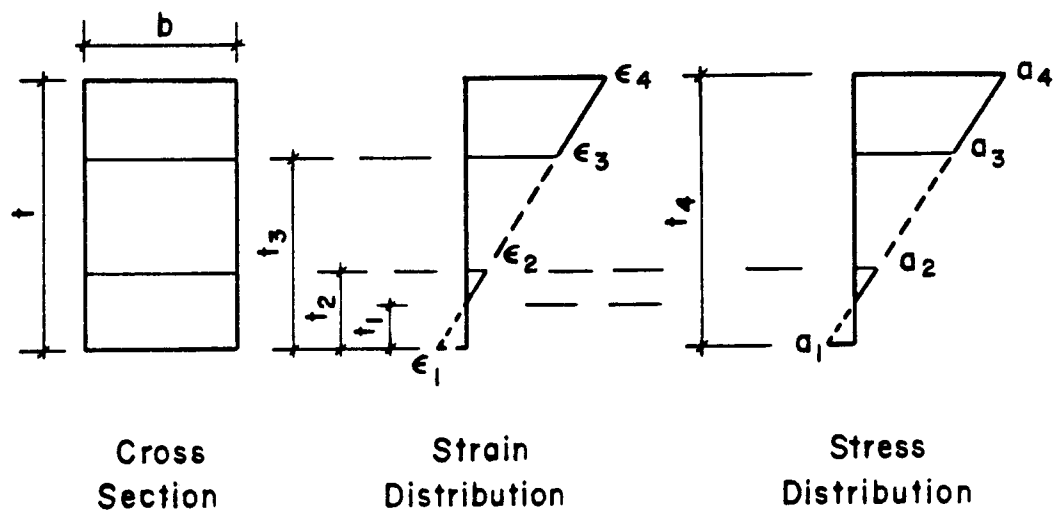
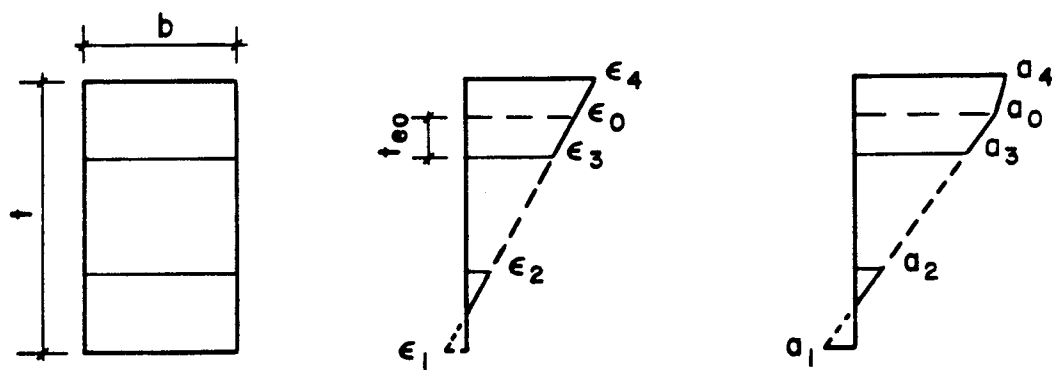


Figure B.6 Case 3: Change in Modulus between ϵ_3 and ϵ_4

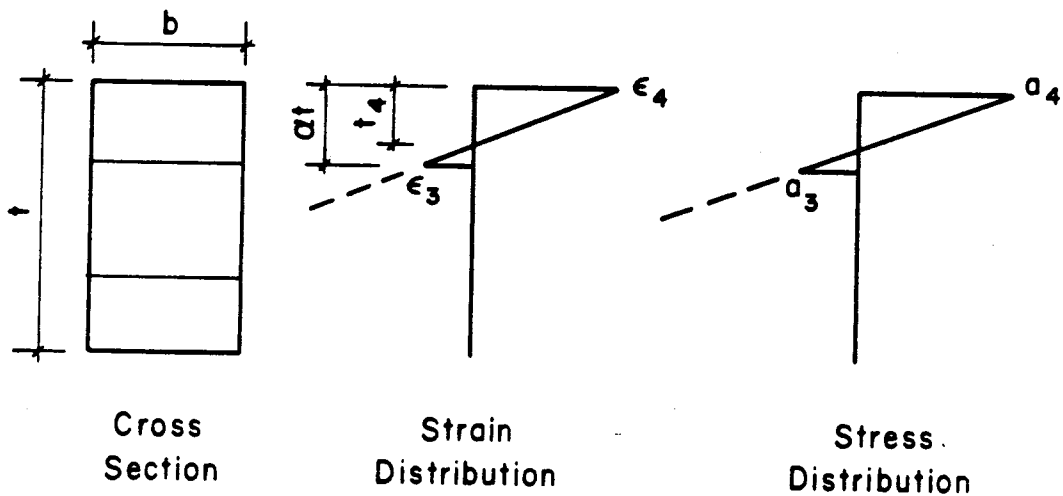


CASE 5A

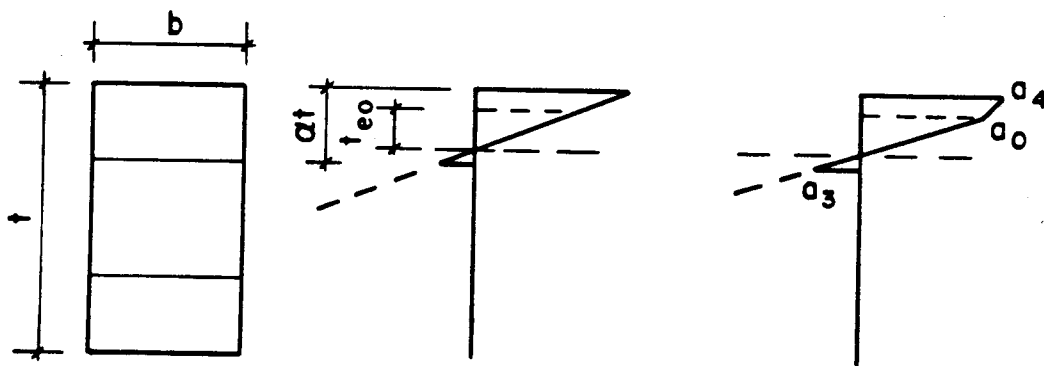


CASE 5B

Figure B.7 Cases 5A and 5B: Tension and Constant/Change in Modulus between ϵ_3 and ϵ_4



CASE 6A



CASE 6B

Figure B.8 Cases 6A and 6B: Large amount of tension on Cross-Section

B1.2 Program Nomenclature

A1, A2, ...	STRESSES AT VARIOUS POINTS ON MASONRY WALL CROSS-SECTION
AS	TOTAL AREA OF STEEL REINFORCEMENT IN WALL
ALPHA	RATIO OF EFFECTIVE THICKNESS TO HALF WALL THICKNESS
DELTA X	INCREMENTAL DISTANCE ALONG WALL HEIGHT
E0	ϵ_0 (AS DEFINED IN FIGURE B.2)
E1, E2, ...	STRAINS AT VARIOUS POINT ON THE CROSS-SECTION
E1M	INITIAL MODULUS OF MASONRY, MPA
E2M	CRACKED MODULUS OF MASONRY, MPA
EMB	MAXIMUM ELASTIC MOMENT ($f'_m b t^2 / 6$)
EMMB	M/M_b
EMMBM	MAXIMUM VALUE OF M/M_b
EMMBT(K)	ARRAY OF M/M_b IN SUBROUTINE 'EMPFY'

EMMBW(N) ARRAY OF M/M_b AT JOINT OF INTEREST (JJ)
WHERE WALL ROTATION IS CALCULATED

ES MODULUS OF ELASTICITY OF STEEL

EUB ULTIMATE COMPRESSION STRAIN OF MASONRY

ER STRAIN IN STEEL REINFORCEMENT

FIFYB(I) ARRAY OF ϕ/ϕ_b IN MAIN PROGRAM

FIFYBT(K) ARRAY OF ϕ/ϕ_b IN SUBROUTINE
'EMPPHI'

FPM MASONRY ULTIMATE COMPRESSION STRESS

FS STRESS IN STEEL REINFORCEMENT

FY YIELD STRENGTH OF STEEL REINFORCEMENT

JJ JOINT ON WALL AT WHICH WALL ACTUAL ROTATION
IS TO BE COMPUTED

ETA RATIO OF DISTANCE FROM BOTTOM FACE OF WALL
CROSS-SECTION TO CENTROID OF STEEL

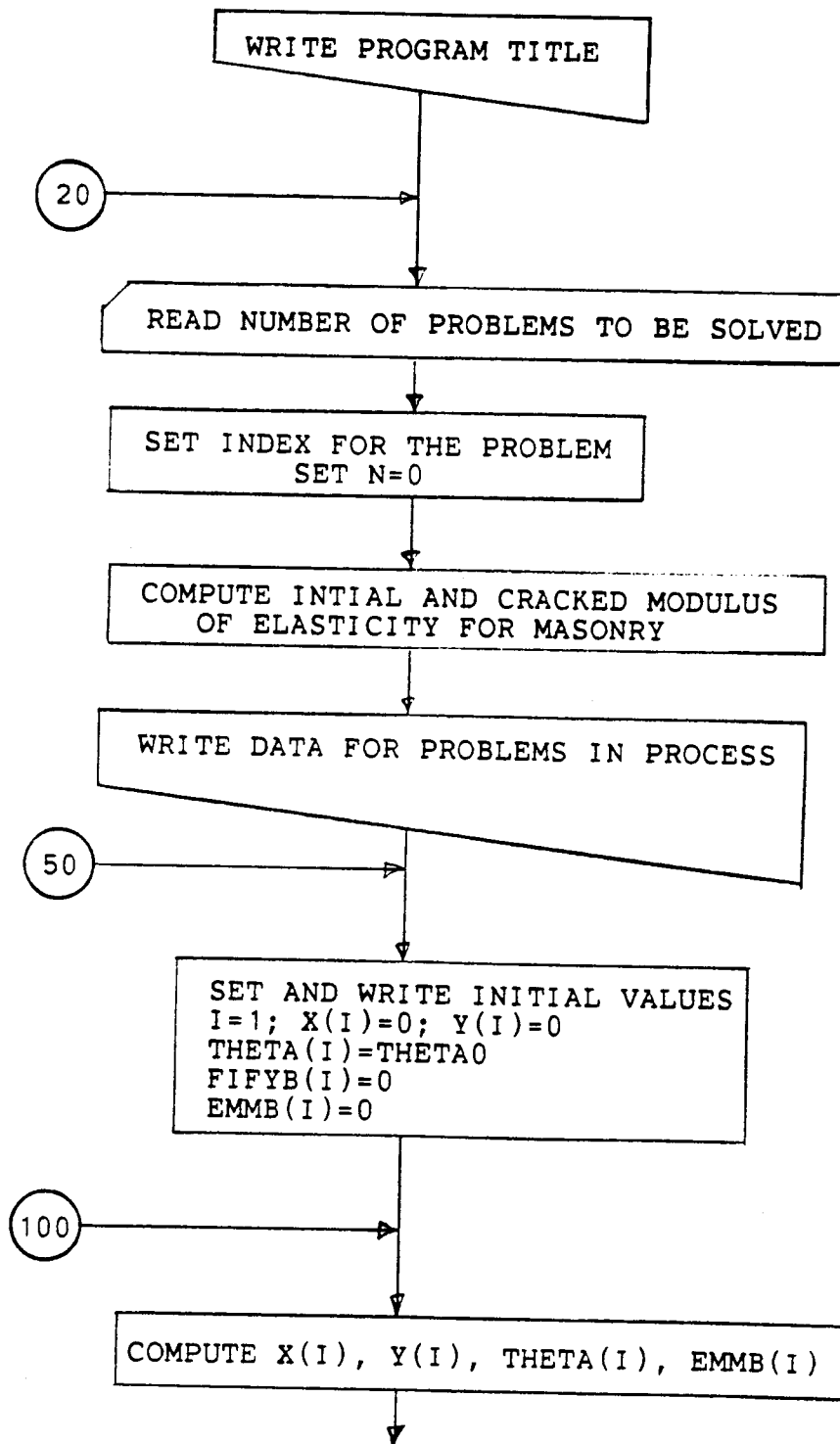
P1, P2, ... AXIAL LOAD FOR VARIOUS CASES CONSIDERED

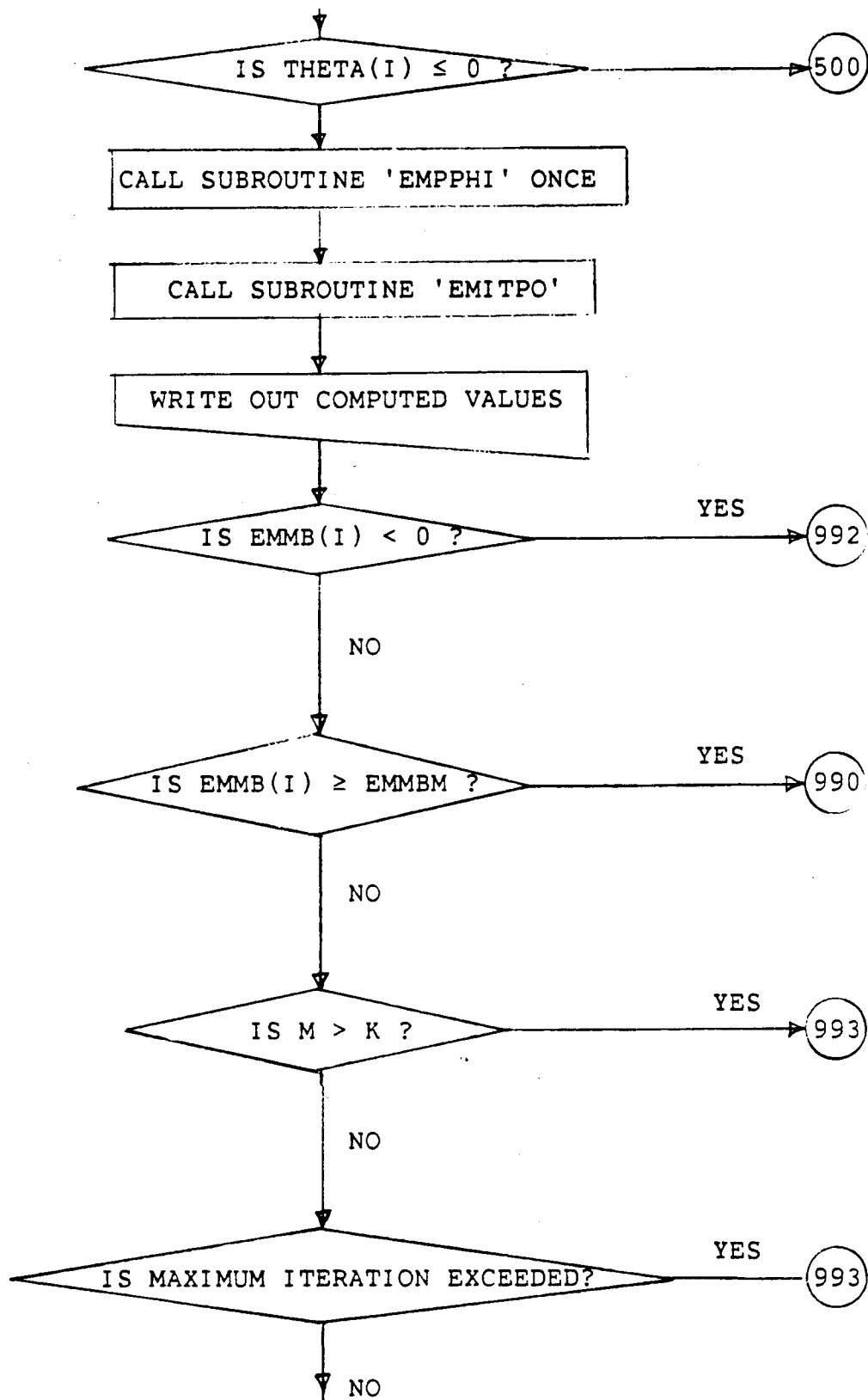
PB CROSS-SECTION AXIAL LOAD CAPACITY

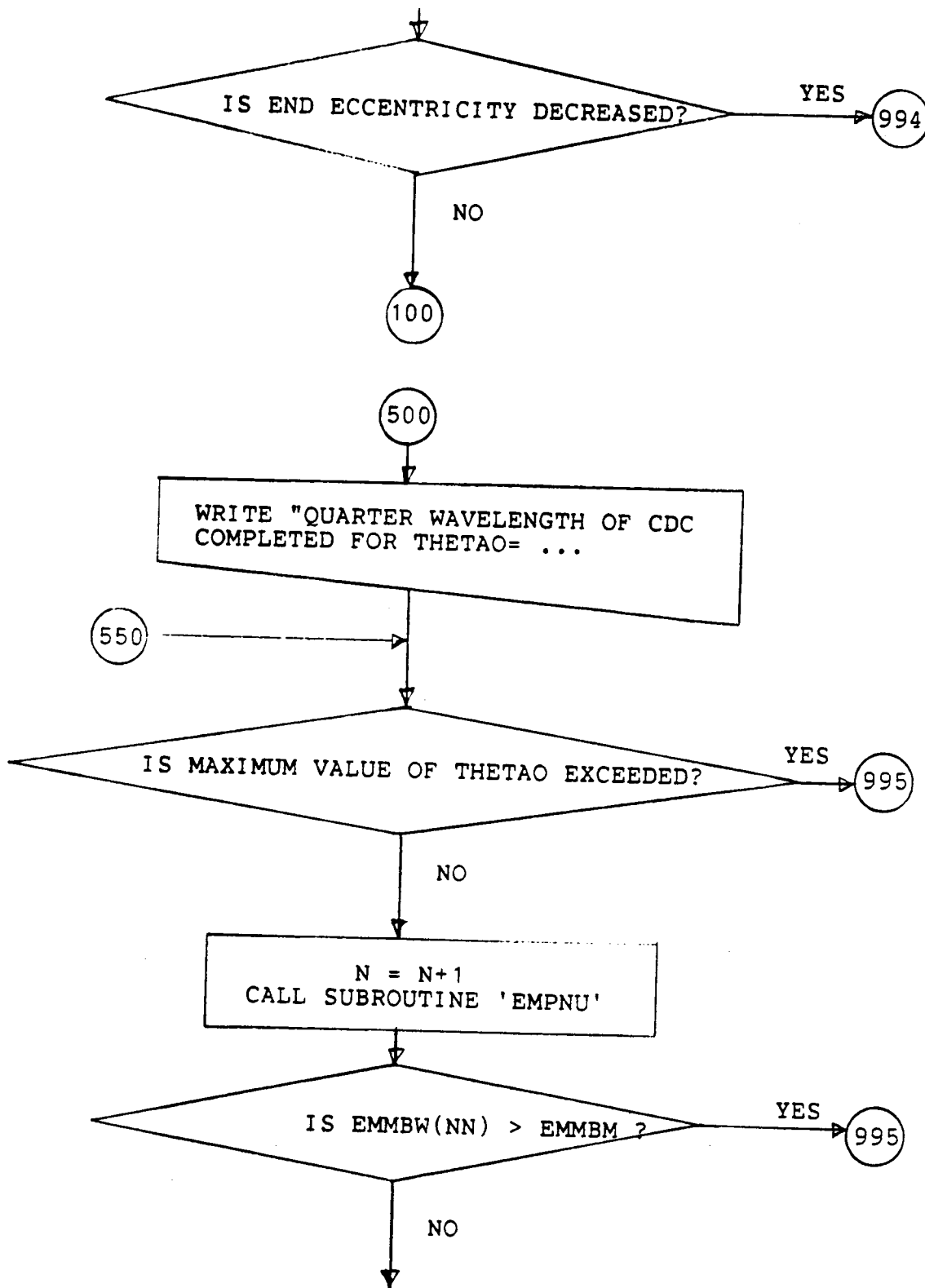
PPB	P/P_b
PPBT(J)	ARRAY FOR TESTING CONVERGENCE TO P/P_b IN SUBROUTINE 'EMPPHI'
RHO	RATIO OF STEEL REINFORCEMENT TO AREA OF WALL CROSS-SECTION
ROTW	WALL ACTUAL ROTATION AT JOINT JJ
T	TOTAL DEPTH OF CROSS-SECTION IN MM
THETA	TANGENTIAL ROTATION AT ANY POINT ON WALL
THETA0	END ROTATION OF THE WALL
X	DISTANCE ALONG WALL LENGTH
Y	DEFLECTION ALONG WALL LENGTH

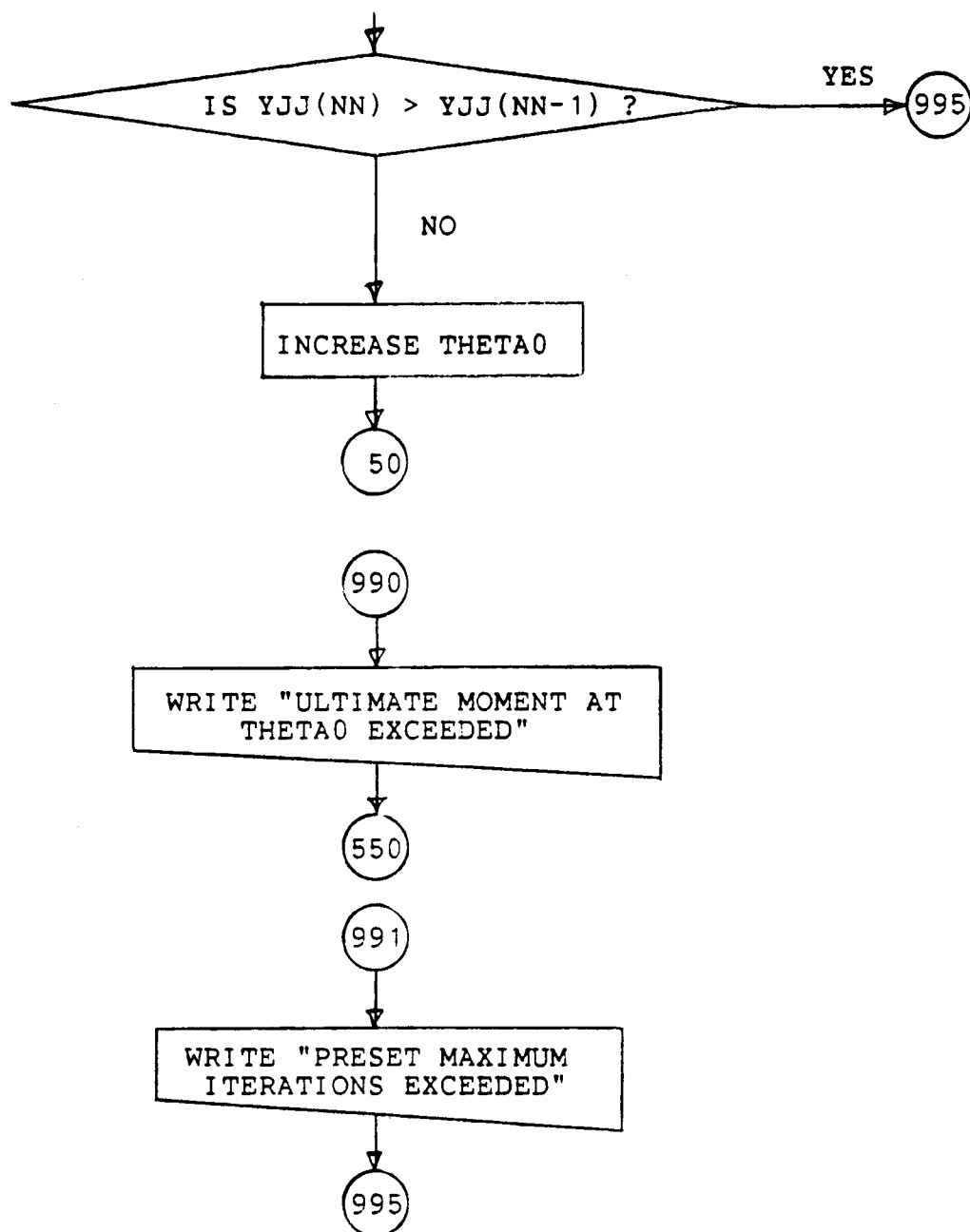
B1.3 FLOW DIAGRAM OF THE COMPUTER PROGRAM

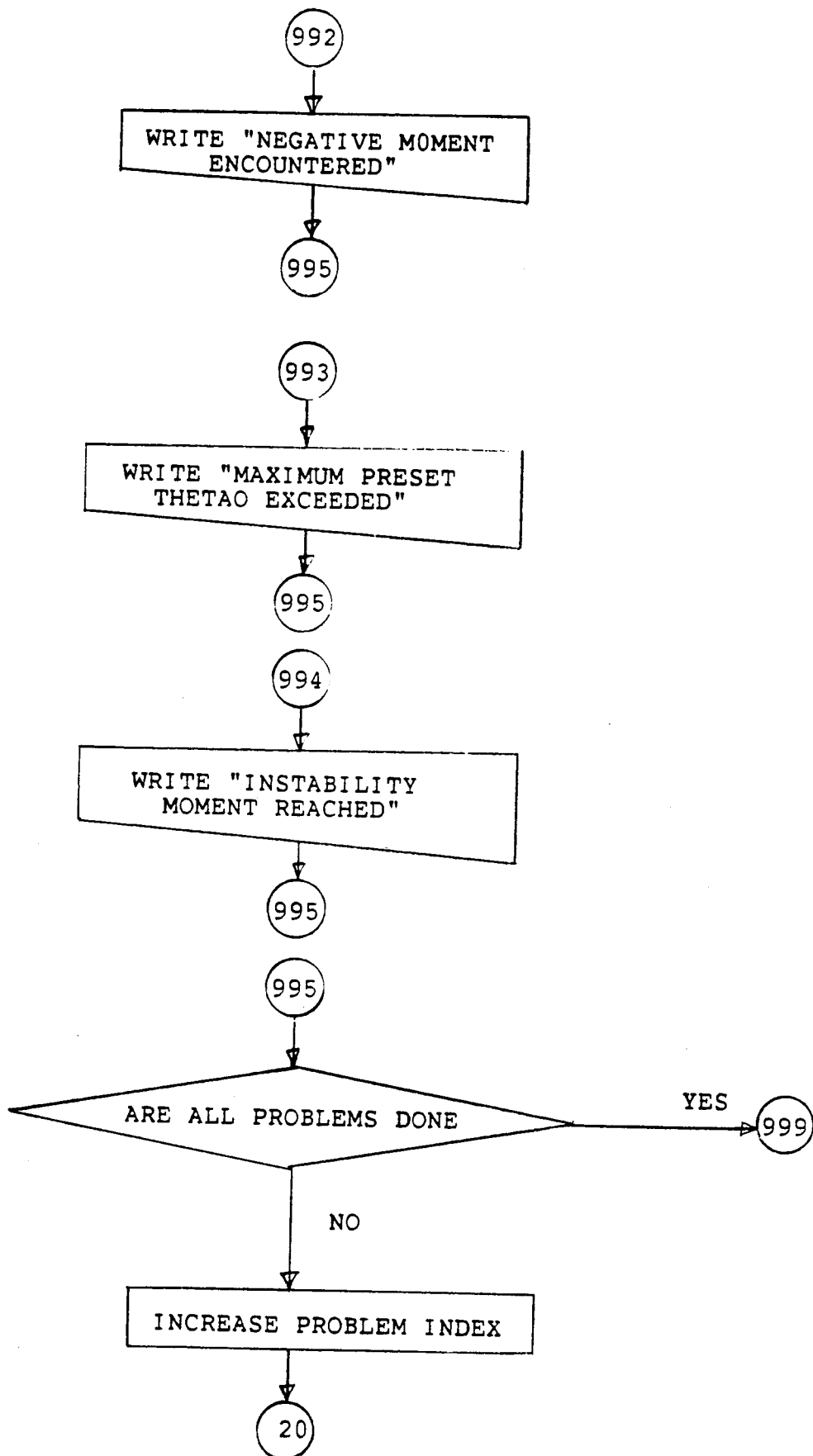
B1.3.1 MAIN PROGRAM



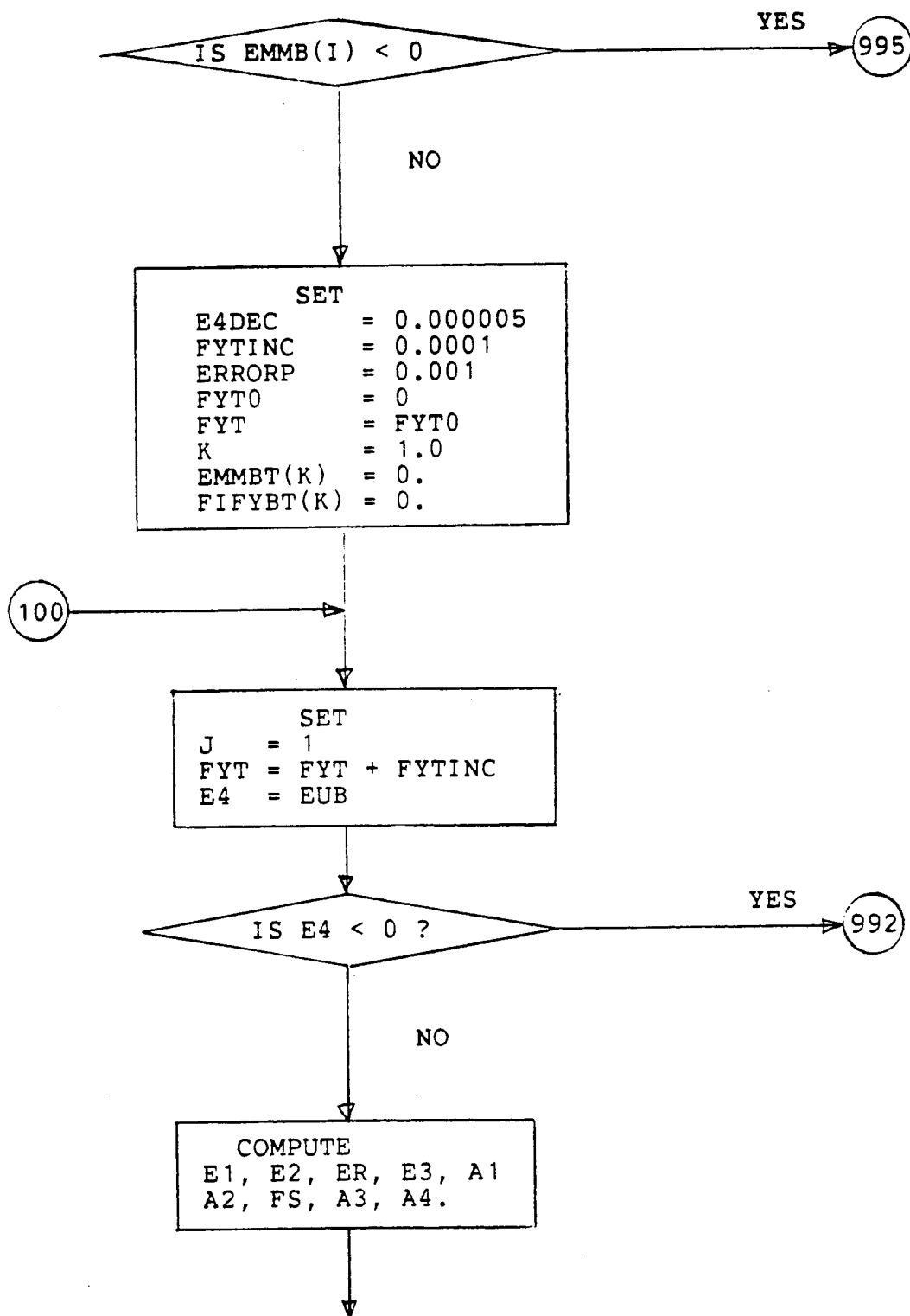


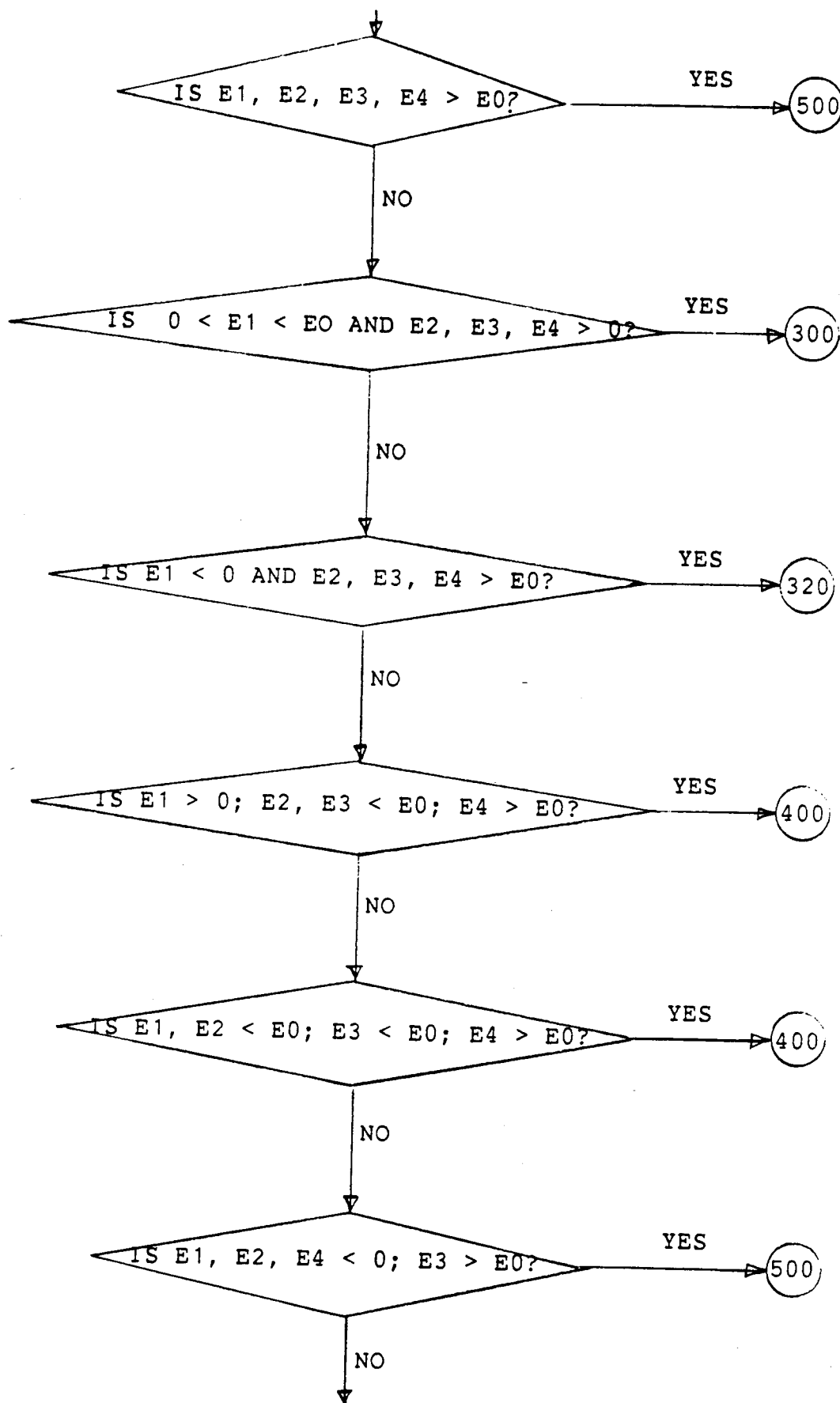


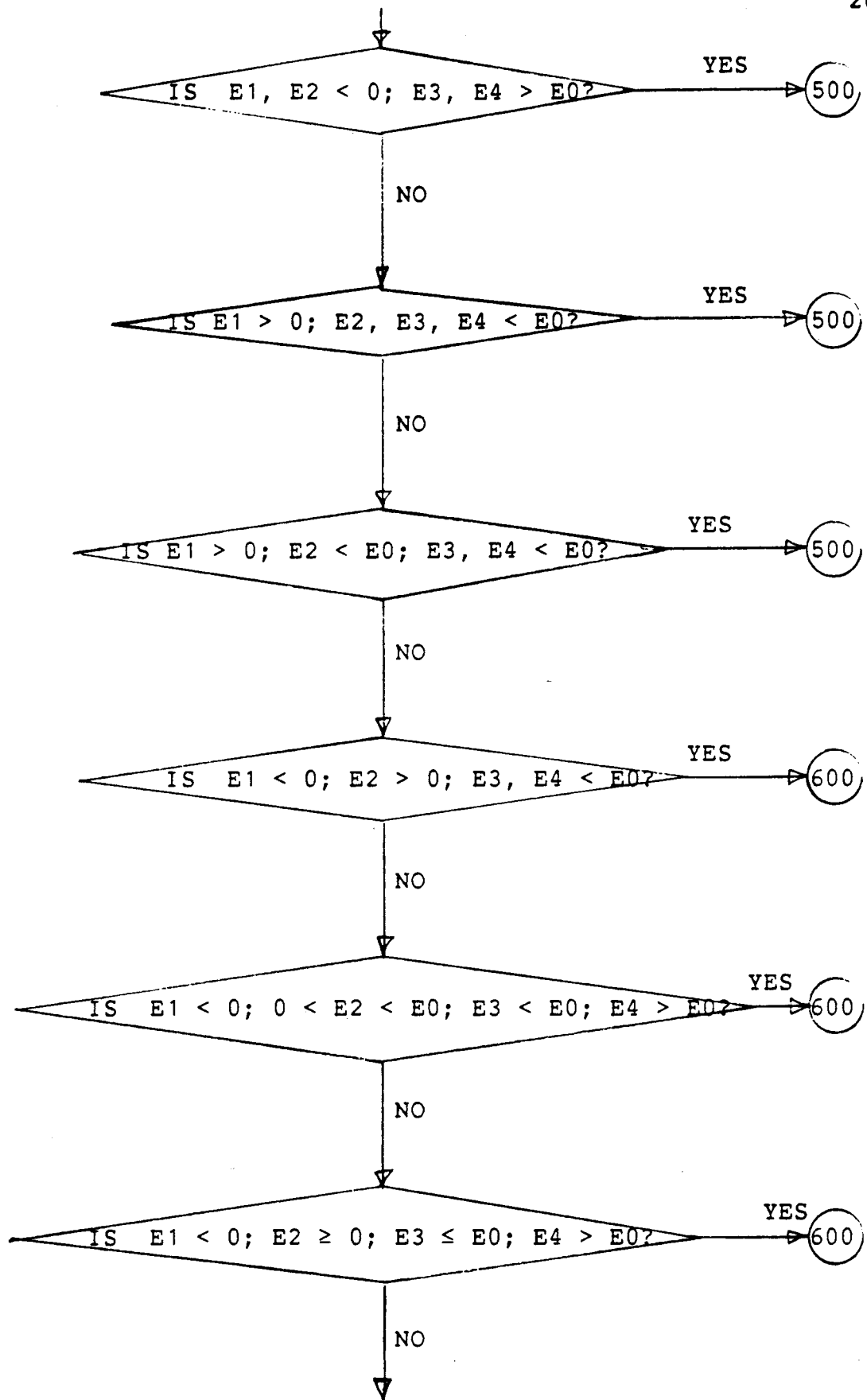


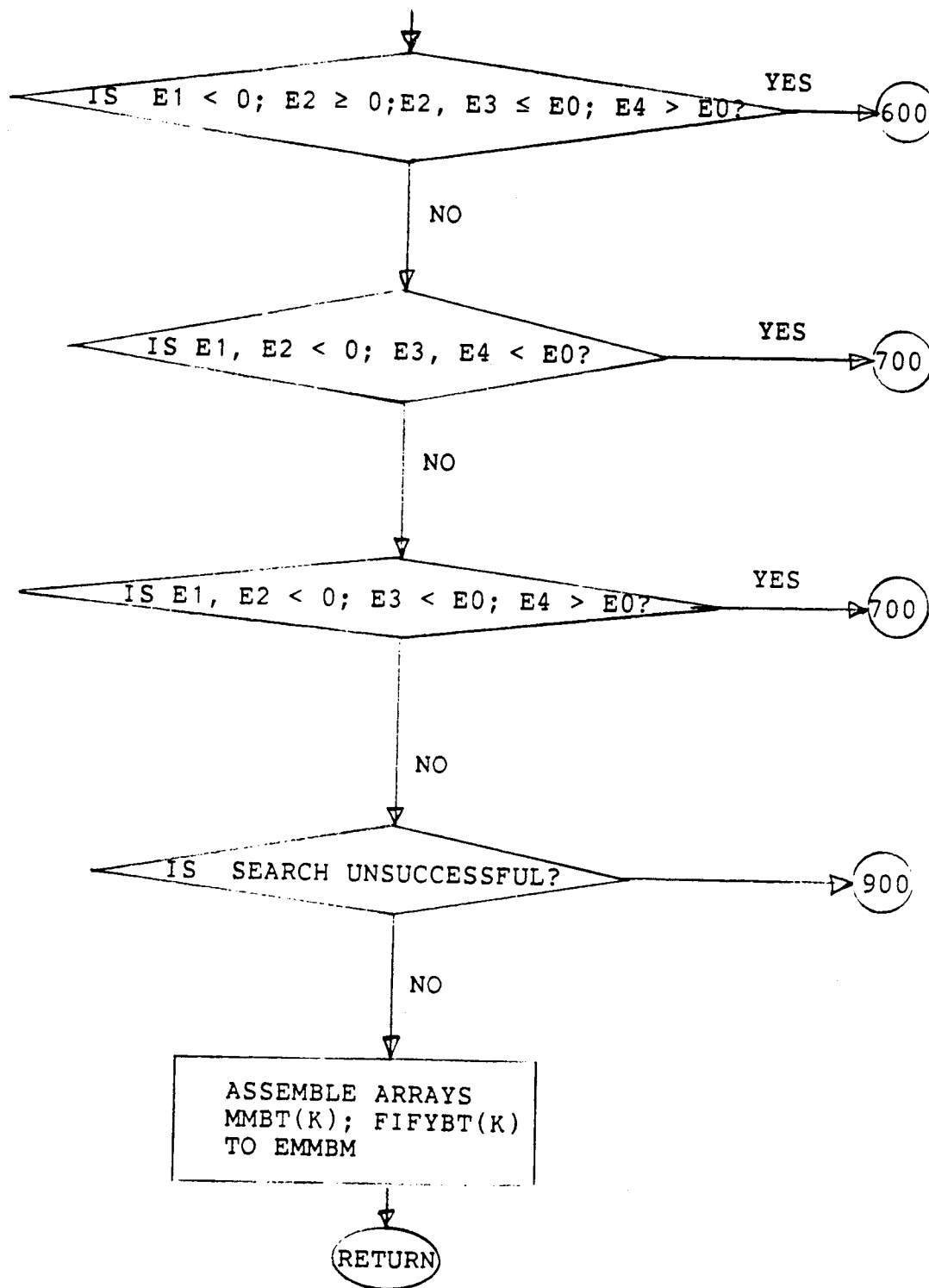


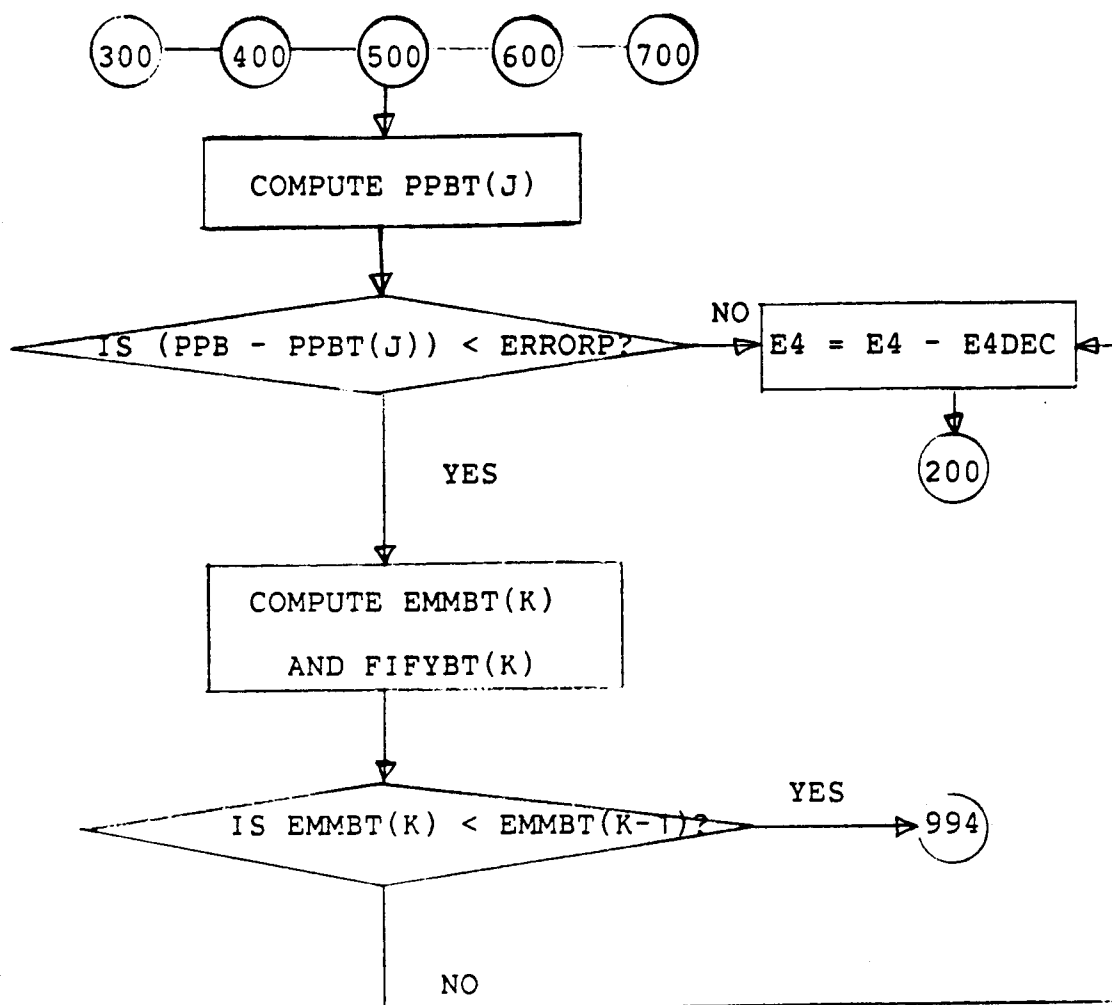
B1.3.2 SUBROUTINE 'EMPPHI'

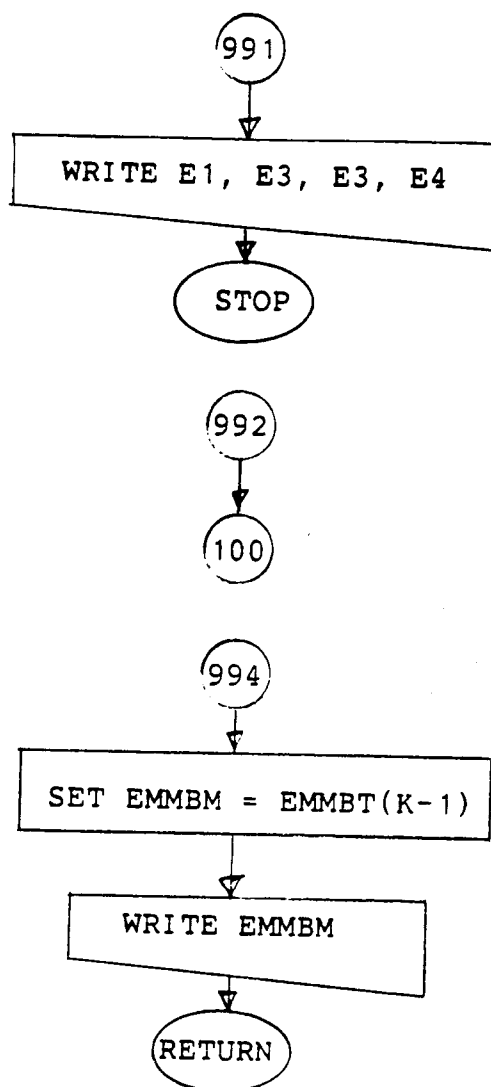


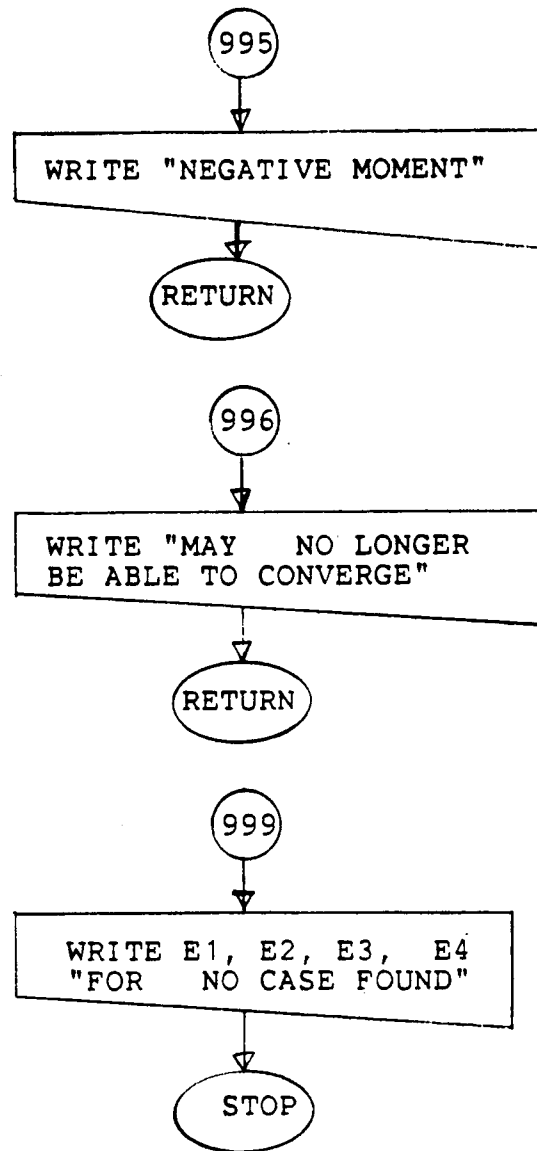




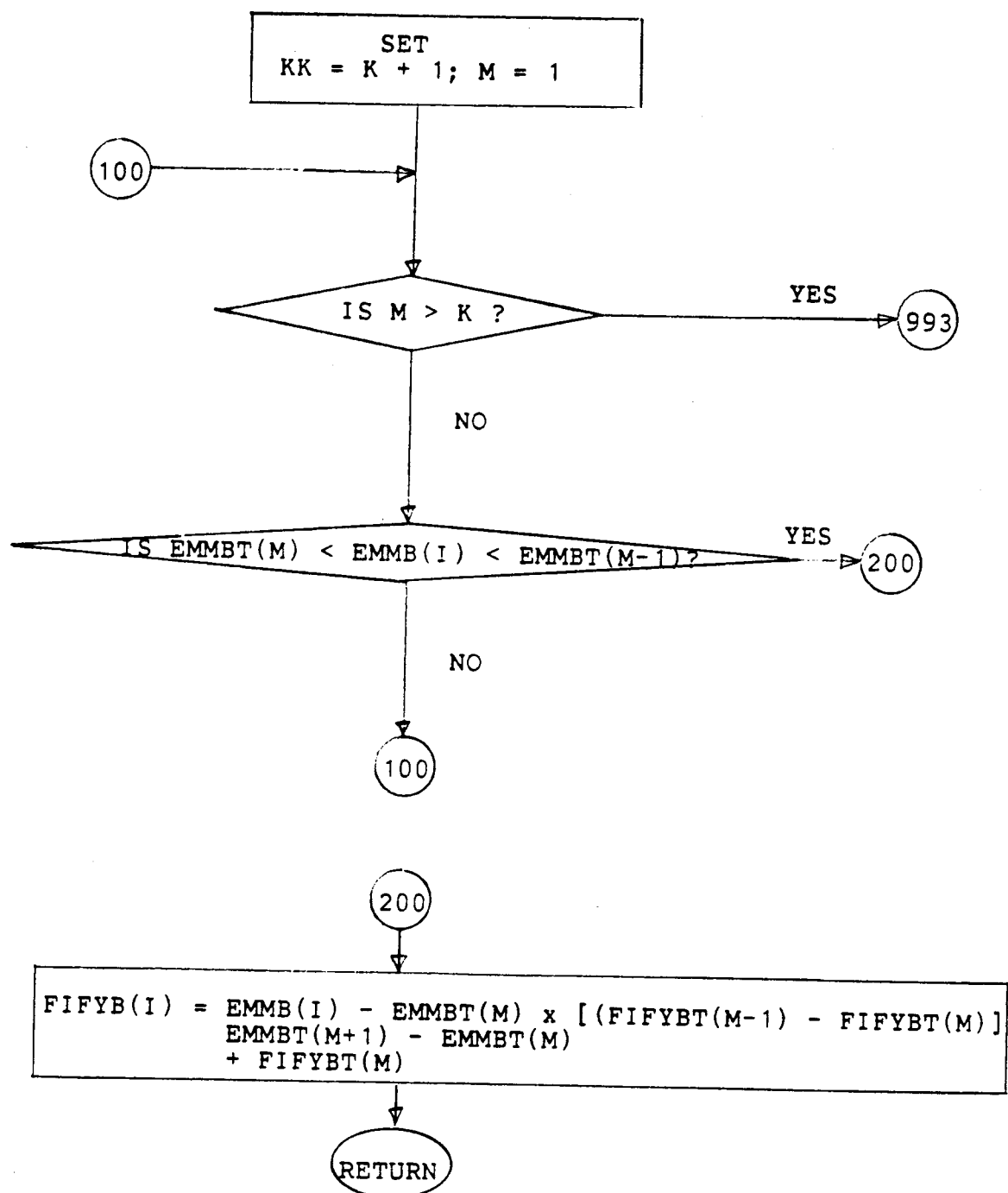


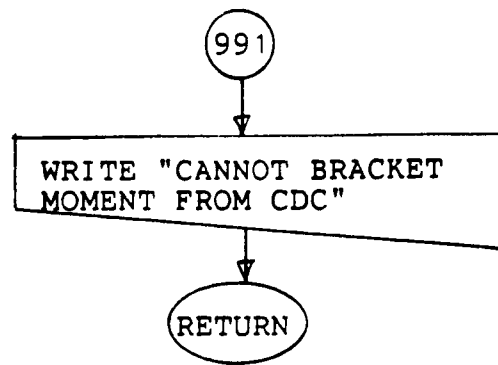




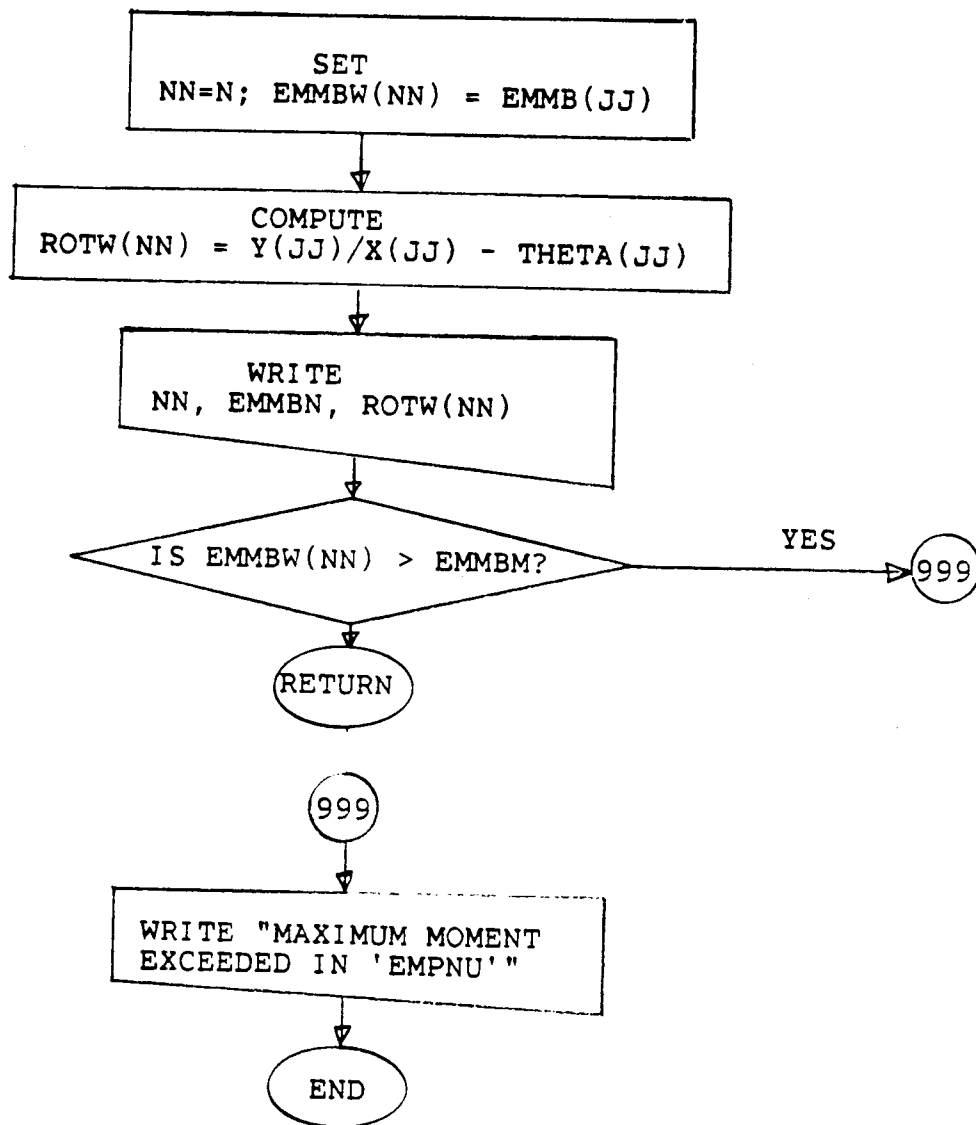


B1.3.3 SUBROUTINE 'EMITPO'





B.3.4 SUBROUTINE "EMPNU"



APPENDIX B2

PROGRAM LISTINGS

```

1  C*****
2  C THIS PROGRAMME CALCULATES THE DEFORMATION AND MAXIMUM
3  C STRENGTH OF A MASONRY WALL USING THE CONCEPTS OF THE
4  C COLUMN DEFLECTION CURVE (CDC)
5  C THIS VERSION CALLED CDC.IE.UA USES TWO MODULI FOR
6  C ANALYSING HOLLOW MASONRY WALLS WITHOUT REINFORCEMENT
7  C
8  C
9  C
10 C*****
11 C
12 C COMMON X(300),Y(300),THETA(300),YJJ(50),
13 C   EMBB(300),FIFYB(300),PPBT(500),EMMBT(300),
14 C   FIFYBT(300),EMMBW(50),ROTHU(50),PPB,FYB,PB,E4,EMB,
15 C   E1M,E2M,EO,EUB,T,FIFYBM,FYT,FYTM,EMMBM,INST,INSTE,
16 C   INSTM,NCIT,NCITH,ERRDRP,ALPHA,I,J,K,M,N,U,JJ
17 C
18 C WRITE(6,2000)
19 C
20 C INPUT AND ECHO CHECK
21 C
22 C READ(5,1000)NPROBM
23 C
24 C NPROB=0
25 C
26 C
27 C 20 READ(5,1100,END=999)ALPHA,T,DELTA,X,EO,EUB,PPB,THETAO,
28 C   THETOM,ERRDRP,NCITM,UJ
29 C
30 C JJ=JJ+1
31 C E1M=0.7/EO
32 C E2M=0.3/(EUB-EO)
33 C
34 C WRITE(6,2100)ALPHA,T,DELTA,X,EO,EUB,PPB,THETAO,E1M,E2M,UJ
35 C EMB=1./6.
36 C
37 C CALL DEMARCATION ROUTINE
38 C
39 C CALL STAR
40 C
41 C
42 C INITIALIZE VARIOUS COUNTERS
43 C
44 C N=0
45 C IR=0
46 C
47 C DO I=1
48 C   X(I)=0
49 C   Y(I)=0
50 C   THETA(I)=THETAO
51 C   EMBB(I)=0
52 C   FIFYB(I)=0
53 C
54 C WRITE HEADINGS AND ECHO CHECK INITIAL VALUES
55 C
56 C WRITE(6,2150)
57 C WRITE(6,2300)I,X(I),Y(I),EMBB(I),FIFYB(I),THETA(I)
58 C
59 C INCREASE COUNTER AND BEGIN CALCULATIONS
60 C
61 C 100 I=I+1
62 C   X(I)=X(I-1)+DELTA
63 C   Y(I)=Y(I-1)+THETA(I-1)*DELTA-DELTA**2/2 *FIFYB(I-1)*2 *EUB/T
64 C   THETA(I)=THETA(I-1)-DELTA*FIFYB(I-1)*2 *EUB/T
65 C   EMBB(I)=EMB+PPB*Y(I)/T
66 C
67 C CHECK IF THETA IS ZERO (QUARTER WAVE OF CDC) FOR NEW THETAO
68 C
69 C IF(THETA(I).LT.0.) GO TO 500
70 C
71 C
72 C WILL NEED CURVATURE FROM M-P-FY RELATIONS
73 C CALL EMPPY ONLY ONCE FOR A PARTICULAR P/PB
74 C
75 C
76 C
77 C IF(IR.LT.1)CALL EMPPH1
78 C IR=IR+1
79 C
80 C CALL EMITPD
81 C
82 C WRITE(6,2300)I,X(I),Y(I),EMBB(I),FIFYB(I),THETA(I)
83 C
84 C IF(EMBB(I).LT.0.)GO TO 992
85 C
86 C IF(EMBB(I).GE.EMMBM)GO TO 990
87 C
88 C
89 C CHECK VARIOUS LIMITS...
90 C
91 C IF(M.GT.K)GO TO 993
92 C
93 C IF(INSTE.GE.5) GO TO 993
94 C
95 C IF(NCIT.GE.NCITH)GO TO 991
96 C
97 C
98 C
99 C GO FOR MORE!!
100 C
101 C GO TO 100
102 C
103 C REACHED CENTRE OF CDC?
104 C
105 C 500 CALL STAR
106 C   WRITE(6,2920)THETAO,I
107 C   CALL STAR
108 C
109 C N=N+1
110 C
111 C CALL EMPPH
112 C
113 C IF(EMMBW(N).GT.EMMBM)GO TO 990
114 C
115 C IF(YJJ(N).LT.YJJ(N-1))GO TO 994
116 C
117 C
118 C HAVE YOU EXCEEDED THE PRESET LIMIT ON THETAO?
119 C
120 C IF(THETAO.GT.THETOM)GO TO 993

```

```

121 C
122 C OTHERWISE INCREASE THETA0
123 C
124 IF (THETA0.LT.0.10)TINC=0.01
125 IF (THETA0.GE.0.10)TINC=0.02
126 THETA0=THETA0+TINC
127 C
128 C MORE THETA0 TO CRANK, MIND BEGINNING AGAIN?
129 C
130 GO TO 50
131 C
132 990 WRITE(6,2600)THETA0
133 CALL STAR
134 C
135 N=N+1
136 C
137 CALL EMPNU
138 C
139 IF (I.LE.JJ1.AND.EMMBW(N).GT.EMMBM)GO TO 995
140 C
141 IF (YJJ(N).LT.YJJ(N-1))GO TO 994
142 C
143 C
144 C
145 C HAVE YOU EXCEEDED THE PRESET LIMIT ON THETA0?
146 C
147 IF (THETA0.GT.THETOM)GO TO 993
148 C
149 C OTHERWISE INCREASE THETA0
150 C
151 IF (THETA0.LT.0.10)TINC=0.01
152 IF (THETA0.GE.0.10)TINC=0.02
153 THETA0=THETA0+TINC
154 C
155 C MORE THETA0 TO CRANK, MIND BEGINNING AGAIN?
156 C
157 GO TO 50
158 C
159 991 WRITE(6,2910)
160 CALL STAR
161 C
162 N=N+1
163 C
164 CALL EMPNU
165 C
166 IF (I.LE.JJ1.AND.EMMBW(N).GT.EMMBM)GO TO 995
167 C
168 IF (YJJ(N).LT.YJJ(N-1))GO TO 994
169 C
170 C
171 C
172 C HAVE YOU EXCEEDED THE PRESET LIMIT ON THETA0?
173 C
174 IF (THETA0.GT.THETOM)GO TO 993
175 C
176 C OTHERWISE INCREASE THETA0
177 C
178 IF (THETA0.LT.0.10)TINC=0.01
179 IF (THETA0.GE.0.10)TINC=0.02
180 THETA0=THETA0+TINC
181 C
182 C MORE THETA0 TO CRANK, MIND BEGINNING AGAIN?
183 C
184 GO TO 50
185 C
186 992 WRITE(6,2700)
187 CALL STAR
188 GO TO 995
189 C
190 C
191 993 CALL STAR
192 WRITE(6,2600)THETOM
193 CALL STAR
194 GO TO 995
195 C
196 994 CALL STAR
197 WRITE(6,2930)ROTNUI(N)
198 CALL STAR
199 C
200 995 CALL STAR
201 IF (NPROB.EQ.NRPOBM)GO TO 999
202 C
203 NPROB=NPROB+1
204 GO TO 20
205 C
206 C
207 999 STOP
208 C
209 C FORMAT STATEMENTS
210 C
211 1000 FORMAT(14)
212 1100 FORMAT(8F10.5,2I5)
213 2000 FORMAT(30X,'1'/'MASONRY WALL DEFORMATION AND STRENGTH',/
214 '26X','USING COLUMN DEFLECTION CURVES - CDC. IE. UR',///)
215 C
216 2100 FORMAT(///10X,'ALPHA= ',F10.4,5X,'DE= ',F10.4,5X,'DELTA= ',
217 F10.5,5X,'EO= ',F10.8,///10X,'EUB= ',F10.8,5X,'P/PB= ',
218 F10.5,5X,'THETA0= ',F10.5,5X,///10X,'E1M= ',F10.5,5X,
219 'E2M= ',F10.5,5X,'AT JOINT #',I4)
220 2150 FORMAT(//9X,'1',9X,'X',9X,'Y',11X,'M/MB',9X,'FI/FYB',
221 5X,'THETA',9X,'E4',9X,'FYT')
222 2300 FORMAT(//5X,I4,4X,F9.3,3X,F9.4,3X,F9.5,3X,F9.5)
223 C
224 2500 FORMAT(//5X,'*****ULTIMATE MOMENT EXCEEDED ',
225 ' WHEN THETA0= ',F8.5,' *****')
226 2600 FORMAT(//5X,'*****MAXIMUM PRESET THETA0 OF ',F8.4,
227 ' EXCEEDED *****')
228 2700 FORMAT(//5X,'***** NEGATIVE M/MB OR FI/FYB *****')
229 2810 FORMAT(//5X,'***** MAX ALLOWED ITERATION EXCEEDED *****')
230 2820 FORMAT(//5X,'*****QUARTER WAVELENGTH OF CDC COMPLETED ',
231 ' FOR THETA0= ',F8.4,' AT I= ',I5,' *****')
232 2930 FORMAT(//5X,'*****INSTABILITY MOMENT IN CDC AT ',
233 ' WALL END ROTATION = ',F8.5,' *****')
234 END
235 C
236 C
237 C
238 C
239 C
240 C*****

```

```

241 C SUBROUTINE TO CALCULATE PHI/PHYS FOR A PARTICULAR P/PB
242 C *****
243 C
244 C
245 C
246 C
247 C SUBROUTINE EMPPH1
248 C
249 C
250 C COMMON X(300),Y(300),THETA(300),YJJ(50),
251 C EMMB(300),FIFYB(300),PPBT(500),EMMBT(300),
252 C FIFYBT(300),EMMBW(50),ROTHU(50),PPB,FYB,PB,E4,EMB,
253 C E1M,E2M,E0,EUB,T,FIFYBM,FYT,FYTM,EMMBM,INST,INSTC,
254 C INSTM,NCIT,NCITM,ERRDRP,ALPHA,I,J,K,M,N,JJ
255 C
256 C IF(EMMB(I).LT.O.)GO TO 995
257 C
258 C ...CALCULATE CONSTANTS AND OUTPUT THEM
259 C
260 C PB=1.
261 C EMB=1./S.
262 C FYB=2 *EUB/D
263 C AO=E1M+E0
264 C
265 C ...INITIALIZE VARIOUS VALUES
266 C
267 C INSTM=5
268 C E4DEC=0.000005
269 C FYTINC=0.00001
270 C FYTO=0
271 C FYT=FYTO
272 C JW=1
273 C INST=0
274 C NCIT=0
275 C IMAX=0
276 C K=1
277 C EMMBT(K)=0.
278 C FIFYB(K)=0.
279 C
280 C 100 J=1
281 C FYT=FYT+FYTINC
282 C E4=EUB
283 C IREP=1
284 C
285 C INCREASE COUNTER AND BEGIN CALCULATIONS
286 C
287 C
288 C 200 IF(E4 LE O..OR.IREP.EO.2)GO TO 992
289 C E1=E4-FYT
290 C E2=E1+ALPHA+FYT
291 C E3=E1+11*(ALPHA)+FYT
292 C
293 C ASSIGN PROPER EM TO STRAIN VALUES AT ANY POINT
294 C
295 C IF(E1 LE EO)A1=E1+E1M
296 C IF(E1 GT EO)A1=(E1-E0)*E2M+AO
297 C IF(E2 LE EO)A2=E2+E1M
298 C IF(E2 GT EO)A2=(E2-E0)*E2M+AO
299 C IF(E3 LE EO)A3=E3+E1M
300 C IF(E3 GT EO)A3=(E3-E0)*E2M+AO
301 C IF(E4 LE EO)A4=E4+E1M
302 C IF(E4 GT EO)A4=(E4-E0)*E2M+AO
303 C IF(E1 LT O.)A1=0.
304 C IF(E2 LT O.)A2=0.
305 C IF(E3 LT O.)A3=0.
306 C IF(E4 LT O.)A4=0.
307 C
308 C TEST FOR VARIOUS STRESS DISTRIBUTION CASES, ACT ACCORDINGLY
309 C CASE 1.
310 C
311 C IF(E1 GT EO AND E2 GT EO AND E3 GT EO AND E4 GT EO)GO TO 500
312 C
313 C CASE 2A AND 2B.
314 C
315 C IF(E1 GT O..AND.E1 LT EO AND E2 GT EO AND E4 GT EO)GO TO 300
316 C IF(E1 LT O..AND.E2 GE EO AND E3 GT EO AND E4 GT EO)GO TO 300
317 C
318 C CASE 3
319 C
320 C IF(E1 GE O..AND.E2 GT O..AND.E3 LT EO AND E4 GT EO)GO TO 400
321 C IF(E1 LT O..AND.E2 LT O..AND.E3 GT O..AND.E3 LT EO AND
322 C *E4 GT EO)GO TO 400
323 C
324 C CASE 4
325 C
326 C IF(E1 LT O..AND.E2 LT O..AND.E3 GE O..AND.E4 LE EO)GO TO 500
327 C IF(E1 LT O..AND.E2 LT O..AND.E3 GT EO AND E4 GT EO)GO TO 500
328 C IF(E1 GE O..AND.E2 LT EO AND E3 LT EO AND E4 LE EO)GO TO 500
329 C IF(E1 GE O..AND.E2 LT EO AND E3 GT EO AND E4 GT EO)GO TO 500
330 C
331 C CASES 5A AND 5B
332 C
333 C IF(E1 LT O..AND.E2 GT O..AND.E3 LE EO AND E4 LE EO)GO TO 500
334 C IF(E1 LT O..AND.E2 GT O..AND.E2 LE EO AND E3 GT EO)GO TO 500
335 C IF(E1 LT O..AND.E2 GE O..AND.E3 LE EO AND E4 GT EO)GO TO 500
336 C IF(E1 LT O..AND.E2 LE O..AND.E3 LE EO AND E4 GT EO)GO TO 500
337 C
338 C CASES 6A AND 6B
339 C
340 C IF(E1 LT O..AND.E2 LT O..AND.E3 LE O..AND.E4 LE EO)GO TO 700
341 C IF(E1 LT O..AND.E2 LT O..AND.E3 LE O..AND.E4 GT EO)GO TO 700
342 C
343 C IF CANNOT SATISFY ANY OF THESE, THEN SOMETHING WRONG
344 C
345 C GO TO 991
346 C
347 C CASE 2A AND 2B: E1 LESS THAN EO OR NEG, E2, E3, GREATER THAN EO
348 C
349 C 300 IF(E1 LT O.)GO TO 320
350 C J=J+1
351 C T1=(EO-E1)/FYT
352 C P2B=(A3+A4)/2 *ALPHA+(AO+A2)/2 *(ALPHA-T1)+(AO+A1)/2 *T1
353 C PPBT(J)=P2B/PB
354 C
355 C
356 C ...CHECK WITH INCOMING PPB
357 C
358 C PDIF=ABS(PPB-PPBT(J))/PPB
359 C IF(PDIF LE ERRDRP)GO TO 350
360 C GO TO 370

```

```

361 C
362 320 J=J+1
363 T4=E4/(E4-E1)
364 IF(T4.GT.1)T4=1.
365 T2=E2/E4+T4
366 TEO=E0/E4+T4
367 T1=ALPHA-T2
368 P2A=(A3+A4)/2 *ALPHA+(A0+A2)/2 *(T2-TEO)+(A0)/2 *TEO
369 PPBT(J)=P2A/PB
370 PDIF=ABS(PPB-PPBT(J))/PPB
371 IF(PDIF.LE.ERRORP)GO TO 340
372 GO TO 370
373 C
374 340 K=K+1
375 NC=21
376 EM2A=A4/2 *ALPHA+(.5-ALPHA/3 )+A3/2 *ALPHA+(.5-2./3 *ALPHA)
377 +A2/2 *(T2-TEO)+(ALPHA-T1)*(ALPHA-T1)/3 *(T2-TEO)+A0/2 *(T2-TEO)+
378 +(.5-T1-(T2-TEO)/3 )-A0/2 *TEO+(.5-T1-2.*TEO/3 )-A1/2 *T1+
379 +(.5-T1/3 )
380 EMMBT(K)=EM2A/EMB
381 FIFYBT(K)=FYT/(2 *EUB)
382 C
383 IF(EMMBT(K).LT.0.)GO TO 395
384 IF(IMAX.GT.0)EMMBT(K)=EMMBM
385 IF(EMMBT(K).LT.EMMBT(K-1).AND.IMAX.EQ.0)GO TO 394
386 IREP=IREP+1
387 C
388 GO TO 370
389 C
390 360 K=K+1
391 NC=22
392 EM2B=A4/2 *ALPHA+(.5-ALPHA/3 )+A3/2 *ALPHA+(.5-2./3 *ALPHA)
393 +A2/2 *(ALPHA-T1)+(ALPHA-T1)*(ALPHA-T1)/3 *(ALPHA-T1)+A0/2 *(ALPHA-T1)+
394 +(.5-T1-(ALPHA-T1)/3 )-A0/2 *T1+(.5-2.*T1/3 )-A1/2 *T1+
395 +(.5-T1/3 )
396 EMMBT(K)=EM2B/EMB
397 FIFYBT(K)=FYT/(2 *EUB)
398 C
399 IF(EMMBT(K).LT.0.)GO TO 395
400 IF(IMAX.GT.0)EMMBT(K)=EMMBM
401 IF(EMMBT(K).LE.EMMBT(K-1).AND.IMAX.EQ.0)GO TO 394
402 IREP=IREP+1
403 C
404 IF(EMMBT(K).EQ.EMMBM)INST=INST+1
405 IF(INST.GE.INSTM)GO TO 393
406 IREP=IREP+1
407 C
408 OR TRY ANOTHER EDGE STRAIN
409 C
410 370 E4=E4-E4DEC
411 C
412 MORE CALCULATIONS
413 C
414 GO TO 200
415 C
416 CASE 3 : E1, E2, E3 LESS THAN E0, E4 GREATER
417 C
418 400 J=J+1
419 T3=(E0-E1)/FYT-(1 *ALPHA)
420 P3=(A0+A4)/2 *(ALPHA-T3)+(A0+A3)/2 *T3+(A1+A2)/2 *ALPHA
421 PPBT(J)=P3/PB
422 C
423 CHECK WITH INCOMING PPB
424 C
425 PDIF=ABS(PPB-PPBT(J))/PPB
426 IF(PDIF.LE.ERRORP)GO TO 450
427 GO TO 480
428 C
429 450 K=K+1
430 NC=3
431 EM3=A4/2 *(ALPHA-T3)+(ALPHA-T3)/3 *(ALPHA-T3)+A0/2 *(ALPHA-T3)+
432 +(.5-2./3 *(ALPHA-T3))+A0/2 *T3+(.5-(ALPHA-T3)-T3/3 )+A3/2 *
433 +T3+(.5-(ALPHA-T3)-2 *T3/3 )-A2/2 *ALPHA+(.5-2./3 *ALPHA)
434 +A1/2 *ALPHA+(.5-ALPHA/3 )
435 EMMBT(K)=EM3/EMB
436 FIFYBT(K)=FYT/(2 *EUB)
437 IF(EMMBT(K).LT.0.)GO TO 395
438 IF(IMAX.GT.0)EMMBT(K)=EMMBM
439 IF(EMMBT(K).LE.EMMBT(K-1).AND.IMAX.EQ.0)GO TO 394
440 IREP=IREP+1
441 C
442 C
443 IF(EMMBT(K).EQ.EMMBM)INST=INST+1
444 IF(INST.GE.INSTM)GO TO 393
445 IREP=IREP+1
446 C
447 OR TRY ANOTHER EDGE STRAIN
448 C
449 460 E4=E4-E4DEC
450 C
451 GO TO 200
452 C
453 CASES 1 AND 4 - MOST COMMON CASES *****
454 INCLUDING BOTH E1 AND E2 NEGATIVE CASES *****
455 C
456 500 J=J+1
457 P4=(A1+A2+A3+A4)/2 *ALPHA
458 PPBT(J)=P4/PB
459 C
460 CHECK WITH INCOMING PPB
461 C
462 PDIF=ABS(PPB-PPBT(J))/PPB
463 IF(PDIF.LE.ERRORP)GO TO 550
464 GO TO 570
465 C
466 550 K=K+1
467 NC=14
468 EM4=0.5*ALPHA*(A4+(.5-ALPHA/3 )+A3+(0.5-2 *ALPHA/3 ))
469 +A2+(.5-2 *ALPHA/3 )-A1+(.5-ALPHA/3 )
470 EMMBT(K)=EM4/EMB
471 FIFYBT(K)=FYT/(2 *EUB)
472 IF(EMMBT(K).LT.0.)GO TO 395
473 IF(IMAX.GT.0)EMMBT(K)=EMMBM
474 IF(EMMBT(K).LE.EMMBT(K-1).AND.IMAX.EQ.0)GO TO 394
475 IREP=IREP+1
476 C
477 C
478 IF(EMMBT(K).EQ.EMMBM)INST=INST+1
479 IF(INST.GE.INSTM)GO TO 393
480

```

```

481       IREP=IREP+1
482     C
483     C
484     C...OTHERWISE...
485     C
486     E70 E4=E4-E4DEC
487     C
488     GO TO 200
489     C
490     C...CASES 5A AND 5B : E1 NEGATIVE, E2 POSITIVE
491     C
492     500 J=J+1
493     T4=E4/(E4-E1)
494     IF(T4.GT.1.)T4=1.
495     T2=E2/E4+T4
496     IF(T2.LT.0.)T2=0.
497     T1=1.-T4
498     IF(E3.LT.E0.AND.E4.GT.E0)GO TO 540
499     C
500     PSA=0.5*A2+T2*(A3+A4)/2 =ALPHA
501     PPBT(J)=PSA/PB
502     C
503     C...CHECK WITH INCOMING PPB
504     C
505     PDIF=ABS(PPB-PPBT(J))/PPB
506     IF(PDIF.LE.ERRORP)GO TO 520
507     GO TO 570
508     C
509     520 K=K+1
510     NC=51
511     EMSA=0.5*ALPHA*((A4*(.5-ALPHA/3.)+A3*(.5-.2*ALPHA/3.))
512     *-0.5*A2+T2*(.5-T1-.2*T2/3.))
513     EMMBT(K)=EMSA/EMB
514     FIFYBT(K)=FYT/(2.*EUB)
515     IF(EMMBT(K).LT.0.)GO TO 555
516     IF(IMAX.GT.0)EMMBT(K)=EMMBM
517     C== IF(EMMBT(K).LE.EMMBT(K-1).AND.IMAX.EQ.0)GO TO 554
518     C
519     C
520     IF(EMMBT(K).EQ.EMMBM)INST=INST+1
521     IF(INST.GE.INSTM)GO TO 553
522     IREP=IREP+1
523     C
524     C...OTHERWISE...
525     C
526     GO TO 570
527     C
528     540 T3=E3/E4+T4
529     TEO=E0/E4+T4
530     T30=T3-T30
531     T30=T30-T3
532     IF(T30.LT.0)GO TO 555
533     T40=T4-TEO
534     C
535     PSB=(A0+A4)/2.*T40+(A0+A3)/2.*T30+0.5*T2+A2
536     PPBT(J)=PSB/PB
537     C
538     C...CHECK WITH INCOMING PPB
539     C
540     PDIF=ABS(PPB-PPBT(J))/PPB
541     IF(PDIF.LE.ERRORP)GO TO 550
542     GO TO 570
543     C
544     550 K=K+1
545     NC=52
546     EMSB=A4/2.*T40*(.5-T40/3.)+A0/2.*T40*(.5-.2./3.*T40)
547     *-A0/2.*T30*(.5-T40-T30/3.)+A3/2.*T30+
548     *-1.5-T40-.2./3.*T30)-0.5*T2+A2*(.5-T1-.2./3.*T2)
549     *-A1/2.*T2*(.5-T1-.2./3.*T2)
550     EMMBT(K)=EMSB/EMB
551     FIFYBT(K)=FYT/(2.*EUB)
552     IF(EMMBT(K).LT.0.)GO TO 555
553     IF(IMAX.GT.0)EMMBT(K)=EMMBM
554     C== IF(EMMBT(K).LE.EMMBT(K-1).AND.IMAX.EQ.0)GO TO 554
555     C
556     C
557     IF(EMMBT(K).EQ.EMMBM)INST=INST+1
558     IF(INST.GE.INSTM)GO TO 553
559     IREP=IREP+1
560     C
561     C
562     C...OTHERWISE...
563     C
564     570 E4=E4-E4DEC
565     C
566     GO TO 200
567     C
568     C...CASE 5 : E1, E2, E3 ALL NEGATIVE, E4 LESS OR EQUAL TO E3
569     C
570     C
571     700 J=J+1
572     E3=E4-ALPHA+FYT
573     T4=E4/(E4-E3)=ALPHA
574     C
575     C...CHECK FOR MAXIMUM E4
576     C
577     IF(E4.GT.E0)GO TO 750
578     C
579     PSA=A4+T4*0.5
580     PPBT(J)=PSA/PB
581     C
582     C...CHECK WITH INCOMING PPB
583     C
584     PDIF=ABS(PPB-PPBT(J))/PPB
585     IF(PDIF.LE.ERRORP)GO TO 720
586     GO TO 750
587     C
588     720 K=K+1
589     NC=51
590     EMSA=A4+T4*.5*(.5-T4/3.)
591     EMMBT(K)=EMSA/EMB
592     FIFYBT(K)=FYT/(2.*EUB)
593     IF(EMMBT(K).LT.0.)GO TO 595
594     IF(IMAX.GT.0)EMMBT(K)=EMMBM
595     C== IF(EMMBT(K).LE.EMMBT(K-1).AND.IMAX.EQ.0)GO TO 594
596     C
597     C
598     IF(EMMBT(K).EQ.EMMBM)INST=INST+1
599     IF(INST.GE.INSTM)GO TO 593
600     IREP=IREP+1

```



```

801 C
802 GO TO 780
803 C
804 CASE 6B
805 C
806
807 780 TO=EO+T4/E4
808 PPS=(AO+A4)/2*(T4-T0)+AO/2*TC
809 PPBT(J)=PPS/PB
810 C
811 CHECK WITH INCOMING PPS
812 C
813 PDIF=ABS(PPS-PPBT(J))/PPS
814 IF(PDIF.LE.ERRDRP)GO TO 770
815 GO TO 780
816 C
817 770 K=K+1
818 NC=52
819 EMBB=A4/2*(T4-T0)+(.5-(T4-T0)/3.)*AO/2*(T4-T0)+
820 (.5-2./3.)*(T4-T0)+AO/2*TO*(.5-(T4-T0)-TO/3.)
821 EMMBT(K)=EMBB/EMB
822 FIFYBT(K)=FYT/(2*EUB)
823 C= IF(IMAX.GT.0)EMMBT(K)=EMMBM
824 IF(EMMBT(K).LE.EMMBT(K-1).AND.IMAX.EC.0)GO TO 994
825 C
826 IF(EMMBT(K).EC.EMMBM)INST=INST+1
827 IF(INST.GE.INSTM)GO TO 993
828 IREP=IREP+1
829 C
830 C
831 C
832 OTHERWISE
833 C
834 780 E4=E4-E4DEC
835 C
836 C
837 GO FOR MORE
838 C
839 GO TO 200
840 C
841 991 WRITE(6,2600)E1,E2,E3,E4
842 STOP
843 C
844 INCREASE FYT AFTER E4 GOES NEGATIVE
845 C
846 992 IF(IREP.LT.2)NCIT=NCIT+1
847 IF(NCIT.GT.NCITM)GO TO 996
848 GO TO 100
849 C
850 993 WRITE(6,2810)EMMBT(K)
851 RETURN
852 C
853 994 EMMBM=EMMBT(K-1)
854 C
855 RAISE A FLAG FOR REACHING MAX MOMENT
856 C
857 IMAX=IMAX+1
858 C
859 C
860 GO FOR SOME MORE CALCULATIONS
861 C
862 E4=E4-E4DEC
863 C
864 GO TO 200
865 C
866 WRITE(6,2810)EMMBM
867 RETURN
868 C
869 995 WRITE(6,2820)
870 RETURN
871 C
872 996 EMMBM=EMMBT(K)
873 WRITE(6,2830)FYT,EMMBM
874 RETURN
875 C
876 999 WRITE(6,2600)E1,E2,E3,E4,NC
877 STOP
878 C
879 C
880 FORMAT STATEMENTS
881 C
882 1000 FORMAT(10F10.5)
883 C
884 2000 FORMAT(30X,'1','MASONRY WALL MOMENT-LOAD-CURVATURE',/
885 '33X','USING INELASTIC BEHAVIOR - MPFY,IE,N',///)
886 C
887 2100 FORMAT(///10X,'ALPHA=',F8.5,5X,'E0=',F8.5,5X,'EUB=',F8.5,
888 5X,'E1M=',F10.5,///10X,'E2M=',F10.5,5X,'PB=',F8.5,5X,'MB=',
889 5X,'FYT0=',F8.5,///10X,'*****P/PB=',F8.5, '*****')
890 C
891 2150 FORMAT(//9X,'I',7X,'M/MB',10X,'P/PB',10X,'E4',9X,'FYT',9X,
892 'F1/FYB')
893 C
894 2300 FORMAT(5X,14,3X,F10.5,3X,F10.5,3X,F10.5,3X,F10.5,3X,F10.5)
895 C
896 2600 FORMAT(//5X,'***** ULTIMATE MOMENT EXCEEDED *****')
897 C
898 2600 FORMAT(//5X,'***** NO CASE SOLUTION FOR E1=',F8.5,'; E2=',
899 5X,'F8.5,30X,'E3=',F8.5,' E4=',F8.5,' NC=',15,' *****')
900 C
901 C
902 C
903 2800 FORMAT(//5X,'*****NEGATIVE COMPRESSION STRAIN AT FYT= ',
904 5X,'F10.5, ' *****')
905 C
906 C
907 2810 FORMAT(//5X,' ***** MAXIMUM MOMENT REACHED!! ***** ',/
908 5X,'***** IN EMPFY AT M/MB =',F8.5, ' *****')
909 C
910 2820 FORMAT(//5X,' ***** NEGATIVE MOMENT REACHED!! ***** ')
911 C
912 2830 FORMAT(//5X,' ***** MAY NO LONGER BE ABLE TO FIND ***** ',/
913 5X,'***** ANOTHER P/PB AFTER FYT= ',F8.5, ' *****',/
914 5X,'*****MAXIMUM M/MB= ',F8.5, '*****')
915 C
916 END
917 C
918 C
919 C
920 C

```

```

721 C
722 C
723 C
724 C.....
725 C...SUBROUTINE TO CALCULATE M/MB BY INTERPOLATION
726 C.....
727 C
728 C
729 C
730 C
731 C      SUBROUTINE EMITPD
732 C
733 C      COMMON X(300),Y(300),THETA(300),YJJ(50),
734 C      *EMMB(300),FIFYB(300),PPBT(500),EMMBT(300),
735 C      *FIFYBT(300),EMMBW(50),ROTHU(50),PPB,FYB,PB,E4,EMB,
736 C      *EIM,E2M,E0,EUB,T,FIFYBM,FYT,FYTM,EMMBM,INST,INSTC,
737 C      *INSTM,NCIT,NCITM,ERRDRP,ALPHA,I,J,K,M,N,JJ
738 C
739 C
740 C      INSTC=0
741 C      KK=K+1
742 C      DO 100 M=1,KK
743 C      IF(EMMB(I))GE.EMMBT(M).AND.EMMB(I).LT.EMMBT(M+1))GO TO 200
744 C      IF(EMMB(I))GT.EMMBT(M).AND.EMMB(I).LE.EMMBT(M+1))GO TO 200
745 C      IF(M.GT.K)GO TO 991
746 C      100 CONTINUE
747 C
748 C      INTERPOLATE TO GET CORRESPONDING PHI/PHIB, CHECK FOR PLATEAU
749 C
750 C      200 ERINST=ABS(EMMBT(M+1)-EMMBT(M))/EMMBT(M+1)
751 C      IF (ERINST.LT.0.005)GO TO 300
752 C
753 C      OTHERWISE
754 C
755 C      FIFYB(I)=(EMMB(I)-EMMBT(M))/(EMMBT(M+1)-EMMBT(M))*
756 C      *(FIFYBT(M+1)-FIFYBT(M))+FIFYBT(M)
757 C      RETURN
758 C
759 C      300 FIFYB(I)=FIFYBT(M)
760 C      INSTC=INSTC+1
761 C      IF(INSTC.GE.5)WRITE(5,3100)
762 C      RETURN
763 C      991 WRITE(5,3000)
764 C      RETURN
765 C
766 C      FORMAT STATEMENTS
767 C
768 C      3000 FORMAT(//10X,'*****CANNOT BRACKET MOMENT FROM CDC')
769 C      3100 FORMAT(//10X,'MAY HAVE REACHED MOMENT PLATEAU FOR CDC')
770 C      END
771 C
772 C
773 C
774 C
775 C
776 C.....
777 C      SUBROUTINE TO GENERATE FINAL EM-P-NU DATA
778 C.....
779 C
780 C      SUBROUTINE EMPNU
781 C
782 C      COMMON X(300),Y(300),THETA(300),YJJ(50),
783 C      *EMMB(300),FIFYB(300),PPBT(500),EMMBT(300),
784 C      *FIFYBT(300),EMMBW(50),ROTHU(50),PPB,FYB,PB,E4,EMB,
785 C      *EIM,E2M,E0,EUB,T,FIFYBM,FYT,FYTM,EMMBM,INST,INSTC,
786 C      *INSTM,NCIT,NCITM,ERRDRP,ALPHA,I,J,K,M,N,JJ
787 C
788 C
789 C      N=NN
790 C      YJJ(NN)=Y(JJ)
791 C      EMMBW(NN)=EMMB(JJ)
792 C      ROTHU(NN)=YJJ(X(JJ)-THETA(JJ))
793 C      WRITE(5,4000)NN,EMMBW(NN),ROTHU(NN)
794 C
795 C      IF(EMMBW(NN).GT.EMMBM.OR.YJJ(NN).LT.YJJ(NN-1))GO TO 999
796 C      999 WRITE(5,4100)
797 C
798 C      N=NN
799 C
800 C      RETURN
801 C
802 C      4000 FORMAT(//5X,'*****
803 C      *      //10X,'#',I2,3X,'(M/MBW)J = ',F8,7,3X,'(NU)J = ',F8,7,
804 C      *//5X,'*****')
805 C      4100 FORMAT(//5X,'*****MAX MOMENT OR ROTATION EXCEEDED IN EMITPD')
806 C      END
807 C
808 C
809 C
810 C
811 C
812 C
813 C.....
814 C      SUBROUTINE STAR
815 C.....
816 C
817 C
818 C
819 C
820 C
821 C      WRITE(5,2000)
822 C      2000 FORMAT(//5X,'*****
823 C      *      //10X,'#',I2,3X,'(M/MBW)J = ',F8,7,3X,'(NU)J = ',F8,7,
824 C      *//5X,'*****')
825 C      RETURN
826 C      END

```

End of #118

```

1 C*****
2 C... THIS PROGRAMME CALCULATES THE DEFORMATION AND MAXIMUM
3 C STRENGTH OF A MASONRY WALL USING THE CONCEPTS OF THE
4 C COLUMN DEFLECTION CURVE (CDC)
5 C THIS VERSION CALLED CDC IE R USES TWO MODULI FOR
6 C ANALYSING REINFORCED MASONRY WALLS
7 C
8 C
9 C
10 C
11 C
12 C*****
13 C
14 C COMMON X(300),Y(300),THETA(300),YJJ(50),
15 C *EMMB(300),FIFYB(300),PPBT(500),EMMBT(300),
16 C *FIFYST(300),EMMBW(50),ROTHU(50),PPB,FYB,PS,E4,EMB,
17 C *E1M,E2M,EO,EUB,T,FIFYBM,FYT,FYTM,EMMBM,INST,INSTC,
18 C *INSTM,NCIT,NCITM,ERRDRP,ALPHA,I,J,K,M,N,UJ,
19 C *PPM,FY,ES,RHO,BETA
20 C
21 C WRITE(6,2000)
22 C
23 C...INPUT AND ECHO CHECK
24 C
25 C READ(5,1000)NPROBM
26 C
27 C NPROB=0
28 C
29 C
30 C 20 READ(5,1100,END=999)ALPHA,T,DELTA,X,EO,EUB,PPB,PPM,FY,
31 C *ES,RHO,BETA,THETAO,THETOM,ERRDRP,NCITM,UJ
32 C
33 C JJ1=JJ-1
34 C E1M=EO *T/EO
35 C E2M=EO *3/(EUB-EO)
36 C
37 C WRITE(6,2100)ALPHA,T,DELTA,X,EO,EUB,PPB,THETAO,E1M,E2M,
38 C *PPM,FY,ES,RHO,BETA,UJ
39 C EMB=1./5
40 C
41 C...CALL DEMARCATION ROUTINE
42 C
43 C CALL STAR
44 C
45 C
46 C INITIALIZE VARIOUS COUNTERS
47 C
48 C N=0
49 C IR=0
50 C
51 C 50 J=1
52 C X(J)=0
53 C Y(J)=0
54 C THETA(J)=THETAO
55 C EMMB(J)=0
56 C FIFYB(J)=0
57 C
58 C...WRITE HEADINGS AND ECHO CHECK INITIAL VALUES
59 C
60 C WRITE(6,2150)
61 C WRITE(6,2300)I,X(1),Y(1),EMMB(1),FIFYB(1),THETA(1)
62 C
63 C... INCREASE COUNTER AND BEGIN CALCULATIONS
64 C
65 C 100 J=J+1
66 C X(J)=X(J-1)+DELTA*X
67 C Y(J)=Y(J-1)+THETA(J-1)*DELTA*X-DELTA*X**2/2 *FIFYB(J-1)*2 *EUB/T
68 C THETA(J)=THETA(J-1)+DELTA*X*FIFYB(J-1)*2 *EUB/T
69 C EMMB(J)=5 *PPB*Y(J)/T
70 C
71 C...CHECK IF THETA IS ZERO (QUARTER WAVE OF CDC) FOR NEW THETAO
72 C
73 C IF(THETA(J).LT.0.) GO TO 500
74 C
75 C
76 C...WILL NEED CURVATURE FROM M-P-FY RELATIONS
77 C...CALL EMPFY ONLY ONCE FOR A PARTICULAR P/PS
78 C
79 C
80 C
81 C IF(IR.LT.1)CALL EMPFY
82 C IR=IR+1
83 C
84 C CALL EMITPD
85 C
86 C WRITE(6,2300)I,X(1),Y(1),EMMB(1),FIFYB(1),THETA(1)
87 C
88 C IF(EMMB(J).LT.0.)GO TO 992
89 C
90 C IF(EMMB(J).GE.EMMBM)GO TO 990
91 C
92 C
93 C...CHECK VARIOUS LIMITS...
94 C
95 C IF(M.GT.K)GO TO 993
96 C
97 C IF(INSTC.GE.5) GO TO 993
98 C
99 C IF(NCIT.GE.NCITM)GO TO 991
100 C
101 C
102 C
103 C...GO FOR MORE!!
104 C
105 C GO TO 100
106 C
107 C...REACHED CENTRE OF CDC?
108 C
109 C 500 CALL STAR
110 C WRITE(6,2920)THETAO,I
111 C CALL STAR
112 C
113 C N=N+1
114 C
115 C CALL EMPNU
116 C
117 C IF(EMMBW(N).GT.EMMBM)GO TO 990
118 C
119 C IF(YJJ(N).LT.YJJ(N-1))GO TO 994
120 C
121 C

```

```

121 C
122 C...HAVE YOU EXCEEDED THE PRESET LIMIT ON THETAO?
123 C
124 IF(THETAO.GT.THETOM)GO TO 993
125 C
126 C...OTHERWISE INCREASE THETAO
127 C
128 IF(THETAO.LT.O.10)TINC=0.01
129 IF(THETAO.GE.O.10)TINC=0.02
130 THETAO=THETAO+TINC
131 C
132 C...MORE THETAO TO CRANK, MIND BEGINNING AGAIN?
133 C
134 GO TO 50
135 C
136 990 WRITE(6,2500)THETAO
137 CALL STAR
138 C
139 N=N+1
140 C
141 CALL EMPNU
142 C
143 IF(1.LE.JJ1.AND.EMMBW(N).GT.EMMBM)GO TO 995
144 C
145 IF(VJJ(N).LT.VJJ(N-1))GO TO 994
146 C
147 C
148 C
149 C
150 C...HAVE YOU EXCEEDED THE PRESET LIMIT ON THETAO?
151 C
152 IF(THETAO.GT.THETOM)GO TO 993
153 C
154 C...OTHERWISE INCREASE THETAO
155 C
156 IF(THETAO.LT.O.10)TINC=0.01
157 IF(THETAO.GE.O.10)TINC=0.02
158 THETAO=THETAO+TINC
159 C
160 C...MORE THETAO TO CRANK, MIND BEGINNING AGAIN?
161 C
162 GO TO 50
163 C
164 991 WRITE(6,2910)
165 CALL STAR
166 C
167 N=N+1
168 C
169 CALL EMPNU
170 C
171 IF(1.LE.JJ1.AND.EMMBW(N).GT.EMMBM)GO TO 995
172 C
173 IF(VJJ(N).LT.VJJ(N-1))GO TO 994
174 C
175 C
176 C
177 C...HAVE YOU EXCEEDED THE PRESET LIMIT ON THETAO?
178 C
179 IF(THETAO.GT.THETOM)GO TO 993
180 C
181 C...OTHERWISE INCREASE THETAO
182 C
183 IF(THETAO.LT.O.10)TINC=0.01
184 IF(THETAO.GE.O.10)TINC=0.02
185 THETAO=THETAO+TINC
186 C
187 C...MORE THETAO TO CRANK, MIND BEGINNING AGAIN?
188 C
189 GO TO 50
190 C
191 992 WRITE(6,2700)
192 CALL STAR
193 GO TO 995
194 C
195 C
196 993 CALL STAR
197 WRITE(6,2600)THETOM
198 CALL STAR
199 GO TO 995
200 C
201 994 CALL STAR
202 WRITE(6,2930)RDTHU(N)
203 CALL STAR
204 C
205 995 CALL STAR
206 IF(NPROB.EQ.NRPOB)GO TO 999
207 C
208 NPROB=NPROB+1
209 GO TO 20
210 C
211 999 STOP
212 C
213 C...FORMAT STATEMENTS
214 C
215 1000 FORMAT(14)
216 1100 FORMAT(14F10.5,215)
217 2000 FORMAT(30X,'1',MASONRY WALL DEFORMATION AND STRENGTH',/
218 '2&X','USING COLUMN DEFLECTION CURVES -CDC IE UR',///)
219 C
220 2100 FORMAT(//10X,'ALPHA= ',F10.4,5X,'T= ',F10.4,5X,'DELTA= ',
221 'F10.5,5X,'E0= ',F10.8,//10X,'EUB= ',F10.8,5X,'P/PB= ',
222 'F10.5,5X,'THETAO= ',F10.5,5X,//10X,'E1M= ',F10.5,5X,
223 'E2M= ',F10.5,5X,'PPM= ',F10.5,//10X,'FY= ',F8.3,5X,
224 'ES= ',F10.3,5X,'RND= ',F10.8,5X,'BETA= ',F5.3,
225 '///10X,'***** AT JOINT #',14)
226 2150 FORMAT(//9X,'1',9X,'X',9X,'Y',11X,'M/MB',8X,'F1/FYB',
227 '5X,'THETA',9X,'E4',8X,'FYT')
228 2300 FORMAT(//6X,14,4X,F9.3,3X,F9.4,3X,F9.5,3X,F9.5)
229 C
230 2500 FORMAT(//5X,'*****ULTIMATE MOMENT EXCEEDED',
231 ' WHEN THETAO= ',F6.5,' *****')
232 2600 FORMAT(//5X,'*****MAXIMUM PRESET THETAO OF ',F6.4,
233 ' EXCEEDED *****')
234 2700 FORMAT(//5X,'***** NEGATIVE M/MB OP F1/FYB *****')
235 2810 FORMAT(//5X,'***** MAX ALLOWED ITERATION EXCEEDED *****')
236 2920 FORMAT(//5X,'*****QUARTER WAVELENGTH OF CDC COMPLETED',
237 ' //FOR THETAO= ',F2.4,' AT J= ',15,' *****')
238 2930 FORMAT(//5X,'*****INSTABILITY MOMENT IN CDC AT ',
239 ' //WALL END ROTATION = ',F6.6,' *****')
240 END

```

```

241 C
242 C
243 C
244 C
245 C
246 C*****
247 C SUBROUTINE TO CALCULATE PHI/PHYS FOR A PARTICULAR P/PS
248 C*****
249 C
250 C
251 C
252 C
253 C SUBROUTINE EMPPH1
254 C
255 C
256 C COMMON X(300),Y(300),THETA(300),YJJ(50),
257 C *EMMB(300),FIFYB(300),PPBT(500),EMMET(300),
258 C *FIFYST(300),EMMBW(50),ROTHU(50),PPB,FYB,PB,E4,EMB,
259 C *E1M,E2M,E0,EUB,T,FIFYBM,FYT,FYTM,EMMBM,INST,INSTC,
260 C *INSTM,NCIT,NCITM,ERRDRP,ALPHA,I,J,K,M,N,UJ,
261 C *PPM,FY,ES,RHO,BETA
262 C
263 C IF(EMMB(1).LT.0.)GO TO 995
264 C
265 C CALCULATE CONSTANTS AND OUTPUT THEM
266 C
267 C PB=1.
268 C EMB=1./5.
269 C FYB=2.*EUB/D
270 C AO=E1M*E0
271 C
272 C INITIALIZE VARIOUS VALUES
273 C
274 C INSTM=5
275 C E4DEC=0.000005
276 C FYTINC=0.00001
277 C FYTO=0
278 C FYT=FYTO
279 C IW=1
280 C INST=0
281 C NCIT=0
282 C IMAX=0
283 C K=1
284 C EMMET(K)=0
285 C FIFYB(K)=0
286 C
287 C 100 J=1
288 C FYT=FYT+FYTINC
289 C E4=EUB
290 C IREP=1
291 C
292 C INCREASE COUNTER AND BEGIN CALCULATIONS
293 C
294 C
295 C 200 IF(E4.LE.0..OR.IREP.EQ.2)GO TO 992
296 C E1=E4-FYT
297 C E2=E1+ALPHA*FYT
298 C ER=E1+BETA*FYT
299 C E3=E1+(1.-ALPHA)*FYT
300 C
301 C ASSIGN PROPER EM TO STRAIN VALUES AT ANY POINT
302 C
303 C IF(E1.LE.E0)A1=E1-E1M
304 C IF(E1.GT.E0)A1=(E1-E0)*E2M*AO
305 C IF(E2.LE.E0)A2=E2-E1M
306 C IF(E2.GT.E0)A2=(E2-E0)*E2M*AO
307 C FS=ER*ES
308 C IF(E3.LE.E0)A3=E3-E1M
309 C IF(E3.GT.E0)A3=(E3-E0)*E2M*AO
310 C IF(E4.LE.E0)A4=E4-E1M
311 C IF(E4.GT.E0)A4=(E4-E0)*E2M*AO
312 C IF(FS.GE.FY)FS=FY
313 C IF(FS.LE.-FY)FS=-FY
314 C IF(E1.LT.0.)A1=0
315 C IF(E2.LT.0.)A2=0
316 C IF(E3.LT.0.)A3=0
317 C IF(E4.LT.0.)A4=0
318 C
319 C TEST FOR VARIOUS STRESS DISTRIBUTION CASES, ACT ACCORDINGLY
320 C CASE 1:
321 C
322 C IF(E1.GE.E0.AND.E2.GT.E0.AND.E3.GT.E0.AND.E4.GT.E0)GO TO 500
323 C
324 C CASE 2A AND 2B:
325 C
326 C IF(E1.GT.0..AND.E1.LT.E0.AND.E2.GT.E0.AND.E4.GT.E0)GO TO 300
327 C IF(E1.LT.0..AND.E2.GE.E0.AND.E3.GT.E0.AND.E4.GT.E0)GO TO 300
328 C
329 C CASE 3
330 C
331 C IF(E1.GE.0..AND.E2.GT.0..AND.E3.LT.E0.AND.E4.GT.E0)GO TO 400
332 C IF(E1.LT.0..AND.E2.LT.0..AND.E3.GT.0..AND.E3.LT.E0.AND.
333 C *E4.GT.E0)GO TO 400
334 C
335 C CASE 4
336 C
337 C IF(E1.LT.0..AND.E2.LT.0..AND.E3.GE.0..AND.E4.LE.E0)GO TO 500
338 C IF(E1.LT.0..AND.E2.LT.0..AND.E3.GT.E0.AND.E4.GT.E0)GO TO 500
339 C IF(E1.GE.0..AND.E2.LT.E0.AND.E3.LT.E0.AND.E4.LE.E0)GO TO 500
340 C IF(E1.GE.0..AND.E2.LE.E0.AND.E3.GE.E0.AND.E4.GT.E0)GO TO 500
341 C IF(E1.GE.0..AND.E2.LT.E0.AND.E3.GT.E0.AND.E4.GT.E0)GO TO 500
342 C
343 C CASES 5A AND 5B
344 C
345 C IF(E1.LT.0..AND.E2.GE.0..AND.E3.LE.E0.AND.E4.LE.E0)GO TO 500
346 C IF(E1.LT.0..AND.E2.GT.0..AND.E2.LE.E0.AND.E3.GT.E0)GO TO 500
347 C IF(E1.LT.0..AND.E2.GE.0..AND.E3.LE.E0.AND.E4.GT.E0)GO TO 500
348 C IF(E1.LT.0..AND.E2.LE.0..AND.E3.LE.E0.AND.E4.GT.E0)GO TO 500
349 C
350 C CASES 6A AND 6B
351 C
352 C IF(E1.LT.0..AND.E2.LT.0..AND.E3.LE.0..AND.E4.LE.E0)GO TO 700
353 C IF(E1.LT.0..AND.E2.LT.0..AND.E3.LE.0..AND.E4.GT.E0)GO TO 700
354 C
355 C IF CANNOT SATISFY ANY OF THESE, THEN SOMETHING WRONG!
356 C
357 C GO TO 991
358 C
359 C CASE 2A AND 2B E1 LESS THAN E0 DP NEC; E2, E3, GREATER THAN E0
360 C

```

```

351 300 IF(E1.LT.0)GO TO 320
352 J=J+1
353 T1=(EO-E1)/PYT
354 P2B=(A3+A4)/2.*ALPHA+(AO+A2)/2.*(ALPHA-T1)+(AO+A1)/2.*T1
355 PPBT(J)=P2B/PB+RHO*FS/PPM
356
357 C
358 C...CHECK WITH INCOMING PPB
359 C
360 PDIF=ABS(PPB-PPBT(J))/PPB
361 IF(PDIF.LE.ERRORP)GO TO 360
362 GO TO 370
363
364 C
365 320 J=J+1
366 T4=E4/(E4-E1)
367 IF(T4.GT.1.)T4=1.
368 T2=E2/E4+T4
369 TEO=EO/E4+T4
370 T1=ALPHA-T2
371 P2A=(A2+A4)/2.*ALPHA+(AO+A2)/2.*(T2-TEO)+(AO)/2.*TEO
372 PPBT(J)=P2A/PB+RHO*FS/PPM
373 PDIF=ABS(PPB-PPBT(J))/PPB
374 IF(PDIF.LE.ERRORP)GO TO 340
375 GO TO 370
376
377 C
378 340 K=K+1
379 NC=21
380 EM2A=A4/2.*ALPHA+(.5-ALPHA/3.)*A3/2.*ALPHA+(.5-2./3.*ALPHA)*
381 A2/2.*(T2-TEO)+(1.5-T1-2.*(T2-TEO)/3.)*AO/2.*(T2-TEO)+
382 (.5-T1-(T2-TEO)/3.)*AO/2.*TEO+(.5-T1-2.*TEO/3.)*A1/2.*T1+
383 (.5-T1/3.)
384 EMMBT(K)=EM2A/EMB
385 FIFYBT(K)=FYT/(2.*EUB)
386
387 C
388 IF(EMMBT(K).LT.0.)GO TO 395
389 IF(IMAX.GT.0)EMMBT(K)=EMMBM
390 IF(EMMBT(K).LT.EMMBT(K-1).AND.IMAX.EQ.0)GO TO 394
391 IREP=IREP+1
392
393 C
394 GO TO 370
395
396 C
397 350 K=K+1
398 NC=22
399 EM2B=A4/2.*ALPHA+(.5-ALPHA/3.)*A3/2.*ALPHA+(.5-2./3.*ALPHA)*
400 A2/2.*(ALPHA-T1)+(1.5-T1-2.*(ALPHA-T1)/3.)*AO/2.*(ALPHA-T1)+
401 (.5-T1-(ALPHA-T1)/3.)*AO/2.*T1+(.5-2.*T1/3.)*A1/2.*T1+
402 (.5-T1/3.)
403 EMMBT(K)=EM2B/EMB
404 FIFYBT(K)=FYT/(2.*EUB)
405
406 C
407 IF(EMMBT(K).LT.0.)GO TO 395
408 IF(IMAX.GT.0)EMMBT(K)=EMMBM
409 IF(EMMBT(K).LT.EMMBT(K-1).AND.IMAX.EQ.0)GO TO 394
410 IREP=IREP+1
411
412 C
413 OR TRY ANOTHER EDGE STRAIN
414 C
415 370 E4=E4-E4DEC
416
417 C
418 MORE CALCULATIONS
419 C
420 GO TO 200
421
422 C
423 CASE 3 : E1, E2, E3 LESS THAN EO, E4 GREATER
424 C
425 400 J=J+1
426 T3=(EO-E1)/PYT*(1.-ALPHA)
427 P3=(AO+A4)/2.*(ALPHA-T3)+(AO+A3)/2.*T3+(A1+A2)/2.*ALPHA
428 PPBT(J)=P3/PB+RHO*FS/PPM
429
430 C
431 CHECK WITH INCOMING PPB
432 C
433 PDIF=ABS(PPB-PPBT(J))/PPB
434 IF(PDIF.LE.ERRORP)GO TO 450
435 GO TO 480
436
437 C
438 450 K=K+1
439 NC=3
440 EM3=A4/2.*(ALPHA-T3)+(1.5-(ALPHA-T3)/3.)*AO/2.*(ALPHA-T3)+
441 (.5-2./3.*(ALPHA-T3))+AO/2.*T3+(1.5-(ALPHA-T3)-T3/3.)*A3/2.*
442 T3+(.5-(ALPHA-T3)-2.*T3/3.)*A2/2.*ALPHA+(.5-2./3.*ALPHA)*
443 A1/2.*ALPHA+(.5-ALPHA/3.)
444 EMMBT(K)=EM3/EMB
445 FIFYBT(K)=FYT/(2.*EUB)
446 IF(EMMBT(K).LT.0.)GO TO 395
447 IF(IMAX.GT.0)EMMBT(K)=EMMBM
448 IF(EMMBT(K).LT.EMMBT(K-1).AND.IMAX.EQ.0)GO TO 394
449 IREP=IREP+1
450
451 C
452 OR TRY ANOTHER EDGE STRAIN
453 C
454 480 E4=E4-E4DEC
455
456 C
457 GO TO 200
458
459 C
460 CASES 1 AND 4 : MOST COMMON CASES *****
461 INCLUDING BOTH E1 AND E2 NEGATIVE CASES *****
462 C
463 500 J=J+1
464 P4=(A1+A2+A3+A4)/2.*ALPHA
465 PPBT(J)=P4/PB+RHO*FS/PPM
466
467 C
468 CHECK WITH INCOMING PPB
469 C
470 PDIF=ABS(PPB-PPBT(J))/PPB
471 IF(PDIF.LE.ERRORP)GO TO 550
472 GO TO 570
473
474 C
475 550 K=K+1

```

```

481      NC=14
482      EM4=0.5*ALPHA*(A4*(.5-ALPHA/3.)+A3*(0.5-2.*ALPHA/3.))
483      A2=(.5-2.*ALPHA/3.)*A1*(.5-ALPHA/3.))
484      EMMBT(K)=EM4/EMB
485      FIFYBT(K)=FYT/(2.*EUB)
486      C** IF(IMAX.GT.0)EMMBT(K)=EMMBM
487      IF(EMMBT(K).LE.EMMBT(K-1).AND.IMAX.EQ.0)GO TO 884
488      C
489      C
490
491      IF(EMMBT(K).EQ.EMMBM)INST=INST+1
492      IF(INST.GE.INSTM)GO TO 883
493      IREP=IREP+1
494      C
495      C
496      C...OTHERWISE...
497      C
498      570 E4=E4-E4DEC
499      C
500      GO TO 200
501      C
502      C...CASES 5A AND 5B : E1 NEGATIVE, E2 POSITIVE
503      C
504      600 J=J+1
505      T4=E4/(E4-E1)
506      IF(T4.GT.1.)T4=1.
507      T2=E2/E4+T4
508      IF(T2.LT.0.)T2=0.
509      T1=1.-T4
510      IF(E3.LT.E0.AND.E4.GT.E0)GO TO 640
511      C
512      C
513      PBA=0.5*A2+T2*(A3+A4)/2.*ALPHA
514      PPBT(J)=PBA/PB/RMD*FS/FPM
515      C
516      C...CHECK WITH INCOMING PPB
517      C
518      PDIF=ABS(PPB-PPBT(J))/PPB
519      IF(PDIF.LE.ERRORP)GO TO 620
520      GO TO 670
521      C
522      620 K=K+1
523      NC=51
524      EM5A=0.5*ALPHA*(A4*(.5-ALPHA/3.)+A3*(.5-2.*ALPHA/3.))
525      A2=(.5-2.*ALPHA/3.)*A1*(.5-2.*T1-2.*T2/3.))
526      EMMBT(K)=EM5A/EMB
527      FIFYBT(K)=FYT/(2.*EUB)
528      IF(EMMBT(K).LT.0.)GO TO 885
529      C** IF(IMAX.GT.0)EMMBT(K)=EMMBM
530      IF(EMMBT(K).LE.EMMBT(K-1).AND.IMAX.EQ.0)GO TO 884
531      C
532      C
533      IF(EMMBT(K).EQ.EMMBM)INST=INST+1
534      IF(INST.GE.INSTM)GO TO 883
535      IREP=IREP+1
536      C
537      C
538      C...OTHERWISE...
539      C
540      GO TO 670
541      C
542      640 T3=E3/E4+T4
543      TEO=E0/E4+T4
544      T3O=TEO-T3
545      IF(T3O.LT.0.)GO TO 888
546      T4O=T4-TEO
547      C
548      PBA=(A0+A4)/2.*T4O+(A0+A3)/2.*T3O+0.5*T2*A2
549      PPBT(J)=PBA/PB/RMD*FS/FPM
550      C
551      C...CHECK WITH INCOMING PPB
552      C
553      PDIF=ABS(PPB-PPBT(J))/PPB
554      IF(PDIF.LE.ERRORP)GO TO 650
555      GO TO 670
556      C
557      650 K=K+1
558      NC=52
559      EM5B=A4/2.*T4O+(.5-T4O/3.)*A0/2.*T4O+(.5-2./3.*T4O)
560      A2=(A0/2.*T3O+(.5-T4O-T3O/3.)*A3/2.*T3O
561      A1=.5-T4O-2./3.*T3O)-0.5*T2*A2*(.5-T1-2./3.*T2)
562      A1/2.*T2*(.5-T1-T2/3.))
563      EMMBT(K)=EM5B/EMB
564      FIFYBT(K)=FYT/(2.*EUB)
565      C** IF(IMAX.GT.0)EMMBT(K)=EMMBM
566      IF(EMMBT(K).LE.EMMBT(K-1).AND.IMAX.EQ.0)GO TO 884
567      C
568      C
569      IF(EMMBT(K).EQ.EMMBM)INST=INST+1
570      IF(INST.GE.INSTM)GO TO 883
571      IREP=IREP+1
572      C
573      C
574      C...OTHERWISE...
575      C
576      670 E4=E4-E4DEC
577      C
578      GO TO 200
579      C
580      C...CASE 6 : E1, E2, E3 ALL NEGATIVE, E4 LESS OR EQUAL TO E8
581      C
582      700 J=J+1
583      E3=E4-ALPHA*FYT
584      T4=E4/(E4-E3)*ALPHA
585      C
586      C...CHECK FOR MAXIMUM E4
587      C
588      IF(E4.GT.E0)GO TO 780
589      C
590      C
591      PBA=A4+T4*0.5
592      PPBT(J)=PBA/PB/RMD*FS/FPM
593      C
594      C...CHECK WITH INCOMING PPB
595      C
596      PDIF=ABS(PPB-PPBT(J))/PPB
597      IF(PDIF.LE.ERRORP)GO TO 720
598      GO TO 780
599      C
600      720 K=K+1

```

```

601      NC=51
602      EMSA=A4+T4*.5*(.5-T4/3.)
603      EMMBT(K)=EMSA/EMB
604      FIFYBT(K)=FYT/(2.*EUB)
605      IF(EMMBT(K).LT.0.)GO TO 995
606      C** IF(IMAX.GT.0)EMMB(I)=EMMBM
607      IF(EMMBT(K).LE.EMMBT(K-1).AND.IMAX.EQ.0)GO TO 994
608      C
609      C
610      IF(EMMBT(K).EQ.EMMBM)INST=INST+1
611      IF(INST.GE.INSTM)GO TO 993
612      IREP=IREP+1
613      C
614      GO TO 780
615      C
616      C...CASE 68 .....
617      C
618
619      750 TO=EO+T4/E4
620      PSB=(AO+A4)/2.*(T4-TO)+AO/2.*TO
621      PPBT(J)=PSB/PS-RHO*FS/FPM
622      C
623      C...CHECK WITH INCOMING PPB
624      C
625      PDIF=ABS(PPB-PPBT(J))/PPB
626      IF(PDIF.LE.ERRDRP)GO TO 770
627      GO TO 780
628      C
629      770 K=K+1
630      NC=52
631      EMBB=A4/2.*(T4-TO)+(.5-(T4-TO)/3.)*AO/2.*(T4-TO)+
632      =(.5-2./3.*(T4-TO))+AO/2.*TO*(.5-(T4-TO)-TO/3.)
633      EMMBT(K)=EMBB/EMB
634      FIFYBT(K)=FYT/(2.*EUB)
635      C** IF(IMAX.GT.0)EMMBT(K)=EMMBM
636      IF(EMMBT(K).LE.EMMBT(K-1).AND.IMAX.EQ.0)GO TO 994
637      C
638      C
639      IF(EMMBT(K).EQ.EMMBM)INST=INST+1
640      IF(INST.GE.INSTM)GO TO 993
641      IREP=IREP+1
642      C
643      C
644      C OTHERWISE...
645      C
646      780 E4=E4-E4DEC
647      C
648      C...GO FOR MORE...
649      C
650      GO TO 200
651      C
652      991 WRITE(6,2600)E1,E2,E3,E4
653      STOP
654
655      C
656      C...INCREASE FYT AFTER E4 GOES NEGATIVE
657      C
658      992 IF(IREP.LT.2)NCIT=NCIT+1
659      IF(NCIT.GT.NCITM)GO TO 996
660      GO TO 100
661      C
662      993 WRITE(6,2810)EMMBT(K)
663      RETURN
664
665      C
666      994 EMMBM=EMMBT(K-1)
667      C
668      C...RAISE A FLAG FOR REACHING MAX MOMENT
669      C
670      IMAX=IMAX+1
671      C
672      C
673      C...GO FOR SOME MORE CALCULATIONS
674      C
675      E4=E4-E4DEC
676      C
677      C** GO TO 200
678      C
679      WRITE(6,2810)EMMBM
680      RETURN
681      C
682      995 WRITE(6,2820)
683      RETURN
684
685      C
686      996 EMMBM=EMMBT(K)
687      WRITE(6,2830)FYT,EMMBM
688      RETURN
689      C
690      999 WRITE(6,2600)E1,E2,E3,E4,NC
691      STOP
692
693      C
694      C...FORMAT STATEMENTS
695      C
696      1000 FORMAT(10F10.5)
697      C
698      2000 FORMAT(30X,' ',MASONRY WALL MOMENT-LOAD-CURVATURE', /
699      *33X,'USING INELASTIC BEHAVIOR - MPFY,IE,N',///)
700      C
701      2100 FORMAT(///10X,'ALPHA= ',F8.5,5X,'EO= ',F8.5,5X,'EUB= ',F8.5,
702      *5X,'E1M= ',F10.5,///10X,'E2M= ',F10.5,5X,'PB= ',F8.5,5X,'MB= ',
703      *F8.5,5X,' FYTO= ',F8.5,///10X,'*****P/PB= ',F8.5, ' *****')
704      C
705      2150 FORMAT(//5X,'1',7X,'M/MB',10X,'P/PB',10X,'E4',5X,'FYT',5X,
706      *'F1/FYB')
707      C
708      2300 FORMAT(//5X,14,3X,F10.5,3X,F10.5,3X,F10.5,3X,F10.5,3X,F10.5)
709      C
710      2500 FORMAT(//5X,'***** ULTIMATE MOMENT EXCEEDED *****')
711      C
712      2600 FORMAT(//5X,'***** NO CASE SOLUTION FOR E1= ',F9.8,', E2= ',
713      *F9.8,/,30X,'E3= ',F9.8,', E4= ',F9.8,', NC= ',I5, ' *****')
714      C
715      C
716      C
717      2800 FORMAT(//5X,'*****NEGATIVE COMPRESSION STRAIN AT FYT= ',
718      *F10.5, ' *****')
719      C
720      C

```



```

721 2810 FORMAT(//,5X,' **** MAXIMUM MOMENT REACHED !! ***** ',/
722 5X,' **** IN EMPFY AT M/MB =',P8.5,' *****')
723 C
724 2820 FORMAT(//,5X,' **** NEGATIVE MOMENT REACHED !! ***** ')
725 C
726 2830 FORMAT(//,5X,' **** MAY NO LONGER BE ABLE TO FIND ***** ',/
727 5X,' **** ANOTHER P/PB AFTER FYT =',P8.5,' *****',
728 5X,' **** MAXIMUM M/MB =',P8.5,' *****')
729 END
730 C
731 C
732 C
733 C
734 C
735 C
736 C
737 C
738 C
739 C
740 C
741 C
742 C
743 C
744 C
745 C
746 C
747 C
748 C
749 C
750 C
751 C
752 C
753 C
754 C
755 C
756 C
757 C
758 C
759 C
760 C
761 C
762 C
763 C
764 C
765 C
766 C
767 C
768 C
769 C
770 C
771 C
772 C
773 C
774 C
775 C
776 C
777 C
778 C
779 C
780 C
781 C
782 C
783 C
784 C
785 C
786 C
787 C
788 C
789 C
790 C
791 C
792 C
793 C
794 C
795 C
796 C
797 C
798 C
799 C
800 C
801 C
802 C
803 C
804 C
805 C
806 C
807 C
808 C
809 C
810 C
811 C
812 C
813 C
814 C
815 C
816 C
817 C
818 C
819 C
820 C
821 C
822 C
823 C
824 C
825 C
826 C
827 C
828 C
829 C
830 C
831 C
832 C
833 C
834 C
835 C
836 C
837 C
838 C
839 C
840 C
841 C
842 C
843 C
844 C
845 C
846 C
847 C
848 C
849 C
850 C
851 C
852 C
853 C
854 C
855 C
856 C
857 C
858 C
859 C
860 C
861 C
862 C
863 C
864 C
865 C
866 C
867 C
868 C
869 C
870 C
871 C
872 C
873 C
874 C
875 C
876 C
877 C
878 C
879 C
880 C
881 C
882 C
883 C
884 C
885 C
886 C
887 C
888 C
889 C
890 C
891 C
892 C
893 C
894 C
895 C
896 C
897 C
898 C
899 C
900 C
901 C
902 C
903 C
904 C
905 C
906 C
907 C
908 C
909 C
910 C
911 C
912 C
913 C
914 C
915 C
916 C
917 C
918 C
919 C
920 C
921 C
922 C
923 C
924 C
925 C
926 C
927 C
928 C
929 C
930 C
931 C
932 C
933 C
934 C
935 C
936 C
937 C
938 C
939 C
940 C
941 C
942 C
943 C
944 C
945 C
946 C
947 C
948 C
949 C
950 C
951 C
952 C
953 C
954 C
955 C
956 C
957 C
958 C
959 C
960 C
961 C
962 C
963 C
964 C
965 C
966 C
967 C
968 C
969 C
970 C
971 C
972 C
973 C
974 C
975 C
976 C
977 C
978 C
979 C
980 C
981 C
982 C
983 C
984 C
985 C
986 C
987 C
988 C
989 C
990 C
991 C
992 C
993 C
994 C
995 C
996 C
997 C
998 C
999 C
1000 C

```

SUBROUTINE TO CALCULATE M/MB BY INTERPOLATION
 SUBROUTINE EMITPD
 COMMON X(300),Y(300),THETA(300),YJJ(50),
 EMMB(300),FIFYB(300),PPBT(600),EMMBT(300),
 FIFYBT(300),EMMBW(50),ROTN(50),PPB,FYB,PB,E4,EMB,
 EIM,E2M,E0,EUB,T,FIFYBM,FYT,FYTM,EMMBM,INST,INSTC,
 INSTM,NCIT,NCITM,ERRDRP,ALPHA,I,J,K,M,N,JJ,
 FPM,FY,ES,RND,BETA
 INSTC=0
 KK=K+1
 DO 100 M=1,KK
 IF(EMMB(I).GE.EMMBT(M).AND.EMMB(I).LT.EMMBT(M+1))GO TO 200
 IF(EMMB(I).GT.EMMBT(M).AND.EMMB(I).LE.EMMBT(M+1))GO TO 200
 IF(M.GT.K)GO TO 991
 100 CONTINUE
 INTERPOLATE TO GET CORRESPONDING PHI/PHIB. CHECK FOR PLATEAU
 200 ERINST=ABS(EMMBT(M+1)-EMMBT(M))/EMMBT(M+1)
 IF (ERINST.LT.0.005)GO TO 300
 OTHERWISE
 FIFYB(I)=(EMMB(I)-EMMBT(M))/(EMMBT(M+1)-EMMBT(M))*
 (FIFYBT(M+1)-FIFYBT(M))+FIFYBT(M)
 RETURN
 300 FIFYB(I)=FIFYBT(M)
 INSTC=INSTC+1
 IF (INSTC.GE.5)WRITE(6,3100)
 RETURN
 991 WRITE(6,3000)
 RETURN
 SUBROUTINE EMPNU
 COMMON X(300),Y(300),THETA(300),YJJ(50),
 EMMB(300),FIFYB(300),PPBT(600),EMMBT(300),
 FIFYBT(300),EMMBW(50),ROTN(50),PPB,FYB,PB,E4,EMB,
 EIM,E2M,E0,EUB,T,FIFYBM,FYT,FYTM,EMMBM,INST,INSTC,
 INSTM,NCIT,NCITM,ERRDRP,ALPHA,I,J,K,M,N,JJ,
 FPM,FY,ES,RND,ETA
 N=NN
 YJJ(NN)=Y(JJ)
 EMMBW(NN)=EMMB(JJ)
 ROTNU(NN)=Y(JJ)/X(JJ)-THETA(JJ)
 WRITE(6,4000)NN,EMMBW(NN),ROTN(NN)
 IF(EMMBW(NN).GT.EMMBM.OR.YJJ(NN).LT.YJJ(NN-1))GO TO 999
 999 WRITE(6,4100)
 N=NN
 RETURN
 4000 FORMAT(//5X,' *****',
 ' *****',/10X,' #',I2,3X,' (M/MBW/J =',P8.7,3X,' (NU/JJ =',P8.7,
 5X,' *****',
 4100 FORMAT(//5X,' *****MAX. MOMENT OR ROTATION EXCEEDED IN EMTITA*'
 END
 SUBROUTINE STAR
 WRITE(6,2000)
 2000 FORMAT(//5X,' *****',
 ' *****',/)
 RETURN
 END

APPENDIX C - OTHER EXAMPLES

C.1 EQUILIBRIUM FAILURE THEORY OF MAURENBRECHER (1970)

The equilibrium theory of Maurenbrecher is applied here to specimens WSA100 and WSA400, with the nomenclature as shown in Figure C.1.

Neglecting the tie-back forces and decrease in H on the lower wall, using Equation 3.6:

$$\frac{P_{smax}}{P_u} = \frac{t/g}{L + t/(2g)}$$

where $g = 1/(1 + h/(2H))$

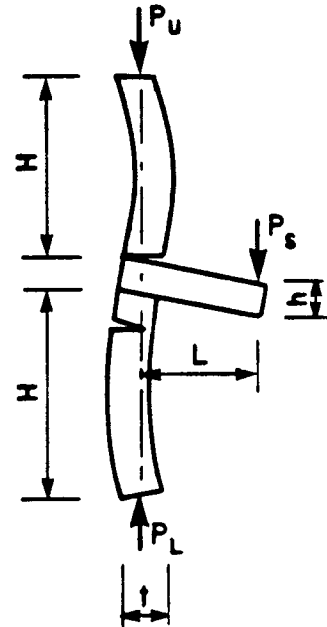


Figure C.1

Specimen WSA100

If $H = 1610 - 100 = 1510$ mm; $h = 200$ mm

and $t = 190$ mm, then $g = 0.9379$ and

$t/g = 190/0.9379 = 202.58$ mm

Thus $P_{smax} = 0.2401P$

From test, $P = 104.7$ kN

Thus $P_{smax} = 25.13$ kN

leading to $M_{smax} = 25.13 \times 0.850 = 21.4$ kNm

This is 11% less than $M = 23.94$ kNm evaluated from test results.

Specimen WSA400

From test, $P = 403.9 \text{ kN}$

Thus $P_{smax} = 0.2401 \times 403.9 = 96.98 \text{ kN}$

leading to $M_{smax} = 96.98 \times 0.850 = 82.42 \text{ kNm}$

This is 5% less than $M = 78.58 \text{ kNm}$ evaluated from test results.

C.2 AWNI/COLVILLE'S METHOD FOR UNREINFORCED FRAMES

Specimen FRA150 at Maximum Joint Moment

1. Floor:

Live load, $P_s = 30$ kN (applied + equipment load)

Equivalent UDL for 2-Point load = $w_{eq} = 3P_s/L = 18.5$ kN/m²

Slab UDL = 4.7 kN/m²

Thickness = 200 mm

$L = 4875$ mm

$I_s = 6.67 \times 10^8$ mm⁴

$E_s = 26\ 646$ MPa

2. Wall

Thickness, $t = 190$ mm

Story height = 3220 mm

Wall Weight = $2.1 \times 1.4 = 2.9$ kN

Equipment = 2.1 kN

$f'_m = 10.2$ MPa

$$I_m = 1/12 \times 995 \times 190^3 - 5(132 \times 126^3)/12$$

$$= 4.62 \times 10^8 \text{ mm}^4$$

(assuming 5 voids, each 132mm wide by 126mm deep)

$$E_m = 750f'_m = 7650 \text{ MPa.}$$

Solution for relative eccentricity, e_r :

With all floor loaded, it may be asumed that the walls are in double curvature with equal end eccentricities, Thus:

$$P_u = 150 + 2.9 + 2.1 = 155 \text{ kN}$$

$$P_L = 155 + 23.2 \times 4.875/2 = 211.6 \text{ kN}$$

$$\psi = P_u/P_L = 0.733$$

$$\psi_1 = 1 + \psi = 1.733$$

AWNI (1980)

$$M_F = \frac{w_{eq} L^2}{12} = 45.95 \text{ kNm}$$

$$\beta = \frac{(EI)_s H}{(EI)_w L} \text{ (Double Curvature)}$$

$$= \frac{17.77 \times 1.610}{3.51 \times 4.875} = 1.67$$

$$M_R = \frac{3M_F}{3 + \beta} = 29.52 \text{ kNm (Double Curvature)}$$

$$\text{Thus } K = 2\beta = 3.34$$

$$\text{Precompression} = P_u/t = 155/190 = 0.83 \text{ MPa}$$

assuming cracked wall, $R = 1.275$

$$e_r = \frac{M_R R \psi}{P_L t (\psi_1 R + K)}$$

$$e_r = \frac{29.52 \times 0.733 \times 1.275}{211.6 \times (1.733 \times 1.275 + 3.34)} = 0.124$$

Thus wall is uncracked and $R = 2.345$, giving $e_r = 0.139$

$$e_r(\text{test}) = \frac{M_{\text{test}}}{(P_u + P_L)t}$$

$$= \frac{29.80}{(155 + 211.6) \times 0.190} = 0.428$$

The ultimate eccentricity ratio, e_{rf} , is (Colville, 1979):

$$e_{rf} = 1/2(1 - P/P_b) = 0.430 > 0.428 \quad \text{OK}$$

where:

$$P_b = f'_m b(2at) = 10.2 \times 995 \times 0.56 \times 190 = 1080 \text{ kN}$$

COLVILLE (1979)

Using the procedure originally proposed by Colville in 1979, e_r was found to be 0.298.

It can be seen that both procedures appear to underestimate the measured eccentricity for the upper wall, which compares very favourably with prediction from interaction curve for a equal to 1.0.